Genetic diversity and spatial patterns of distribution of Citrus greening disease and its vectors in East Africa

by

Inusa Jacob Ajene

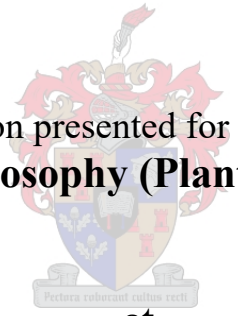

Dissertation presented for the degree of
Doctor of Philosophy (Plant Biotechnology)

at

Stellenbosch University
Department of Genetics, Faculty of AgriSciences

Supervisor: Prof. Gerhard Pietersen
Co-supervisor: Dr Barbara van Asch
Co-supervisor: Dr Fathiya Khamis
Co-supervisor: Dr Sunday Ekesi

December 2020

Declaration

By submitting this dissertation electronically, I declare that the entirety of the work contained therein is my own, original work, that I am the sole author thereof (save to the extent explicitly otherwise stated) that reproduction and publication thereof by Stellenbosch University will not infringe any third party rights and that I have not previously in its entirety or in part submitted it for obtaining any qualification.

Date: 10/05/2020

This dissertation includes five original papers published in peer-reviewed journals and two unpublished manuscripts (finalised with a view to submission for publication). The development and writing of the papers (published and unpublished) were the principal responsibility of myself and, for each of the cases where this is not the case, a declaration is included in the dissertation as an appendix indicating the nature and extent of the contributions of co-authors. Declaration with signature in possession of candidate and supervisor.

Summary

Citrus spp is an important cash crop supporting millions of households in East Africa. However, the crop faces challenges of infestation by pests and diseases that lead to substantial economic loss. Citrus greening disease is the most destructive disease on citrus worldwide. The disease is caused by a phloem-limited, bacteria of the "*Candidatus"* Liberibacter species. The Asian citrus greening also known as Huanglongbing (HLB), is associated with the pathogen "*Candidatus* Liberibacter asiaticus" (CLas) which is transmitted by the Asian citrus psyllid (*Diaphorina citri* Kuwayama). The African citrus greening disease (ACG) associated with "*Candidatus* Liberibacter africanus" (CLaf) is transmitted by the African citrus triozid (*Trioza erytreae* del Guercio). *Trioza erytreae* is widespread in Africa and has been reported in 21 countries in Africa while *D. citri* has been reported in Asia and the Americas with recent invasions into Kenya and Tanzania. Currently, management of the diseases rely on the control of the psyllid vectors. Furthermore, targeted control measures against the vectors are dependent on the knowledge of its biology and genetic diversity. Therefore, the objectives of this study were to i) To identify the Liberibacters associated with citrus greening disease in Eastern Africa, ii) determine current and predicted regional and global climate suitability of Liberibacter species associated with Huanglongbing, iii) unravel the genetic diversity of the greening disease vectors using microsatellite markers and mitochondrial genome analysis and iv) assess the microbiome diversity and genes for resistance to antibiotics within populations of *D. citri.* Field surveys were conducted in Ethiopia, Kenya and Uganda to assess the spatial distribution of the Liberibacters and vectors in the region. Quantitative PCR and Sanger sequencing were used to identify and characterise the Liberibacters. Future distribution of CLas in Africa and CLaf globally was predicted using an ensemble modelling approach. The genetic diversity of *D. citri* was assessed by analysing the complete mitochondrial genome of the African populations as well as assessing the simple sequence repeats within the genome of the psyllid. This provided the population structure and the possible route of invasion of *D. citri* into Africa. Finally, the bacterial microbiome diversity of the *D. citri* populations was assessed. Our findings showed that CLas was more widespread in Ethiopia than previously reported, CLas was detected in Kenya for the first time and *D. citri* was detected in Ethiopia for the first time. Furthermore, we found CLas in field populations of *T. erytreae*. The predictive modelling showed that most citrus producing countries in Africa are highly suitable for the establishment of CLas. The assessment of the genetic diversity revealed *D. citri* from Kenya and Tanzania had a close genetic relationship with *D. citri* from China while *D. citri* from Ethiopia had a close relationship with *D. citri* from the USA. Thus, two separate introduction events for *D. citri* into Africa was concluded. Finally, the microbiome analysis also showed that *D. citri* from Kenya and Tanzania had a similar microbiome composition to the *D. citri* from China.

Opsomming

Sitrus is 'n belangrike kontantgewas wat miljoene huishoudings in Oos-Afrika ondersteun. Die oes staar egter uitdagings van besmetting deur peste en siektes in die gesig wat tot aansienlike ekonomiese verliese kan lei. Sitrusvergroeningsiekte is die mees vernietigende siekte op sitrus wêreldwyd. Die siekte word veroorsaak deur 'n floeëmbeperkte, bakterieë van die "*Candidatus*" Liberibacter spesie. Die Asiatiese sitrus vergroening, ook bekend as Huanglongbing (HLB), word geassosieer met die patogeen "*Candidatus* Liberibacter asiaticus" (CLas) wat oorgedra word deur die Asiatiese sitrus psyllid (*Diaphorina citri* Kuwayama). Die Afrika-sitrusvergroeningsiekte (ACG) wat met "*Candidatus* Liberibacter africanus" (CLaf) geassosieer word, word deur die Afrika-sitrus triozid (*Trioza erytreae* del Guercio) oorgedra. *Trioza erytreae* is wydverspreid in Afrika en is al in 21 lande in Afrika aangemeld, terwyl *D. citri* in Asië en die Amerikas aangemeld is met onlangse invalle in Kenia en Tanzanië. Tans word daar staat gemaak op die beheer van die psyllid vektore om die siekte te bestuur. Geteikende beheermaatreëls teen die vektore is afhanklik van die kennis oor hul biologie en genetiese diversiteit. Daarom was die doelwitte van hierdie studie om; i) die Liberibacters wat met sitrusvergroeningsiekte in Oos-Afrika geassosieer word, te identifiseer, ii) te bepaal wat die huidige en voorspelde streeks- en globale klimaatgeskiktheid van Liberibacter spesies wat verband hou met Huanglongbing, iii) die genetiese diversiteit van die vergroeningsiekte vektore met behulp van mikrosatelliet merkers en mitokondriale genoom analise te ontrafel en iv) die mikrobiome diversiteit en gene vir weerstand teen antibiotika te evalueer. Veldopnames is in Ethiopië, Kenia en Uganda gedoen om die ruimtelike verspreiding van die Liberibacters en vektore in die streke te evalueer. Kwantitatiewe PKR- en Sangervolgordebepalings is gebruik om die Liberibacters te identifiseer en te kenmerk. Toekomstige verspreiding van CLas in Afrika en CLaf wêreldwyd is voorspel met behulp van 'n ensemble modellering benadering. Die genetiese diversiteit van *D. citri* is geassesseer deur die volledige mitokondriale genoom van die Afrika-bevolking te ontleed, asook die beoordeling van die eenvoudige reeks herhalings binne die genoom van die psyllid. Dit het die bevolkingstruktuur en die moontlike roete van inval van *D. citri* in Afrika verskaf. Uiteindelik is die bakteriële mikrobioomdiversiteit van die D. citri populasies bepaal. Ons bevindinge het getoon dat CLas meer wydverspreid in Ethiopië was as wat voorheen berig is, CLas is vir die eerste keer in Kenia opgespoor en *D. citri* is vir die eerste keer in Ethiopië opgespoor. Verder het ons CLas gevind in veldbevolkings van *T. erytreae*. Die voorspellende modellering het getoon dat die meeste sitrusproduserende lande in Afrika hoogs geskik is vir die vestiging van CLas. Die assessering van die genetiese diversiteit het *D. citri* in Kenia en Tanzanië het 'n noue genetiese verband met *D. citri* uit Sjina, terwyl *D. citri* van Ethiopië 'n noue verband met *D. citri* uit die USA het. Twee afsonderlike bekendstellingsgeleenthede vir *D. citri* in Afrika is dus voorgestel. Uiteindelik het die mikrobioom analise ook getoon dat *D. citri* van Kenia en Tanzanië het 'n soortgelyke mikrobiome samestelling aan die *D. citri* uit Sjina.

This dissertation is dedicated
With love to my mother, father and brothers.

Biographical sketch

Inusa Jacob Ajene is a Lecturer and research scientist at the Department of Crop protection, Faculty of Agriculture/Institute for Agricultural research, Ahmadu Bello University Zaria, Nigeria with a background in molecular plant pathology and epidemics. He obtained his Bachelor of Agriculture (B. Agric) and Master of Science in Crop protection (M.Sc. Crop Protection) at Ahmadu Bello University, Zaria. He obtained a PhD Scholarship from the Deutscher Akademischer Austauschdienst (DAAD) under the African Regional Postgraduate Programme in Insect Science (ARPPIS) scholarship program at the International Center of Insect Physiology and Ecology (ICIPE), Nairobi, Kenya under the project; 'Strengthening Citrus Production Systems through the Introduction of Integrated Pest Management Measures for Pests and Diseases in Kenya and Tanzania' which focused on the different aspects of pests and diseases of citrus in Eastern Africa. The specific aim of his current research is to assess the current status of the greening disease on citrus and the genetic diversity of its vector in Eastern Africa, resolve the identities of *Candidatus* Liberibacter species associated with citrus greening disease and identify potential management strategies against the disease to protect the citrus industry on the continent.

Acknowledgements

I wish to express my sincere gratitude and appreciation to the following institutions and persons:

- Stellenbosch University for providing ample academic and administrative resources which led to a relatively smooth attainment of my degree as well as Ahmadu Bello University for granting me a study leave to pursue my PhD.
- The German Academic Exchange (DAAD)
- The German Ministry for Economic Cooperation and Development (BMZ)
- The International Center for insect Physiology and Ecology (*icipe*) for hosting me during my field and lab work and for the trainings and workshops offered during my graduate experience.
- My Supervisors; Prof. Gerhard Pietersen, for his guidance, motivation, patience and unrelenting support throughout my doctoral study. I sincerely thank him for painstakingly reviewing my work amidst his busy schedules. His insightful comments and suggestions which greatly improved my work. Dr Barbara van Ash, who kept me on my toes and worked tirelessly on my data analysis and greatly improved my writing skills. I appreciate her awesome mentorship, patience and generous heart. Dr Fathiya Khamis for her care, guidance, motivation, patience and support throughout my doctoral study. Dr Sunday Ekesi for his guidance, motivation and unrelenting support amidst his busy schedules, facilitating the smooth operations and approved every request I brought before him throughout my doctoral study. Dr Samira Mohamed, for her care and immense support in the course of my work.
- My sincere appreciation to the entire academic and administrative staff at the Genetics department, Stellenbosch University. In particular, the staff and students of the Vitis Lab and the Molecular Breeding and Biodiversity Lab for their awesome support. I am highly indebted to my team from *icipe* Levi Ombura, Maureen Adhiambo, Dr Brenda Rasowo, Dr Joseph Gichuhi, Anne Wairimu, my team from Ethiopia Dr Shifa Ballo and Nurhussen Seid and the entire staff at the Crop Protection department, Ahmadu Bello University, Zaria.
- Most importantly, I thank my supportive Family; My parents, Prof Oga Ajene and Mrs. Alice Ajene. To my siblings, Adam, Paul-Ben, Oga Jr. and Ogo Jet Jason-Charles, I thank them for their love, support, encouragement, prayers and well wishes.
- Above all, I thank God for his grace and for giving me good health and strength to go through my studies.

Preface

This dissertation is presented as a compilation of eight chapters. Each chapter has been prepared as stand-alone publications or manuscripts submitted to different scientific journals for publication. Consequently, unavoidable overlaps and/or repetitions may occur.

Chapter 1	**General Introduction and project aim**
Chapter 2	**Distribution of *Candidatus* Liberibacter species in Eastern Africa, and the First Report of "*Candidatus* Liberibacter asiaticus" in Kenya. *Scientific reports*. 2020; 10, 3919. https://doi.org/10.1038/s41598-020-60712-0**
Chapter 3	**Habitat Suitability and Distribution Potential of Liberibacter Species ("*Candidatus* Liberibacter asiaticus" and "*Candidatus* Liberibacter africanus") associated with Citrus Greening disease. *Diversity and Distributions.* 2020; 00:1–14. https://doi.org/10.1111/ddi.13051.**
Chapter 4	**Detection of Asian citrus psyllid *Diaphorina citri* (Hemiptera: Psyllidae) in Ethiopia: A new haplotype and its implication to the Proliferation of Huanglongbing. *Journal of Economic Entomology*. 2020. https://doi.org/10.1093/jee/toaa113.** **First report of field population of *Trioza erytreae* carrying the Huanglongbing associated pathogen, "*Candidatus* Liberibacter asiaticus", in Ethiopia. *Plant Disease Notes*. 103:7 https://doi.org/10.1094/PDIS-01-19-0238-PDN.**
Chapter 5	**Comparative Analyses of *Diaphorina citri* Mitogenome revealed different African Populations of are linked to Populations from USA and China. *(Manuscript finalised with a view to submission for publication)***
Chapter 6	**Genetic diversity and population structure of *Diaphorina citri* in East Africa inferred from microsatellite markers. *Manuscript finalised with a view to submission for publication)***
Chapter 7	**Microbiome diversity in *Diaphorina citri* populations from Kenya and Tanzania shows links to China. *PLoS one.* 2020. 15(6): e0235348. https://doi.org/10.1371/journal.pone.0235348.**
Chapter 8	**General discussion and conclusions**

Outline of the thesis

Chapter One presents a general introduction and overview of literature on citrus greening disease and its vectors and the implications for the African citrus industry. **Chapter two** presents survey and molecular identification of the *Candidatus* Liberibacter species in three eastern African countries (Ethiopia, Kenya and Uganda). It provides an overview of the distribution of the Liberibacter species in each country and the characterization of the different species. **Chapter three** assessed the habitat suitability of "*Candidatus* Liberibacter asiaticus" (CLas) in Africa using current and future bioclimatic variables and predicted its future distribution in a changing climate (raising temperatures) using three species distribution models. Also, the habitat suitability of "*Candidatus* Liberibacter africanus" (CLaf) was assessed globally. **Chapter four** highlights the first report of the Asian citrus psyllid *Diaphorina citri* (Kuwayama) vector of CLas in Ethiopia, the identification of a new haplotype and its implication for the proliferation of HLB in the region. Also, the first report of field populations of the African citrus triozid *Trioza erytreae* (Del Guercio) carrying CLas in Ethiopia. *Trioza erytreae* is the known vector of CLaf but this report highlights the possibility that *T. erytreae* may be able to transmit CLas. **Chapter five** evaluates the phylogeographic diversity of *D. citri* using the complete mitochondrial genome in an attempt to infer the routes of invasion of *D. citri* into Africa. **Chapter six** evaluates the genetic diversity and population structure of *D. citri* populations from the three African countries (Ethiopia, Kenya and Tanzania) where the psyllid has been reported as well as the probable founder populations (China and USA). **Chapter seven** analyses the microbiome of *D. citri* from four countries and evaluates the bacterial endosymbionts as well as identifies genes for resistance to antibiotics present in the psyllid. **General conclusions** looked at the findings from all chapters and proposed recommendations and highlighted areas for future research.

Table of Contents

List of Figures

CHAPTER THREE

CHAPTER FOUR

List of Tables

List of Abbreviations

ACG	Africa citrus greening disease
AMOVA	Analysis of molecular Variance
ARGs	antibiotic resistance genes
ATP6	ATP synthase F0 subunit 6
ATP8	ATP synthase F0 subunit 8
AUROC	Area Under the Receiver Operator Curve
BLAST	Basic Local Alignment Search Tool
BRT	Boosted Regression Trees
CARD	Comprehensive Antibiotic Resistance Database.
CGD	Citrus greening disease
CMIP	Coupled Model Intercomparison Project
COI	cytochrome c oxidase subunit I
COII	cytochrome c oxidase subunit II
COXIII	cytochrome c oxidase subunit III
Ct	Cycling threshold
CYTB	cytochrome b
DAPC	discriminate analysis of principal components
He	Expected Heterozygosity
HLB	Huanglongbing disease
Ho	Observed Heterozygosity
CLaf	"*Candidatus* Liberibacter africanus"
CLafC	"*Candidatus* Liberibacter africanus subspecies clausenae"
CLafT	"*Candidatus* Liberibacter africanus subspecies teclae"
CLafV	"Candidatus Liberibacter africanus subspecies vepridis"
CLam	"*Candidatus* Liberibacter americanus"
CLas	"*Candidatus* Liberibacter asiaticus"

M. A. S. L	meters above sea level
MaxEnt	Maximum Entropy
MT	metric tons
Na	No. of Different Alleles,
ND1	NADH dehydrogenase subunit 1
ND2	NADH dehydrogenase subunit 2
ND3	NADH dehydrogenase subunit 3
ND4	NADH dehydrogenase subunit 4
ND5	NADH dehydrogenase subunit 5
ND6	NADH dehydrogenase subunit 6
Ne	No. of Effective Alleles
ONT	Oxford Nanopore Technologies
PCG	Protein Coding Gene
PCoA	principal coordinate axis
PCR	Polymerase Chain Reaction
QGIS	Quantum Geographical Information Systems
qPCR	Quantitative PCR
RCPs	Representative Concentration Pathways scenarios
rplJ	ribosomal protein L10
tRNA	Transfer RNA
uHe	Unbiased Expected Heterozygosity
WIMP	What's in my Pot

Chapter One: General Introduction

Introduction

Citrus is an economically important crop with annual production estimates standing at over 122 million metric tons (MT) of fruit from the top producing countries (Brazil, USA and China) (Mendonça, et al., 2017). In Africa, the average annual production is over 73 million metric tons (MT) (FAOSTAT, 2018). There are a wide variety of cultivated species of citrus, including sweet orange (*Citrus sinensis* Osbeck), lemon (*Citrus limon* [L.] Burm. f.), lime (*Citrus aurantifolia* [Cristm.] Swingle), grapefruit (*Citrus paradisi* Macfad), and mandarin (*Citrus reticulata* Blanco). Egypt and South Africa are the largest producers of citrus fruits in Africa (FAOSTAT, 2018). In eastern Africa, citrus is widely cultivated in Ethiopia, Kenya, Tanzania and Uganda where citrus production is a key source of livelihood for smallholder farmers with production ranging from small to medium scale (>1 to 5 hectares) (Aidoo et al., 2018). The annual production in East Africa ranged from 61 to 135 MT between 2012 and 2016 (FAOSTAT, 2018). However, production has been on the decline in East Africa, particularly in the highland regions (Sengoba et al., 2002; Aidoo et al., 2018). Furthermore, fruit yield at the smallholder level is about 10 t/ha, far below the potential of 75 t/ha (Obukosia and Waithaka, 2000; Kilalo et al., 2009). Several biotic and abiotic factors have been attributed to the decreasing yields in sub-Saharan Africa, with pests and diseases among the most important (Ekesi, 2012). A large portion of economic losses in citrus production in Africa, Asia and the American continent is attributed to citrus greening disease (Krishna, 2015).

Based on the associated cause, citrus greening disease (CGD) commonly referred to as Huanglongbing, or specifically in Africa as Africa citrus greening disease (ACG), is reported as one of the major limitations to citrus production (Ministry of Agriculture, 1982; Kilalo et al., 2009; Tschirley et al., 2004).

Citrus greening disease

Candidatus Liberibacter pathogens

Citrus greening disease is associated with *Candidatus* Liberibacter species infections. The bacterial pathogens belong to the alpha sub-division of Proteobacteria. They are phloem-limited, non-culturable, Gram negative bacteria. (Garnier and Bove, 1983; Jagoueix et al., 1996). Three species of the bacteria have been associated with citrus greening disease. "*Candidatus* Liberibacter africanus" (CLaf) is the pathogen associated with the African citrus greening

(ACG), "*Candidatus* Liberibacter americanus" (CLam) and "*Candidatus* Liberibacter asiaticus" (CLas) are associated with the more severe Huanglongbing disease (HLB) (Bassanezi and Gottwald, 2004; Garnier et al., 2000; Teixeira, 2005). CLas is more heat-tolerant and can withstand temperatures of 30 to 35 °C (da Graca & Korsten, 2004). CLaf usually occurs in cool highland regions, mostly above 900 meters above sea level (m.a.s.l.) (Narouei-Khandan et al., 2016). Several subspecies of CLaf have been identified from indigenous rutaceous trees including "*Candidatus* Liberibacter africanus subspecies clausenae" (CLafCl) (Roberts et al., 2015) detected from *Clausena anisata* (Wild) Hook. f. ex Benth., "*Candidatus* Liberibacter africanus subspecies vepridis" (CLafV) (Roberts et al., 2015) detected from *Vepris lanceolata* (CLam.) G.Don, "*Candidatus* Liberibacter africanus subspecies teclae" (CLafT) (Roberts and Pietersen 2017) detected from *Teclea gerrardii* Verdoorn.

Geographic distribution

"*Candidatus* Liberibacter asiaticus" is the most widely distributed and devastating species associated with HLB that has been reported from citrus crops in Asia (Garnier and Bove, 1996), the Mascarene Islands (Garnier et al., 1996), South and Central America (Halbert and Manjunath ,2004), Papua New Guinea (Weinert et al., 2004) and in Ethiopia (Saponari et al., 2010) (Fig 1.1). "*Candidatus* Liberibacter americanus" has been found in Brazil and Texas (Bové, 2006; Teixeira, 2005) while "*Candidatus* Liberibacter africanus" has been reported in southern, eastern and central African countries including Madagascar (van Vuuren, 1978; Moll et al., 1980; Da Graca 1991; Batool et al., 2007; Magomere et al., 2009).

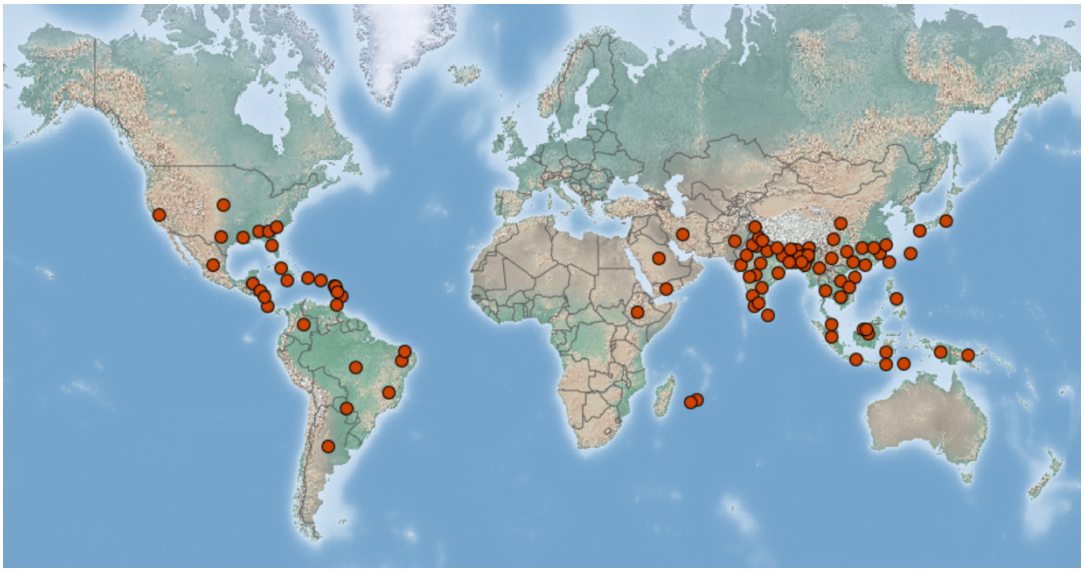

Figure 1.1. Global occurrence of citrus Huanglongbing disease (HLB) associated with the bacterial pathogen "*Candidatus* Liberibacter asiaticus" (CLas), as reported in previous studies. Source: Centre for Agriculture and Bioscience International CABI/EPPO, 2017. "*Candidatus*

Liberibacter asiaticus". [Distribution map]. In: Distribution Maps of Plant Diseases, (No.April) Wallingford, UK: CABI.Map 766 (Edition 4).

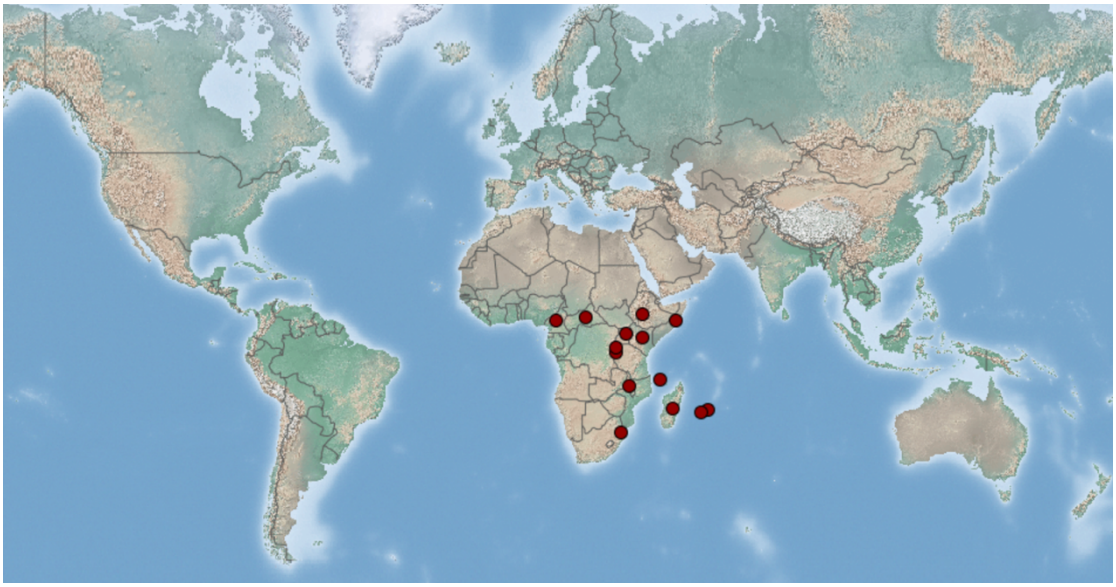

Figure 1.2 Occurrence of African citrus greening disease associated with the bacterial pathogen "*Candidatus* Liberibacter africanus" (CLaf), as reported in previous studies. Source: Centre for Agriculture and Bioscience International CABI/EPPO, 1998. Liberobacter africanum (sic). [Distribution map]. Distribution Maps of Plant Diseases, October (Edition 1). Wallingford, UK: CAB International, Map 765

Transmission

The primary mode of transmission of the citrus greening pathogen from one plant to another is through insect vectors. Mechanical transmission through vegetative propagation with infected plant materials is also an important means of transmission (Capoor et al., 1974; Roistacher, 1996). Vegetative transmission occurs through the use of infected bud wood (Oberholzer et al., 1965). There are two known vectors of the pathogens; the African citrus triozid, *Trioza erytreae* (Del Guercio) (Hemiptera: Triozidae) (Fig 1.3a) which is widespread in Africa and has been reported in 19 African countries (Angola, Kenya, Ethiopia, Eritrea, Madagascar, Malawi, Mauritius, La Réunion, South Africa, Sudan, Swaziland, St. Helen, Tanzania, Uganda, Zambia, DR Congo, Rwanda, Comoros, and Cameroon) (EPPO, 2014), and then the Asian citrus psyllid *Diaphorina citri* (Kuwayama) (Hemiptera: Liviidae) (Fig 1.3b) which has been reported in 55 countries in Asia, Africa, the Americas and Oceania (EPPO, 2014).

D. citri can withstand temperatures above 30°C and is able to transmit CLas or CLam pathogen via salivary secretions to an uninfected plant during 15–30 minutes of phloem-feeding with a latent period of 8–12 days (Salibe and Cortez, 1966). The *Candidatus* Liberibacter pathogens can also be passed vertically from infected mothers to uninfected offspring via the egg, or through venereal transmission where infected males or females transfer and infect the other sex during

mating (Tabachnick, 2015). *T. erytreae* develops at temperatures of 22-25°C. The bacterium is ingested by the psyllid and multiplies in the insect hemolymph (Batool et al., 2007). The pathogen is then injected along with saliva into the plant during feeding. T. *erytreae* can acquire the inoculum within five days of feeding and transmits the disease in less than 60 minutes of feeding (van Vuuren and da Graça, 1978). Experimentally both psyllid species have been shown to transmit either Liberibacter specie (Massonié et al., 1976).

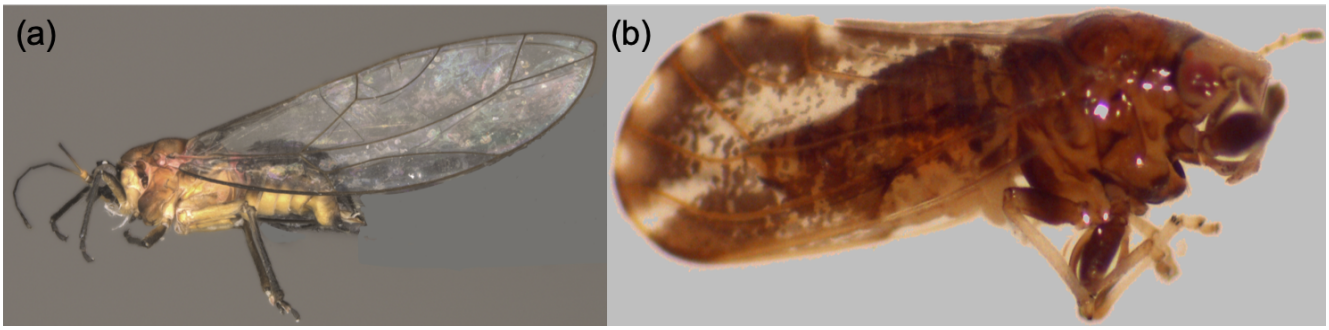

Figure 1.3. Lateral view of representative adult specimens of (a) *Trioza erytreae* (Del Guercio) and (b) *Diaphorina citri* (Kuwayama)

Symptoms

Trees infected with the Liberibacter pathogens, show mild to severe yellowing on the shoots and subsequently progressive yellowing of the entire tree. Leaves may also become thicker, leathery, and midribs and lateral veins are sometimes enlarged, swollen, and corky (Batool et al., 2007). Mottling and chlorosis are the main characteristics of leaf symptoms. The asymmetric blotchy mottle pattern distinguishes it from zinc, manganese, magnesium, calcium, and iron deficiency symptoms (Da Graça, 1991). The fruits are often underdeveloped, lopsided, show color inversion and can have a sour or bitter taste (Garnier and Bové, 1983; Akhtar and Ahmad, 1999; Jepson, 2009; ANR, 2010)

Figure 1.4 Symptoms typical of Huanglongbing disease; (a) Progressive yellowing of leaves on tree, (b) defoliation, yellowing and dieback on an orange tree, (c) severe yellowing of leaves and (d) color inversion on fruit.

Rationale

Huanglongbing is one of the most destructive diseases of citrus worldwide and currently there is still no known cure (Bové, 2006; McClean, 1970). The detection of CLas associated HLB in Ethiopia by Saponari et al, (2010) has highlighted the increased risk of spread of the disease to other citrus-producing countries in the continent. The presence of this disease in addition to the presence of CLaf associated ACG which is already widespread in Africa and causes losses ranging from 25 to 100% in Kenya and Tanzania (Tschirley et al., 2004; Swai et al., 1988), increases the threat of the collapse of the citrus industry in Africa. Furthermore, the detection of the native vector of CLas *D. citri* in Tanzania and Kenya (Shimwela et al., 2016, Rwomushana et al., 2017) increases the potential for rapid spread of the disease. However, critical information on the distribution of the Liberibacter species, the genetic diversity of the African populations of the vector, vector-pathogen interactions and their implications for the establishment and spread of HLB is limited in Africa. In addition, considering the economic importance of *D. citri* with regard to HLB transmission, research into the population structure and microbiome diversity of

the vector to provide insight into probable biological control measures using endosymbionts associated with *D. citri* is necessary.

Research aim and objectives

This study aims to identify the Liberibacter species and vectors associated with citrus greening disease in eastern Africa, establish the current and potential distribution of the Liberibacter pathogens and establish the genetic diversity of their associated vectors.

The specific objectives of this study are;

1. To identify and characterise the Liberibacters associated with citrus greening disease in Eastern Africa using molecular tools.
2. To determine current and predicted regional and global climate suitability of Liberibacter species associated with citrus Huanglongbing, using three species distribution models.
3. To unravel the genetic diversity of the greening disease vectors using microsatellite markers and complete mitochondrial genome analysis
4. To asses Microbiome Diversity, identify endosymbionts and genes for resistance to antibiotics within populations of *Diaphorina citri*

Chapter Two: Distribution of *Candidatus* Liberibacter species in Eastern Africa, and the First Report of "*Candidatus* Liberibacter asiaticus" in Kenya

1.1 Abstract

Abstract

Huanglongbing (HLB) is a serious disease of *Citrus* sp. worldwide. In Africa and the Mascarene Islands, a similar disease, known as African citrus greening (ACG) is associated with the bacterium "*Candidatus* Liberibacter africanus" (CLaf). In recent years, "*Candidatus* Liberibacter asiaticus" (CLas) associated with the severe HLB has been reported in Ethiopia. Thus, we aimed to identify the Liberibacter species affecting citrus, the associated vectors in Eastern Africa and their ecological distribution. We assessed the presence of Liberibacters in symptomatic leaf samples by a generic Liberibacter quantitative PCR. Subsequently, we sequenced the 50S ribosomal protein L10 (*rplJ*) gene region in samples positive for Liberibacters and identified the species by comparison with public sequence data using phylogenetic reconstruction and genetic distances. We detected generic Liberibacter in 26%, 21% and 66% of plants tested from Uganda, Ethiopia and Kenya, respectively. The *rplJ* sequences revealed the most prevalent Liberibacters in Uganda and Ethiopia were "*Candidatus* Liberibacter africanus subsp. clausenae" (CLafCl) (22%) and CLas (17%), respectively. We detected CLas in Kenya for the first time from three sites in the coastal region. Finally, we modelled the potential habitat suitability of CLas in Eastern Africa using MaxEnt. The projection showed large areas of suitability for the pathogen in the three countries surveyed. Moreover, the potential distribution in Eastern Africa covered important citrus-producing parts of Ethiopia, Kenya, Uganda and Tanzania, and included regions where the disease has not yet been reported. These findings will guide in the development of an integrated pest management strategy to ACG/HLB management in Africa.

Introduction

Huanglongbing (HLB) is presently one of the most destructive plant diseases affecting citrus groves worldwide (Da Graça, 1991). The disease is associated with "*Candidatus* Liberibacter asiaticus" (CLas) and "*Candidatus* Liberibacter americanus" (CLam), which are phloem-limited, fastidious, gram-negative bacteria belonging to the alpha subdivision of Proteobacteria (Jagoueix et al., 1996; Damsteegt et al., 2010). CLas is heat-tolerant and associated with the severe HLB which is transmitted by the Asian citrus psyllid *Diaphorina citri* Kuwayama (Liviidae) (Hall et

al., 2013). *Diaphorina citri* is distributed in Asia, the United States, Central America, Ethiopia and Brazil (Jagoueix et al., 1994; Halbert and Manjunath, 2004; Bruce et al., 2005; Teixeira, 2005; Li et al., 2006; Saponari et al., 2010). In addition to CLas and CLam, the citrus-infecting Liberibacter genus contains another species: "*Candidatus* Liberibacter africanus" (CLaf) (Da Graça, 1991). CLaf is heat-sensitive and is associated with African citrus greening disease (ACG) (Oberholzer et al., 1965; Garnier and Bové, 1993; Garnier et al., 2000). This pathogen is principally transmitted by *Trioza erytreae* (Del Guercio) (Triozidae), also known as the African citrus triozid (Aubert, 1987; Gottwald, 2010). Additionally, several subspecies of CLaf have been reported, including "*Candidatus* Liberibacter subsp. capensis (CLafC), "*Candidatus* Liberibacter africanus subsp. clausenae" (CLafCl), "*Candidatus* Liberibacter africanus subsp. teclae" (CLafT), "*Candidatus* Liberibacter africanus subsp. vepridis" (CLafV), and "*Candidatus* Liberibacter africanus subsp. zanthoxyli" (CLafZ) (Garnier et al., 2000; Roberts et al., 2015; Roberts and Pietersen, 2017).

Citrus is the most extensively cultivated fruit crop in Kenya (Kilalo et al., 2009; Aidoo et al., 2018). with annual production ranging from 61 to 135 metric tons between 2012 and 2016 (FAOSTAT, 2018). Citrus production provides a source of income for farmers, as well as a ready source of vitamins in diet (Aidoo et al., 2018). However, production has been on the decline in East Africa, particularly in the highland regions (Aidoo et al., 2018; Sengoba et al., 2002). Furthermore, fruit yield at the smallholder level is about 10 t/ha, far below the potential of 75 t/ha (Kilalo et al., 2009; Obukosia and Waithaka, 2000). Several biotic and abiotic factors have been responsible for the decreasing yields, with pests and diseases among the most important (Ekesi 2012). Among the diseases, ACG remains the most prevalent, particularly in the mid to high altitude areas of Eastern Africa and is primarily attributed to CLaf (Magomere et al., 2009; Kalyebi et al., 2016; Shimwela et al., 2016).

However, in the last decade, CLas was reported for the first time in Ethiopia (Saponari et al., 2010) and more recently in Uganda in 2016 (Kalyebi et al., 2016), although the reported occurrences in Uganda were subsequently shown to have been misidentifications (Roberts et al., 2017). That notwithstanding, the confirmed presence of CLas in at least one country in Eastern Africa represents a real threat to citrus production, as CLas is more heat-tolerant and adapted to the various altitudinal ranges' characteristic of the countries in this region. Furthermore, recent studies have established that *D. citri* is now established in Kenya and Tanzania (Shimwela et al., 2016; Rwomushana et al., 2017). This could potentially have even more impact than envisaged as *D. citri* possesses a superior ability as a CLas vector (Gottwald, 2010; Grafton-Cardwell et al., 2013). It is likely that with the increasing regional trade, similar climatic patterns and the presence of reservoir hosts plants, CLas could be more widespread than is currently known and

its interactions with CLaf and related subspecies is still largely unknown. Current models on the potential spread of HLB are based on suitable climate conditions for the psyllid vector *D. citri* (Aurambout et al., 2009; Gutierrez and Ponti, 2013). However, the risk of the establishment of HLB is not based solely on the distribution of the vector, because other factors such as environmental requirements may differ between the psyllid and the bacterial pathogen (Gottwald, 2010; Narouei-Khandan et al., 2016). Thus, it becomes therefore necessary to confirm the status and distribution of Liberibacter species and the subspecies in the region. Therefore, this study aimed to asses the status of HLB and ACG in three Eastern Africa countries (Ethiopia, Kenya and Uganda) by identifying the associated Liberibacter species in citrus plants and their psyllid vectors, establishing their occurrence, and determining the potential spread to other citrus-producing parts of the region.

Methods

Sample collection and DNA extraction

Field surveys were carried out for ACG, HLB and their associated insect vectors (*T. erytreae* and *D. citri*) in citrus orchards and backyard gardens in Uganda (300 sites), Ethiopia (170 sites) and Kenya (9 sites), from March 2017 to December 2018. The citrus species sampled included sweet orange (*Citrus sinensis* L. Osbeck.), lemon (*Citrus limon* L. Osbeck) and tangerine (*Citrus reticulata* Blanco). Leaf samples were collected from plants that exhibited the typical citrus greening symptoms; defoliation, mottling, twig and tree dieback, and lopsided fruit in the most severe cases. Infected leaf samples (four leaves per tree) were individually collected into plastic bags, and stored at 4°C. Psyllids encountered on infected trees were also aspirated from the trees and stored in vials with 96% ethanol for later DNA extraction. At each site where psyllids were found, 20 specimens per site were collected for screening which bacterium was present. Geographic positioning coordinates (GPS) of the sampling sites were obtained using a Garmin eTrex20 instrument (GARMIN, USA) and recorded for each site.

In the laboratory, individual psyllids and plant leaves were surface-sterilised by completely submerging the insect/leaf in a petri dish containing 3% sodium hypochlorite for three seconds and rinsing thrice with distilled water. Total DNA from individual petioles was extracted using the Isolate II Plant DNA Kit (Bioline, London, UK), while total DNA from individual psyllids was extracted using the Isolate II Genomic DNA Kit (Bioline) then eluted to a final volume of 50 µl. DNA extracts were checked for purity and concentration using a Nanodrop 2000/2000c Spectrophotometer (Thermo Fischer Scientific, Wilmington, USA). DNA extracts within the $A_{260\ nm}/A_{280nm}$ ratio range of 1.8 to 2.0 were stored at – 20°C then used in downstream processes.

Quantitative PCR assay for the generic detection of Liberibacters

Quantitative PCR (qPCR) was used to screen for the presence of generic Liberibacter in each plant and psyllid DNA extract. A 1160 bp region of a mitochondrial gene (16s rRNA) conserved in Liberibacter was targeted using the forward primer LibUF(Roberts et al., 2015; Phahladira et al., 2012) and the reverse primer HLBr (Li et al., 2006) (Appendix 7). Reactions were prepared in a final volume of 10 µl containing 0.5 pmol μl^{-1} of each primer, 2x Maxima SYBR Green/ROX qPCR Master Mix (Thermo Fischer Scientific, Wilmington, USA), and 15 ng μl^{-1} of DNA template. The assays were performed in a Stratagene MX3005P qPCR instrument (Agilent Technologies, California, USA), under the following conditions: an initial denaturation step of 10 min at 95ºC, 40 cycles of 95ºC for 30 s, 61ºC for 45 s and 72ºC for 1 min, followed by one dissociation cycle of 95ºC for 1 min, 55ºC for 30 s and 95ºC for 30 s. All assays were performed using three replicates and a negative control. Fluorescence was measured, and quantification cycle (Ct) values were determined using MxPro – Mx3005P Software (Agilent Technologies). The specificity and purity of the amplicons were determined by the dissociation curve. A threshold of Ct <31 was used as the cut-off value for the detection of generic Liberibacter as the HLB primers, are reliable at Ct <30 while at Ct >30 they are unreliable in differentiating whether the Liberibacter is present (Bao et al., 2019). Ct values were recorded for all the reactions. The amplification curves for Ct determination and the melting curves for temperature estimations at the peak of the curves were analysed using the MxPro – Mx 3005P qPCR software.

PCR amplification and Sanger sequencing for species identification of Liberibacters

Species identification was done on all samples positive for generic Liberibacter in the qPCR assays. A 650 bp region of the 50S ribosomal protein L10 (*rplJ*) gene was used in conventional PCR for the identification of the Liberibacter species CLas, CLaf, CLafCl, CLafZ, CLafC and CLafZ. The fragment was amplified using primer pair A2 and J5 (Appendix 7) (Hocquellet, 1999). Reactions were carried out in a total volume of 20 µl containing 5X My Taq reaction buffer (5 mM dNTPs, 15 mM $MgCl_2$, stabilizer and enhancer) (Bioline), 0.5 pmol μl^{-1} of each primer, 0.5 mM $MgCl_2$ (Thermo Fischer Scientific, Wilmington, USA), 0.0625 U μl^{-1} MyTaq DNA polymerase (Bioline), and 15 ng μl^{-1} of DNA template. PCR was run in a Mastercycler Nexus gradient thermal cycler (Eppendorf, Germany), using the following conditions: initial denaturation for 2 min at 95°C, followed by 40 cycles of denaturation for 30 s at 95°C, annealing for 45 s at an optimized annealing temperature of 58.7°C and extension for 1 min at 72°C, and a final extension step of 10 min at 72°C. PCR products were separated in a 1.5% agarose gel stained with 10 mg ml^{-1} ethidium bromide (Sigma-Aldrich, Gmbh, Germany). Gel bands were analysed and documented using KETA GL imaging system trans-illuminator (Wealtec Corp,

Meadowvale Way Sparks, Nevada, USA). PCR products were purified using Isolate II PCR and Gel Kit (Bioline) following the manufacturer's instructions. The purified PCR products were bi-directionally sequenced by Macrogen Inc Europe Laboratory, The Netherlands, using the forward and reverse PCR primers. Forward and reverse sequences for each sample were trimmed to remove primer regions and assembled to obtain a consensus using BioEdit v7.2.5 (Hall, 1999). All new sequences were deposited in GenBank (accession numbers MK542517- MK542519).

Liberibacter sequence analyses

Sequence identity was determined for all sequences using Basic Local Alignment Search Tool (BLAST). Multiple sequence alignments for phylogenetic reconstruction and estimates of pairwise genetic distances were performed using MAFFT (Katoh and Standley, 2013) in Geneious Prime version 2019.0.4. (https://www.geneious.com).

Phylogenetic reconstruction for the representation of the patterns of evolutionary divergence included all sequences generated in this study and 144 additional sequences of Liberibacter species available in GenBank (Appendix 8), with *Candidatus* Liberibacter solanacearum as an outgroup. Public sequences shorter than 650 bp, containing nucleotide ambiguities, and non-overlapping with the *rplJ* region were excluded from downstream analyses. To avoid excessively dense trees in the genetic clustering analyses, duplicate haplotypes in the public sequences were identified and deleted using Geneious, and only one sequence per species was used as a representative. Maximum-likelihood (ML) trees were reconstructed using the Tamura-Nei model (Tamura and Nei, 1993) implemented in MEGA X (Kumar et al., 2018). Branch support was estimated by 1,000 bootstrap replicates.

Intra and interspecific sequence divergence were calculated using the uncorrected p-distance model in MEGA X. Standard errors were obtained using 1,000 bootstrap replicates. All the new and publicly available sequences were used, and duplicate sequences were not removed. Multidimensional scaling analysis was carried out using the 'cmdscale' function in R software version 3.5.1 (R Development Core Team, 2008) on the genetic distance matrix to generate the plot for principal coordinate axis (PCoA). The R code is publicly available at https://github.com/InusaJacob/Principal-Coordinate-axes.

Predicted distribution HLB in Eastern Africa

The potential distribution of CLas and the high-risk areas for HLB in Eastern Africa were predicted using the Maximum Entropy (MaxEnt) model (Phillips et al., 2006). Both the bacteria and its vector (*D. citri*) were modelled individually and the resulting risk maps were overlaid to

get a consensus map of the potential distribution of HLB in Eastern Africa. In addition to the results of the current survey, reports of HLB and *D. citri* occurrence were obtained from the CABI Invasive Species Compendium (CABI 2018). All points positive for CLas from the current study areas were excluded from the presence points and added to the background points used in the model to avoid sampling bias. Environmental predictors used for the modelling of CLas and *D. citri* included 19 bioclimatic variables for the current baseline average (1950–2000) acquired from the WorldClim database (http://www.worldclim.org/). For each model, presence locations (occurrence data) were compared against background points to avoid model overfitting of spatially clustered presence points, and inability to predict spatially independent data. We used 75% of the presence data to train the model, and 25% for model validation. The models were run with 5,000 iterations and >10,000 background points. The Area Under the Receiver Operator Curve (AUROC) was used to validate the performance of each model. AUC values above 0.5 connote sites with high predicted suitability. To obtain a consensus of the two models, we rescaled the raster outputs from the individual models to uniform values between 0 and 1. We combined the individual models weighted by their AUC scores, subtracted 0.5 and squared the results to give further weight to the higher AUC values, thus obtaing the weighted average. Finally, we made a Raster Stack of our individual model predictions and computed the average. All models were run in Maxent version 3.3.3k, and the data was exported as ASCII files for enhanced visualization with QGIS software version 2.18.1. (QGIS development team, 2016)

Results

Presence of citrus greening disease and psyllid vectors

Fields were monitored in Uganda (300 sites), Ethiopia (170 sites) and Kenya (9 sites). Symptoms typical of citrus greening disease were encountered at study sites in all three countries surveyed and included yellowing, galls and vein degeneration of leaf veins, while dieback was observed in trees with severe disease progression (Appendix 1). Infected trees which were subsequently shown to be CLaf-infected showed milder yellowing on the leaves and in most cases, infected leaves were observed on one side of the tree. In cases where CLas was detected, the leaf symptoms were more severe and encompassed the entire tree. The survey covered altitudes ranging from lowlands (<1000 m.a.s.l), midlands (1000 -1500 m.a.s.l) to highlands (>1500 m.a.s.l.) (Appendix 5). In Ethiopia, HLB symptoms were not seen at low altitudes (<1000 m; Oromia region) but were found at high altitudes (1,876 – 2,116 m; Gondar region). Greening disease symptoms were found in 26% of the Ugandan sites, 20.6% of the Ethiopian sites and 66.6% of the sites surveyed in Kenya. (Fig. 2.1a). *Trioza erytreae* was found at 10 sites in Uganda and seven sites in Ethiopia, but not in any of the sites in Kenya. Conversely, *D. citri* was found at all sites in Kenya at the time of the survey, but not in Uganda or Ethiopia (Fig. 2.1b).

Detection of Liberibacter generically by qPCR

The presence of generic Liberibacter in the plant and insect samples collected in Uganda, Ethiopia and Kenya was assessed by qPCR . All samples had the same melting peak as the positive control (Appendix 2). Generic Liberibacter was detected in 78 plant samples collected in Uganda (26%), 35 plant samples in Ethiopia (21%), and six plant samples in Kenya (66%) (Fig. 2.1c). Liberibacter was also detected in adult *T. erytreae* collected in Uganda (five sites) and Ethiopia (five sites), and from adult *D. citri* collected in Kenya (three sites) (Fig. 2.1d).

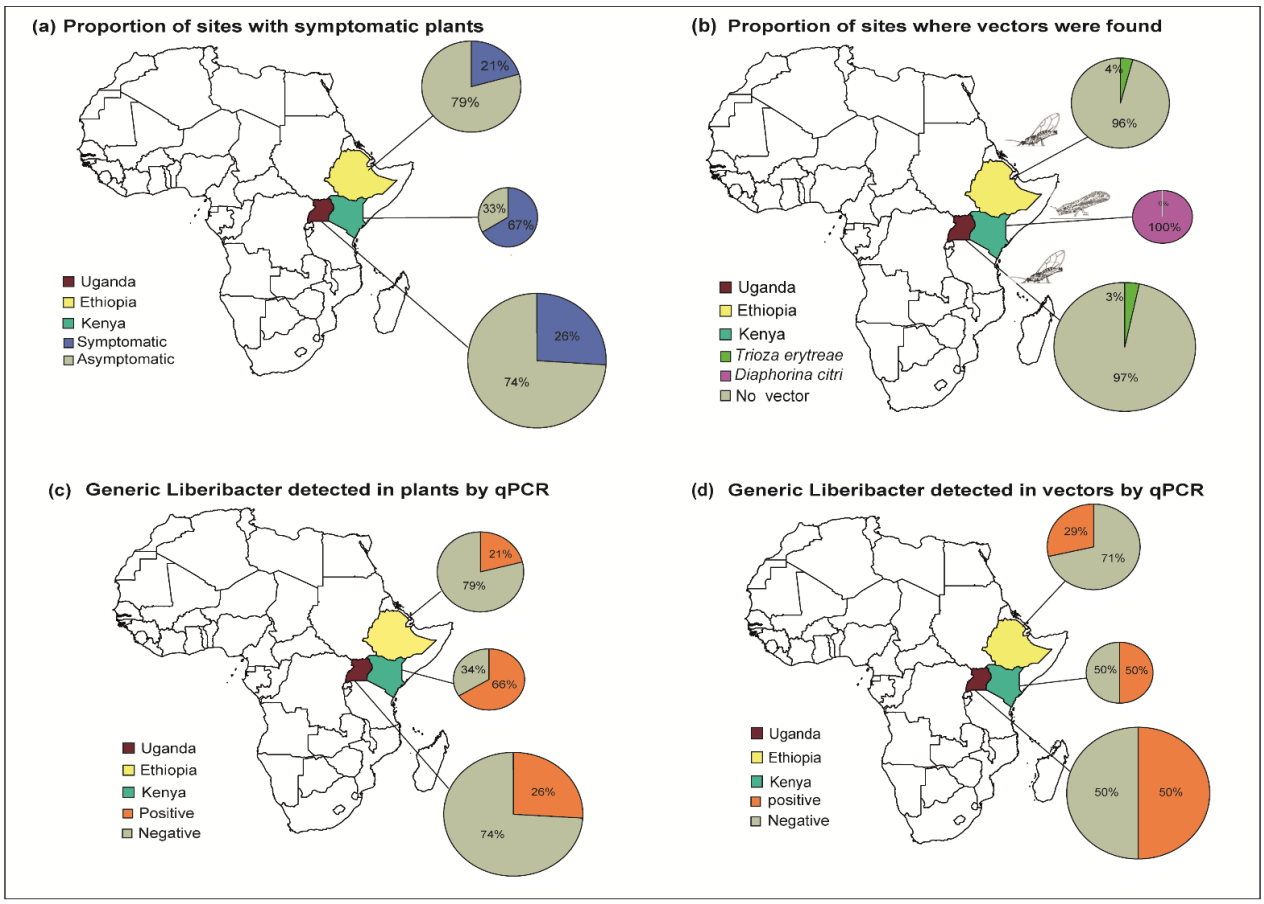

Figure 2.1. Presence of citrus greening disease symptoms, *Candidatus* Liberibacter species and psyllid vectors, from the survey of citrus in Uganda, Ethiopia and Kenya. (a) Proportion of sites where symptomatic trees were found, (b) Proportion of sites where the insect vectors *Trioza erytreae* and *Diaphorina citri* were found, (c) Generic Liberibacter detected in plants by qPCR, and (d) Generic Liberibacters detected in vectors by qPCR. The size of the pie charts is proportional to the total number of sites surveyed.

Identification of Liberibacter species using Sanger sequencing

PCR amplifications consistently resulted in the expected product size (approx. 650 bp) from all samples positive for generic Liberibacter in the qPCR assays. BLASTn analyses showed high homology of the new sequences with publicly available CLas, CLaf and CLafCl sequences. In Uganda, 66 sites (22%) were positive for CLafCl, while 12 sites (4%) were positive for CLaf (Fig. 2.2). The sequences showed high homology (up to 99% identity) with publicly available CLafCl and CLaf sequences. In Ethiopia, 29 sites (17%) were positive for CLas, 15 sites (9%) for CLafCl, and one site (1%) for CLaf (Fig. 2.2a), and the sequences showed high homology with publicly available CLas, CLaf and CLafCl (all 100%) sequences. In Kenya, three sites (33%) were positive for CLas and three sites (33%) for CLafCl. The sequences showed high homology with publicly available sequences for CLas (100%) and CLafCl (99%). The spatial distribution of the species showed that CLaf and CLafCl occurred together in the western region in Uganda, with CLafCl the only species in the eastern region (Fig. 2.3). In Ethiopia, CLafCl

(75%), CLas (25%) and CLaf (4%) occurred in the Gonder region while only CLas was found in Tigray and Wollo regions. In Kenya, CLas was present at the Coastal region, while CLafCl was found in the western region.

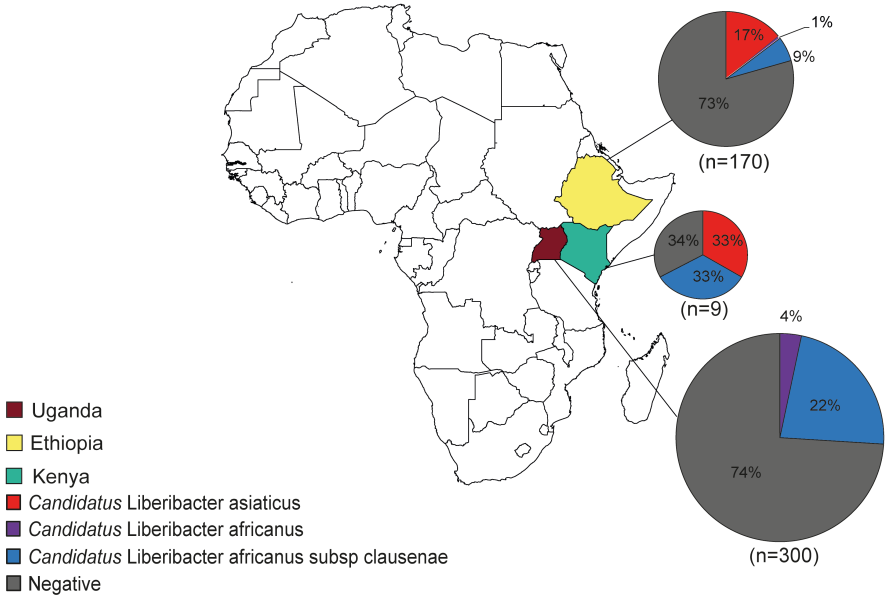

Figure 2.2. Proportion of *Candidatus* Liberibacter species identified from sampled sites in Uganda, Ethiopia and Kenya. The size of the pie charts is proportional to the total number of sites surveyed.

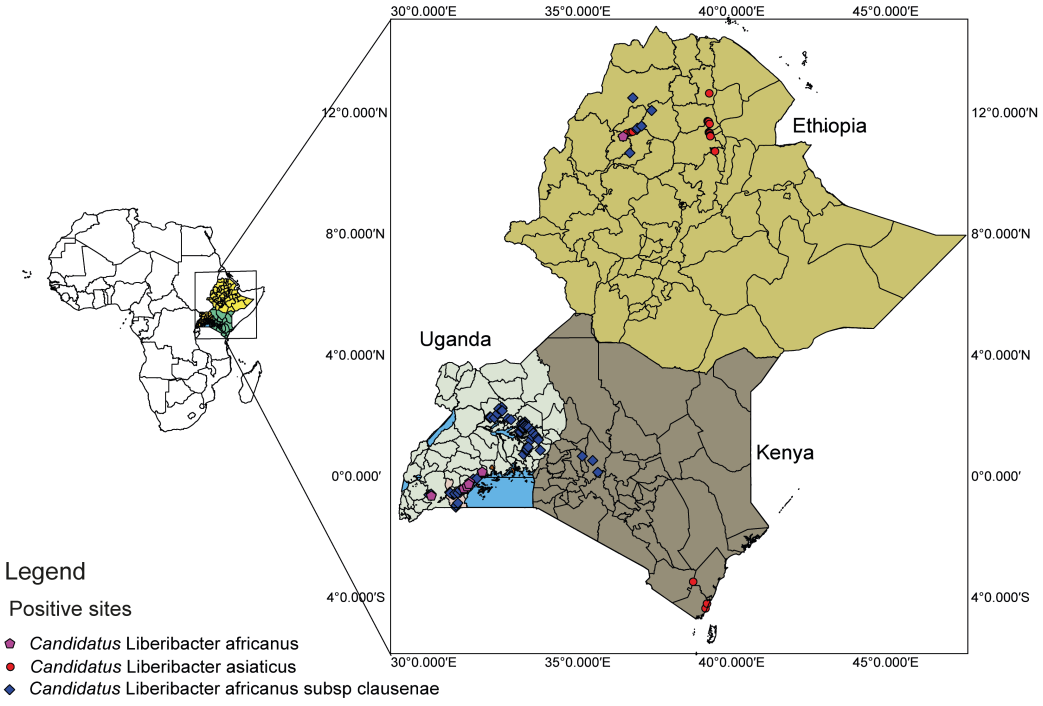

Figure 2.3. Distribution of *Candidatus* Liberibacter species in Uganda, Ethiopia and Kenya, showing the sampling sites positive for each *Candidatus* Liberibacter species.

Identification of Liberibacter species found in Uganda, Ethiopia and Kenya

A Maximum Likelihood tree was built using the sequences obtained in this study combined with representative sequences available in GenBank to assess the phylogenetic and phylogeographic structure of the *rplJ* sequences (Fig. 2.4). The tree topology indicated that all new sequences were identical to either CLas, CLaf or CLafCl, and no other known Liberibacter species were found. The new sequences from Ethiopia clustered in three distinct clades: one clade with CLas, one clade of CLaf, and one clade of CLafCl. The sequences from Kenya clustered in two clades: one clade with CLas, and another formed by CLafCl. The new sequences from Uganda clustered in two clades: one clade including publicly available CLaf sequences, and another formed by CLafCl (Fig. 2.4). Separate trees were constructed for each country (Appendix 3).

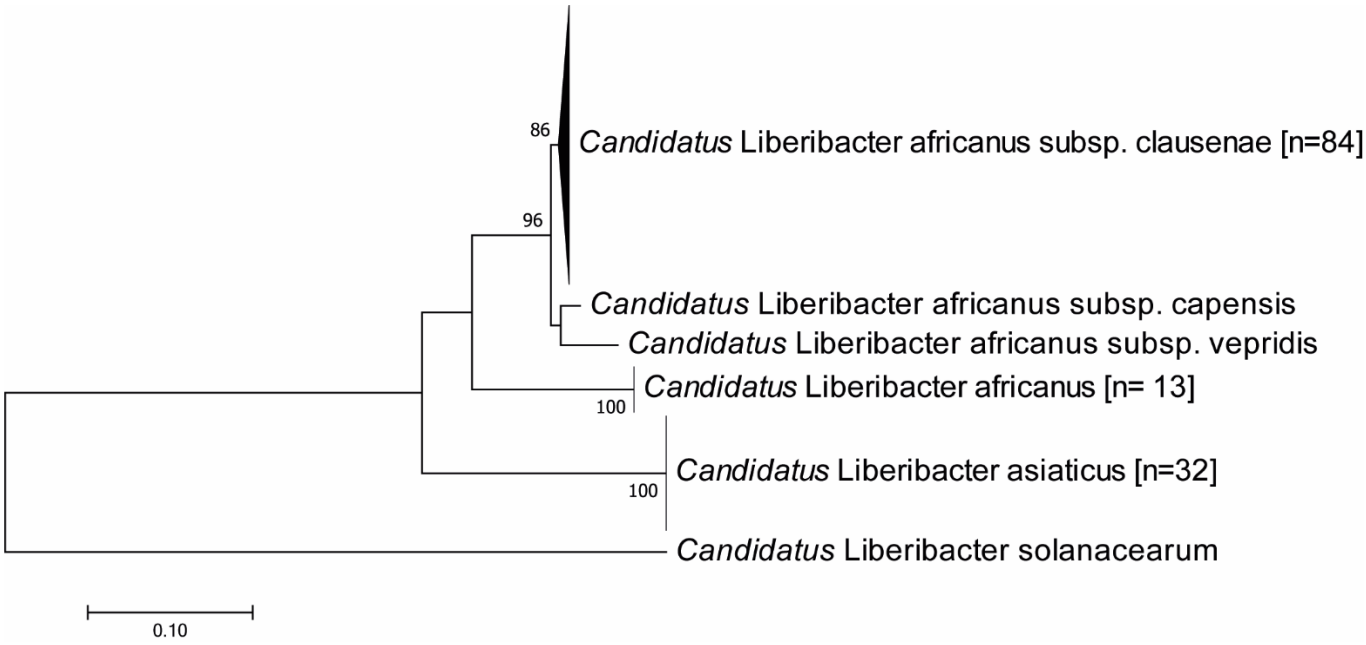

Figure 2.4. Maximum-Likelihood tree based on a 650 bp alignment of 129 *Candidatus* Liberibacter sequences of the 50S ribosomal protein L10 (*rplJ)* gene from symptomatic citrus samples collected from Ethiopia (n = 45), Kenya (n = 6) and Uganda (n = 78), and other Liberibacter sequences available in GenBank (n = 6), with *Candidatus* Liberibacter solanacearum as an outgroup. The number of Liberibacter sequences obtained in this study is indicated in square brackets. Branchsupport was based on 1,000 bootstrap replicates.

Genetic distance analyses for the Liberibacter species identification included 129 new sequences and 144 publicly available sequences (Appendix 8). For CLaf and CLafCl, no difference was found between the new sequences and the sequences available on GenBank, as only one haplotype was found for each species (Appendix 6). All new CLas sequences were identical to one of the four haplotypes previously found for CLas (Appendix 4). Interspecific genetic distances showed that CLas/CLaf was the most diverged pair (23.23%) (Table 2.1). CLas was similarly diverged from CLafV (22.32%), CLafC (20.51%) and CLafCl (20.33%). CLaf had slightly lower distances from CLafCl (15.43%), CLafC (16.88%) and CLafV (16.88%). The

lowest divergences were found between the pairs CLafC/CLafV (4.36%), CLafCl/CLafV (3.81%) and CLafCl/CLafC (2.72%). The PCoA plot based on genetic distances among all Liberibacter showed overlap of the new and publicly available CLaf, CLafCl and CLas sequences, and evidenced the divergence of between CLas, CLaf, and the cluster comprising CLafCl, CLafC and CLafV (Fig. 2.5).

Table 2.1. Interspecific mean uncorrected p-distances (%) for *Candidatus* Liberibacter species and subspecies: CLas – "Candidatus Liberibacter asiaticus", CLaf – "*Candidatus* Liberibacter africanus", CLafCl – "*Candidatus* Liberibacter africanus subsp. clausenae", CLafC – "*Candidatus* Liberibacter africanus subsp. capensis" and CLafV – "*Candidatus* Liberibacter africanus subsp. vepridis". Distances were calculated based on a 649 bp alignment of 273 new and publicly available sequences. Standard error estimates are shown above the diagonal. * - Sequences from this study combined with publicly available sequences

	CLaf*	CLafC (GenBank)	CLafCl*	CLafV (GenBank)	CLas*
CLaf*	-	0.016	0.015	0.015	0.017
CLafC (GenBank)	16.88	-	0.007	0.008	0.017
CLafCl*	15.43	2.72	-	0.008	0.017
CLafV (GenBank)	16.88	4.36	3.81	-	0.018
CLas*	23.23	20.51	20.33	22.32	-

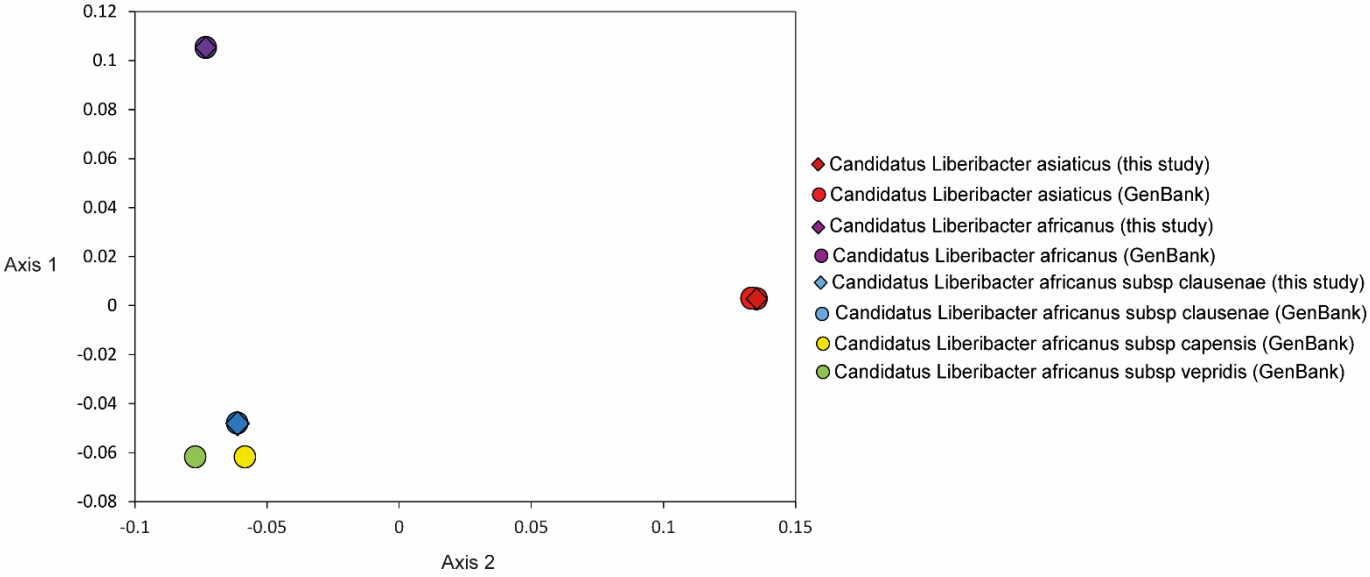

Figure 2.5. Principal Coordinate Analysis (PCoA) plot representing the genetic distances among Liberibacter sequences (n = 129) from Ethiopia, Kenya, Uganda, and publicly available sequences available in GenBank (n = 144) based on the ribosomal protein L10 (*rplJ*) gene computed using the classic multidimensional scaling function 'cmdscale' in R version 3.5.1.

Potential distribution of CLas in Africa

The modelling of the potential distribution of CLas resulted in an AUC value for the current distribution of 0.76125, and the distribution of *D. citri* resulted in an AUC value of 0.84332, indicating a good fit of the prediction in relation to the datasets used. The consensus model showed a potential distribution for HLB covering most of the citrus-producing areas of Eastern Africa. Large areas of optimum potential distribution of HLB were predicted in Ethiopia including Tigray, Gonder, Dire Dawa, Awasa and Jimma, whereas most parts of Uganda showed marginal suitability. The predicted distribution of HLB in Kenya covered the coastal, western and central regions including the areas surveyed (Lunga-Lunga, Matuga and Awasi), while large areas of northern Kenya were predicted to be unsuitable. Large areas of Tanzania showed marginal to optimal suitability for HLB including Arusha, Morogoro, Tanga and Dar es Salaam. The islands of Zanzibar also showed high suitability for this pathogen (Fig. 2.6).

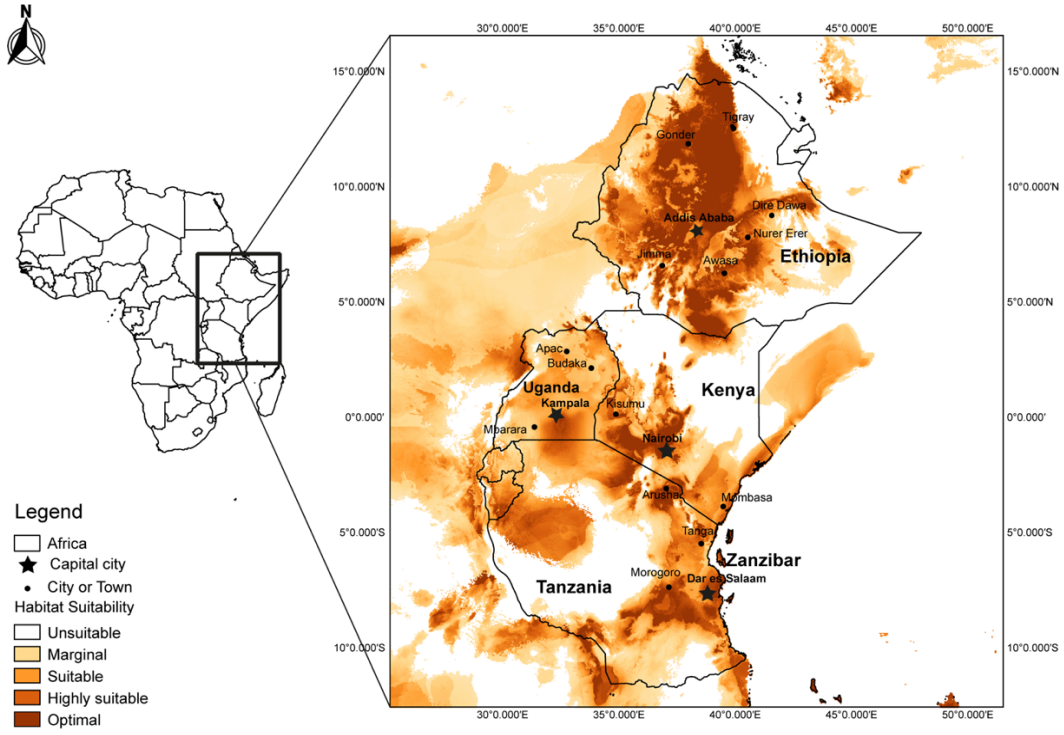

Figure 2.6. Potential distribution of the Huanglongbing associated with "*Candidatus* Liberibacter asiaticus" in Eastern Africa, as predicted from the current occurrence locations using global 50-year climate data with MaxEnt.

Discussion

In this study, we assessed the distribution of Liberibacter species in three Eastern African countries, as well as determined the potential spread of CLas in the region. Mild to severe symptoms of citrus greening disease were encountered in different citrus growing agro-ecologies across a range of altitudes from low to high altitude regions in Ethiopia, Kenya and Uganda.

Furthermore, HLB symptoms in the Ethiopian highlands appeared to be severe, in contrast to reports that they are less pronounced and disappear above 1,500 m (Aubert, 1987). These symptoms were observed in the absence of the vector *D. citri.* In Uganda, symptomatic plants in the Eastern region presented severe symptoms akin to the HLB infected plants observed in Ethiopia, but we identified the pathogen as CLafCl. Citrus plants in the western region, which were infected by CLaf, had milder symptoms typical of ACGD.

Trioza erytreae adults were found on citrus trees in Ethiopia and Uganda, while *D. citri* adults were found in Kenya. In the three countries, both insect species tested positive for generic Liberibacter. Previous studies have postulated the probable transmission of CLas by *T.* erytreae (Da Graça, 1991; Van de Merwe and Andersen, 1937; McLean and Oberholzer, 1965; Aubert et al., 1988). Furthermore, previous studies experimentally determined that *T. erytreae* and *D. citri* could both transmit ACG (associated with CLaf) and HLB (associated with CLas) (Massonie et al., 1976; Lallemand et al., 1986), although *D. citri* was the more effective vector for HLB. The detection of CLas in field populations of *T. erytreae* in a previous study (Ajene et al., 2019) suggests that this species has the potential for also transmitting HLB, particularly to citrus groves at the mid to higher altitude areas of Eastern Africa. Rwomushana et al., (2017) have also reported a niche overlap between *D. citri* and *T. erytreae*, which is likely to result in *T. erytreae* picking up HLB from lower-lying areas and potentially spreading it alongside ACG at the mid-altitude areas whose conditions are suitable for this disease. We as yet have no evidence if HLB and ACG can co-exist on the same citrus plant, and we propose further studies to understand the epidemiology of citrus greening in the midst of both pathogens. The risk of spread of HLB to Tanzania also remains high due to the recent invasion of *D. citri* in the country (Shimwela et al., 2016).

The detection of low concentrations of Liberibacter in asymptomatic plants has been problematic even with sensitive diagnostic methods (Manjunath et al., 2008). In Florida, for example, the detection of the pathogen from psyllid vectors is commonly reported long before the detection from the plants (Manjunath et al., 2008). Although the quantity of the CLas detected in citrus material was generally low in the Kenyan samples, the Liberibacter was unambiguously identified in plants and vectors.

Phylogenetic relationships and genetic divergence within and between Liberibacter groups were assessed to assist in species identification, as these methods have proven useful provided that the groups under consideration are well represented in the reference dataset (Hebert et al., 2003; Ross et al., 2008; Powell et al., 2018). Publicly available sequences identified as CLas, CLaf, CLafCl, CLafC and CLafV provided references for the identification of the new sequences. Our

sequences formed a monophyletic cluster with sequences publicly available CLas, CLaf and CLafCl.

No intraspecific divergence of the *rplJ* gene region was found in CLaf or CLafCl, as the new sequences were identical to previously reported sequences. For CLas, the publicly available sequences comprised four haplotypes, with the most frequent haplotype found in the Americas and Asia. The remaining haplotypes were unique to Oman, India and China, respectively. The new CLas sequences were identical to the most frequently occurring haplotype. The intraspecific genetic divergence of CLas was less than 0.07%, thus supporting correct species identification of all public and new CLas sequences. Interestingly, interspecific comparisons showed low genetic divergence between CLafCl, CLafC and CLafV (average = 3.63%). These Liberibacter are currently classified as subspecies of CLaf and were recovered as a group separated from CLaf in the maximum likelihood (ML) analysis. Additionally, the average genetic divergence between CLaf and the cluster CLafCl/CLafC/CLafV (16.40%) was only slightly lower than the average between CLas and the cluster CLafCl/CLafC/CLafV (21.59%). This suggests that the sequences CLafCl, CLafC and CLafV could be different haplotypes representing the same species. Therefore, further analyses will be necessary to establish the species status of this genetic group. Future whole-genome comparisons among Liberibacter will contribute to clarify the relationships among CLaf and the haplotypes currently classified as its subspecies.

We identified both CLaf and CLafCl in Uganda; the two Liberibacter previously found to be widely distributed in the citrus-growing areas in the western and central regions of the country (Roberts et al., 2017). In our study, CLafCl was dominant in the eastern region of the country where Las had been previously misreported (Kalyebi et al., 2016). Our results support the hypothesis that the previous record of CLas in Uganda was probably a misidentification (Roberts et al., 2017) therefore, the presence of CLas in Uganda remains unconfirmed. On the contrary, our survey in Ethiopia showed that, in addition to CLafCl, CLas was also widely distributed in the citrus-growing areas of the Amhara region. Our survey in Kenya covered relatively fewer sites than in the other countries; however, we found CLas both in citrus plants and in the insect vector *D. citri* in the coastal region. In the western and central parts of the country, we only identified CLafCl, as previously reported (Rasowo et al., 2019). Overall, our survey confirms that CLas is present in Kenya and that the distribution of CLafCl in Uganda and CLas in Ethiopia is much more widespread than previously described (Saponari et al., 2010; Roberts et al., 2017).

Vector-based modelling has been the usual practice for establishing the distribution of HLB. However, a consensus model of the vector and pathogen will give a more robust view of the potential distribution of the disease. Environmental and climate data, including monthly

temperature and rain, are assumed to reflect the climate suitability for the growth and development of different organisms, including plant pathogens (Hijmans et al., 2005). Ecological factors such as; temperature, light and water availability, soil fertility, methane and CO_2 concentration can have varying effects disease development, as pathogens show different responses to these factors (Velásquez et al., 2018). Precipitation and soil moisture have a crucial effect on plant disease establishment, because, most plant diseases are favored by conditions of rain and high air humidity (Velásquez et al., 2018). Temperature is also a key factor in the development of plant diseases, has a significant effect on vector-borne pathogens like CLas, CLaf and Banana bunchy top virus (BBTV) transmitted by *Pentalonia nigronervosa* and influences the incidence and severity by affecting the vector (Robson et al., 2007).

The ensemble approach to HLB distribution carried out in this study indicated large areas of optimum habitat suitability for the pathogen in Ethiopia, including the areas where the disease was detected in our study, as well as the areas where it has previously been reported (Saponari et al., 2010; Narouei-Khandan et al., 2016). It also showed areas of habitat suitability in other citrus-producing areas of the country such as Nura-Hera, Awasa, Jimma and Dire Dawa where the disease has not yet been detected. The model showed marginal suitability for CLas in eastern Uganda, the major citrus-producing region of the country. Large areas of Tanzania ranged from marginal to optimal suitability for the pathogen, and the regions where *D. citri* has been detected (Rwomushana et al., 2018) were highly suitable. Likewise, the island of Zanzibar, where *D. citri* is present, showed high suitability for the pathogen. The coastal and western regions of Kenya, where citrus production is high, showed optimum suitability**.** The previous detection of *D. citri* in these regions (Rwomushana et al., 2018) and, the subsequent detection of CLas in our survey suggests an increased risk of spread of the disease to the citrus producing parts of the central region of Kenya. Kobori et al. (2011) reported that adult *D. citri* hardly move after finding a suitable host, they can potentially disperse for at least 2 km within 12 days (Lewis-Rosenblum et al., 2015). Further efforts by phytosanitary authorities are therefore recommended towards preventing further spread of *D. citri* to suitable areas in neighbouring Uganda where this vector was absent.

The spread of CLas depends, not only on climate suitability, but also on the presence/absence of the vectors (*D. citri* and *T. erytreae*) (Roberts et al., 2017). Additionally, human-mediated activities such as movement of infected plants and use of infected budwood have been implicated in the long-distance transmission of HLB (Manjunath et al., 2018; Halbert et al., 2012; Islam et al., 2012). Therefore, phytosanitary and quarantine measures need to be implemented particularly in countries where the pathogen is not yet present and included in integrated management strategies. Considering the potential ability of *T. erytreae* to transmit

CLas, the monitoring and detection of the vector is now of utmost importance for successful management. An integrated strategy involving the systematic destruction of infected trees and effective psyllid control should be deployed to stem the spread of the disease.

Despite the increasing knowledge on the complex of bacteria causing citrus greening disease in Ethiopia, Kenya and Uganda, the genetic diversity of the vector populations in both countries remain unknown. Some citrus psyllid populations may have inherently differential ability to transmit citrus greening disease, and certain types and strains of Liberibacter may be inherently more transmissible than others[6]. Therefore, research to unravel the population genetic structure of the citrus psyllids in different agro-ecological zones of the region needs to be carried out to inform the integrated pest management approaches for citrus greening disease in Africa.

The HLB threat to the citrus industry in Africa is clearly increasing. This study showed that the CLas pathogen associated with HLB is widespread in Ethiopia and present in other regions of the country far dispersed from previously surveyed areas. We also report the presence of CLas in Kenya for the first time, suggesting that there is an increased risk for the geographical spread of HLB further afar on the continent. Our modelling of the potential distribution of HLB highlights the high risk of disease spread to areas previously deemed unsuitable. We found Las thriving at higher -altitude regions with cooler temperatures in Ethiopia and the warm climate regions of Kenya; therefore, the spread of HLB is presently more evident. Our study highlighted the dominance of CLaf distribution in Uganda and the potential spread of HLB to other citrus-producing parts of East Africa. We recommend that urgent measures need to be put in place to halt the further spread of the disease in other neighbouring areas, including strict phytosanitary measures particularly for citrus seedlings and propagations.

Chapter Three: Habitat Suitability and Distribution Potential of Liberibacter Species ("*Candidatus* Liberibacter asiaticus" and "*Candidatus* Liberibacter africanus") associated with Citrus Greening disease

Abstract

This study sought to quantify current and predict future distribution of the citrus greening pathogens "*Candidatus* Liberibacter asiaticus" (CLas) in Africa and "*Candidatus* Liberibacter africanus" (CLaf) globally. Three species distribution models (MaxEnt, BIOCLIM and Boosted Regression Trees) were used to predict the current and future potential distribution of CLas in Africa, and the potential global distribution of CLaf, using long-term bioclimatic variables. Two climate change scenarios (moderate and extreme) were employed to determine how future climate alterations may affect the potential distribution of CLas in Africa. Occurrence of HLB from global reports of CLas, as well as the new positional points obtained in this survey were used to predict the habitat suitability of the pathogen in Africa, while the presence of CLaf were used to predict the global habitat suitability. Testing data comprised 25% of the presence only points. Consensus of the three models predicted a potential distribution of CLas in large areas of Western, Eastern and sub-Saharan Africa. North Africa was mostly unsuitable for CLas, except for the northern fringes. The potential distribution of CLaf included South and Central America, Asia and Australia. In Europe, the United Kingdom and the Iberian Peninsula showed marginal suitability for CLaf. The projections under the future climate change scenarios showed an increase in the hotspots under the extreme scenario. This study highlights the potential establishment and distribution in Africa of CLas-associated Huanglongbing disease, and globally for CLaf-associated with African citrus greening disease. The ensemble modelling approach for the distribution of plant pathogens is a valuable tool for the development of strategies for crop protection. These results constitute an early alert for citrus-producing regions that should inform

strategies for surveillance and preventive management against the invasion and spread of this destructive disease.

Introduction

Citrus is an economically important crop with annual production estimates standing at over 122 million metric tons of fruits from the top producing countries (Brazil, USA and China) (Mendonça et al., 2017). A significant portion of economic losses in citrus production in Africa, Asia and the American continent is attributed to Huanglongbing (HLB) (Krishna, 2015). HLB is associated with the phloem-limited bacterium *"Candidatus* Liberibacter asiaticus" (CLas) (Gottwald, 2010) occurring in Asia and the Americas, and recently reported in Africa (Saponari et al., 2010). In addition to the CLas-HLB association, there are two other citrus-infecting Liberibacter species: "*Candidatus* Liberibacter americanus" (CLam) and *"Candidatus* Liberibacter africanus" (CLaf). CLaf, which causes African citrus greening disease (ACG), is widespread in Africa, where a number of subspecies have been reported recently including *"Candidatus* Liberibacter africanus subsp. clausenae" (CLafCl), *"Candidatus* Liberibacter africanus subsp. capensis" (CLafC), *"Candidatus* Liberibacter africanus subsp. tecleae" (CLafT), *"Candidatus* Liberibacter africanus subsp. vepridis" (CLafV), and *"Candidatus* Liberibacter africanus subsp. zanthoxyli" (CLafZ) (Roberts et al., 2015). CLaf is transmitted by the African citrus psyllid *Trioza erytreae* (del Guercio), and usually occurs in cool highland regions, mostly above 900 meters above sea level (Narouei-Khandan et al.,2016). In contrast, CLas is transmitted by the Asian citrus psyllid *Diaphorina citri* Kuwayama and is more heat-tolerant and can withstand temperatures of 30 to 35 °C (da Graça & Korsten, 2004). All citrus species and cultivars have been reported to be susceptible to infection by CLas, which also infects some related plant genera such as *Murraya* and *Clausena* (Manjunath et al., 2008; Halbert et al., 2012). Dispersal takes place by movement of and feeding of infective adult psyllids and transportation and planting of infected nursery citrus stock or use of infected budwood (Lopes & Frare, 2007; Gottwald, 2010), with the latter being the most important factor in the long-distance dispersal of HLB and hitch-hiking of the vector (Halbert et al., 2010; Halbert et al., 2012; Narouei-Khandan et al., 2016). Trees infected with the Liberibacter pathogens, show mild to severe yellowing on the shoots and subsequently progressive yellowing of the entire tree (Batool et al. 2007). Leaves may also become thicker, leathery and midribs and lateral veins are sometimes enlarged, swollen, and corky (Batool et al., 2007). Mottling and chlorosis are the main characteristic leaf symptoms. The fruits are often underdeveloped, lopsided, show color inversion and can have a sour or bitter taste (Garnier and Bové 1983; Akhtar & Ahmad 1999; Jepson, 2009; ANR, 2010). Ultimately the infected tree dies as there is currently no treatment for infected trees and all commonly grown citrus varieties are susceptible to the disease (Li et al.,

2019). This will lead to a decline in the production and subsequent collapse of the citrus industry in the region.

Presently, Huanglongbing has been reported in 44 countries in the Americas and Asia (CABI/EPPO, 2017). The first report of HLB on the African mainland was in Ethiopia (Saponari et al., 2010). African citrus greening disease on the other hand, has been reported only in 19 countries within Africa since the 1920's (McClean & Oberholzer, 1965; Massonié et al., 1976; Buitendag & von Broembsen 1993; CABI/EPPO, 1998; EPPO, 2014; Roberts et al., 2017; Rasowo et al., 2019).

Currently, the habitat suitability for Liberibacter infection in Africa is poorly known. As a consequence, the design of spatially-explicit management strategies to minimise losses in the citrus industry is challenging. Africa is an ecologically diverse continent with great diversity of agro-ecological zones varying in natural resources and land use patterns, which could lead to differences in the habitat suitability of Liberibacter in the continent. Generally, the distribution of species is significantly affected by climate change (Kerr, 2001), but no studies have assessed the role of climate change in the current and future suitability and distribution of Liberabacter in Africa.

Few risk assessment models are available currently for predicting the potential establishment of HLB (Gutierrez & Ponti, 2013), despite a call for predictive global mapping of the disease fifteen years ago (da Graça & Korsten, 2004). Most available models on the potential spread of HLB are based on suitable climate conditions for the psyllid vector *D. citri* (Aurambout et al., 2009; Gutierrez & Ponti, 2013; Torres-Pacheco et al., 2013). However, the risk of the establishment of HLB is not based solely on the distribution of the vector, because other factors such as environmental requirements may differ between the psyllid and the bacterial pathogen (Gottwald, 2010; Narouei-Khandan et al., 2016).

Species distribution models are important tools for investigating the potential impacts of climate change on the distribution of species (Wiens et al., 2009). These models are employed to project potential future changes in the geographic ranges of species (Gritti et al., 2006; Barrows et al., 2010), estimate rates of extinction (Williams, Bolitho & Fox, 2003; Thomas et al., 2004), examine the efficacy of existing reserve systems (Tellez-Valdes & Davila-Aranda, 2003; Araujo, Cabeza, Thuiller, Hannah & Williams, 2004), and help to prioritize biodiversity conservation efforts (Pyke, Andelman & Midgley, 2005). Emissions scenarios represent probable futures and are used in species distribution predictions (Rosentrater 2010; Weaver et al., 2013; Porfirio et al., 2014). They comprise of representative concentration pathways (RCPs) which are scenarios that describe alternate trajectories for carbon dioxide emmissions and the resulting atmospheric concentration from the year 2000 to 2100. Four representative concentration pathway scenarios

(rcp2.6, rcp4.5, rcp6 and rcp8.5) have been selected for climate modelling. The moderate scenario (rcp4.5) is a stabilization scenario where total radiative forcing (the difference between sunlight absorbed by the earth and energy radiated back to space) is stabilized shortly after the year 2100, without overshooting the long-run radiative forcing target level (Clarke et al., 2007; Wise et al., 2009). The extreme scenario (rcp8.5) is characterized by continuous rapid increase in concentrations of atmospheric carbon dioxide reaching 950 ppm by the year 2100, and continued increase for another 100 years (Riahi et al., 2007). Representative concentration pathways are useful in species distribution modelling, as they aid in clarifying future climate scenarios and their impact on distribution range and the suitable habitat of species based on possible future greenhouse gas emission trajectories (Chhetri et al., 2018). The use of the moderate and extreme scenarios in this study seek to establish a wide prediction range on effects of change in climate on species distribution whilst being realistic on the current global climatic trends. The use of the moderate and extreme scenarios in this study seeks to establish a wide range for predicting the effects of change in climate on species distribution whilst being realistic about the current global climate trends.

As a vector-borne plant pathogen, the *Candidatus* Liberibacter species resides mainly in the plant tissue. Therefore, the presence of the host plant under a particular bioclimatic condition will almost certainly mean the probable survivability of the Liberibacter species. Furthermore, the habitat suitability of certain bacterial species has been shown to be influenced by bioclimatic conditions for example; Stream ecosystem specificities related to the climatic and biogeochemical context can influence the microbial colonization (Sabater et al., 2008). The hydrological regime, nutrient content, temperature conditions, and biological interactions depend on the climate (Sabater et al., 2008). Bioclimatic conditions have also been shown to influence the abundance of the bacterial microbiome in amphibian microbiome (Kueneman et al., 2019). Thus, our approach seeks to provide an alternative method for surveillance purposes in addition to vector surveillance since non-vector transmission (human-mediated) is also a factor in the spread of the pathogen.

This study aimed to quantify the current and predict the future habitat suitability and distribution of CLas in Africa under different climate change scenarios, and to identify hotspots of habitat suitability of CLas using consensus models. We also aimed to quantify the current and predict the future global habitat suitability of CLaf to establish the potential worldwide distribution and risk of spread of African citrus greening disease.

Methods

Species data

Global presence points from previous reports of CLas and CLaf were obtained from the Centre for Agriculture and Bioscience International (CABI) Invasive Species Compendium (CABI, 2018), and European Plant Protection Organization (EPPO) Global Database (EPPO, 2018) (Appendix 9 and 10).

New presence points in Ethiopia, Kenya, Tanzania and Uganda were obtained during surveys on the incidence of HLB and African citrus greening carried out on citrus orchards located in various regions to determine the extent of the spread of the disease in the sampled areas (Appendix 11). Assessment of affected trees was made by visual inspection of foliage on site, and symptomatic tissue was tested for the presence of CLas and CLaf by PCR and identities were confirmed by sanger sequencing (Ajene et al., 2019; Rasowo et al., 2019). All sites in Africa found to be positive for CLas in previous studies and the current study were included as background points in the models. The presence data was cleaned by removing duplicate coordinates from the final dataset before running the models.

Models

Three species distribution models were selected to study the potential distribution of Huanglongbing in Africa, and African citrus greening disease in other parts of the world; (a) The classic climate-envelope-model BIOCLIM (Booth et al., 2014), which employs only occurrence data to define a multi-dimensional environmental space in which a species can occur. The model predicts suitable conditions in a “bioclimatic envelope”, consisting of a rectilinear region in environmental space representing the range (or some percentage thereof) of observed presence values in each environmental dimension (Phillips et al., 2006). To avoid the over predictive effect of outliers, the resulting envelope can be reduced at specified percentiles or standard deviations (Araujo & Petersen 2012).

(b) Maximum Entropy (MaxEnt) (Phillips et al., 2006), which is a general-purpose method for making predictions from incomplete information (Phillips et al., 2006). It requires only presence data, together with environmental data of the study area, employs both continuous and categorical data, can incorporate interactions between different variables and can converge to the optimal probability distribution as a result of deterministic algorithms which have been developed within the model (Phillips et al., 2006).

(c) Boosted Regression Trees (BRT) (Friedman, 2001), which is one of several techniques that enhances the accuracy of a single model by using two algorithms: regression trees and boosting.

Boosting improves the model accuracy (Schapire 2003). It is a forward, stagewise procedure. In boosting, models are fitted in a stepwise manner to the training data, subsequently, appropriate methods are employed to gradually to increase emphasis on poorly modeled observations by the existing collection of trees (Friedman, 2001). These models were selected to represent a spectrum of model complexity as well as make up for the limitations of each individual model via the consensus approach.

Selection of bioclimatic variables

Environmental predictors included 19 bioclimatic variables (Table 3.1) of 2.5 km spatial resolution for the current scenario using the baseline average [1950–2000] (Fick & Hijmans, 2017), and for each future scenario using the Coupled Model Intercomparison Project, Phase 5 (CMIP) 2055 average [2041-2070] (Taylor et al., 2012). To assess the effect of climate change in the potential distribution of CLas, we used two representative concentration pathways (RCPs): CMIP5 rcp4.5 (moderate scenario) and CMIP5 rcp8.5 (extreme scenario). The environmental variables were obtained from the WorldClim database (http://www.worldclim.org/).

Expected multi-collinearity among all the predictor bioclimatic variables were tested using the Pearson correlation test. The highly correlated variables were eliminated using the "findCorrelation" function in the 'Caret' package (Kuhn et al., 2016) in R v3.5.1 environment via R-Studio (R Development Core Team 2008). The correlation coefficient of $|r| > 0.7$ was set as a collinearity indicator for variables that would affect the models (Dormann et al., 2012). Variables within this range were eliminated from the analysis, and only the uncorrelated predictor variables were used in the models. A Jacknife test for variable importance was run on the selected variables in Maxent to determine the percentage contribution of each selected variable to the model.

Model evaluations

Model accuracy was assessed using the area under receiver operating characteristic curve (ROC curve) (Thuiller et al., 2003). The ROC curve is a graphical technique that represents the relation between the False Positive fraction (1 - specificity) and the sensitivity for a number of thresholds. (Fielding & Bell, 1997; Phillips et al., 2006). A curve that maximizes sensitivity for low values of (1-specificity) infers good model performance. The classification of the accuracy of a diagnostic test is the traditional academic point system (Swets 1988): 0.90-1.00 = excellent; 0.80-0.90 = good; 0.70-0.80 = fair; 0.60-0.70 = poor; 0.50-0.60 = fail. The difference between the areas under ROC curves generated by two or more models provides a measure of comparative discrimination ability of these models when applied to independent evaluation data.

All models were run in R v3.5.1 environment via R-Studio, and the data was exported as ASCII files for enhanced visualisation with QGIS software v2.18.15 (QGIS Development Team, 2016).

Model calibration

MaxEnt

Presence locations for CLas and CLaf (occurrence data) were compared against all the pseudo-absence points that are available in the study area (also known as "background points") to avoid model overfitting of spatially clustered presence points and inability to predict spatially independent data. Pseudo-absence points were generated by automatically in MaxEnt by random selection from all points within the studied area excluding available presence points (Barbet-Massin et al., 2012). The model was trained using 75 % of the presence data and validated using 25 %. The model was run with 5,000 iterations and >10,000 background points for both current and future climate scenarios.

BIOCLIM

The mean and standard deviation for each environmental variable were used individually to compute bioclimatic envelopes. The level of fitness between the environmental values on a point and the respective envelopes classifies each point as Suitable, Marginal, or Unsuitable for presence. The categorical output is mapped to probabilities of 1.0, 0.5 and 0.0, respectively. The presence points were used to find the bioclimatic envelope during model creation, and the occurrence data were compared versus 10,000 background points generated by random selection of points from all points outside of the suitable area estimated by a rectilinear surface envelope from the presence sample (Thuiller et al., 2009; Barbet-Massin et al., 2012).

Boosted Regression Trees

The model was calibrated using the gradient boosting function "gbm.step" in the 'dismo' package (Hijmans et al., 2017) in R. The data and settings were as follows: the data frame containing the trained data, the predictor variables – gbm.x = 2.20, the response variable – gbm.y = 1, the nature of the error structure (family = 'bernoulli'), the tree complexity (5), the learning rate (0.01), the bag fraction (0.5). All other parameters not named in the call were set at as default.

Model consensus

Consensus models have been shown to have higher predictive capacity than any of the single SDMs alone (Forester et al., 2013). Furthermore, they have been shown to outperform individual

models thereby providing more robust projections of habitat distributions (Marmion et al., 2009; Grenouillet et al., 2011). Additionally, the use of several algorithms to project species distributions is important because models with the highest accuracy on current climate data may not be optimal in projecting onto new areas or climate conditions (Heikkinen et al., 2012). We employed an ensemble modelling method of obtaining a consensus of the three models, weighted by their AUC scores. Averaging several models, has shown that the 'output' of interest is isolated from the 'noise' associated with individual model errors and uncertainties. When combining forecasts for consensus, one can produce weighted and unweighted averages (Araújo & New, 2007). To obtain a three-model consensus, the raster outputs from the individual models were rescaled to uniform values between 0 and 1. The individual models weighted by their AUC scores were combined, 0.5 was subtracted and the results squared to give further weight to the higher AUC values, thus obtaining the weighted average. Finally, a Raster Stack of the individual model predictions and computed the average. Habitat suitability hotspots were identified by points on the final raster with a probability of occurrence of >0.05.

The final output of level of fitness on the consensus models which ranged between 0 and 1 was classified based on the estimated value cut of the full extent in QGIS as follows: > 0.2 = optimal, 0.2- 0.01 = Highly suitable, 0.01 - 0 = marginal, 0 = unsuitable.

Effect of climate change

The impact of climate change on the future distribution of HLB was determined using the raster calculator in QGIS to resolve the differences between the outputs of the two scenarios assessed. The effect of climate change was calculated by subtracting the raster outputs. The potential distribution due to a change from the extreme emission scenario to the moderate emission scenario was calculated as CMIP5 rcp 4.5 – CMIP5 rcp 8.5 = change. The potential distribution due to a change from the moderate emission scenario to the extreme emission scenario was calculated as CMIP5 rcp 8.5 – CMIP5 rcp 4.5 = change. The final output was streamlined to project only the optimum habitat suitability for better visualisation of the change in the distribution of the hotspots.

Results

Environmental variables affecting the model

Expected multi-collinearity among all the predictor bioclimatic variables tested using the "findCorrelation" function showed high correlation between 10 of the 19 bioclimatic variables, while nine bioclimatic variables were uncorrelated (Appendix 12). The uncorrelated predictor variables (Table 3.1) were used in the models. The jackknife test for variable importance showed

that the precipitation of the wettest month and the annual mean temperature had the highest percentage contribution and permutation importance to the model, respectively. Precipitation of the driest month had the least percentage contribution, while the mean temperature of the warmest quarter had the least permutation importance (Table 3.2).

Table 3.1. Predictor bioclimatic variables used for modelling the ecological niche for "*Candidatus* Liberibacter asiaticus" and "*Candidatus* Liberibacter africanus". Variables selected through a multi-collinearity test using the "Find correlation" function in the caret package in the R software are shown in bold. Data was sourced from the WorldClim database accessed on November 2018.

Variable	Code	Units
Annual mean temperature	**Bio 1**	**ºC**
Mean diurnal range	**Bio 2**	**ºC**
Isothermality	Bio 3	ºC
Temperature Seasonality	Bio 4	ºC
Max temperature of warmest month	Bio 5	ºC
Min temperature of coldest month quarter	Bio 6	ºC
Temperature annual range	**Bio 7**	**ºC**
Mean temperature of wettest quarter	Bio 8	ºC
Mean temperature of driest quarter	Bio 9	ºC
Mean temperature of warmest quarter	**Bio 10**	**ºC**
Mean temperature of coldest quarter	Bio 11	ºC
Annual precipitation	**Bio 12**	**mm**
Precipitation of wettest month	**Bio 13**	**mm**
Precipitation of driest month	**Bio 14**	**mm**
Precipitation seasonality (coefficient of variation)	**Bio 15**	**mm**
Precipitation of wettest quarter	Bio 16	mm
Precipitation of driest quarter	**Bio 17**	**mm**
Precipitation of warmest quarter	**Bio 18**	**mm**
Precipitation of coldest quarter	**Bio19**	**mm**

Table 3.2. Percent contribution and permutation importance of predictor variables as obtained from Jacknife test, used for modelling the ecological niche for "*Candidatus* Liberibacter asiaticus" (CLas) and "*Candidatus* Liberibacter africanus" (CLaf).

Variable	Percent contribution	Permutation importance
Precipitation of wettest month	35.6	25.6
Annual mean temperature	21.5	25.7
Precipitation of warmest quarter	20.6	4.4
Precipitation of coldest quarter	8.5	17.1
Temperature annual range	6	10.5
Mean temperature of warmest quarter	2.9	1.7
Precipitation seasonality	2.5	3.9
Mean diurnal range	1.5	8
Precipitation of driest month	1	3.1
Precipitation of driest quarter	0.5	2.9
Annual precipitation	0.1	0
Precipitation of wettest quarter	0	0

Predicted current distribution of Huanglongbing in Africa

The predicted current distribution of HLB, as obtained from the three-model consensus, showed all countries of Central, Eastern, Southern and Western Africa having marginal to optimal habitat suitability for CLas (Fig. 3.1). In contrast, large areas of North Africa were predicted to have habitat unsuitable for CLas, but the northern fringes of Morocco, Algeria, Tunisia and Egypt showed marginal habitat suitability.

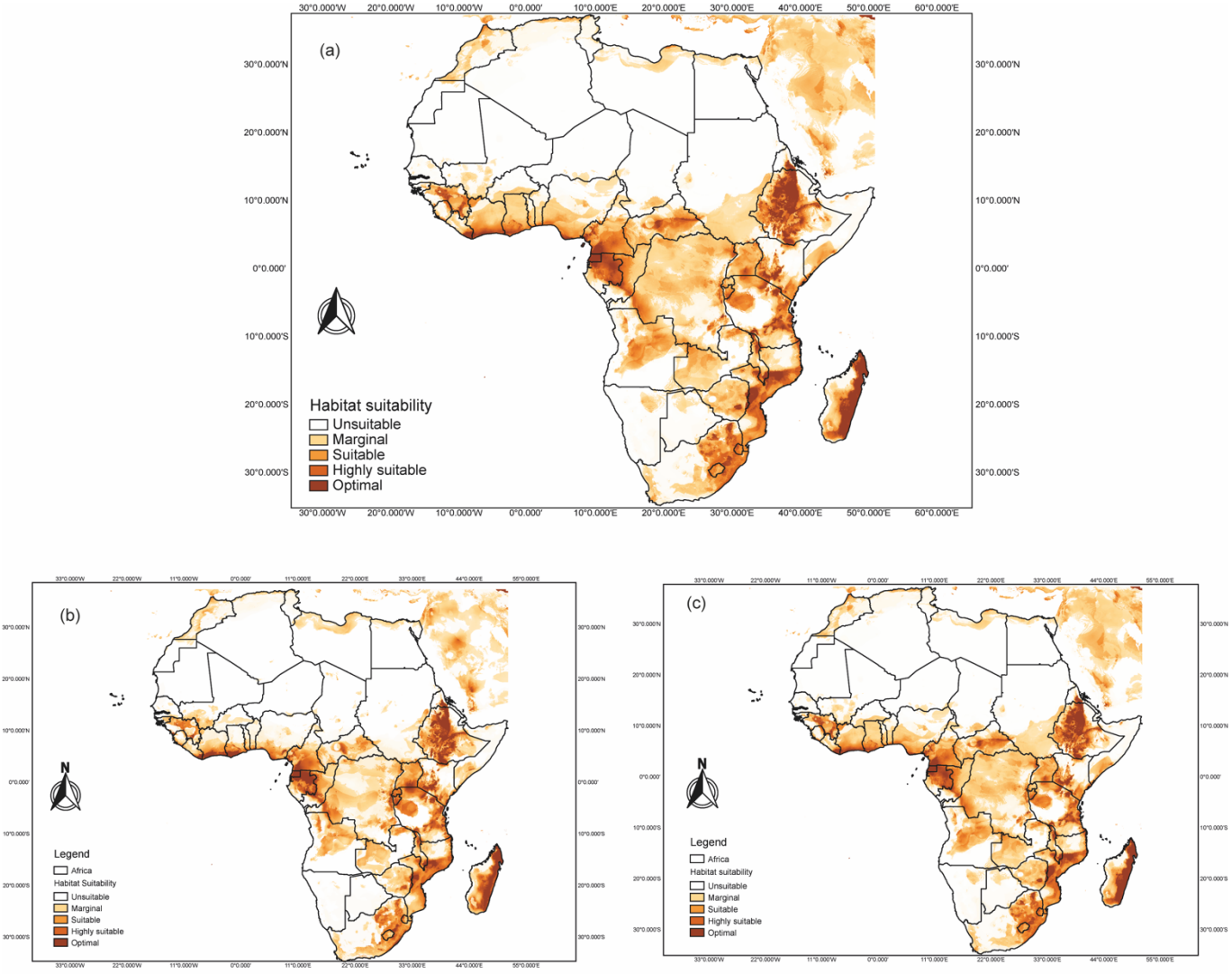

Figure 3.1 Potential distribution of Huanglongbing in Africa, as predicted by three-model consensus (BIOCLIM, MaxEnt and Boosted Regression Trees) showing: (a) Potential current distribution of Huanglongbing in Africa, (b) future (2055) potential distribution of Huanglongbing (HLB) in Africa under moderate scenario (Representative Concentration Pathway 4.5) and (c) future (2055) potential distribution of Huanglongbing (HLB) in Africa under extreme scenario (Representative Concentration Pathway 8.5). The maps were generated using the World Geodetic System 1984 (WGS84) projection.

Predicted future (2050) distribution of Huanglongbing in Africa

The future distribution of HLB in Africa predicted using the three-model consensus also showed a wide distribution under the moderate (CMIP5 rcp4.5) climate scenario and the extreme (CMIP5 rcp8.5) climate change scenarios. All countries of Central, Eastern, Southern and Western Africa showed marginal to optimal habitat suitability for CLas (Fig 3.1). The extreme scenario (Fig 3.1c) showed increased areas of habitat suitability compared to the moderate scenario (Fig 3.1b). A shift in the distribution of HLB was shown by the difference in the hotspots between the current and the future scenarios showed. Under the extreme scenario, the areas of optimum habitat suitability absent in the current distribution and present in the future

distribution were predominantly in Western, Central and Eastern Africa (Fig 3.2a), whereas under the moderate scenario, these areas were predominantly in Southern Africa (Fig 3.2b).

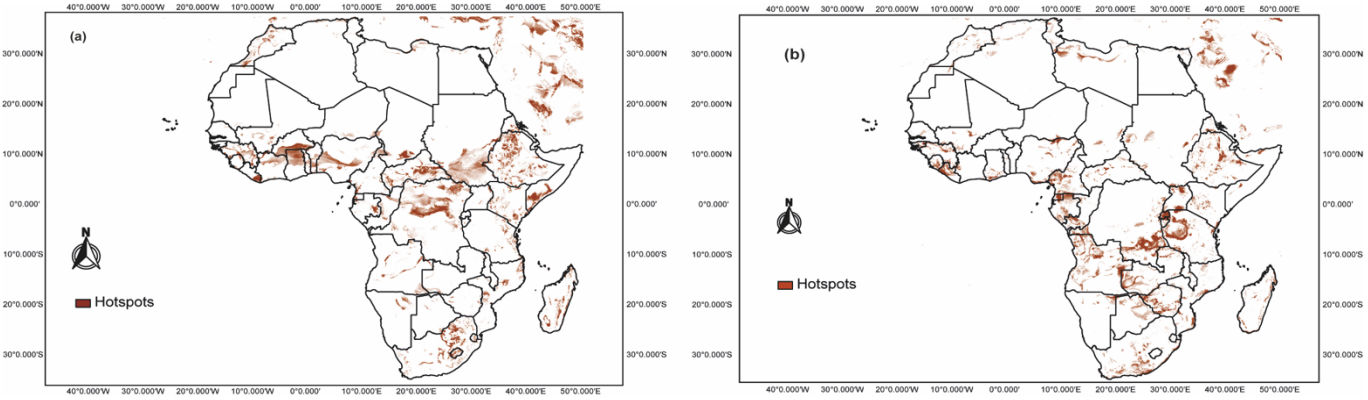

Figure 3.2. Difference in CLas habitat suitability hotspots between the current distribution and future distribution under (a) Extreme scenario (Representative Concentration Pathway 8.5), and (b) Moderate scenario (Representative Concentration Pathway 4.5). The maps were generated using the World Geodetic System 1984 (WGS84) projection.

Predicted effect of climate change on habitat suitability of Huanglongbing in Africa

Assessment of predicted habitat suitability showed that there are more areas of optimal habitat suitability for CLas under the extreme scenario (CMIP5 rcp8.5) than in the moderate scenario (CMIP5 rcp4.5) (Fig 3.3a). The major citrus exporting countries in Africa (Egypt, Ethiopia and South Africa) showed fewer hotspots in the moderate scenario than in the extreme scenario (Fig 3.3b).

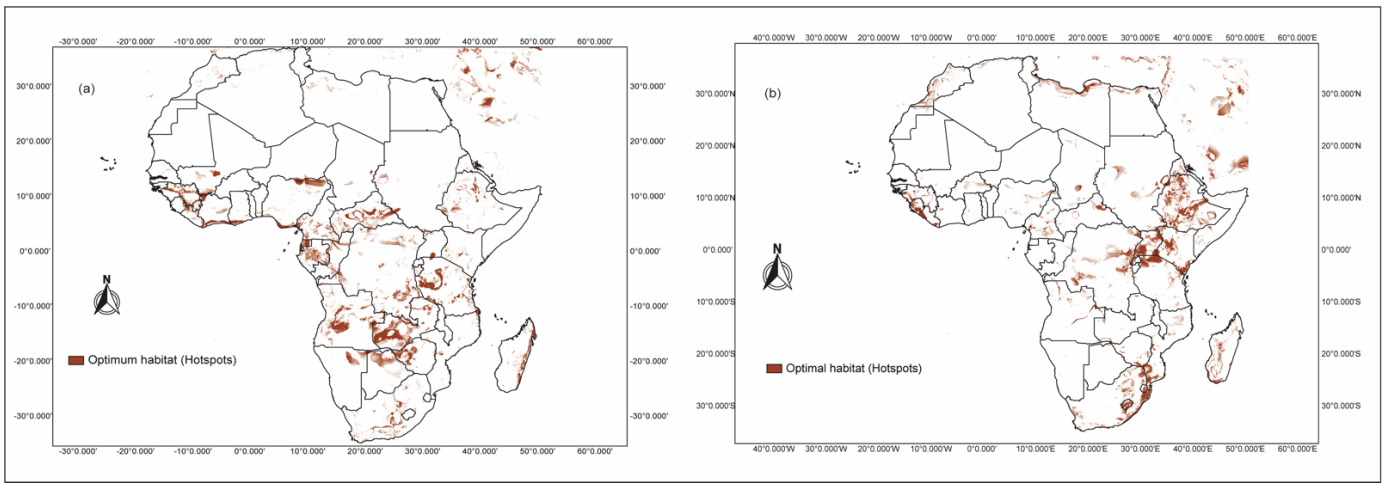

Figure 3.3. Predicted effect of climate change on CLas habitat suitability hotspots areas: (a) Hotspot areas present under the moderate scenario (Representative Concentration Pathway 4.5) and absent under the extreme scenario (Representative Concentration Pathway 8.5) and (b) Hotspot areas present under the extreme and absent under the moderate scenario. The maps were generated using the World Geodetic System 1984 (WGS84) projection.

Predicted current distribution of African citrus greening globally

The predicted current global distribution of ACG obtained from the three-model consensus showed a marked distribution in large areas of Africa, South and Central America, Asia and Australia. Countries of South and Central America showed marginal to optimal suitability for the pathogen, while the southern fringe of North America, especially Florida, showed marginal suitability. Most Asian countries, as well as Australia, showed marginal suitability for CLaf, while Indonesia, Papua New Guinea, Singapore and the Philippines were highly suitable. The United Kingdom, Spain and Portugal showed areas of marginal suitability (Fig. 3.4).

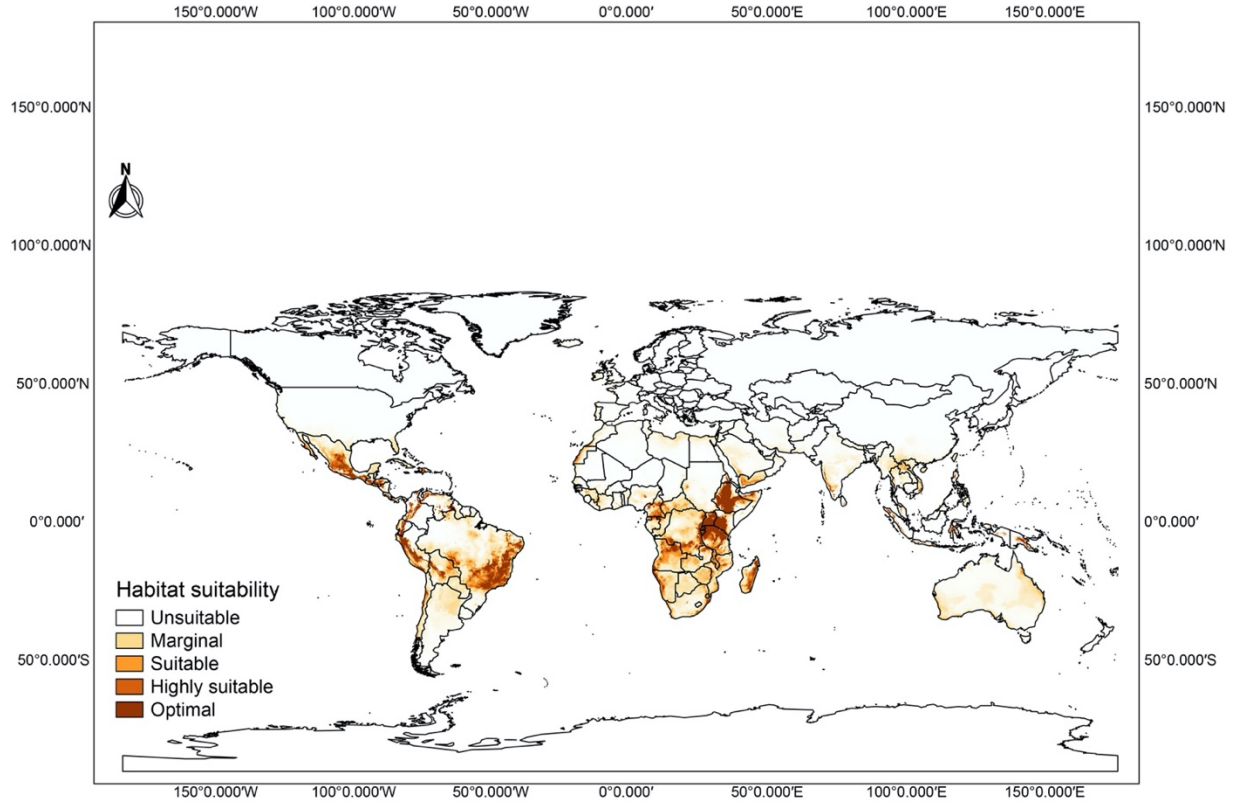

Figure 3.4. Three-model consensus (BIOCLIM, MaxEnt and Boosted Regression Trees) of global potential current distribution of African citrus greening disease. The map was generated using the World Geodetic System 1984 (WGS84) projection.

Predicted current distribution of African citrus greening globally

The predicted current global distribution of ACG obtained from the three-model consensus showed a marked distribution in large areas of Africa, South and Central America, Asia and Australia. Countries of South and Central America showed marginal to optimal suitability for the pathogen, while the southern fringe of North America, especially Florida, showed marginal suitability. Most Asian countries, as well as Australia, showed marginal suitability for CLaf, while Indonesia, Papua New Guinea, Singapore and the Philippines were highly suitable. The United Kingdom, Spain and Portugal showed areas of marginal suitability (Fig. 4).

Predicted future (2050) distribution of African citrus greening globally

The predicted future distribution of ACG globally under the extreme scenario (CMIP5 rcp8.5) showed an increase in the areas of habitat suitability from the current distribution from the current scenario (Fig 3.5). Specifically, few areas showed a slight alteration: Papua New Guinea showed a slight increase, while Australia showed a decrease. The predicted future distribution of ACG globally under the moderate scenario (CMIP5 rcp4.5) showed a decrease in the areas of habitat suitability from the current distribution from the current scenario (Fig 3.6).

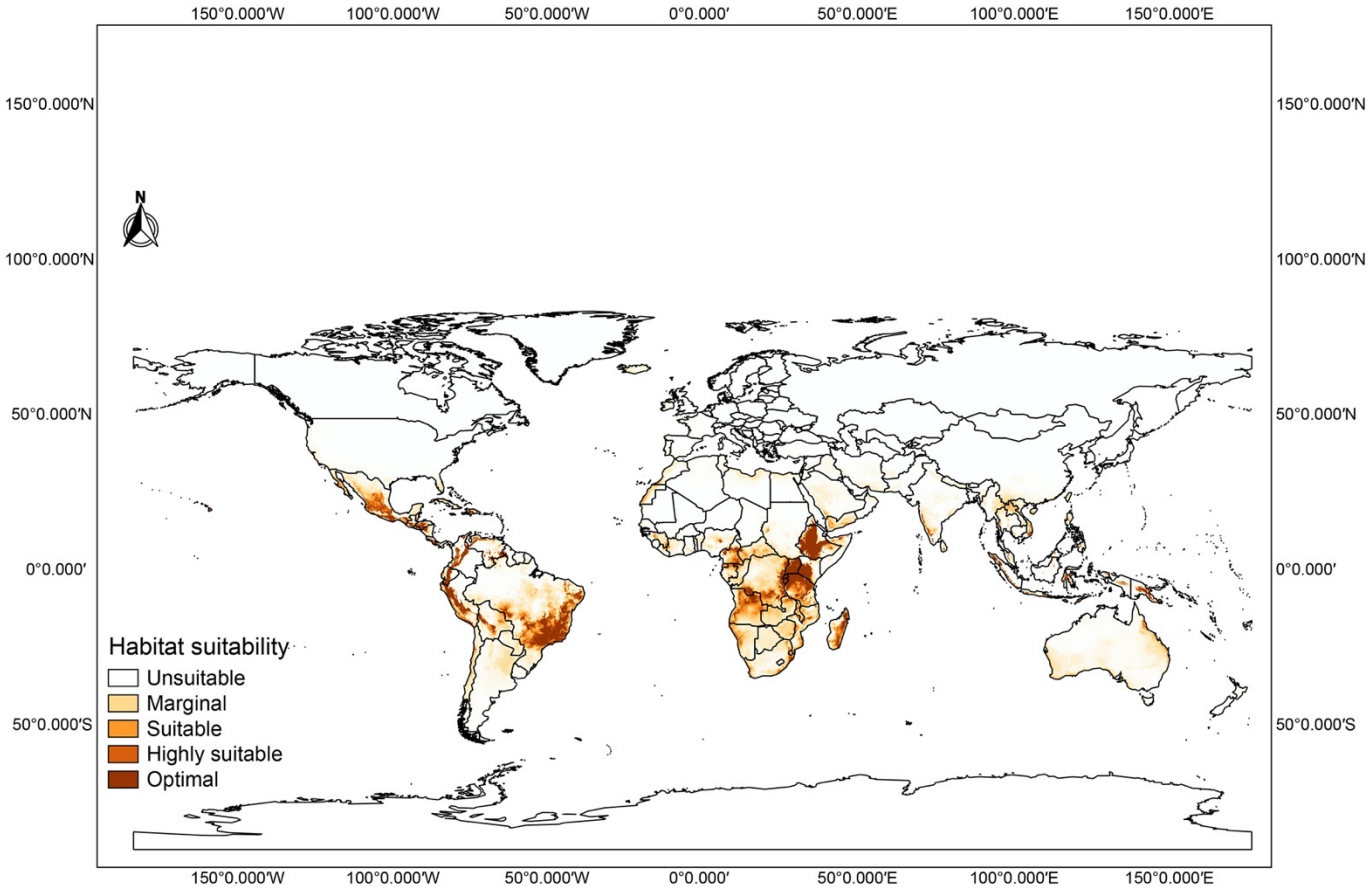

Figure 3.5. Three-model consensus (BIOCLIM, MaxEnt and Boosted Regression Trees) of global potential future (2055) distribution of African citrus greening disease under Representative Concentration Pathway 4.5 (moderate scenario). The map was generated using the World Geodetic System 1984 (WGS84) projection.

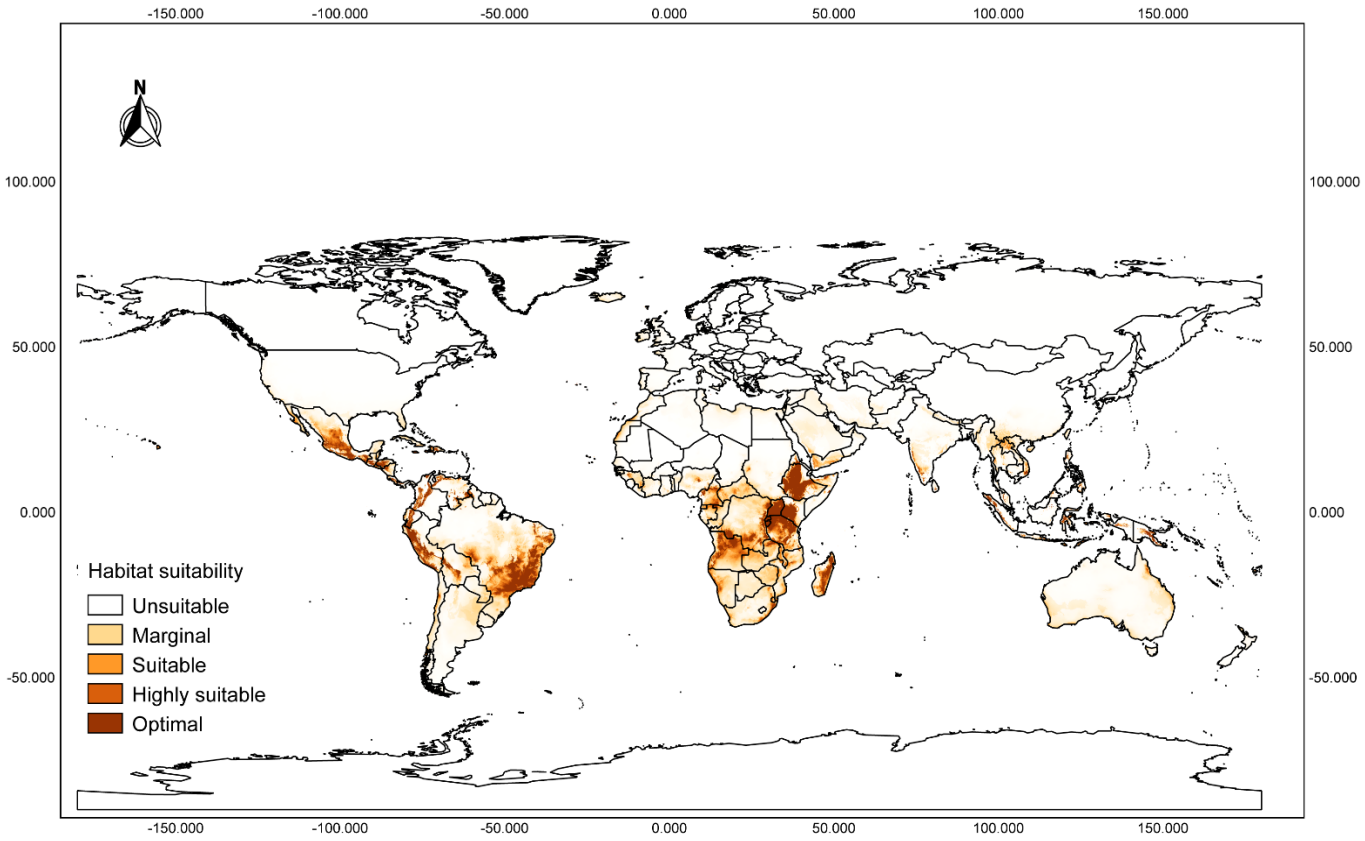

Figure 3.6. Three-model consensus (BIOCLIM, MaxEnt and Boosted Regression Trees) of global potential future (2055) distribution of African citrus greening disease under Representative Concentration Pathway 4.5 (moderate scenario). The map was generated using the World Geodetic System 1984 (WGS84) projection.

Discussion

Huanglongbing (HLB) associated with CLas is a destructive disease of citrus worldwide and has recently been reported on the African continent (Saponari et al., 2010; Ajene et al., 2019), while CLaf-associated African citrus greening disease (ACGD) has been reported in Africa since the 1920's (McClean & Oberholzer, 1965; Massonié et al.,1976; Buitendag & von Broembsen 1993; Roberts et al., 2017; Rasowo et al., 2019). Vector-based modelling has been the norm for predicting the distribution of HLB because modelling ecological niches for plant pathogens can be a problematic endeavour considering the different variables involved. However, environmental and climate data, including monthly temperature and rain, are assumed to reflect the climate suitability for the growth and development of different organisms, including plant pathogens (Hijmans, Cameron, Parra, Jones & Jarvis, 2005). Ecological factors such as; temperature, light and water availability, soil fertility, methane and CO_2 concentration can have positive, neutral, or negative effects on disease development, as pathogens show varying responses to these factors (Velásquez et al., 2018). Furthermore, increased industrialization of developing countries leads to has a direct effect on the CO2 emissions and hence an effect on the distribution of plant pathogens (Anderson, 2010). Studies have shown CO2 levels affect the photosynthetic rate and crop yield of C3 plants such as soybean, cotton, oranges and lemon. The

increase in CO2 concentrations have also been shown to increase disease severity in some plants such as rice and wheat (Kobayashi et al., 2006; Mullins et al., 2015). Precipitation and soil moisture have a crucial effect on plant disease establishment, because, most plant diseases are favored by conditions of rain, high air humidity and high soil moisture (Velásquez et al., 2018). For instance, fungal pathogens such as *Magnaporthe oryzae* requires a minimum of five hours of leaf wetness for disease establishment (Magarey, Sutton & Thayer 2015). Temperature also plays a vital role in plant-pathogen interaction. Disease development in plants generally have an optimal range, for example *Xanthomonas oryzae* has been shown to have an optimal daytime temperature of 350C and night time temperature of 270C for the infection of rice (Horino et al.,1982), while a temperature range between 26^0C to 31^0C are optimal for papaya ringspot virus to colonize papaya (Mangrauthia et al.,2009). Temperature is a crucial factor in the development of plant diseases, as the projected increase in the global temperature may change the areas where crops are susceptible to a particular pathogen (Velásquez et al., 2018). Furthermore, certain diseases with the potential to cause epidemics may never do so due to transient shifts in temperature (Velásquez et al., 2018). Temperature also has a significant effect on vector-borne pathogens like CLas transmitted by *Diaphorina citri*, CLaf transmitted by *Trioza erytreae* and Banana bunchy top virus (BBTV) transmitted by *Pentalonia nigronervosa* (Robson et al.,2007) and influences the incidence and severity by affecting the vector (Robson et al., 2007). Temperatures favorable for the *D. citri* and *T. erytreae* could explain epidemics in CLas and CLaf even if the conditions are suboptimal for the bacterial replication.

HLB is known to be most severe in warm and wet climates (Bové, 2014), which are common in the areas that showed optimal habitat suitability in this study. We found that the environmental variables which had the highest contribution to the models were the temperature and temperature-dependent precipitation variables. Specifically, the precipitation of the wettest month had the highest contribution to the habitat suitability of Liberibacter while the annual mean temperature was the most important variable when considered in combination with other variables. These results are in agreement with a previous study that showed that optimal and limiting temperature conditions for HLB depend on rainfall (Shimwela et al., 2016). Also, the vector *D. citri* is heat-tolerant and survives in tropical and sub-tropical climates.

The ensemble approach to plant pathogen predictive modelling carried out in this study corroborates previous vector-based approaches to HLB prediction. Our results highlight the potential distribution of CLas in Africa, and show that large areas of Central Africa, Eastern Africa, Southern Africa, and some parts of Western Africa are highly suitable for HLB establishment. This is in agreement with a global study on the potential spread of HLB that used two correlative modelling approaches to predict the potential distribution of CLas based on the

distribution of the insect vector (Narouei-Khandan et al., 2015). The authors also pointed to central and southeastern parts of Africa as highly suitable for HLB. Our results concur with a previous study highlighting areas in West Africa as highly suitable for HLB, also based on habitat suitability of the vector, as obtained from a multi-model framework (Shimwela et al., 2016). The differences in the predictions between the current and future distributions showed clear variations between the distributions under the moderate and extreme scenarios and, overall, the extreme scenario showed an increased distribution of the disease. The inclusion of the presence points of CLas in Ethiopia from previous studies to the background points validated the accuracy of the ensemble approach to plant pathogen predictive modelling. The predicted optimal areas for the establishment of CLas were the same areas where the pathogen was found in previous studies (Saponari et al., 2010; Ajene et al., 2019). In 2016, the presence of CLas was reported in Uganda (Kalyebi et al., 2016). However, the presence points from Uganda were not included in the models as the report was shown to be a misidentification of CLafCl (Roberts et al., (2017). In Uganda, large areas of marginal suitability and a few areas of high suitability for CLas were predicted but no areas of optimal suitability for the pathogen were observed.

Citrus cultivation in most parts of Africa is a key source of livelihood for small holder farmers as production ranges from small to medium scale (Aidoo et al., 2019). In Kenya and Tanzania, ACG has had the greatest impact on citrus production in the cooler highland regions, causing yield losses of 25–100% (Pole et al., 2010). The small-scale production is mostly in backyard gardens with minimal pest control measures applied this is usually problematic as it serves as reservoirs for plant diseases and their vectors. This is key in the distribution of CLas and CLaf because these backyard gardens may become a constant source of infestation by the vectors of CLas and CLaf to the large-scale commercial orchards which are constantly surveyed, and pest control measures applied.

African citrus greening, the disease associated with the pathogen CLaf, has only been reported in Africa thus far. However, our study highlighted the potential areas of suitability for CLaf in other parts of the world. Our predictive maps showed large areas of the Americas, Asia and Australia included in the potential distributional range of ACG in the world. In Europe, only the Iberian Peninsula showed suitability for the disease, although marginal. However, the recent introduction of *T. erytreae,* the native African vector of CLaf, to Spain and Portugal (Cocuzza, et al., 2017; Siverio et al., 2019) highlights increased potential for spread of ACG outside Africa. Thus, the prediction of potential habitat suitability of the bacteria in other areas of the world provides valuable information required for monitoring and implementation of preventive measures.

Vector-based modelling has shown that it took more than seven years after documented individual insect-based infections for the entire grove to become fully symptomatic for HLB (Kobori et al., 2012). In the context of invasive pathogens such as CLas, this approach could prove fatal as infected saplings from seemingly uninfected orchards can be unintentionally transferred to new groves, thereby facilitating non-vector dissemination of the disease. Infection of trees due to the presence of *D. citri* can occur such that within 1- 2 years the entire grove can be asymptomatically infected (Lee et al., 2015). HLB surveillance has been problematic because infected citrus groves may not show symptoms of the disease until up to 5 years after infection (Manjunath et al., 2008). Therefore, surveillance has relied on the detection of the pathogen within insects because the infection can be detected in the vector months before the plants develop symptoms (Manjunath et al., 2008; Shen et al., 2013). Our projection of the distribution of CLas will inform; closer vector monitoring in citrus producing areas with high suitability for HLB establishment, as well as periodic testing of asymptomatic citrus plants in these high-risk areas.

Liberibacter presence points obtained from detection in citrus plants and used in the models show that the habitat suitability for citrus production has an implicit impact on the potential distribution of HLB, ACG and their vectors *D. citri and T. erytreae* (Narouei-Khandan et al., 2016). Our study showed variations between the current predicted habitat suitability of CLas and the future predictions under different climate change scenarios. This suggests that extreme changes in climate influence the potential establishment of the disease in areas suitable for citrus production. The change in the distribution of HLB in climate change scenarios showed a dramatic shift from a sparse distribution in Western, Central and Southern Africa under a moderate scenario to a higher distribution concentrated in Northern, Eastern and Southern Africa under the extreme scenario. This prediction alerts to the possibility that the top citrus exporting countries in Africa may be greatly affected, as rising temperatures and rainfall patterns will affect the distribution of HLB and its vector.

We demonstrated the potential of an ensemble approach using bioclimatic variables to model the distribution of plant pathogens and predict future habitat suitability of Liberibacter species. These results constitute an early alert for citrus-producing regions where HLB and ACG are not yet present. Plant protection strategies based on future habitat suitability of plant pathogens would be an important inclusion in the integrated pest management systems for citrus production.

Chapter Four: Detection of Asian citrus psyllid *Diaphorina citri* (Hemiptera: Psyllidae) in Ethiopia: A new haplotype and its implication to the Proliferation of Huanglongbing

Abstract

Diaphorina citri Kuwayama (Hemiptera: Psyllidae) also known as the Asian citrus psyllid is a pest of citrus known for its transmission of "*Candidatus* Liberibacter asiaticus" (CLas), the causal bacterium associated with Huanglongbing. The African citrus triozid *Trioza erytreae* (Del Guercio) (Hemiptera: Triozidae) has been shown to vector "*Candidatus* Liberibacter africanus" (CLaf) which causes the African citrus greening disease. Following reports of *D. citri* in Kenya and Tanzania, we surveyed citrus plants to establish the presence/absence of *D. citri* in Ethiopia in citrus growing regions ranging from 900 to 2460m above sea level (masl). *D. citri* adults were detected in five of the surveyed sites in Ethiopia. Adult insects encountered were collected using an aspirator and stored in 97% ethanol. The mitochondrial cytochrome oxidase 1 (*mt COI*) gene of the collected insects was amplified using LepF1/LepR1 primers, and sequences obtained showed low variation, which fell within the acceptable range of species. BLAST was used to query the sequences obtained, and all the sequences linked to *D. citri* accessions that are available in GenBank. The analysis of the sequences revealed a new haplotype of the species that differs from haplotypes previously reported. Phylogenetic relationships of our samples and other *D. citri* reference sequences was inferred using the Maximum likelihood method. Monophyly was observed between the samples and the publicly available sequences from global accessions. This is the first report of the presence of *D. citri* in Ethiopia.

Introduction

Citrus greening has been known to be one of the most destructive diseases affecting citrus plants worldwide (Halbert and Manjunath, 2004). The disease is associated with Candidatus Liberibacter, an alpha Proteobacteria which is gram-negative, fastidious and phloem-limited (Damsteegt et al. 2010, Jagoueix et al., 1996). The Candidatus Liberibacter genus contains three species that are known to cause disease in citrus: "Candidatus Liberibacter asiaticus" (CLas), "*Candidatus* Liberibacter americanus" (CLam), and "*Candidatus* Liberibacter africanus" (CLaf). CLas is the pathogen associated with Huanglongbing (HLB), transmitted by *Diaphorina citri*

Kuwayama also known as the Asian citrus psyllid (ACP). CLas is present in Asia, the United States and Brazil (Jagoueix et al., 1994; Sutton et al., 2005; Halbert and Manjunath, 2004; Teixeira, 2005; Li et al., 2006). The heat-sensitive CLaf causes the African citrus greening disease (ACG) that is transmitted principally by *Trioza erytreae* (del Guercio) also known as the African citrus triozid (ACT). Both vectors have been shown to transmit either bacteria experimentally (Lallemand et al., 1986).

The Asian citrus psyllid was described from citrus in Taiwan in 1907 (Kuwayama 1908). Six other members of the genus *Diaphorina* have been reported on citrus: *Diaphorina amoena* Caperner, *Diaphorina auberti* Holis, *Diaphorina communis* Mather, *Diaphorina murrayi* Kandasamy, *Diaphorina punctulata* Pettey, and *Diaphorina zebrana* Capener (Pettey, 1924; Capener, 1970; Catling and Atkinson, 1974; Mather, 1975; Kandasamy, 1986; Aubert, 1987; Hollis, 1987; da Graça, 1991). Of these, only *D. citri* and *D. auberti* are primarily on citrus. *Diaphorina communis* is primarily on *Bergera* but occasionally infests citrus. *Diaphorina murrayi* was described from *Murraya paniculata* (L.) Jack, but presumably could be on citrus. Differences between *D. murrayi* and *D. citri* are small, so the two might be synonyms. Other species of *Diaphorina* reported on citrus do not reproduce on the crop (Halbert and Manjunath 2004). Most species on citrus can be differentiated based on the pattern of spots on the forewing as well as the shape of the genal cones (Halbert and Manjunath, 2004). The wing pattern of ACP is distinct and is easily distinguishable from the other species (Halbert and Manjunath, 2004). ACP recently was detected in Africa in 2016 and 2017 in Tanzania and Kenya respectively (Shimwela et al., 2016, Rwomushana et al., 2017). The putative dispersal patterns of ACP suggest that it may have spread from the regions of the initial detection into other countries. The natural movement of ACP may be an unlikely route of long-distance dispersal, but the free flow of plant products such as budwood and rootstock seedlings along with infested ornamentals such as *Murraya paniculata* through trade within the eastern African region could assist the long-distance dispersal of the eggs and nymphs (Rwomushana et al., 2017).

The African citrus triozid was recorded first in 1929 in South Africa (Jagoueix et al., 1994), and the insect currently is widely distributed in Africa. The insect has been reported in 21 out of 54 African countries (Fig. 4.1) (EPPO, 2020). Outside Africa, ACT was detected in 1994 in Portugal (Fernandes and Franquinho Aguiar, 2001), and it is spreading now to the south-western part of the Iberian peninsula (Cocuzza et al., 2017). ACT vectors CLaf, causing ACG in Africa and the Mascarene islands (Magomere et al., 2009; Bové, 2014b). In Ethiopia, the distribution of ACT showed an irregular pattern of distribution and severity (Hailu and Wakgari, 2019). The highest infestation of ACT has been reported on White sapota (*Casimiroa edulis*) in Oromia and Dire Dawa (Hailu and Wakgari, 2019) which is among the alternative host plants of the pest. The

widespread presence of ACT in Ethiopia, as well as, the presence of CLas associated HLB already presents a significant risk to citrus production in the region.

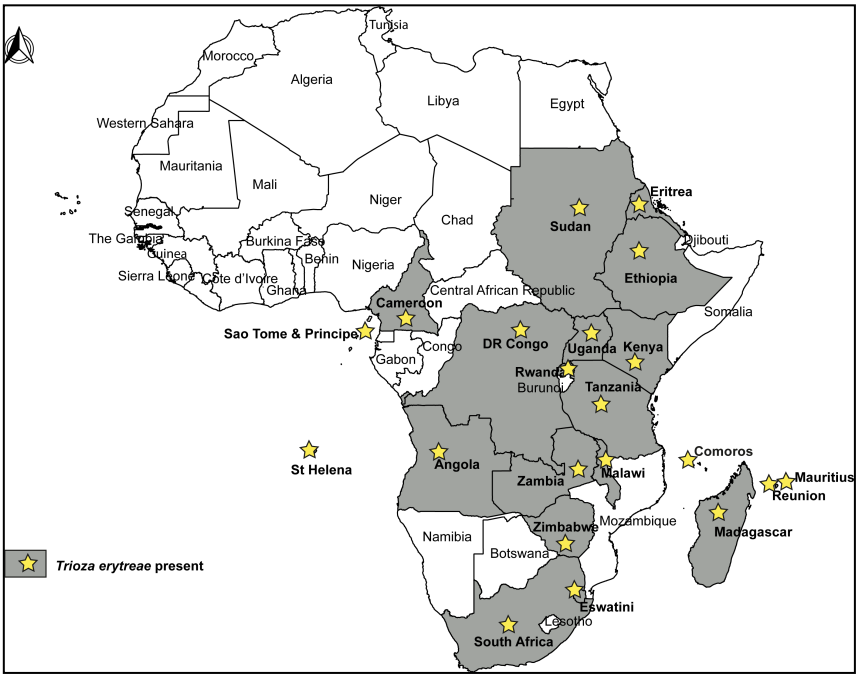

Figure 4.1. Distribution of the African Citrus Triozid (*Trioza erytreae*) in Africa.

Due to the presence of the CLas in Ethiopia, recent detection of ACP in the African continent, free trade movement, presence of reservoir hosts plants and similar climatic patterns, there is a need to confirm the presence and status of ACP in the country. Therefore, this study aimed to establish the presence or absence of ACP in Ethiopia and characterize the population in relation to other populations in Eastern Africa and beyond.

Methods

Vector Sampling

Surveys for the psyllid vectors of greening disease (ACP and ACT) were done in Ethiopia, between June 2017 and November 2017. The sites sampled included large orchards, small-scale rural farms and homestead gardens. The survey covered the Districts of West Gojjam, North Gondar, South Gondar, Adwa, Central Tigray, Eastern Tigray, North Wollo, South Wollo, Oromia Special Zone East Shewa and North Shewa. Each sampling location was geotagged using the Garmin, eTrek_ 209 (Garmin, USA) global positioning system device. In smaller orchards (<50 trees), all trees were surveyed for ACP and ACT adults, while in large orchards (> 50 trees), a transect sampling method was used, by beginning from the center of the grove and moving diagonally to the four corners of the grove. Ten trees on each transect, were checked for the presence of the psyllids. In the backyard gardens, every available tree was inspected. *Diaphorina citri* were identified by their distinct wing pattern and their posture (head down, tail

up). *Trioza erytreae* also were identified by their light brown appearance, wing size and clear venation patterns, and feeding posture. The adult psyllids, when encountered, were collected with an aspirator. Morphological identification of ACP and ACT were made according to OEPP/EPPO (2005a) and OEPP/EPPO (2005b) respectively. Voucher specimens of the insects are deposited at the Biosystematics Unit of the International Centre of Insect Physiology and Ecology (ICIPE), Nairobi, Kenya.

DNA Extraction, Polymerase Chain Reaction and Sequencing

Genomic DNA extraction was carried out on individual psyllids using the Isolate II genomic DNA Kit (Bioline, United Kingdom), following the manufacturer's instructions. DNA was extracted from ten psyllids per site, in locations where less than ten psyllids were encountered, one psyllid was reserved as a voucher specimen while DNA was extracted from the remaining psyllids. Quality and quantity of the DNA extracts were checked using Nanodrop 2000/2000c Spectrophotometer (Thermo Scientific, USA). Polymerase chain reaction (PCR) was done using the primer pairs LepF1 and LepR1(Hebert et al., 2004) to amplify the *mt COI* gene region. For each assay, three technical replicates were used. The PCR reaction volume was 20 µl containing 5× MyTaq reaction buffer (5 mM dNTPs, 15 mM MgCl2) (Bioline), 10 picomole of each primer, 0.5 mM MgCl2 (Thermo Scientific), 0.25 µl MyTaq DNA polymerase (Bioline), and 15 ng/µl of DNA template. The reactions were set up in the Master Cycler Nexus gradient (Thermo Scientific). The cycling conditions used were as follows; initial denaturation for 2 min at 95°C, followed by 40 cycles of denaturation for 30 s at 95°C, annealing for 45 s at an optimized annealing temperature of 52°C, and extension for 1 min at 72°C. Then a final extension step of 10 min at 72°C. The amplified PCR products were resolved through a 1.2% agarose gel. DNA bands on the gel were analyzed and documented using KETA GL imaging system trans-illuminator (Wealtec Corp, USA). Successfully amplified products were bidirectionally sequenced.

Data analyses

The *mt COI* sequences obtained from this study were aligned with 148 *D. citri mt COI* sequences retrieved from GenBank (**www.ncbi.nlm.nih.gov/genbank/**). Multiple sequence alignments were done using the MUSCLE tool in MEGA X (Kumar et al., 2018). The sequence alignment was used to construct a median-joining network using Network software (http://www.fluxus-engineering.com/sharenet.htm), under the default settings (Bandelt et al., 1999). Interspecific sequence divergences were calculated using the uncorrected p-distance model and Standard

errors were obtained using 1,000 bootstrap replicates. The phylogenetic tree was constructed using the Maximum likelihood (ML) method implemented in MEGA X based on p-distances, with 1,000 bootstrap replicates.

Results

The survey included 70 sites in Amhara, Oromia and Tigray regions in Ethiopia (Fig. 4.2). The study areas ranged in altitude from 900 meters above sea level (masl) in Nura Hera to 2460 masl at Bure. *D. citri* was detected in five locations while *T. erytreae* was detected in 14 locations. Adult *D. citri* were found on mature leaves, with white excretory deposits on the leaves. The highest number of *D. citri* adults were found in Pasomile (10). In total, 28 *D. citri* were collected from Pasomile (10), Goshuha (7), Mersa (5), Hayk (3) and Abuabu (3) (Table 4.1). *T. erytreae* was not found at the locations where *D. citri* was detected during the survey. There were no *D. citri* adults detected below 1000 masl, but, surprisingly, they were detected between 1619 and 2112 masl in Ethiopia (Table 4.1). *Trioza erytreae* occurred mostly in the highland areas of Amhara between 1867 – 2460 masl (Fig. 4.2).

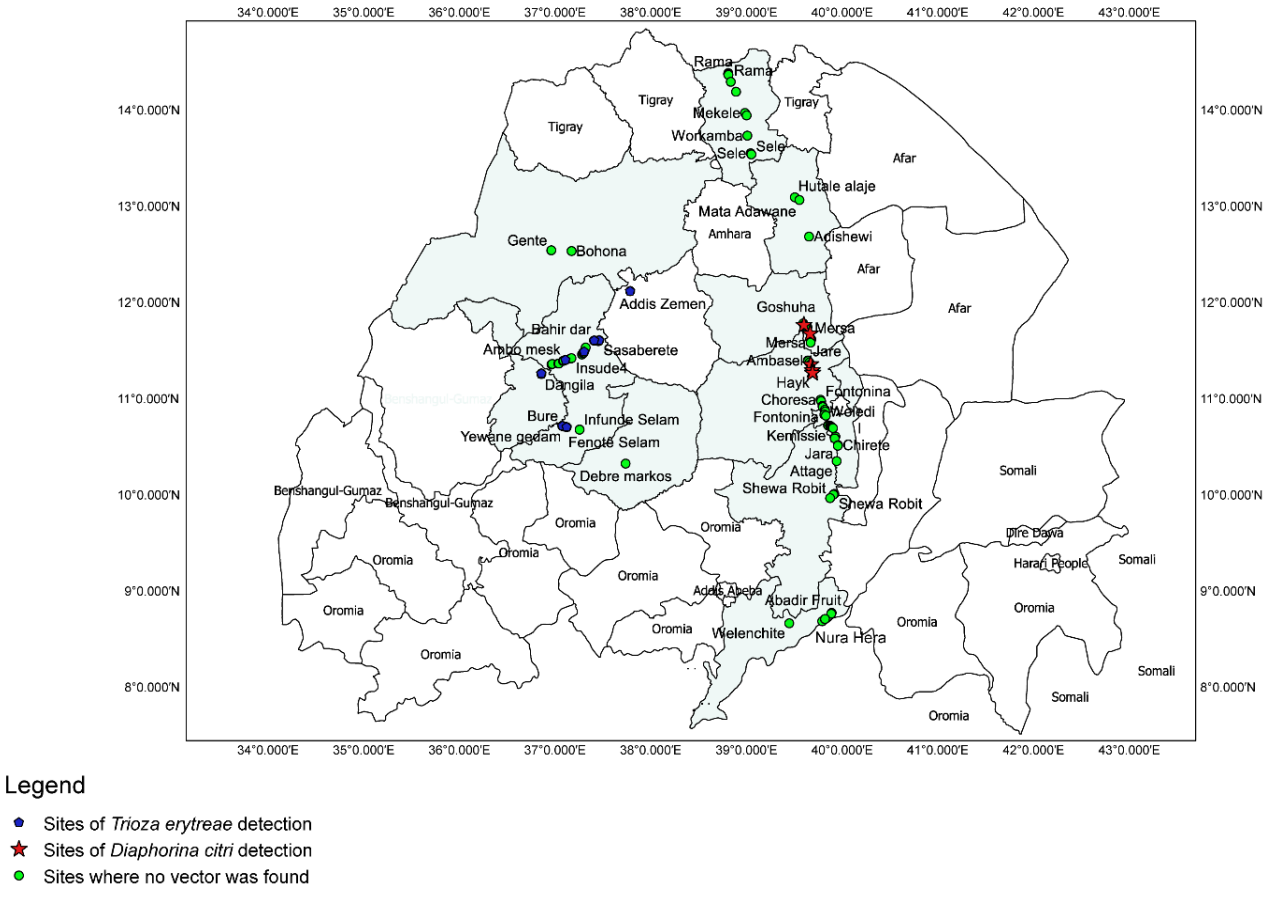

Figure 4.2. Sampling Locations and locations of positive detection of *Diaphorina citri* and *Trioza erytreae* in Ethiopia

Table 4.1. Locations of *D. citri* detection in Ethiopia

Country	Location	Latitude	Longitude	Altitude	*D. citri* adults	Citrus system
Ethiopia	Abuabu	11.26593	39.68184	2112	3	Back yard garden
	Goshuha	11.76407	39.59168	1880	7	Back yard garden
	Hayk	11.29428	39.67969	2001	3	Back yard garden
	Mersa	11.67397	39.65604	1619	5	Back yard garden
	Pasomile	11.3551	39.66207	1804	10	Back yard garden

The PCR assays of *D. citri* DNA extracts using the Lep primer had stable amplicon sizes of approximately 650 to 700 base pairs. The sequencing reads were of high quality (≥98%). Twenty-eight samples from Ethiopia were sequenced, and *mt COI* sequences obtained were analyzed. Sequences from this study (MN449343 - MN449347) had 94% base-pair matches with *mt COI* region of the *D. citri* mitochondrial genome found in Genbank (KU647697.1).

The Interspecific genetic distances showed that *D. citri* from Ethiopia was least diverged from *D. citri* from Brazil (0.11) while it was most diverged from *D. citri* from the other east African *D. citri* as well as *D. citri* from China (Table 4.2). The Maximum-Likelihood tree was built using *mt COI* sequences obtained from the samples in this study combined with *mt COI* sequences of the representative sequences available in GenBank to assess the phylogeographic structure of *D. citri*. The tree topology indicated that *D. citri* from Ethiopia formed a distinct clade separate from the *D. citri* in other countries. The Ethiopian clade was closely related to the sequences from Brazil (Fig. 4.3). The analysis of the haplotype network based on the variation in the *mt COI* sequences showed that *D. citri* from Ethiopia formed a singleton haplotype, differing from *D. citri* found in other countries (Fig. 4.4).

Table 4.2. Estimates of evolutionary divergence of COI gene region over sequence pairs between groups of *Diaphorina citri* as determined using p-distance model.

		1	2	3	4	5	6	7	8	9	10	11	12	13	14
1	Kenya	0.00													
2	Tanzania	0.00	0.00												
3	China	0.00	0.00	0.00											
4	Vietnam	0.00	0.00	0.00	0.00										
5	India	0.62	0.62	0.62	0.62	0.00									
6	Guadeloupe	0.44	0.44	0.44	0.44	0.75	0.00								
7	USA	0.85	0.85	0.85	0.85	0.71	0.93	0.00							
8	Mexico	0.00	0.00	0.00	0.00	0.62	0.44	0.84	0.00						
9	Pakistan	0.01	0.01	0.01	0.01	0.61	0.45	0.84	0.00	0.00					
10	Saudi Arabia	1.09	1.09	1.09	1.09	0.95	0.67	1.07	1.11	1.12	0.00				
11	Brazil	1.28	1.28	1.28	1.28	0.78	1.19	0.44	1.28	1.27	1.06	0.00			
12	Argentina	1.26	1.26	1.26	1.26	0.76	1.17	0.42	1.26	1.25	1.04	0.02	0.00		
13	Paraguay	1.25	1.25	1.25	1.25	0.75	1.16	0.42	1.25	1.23	1.04	0.02	0.00	0.00	
14	Ethiopia	1.35	1.35	1.35	1.35	0.85	1.24	0.53	1.35	1.33	1.09	0.11	0.13	0.12	0.00

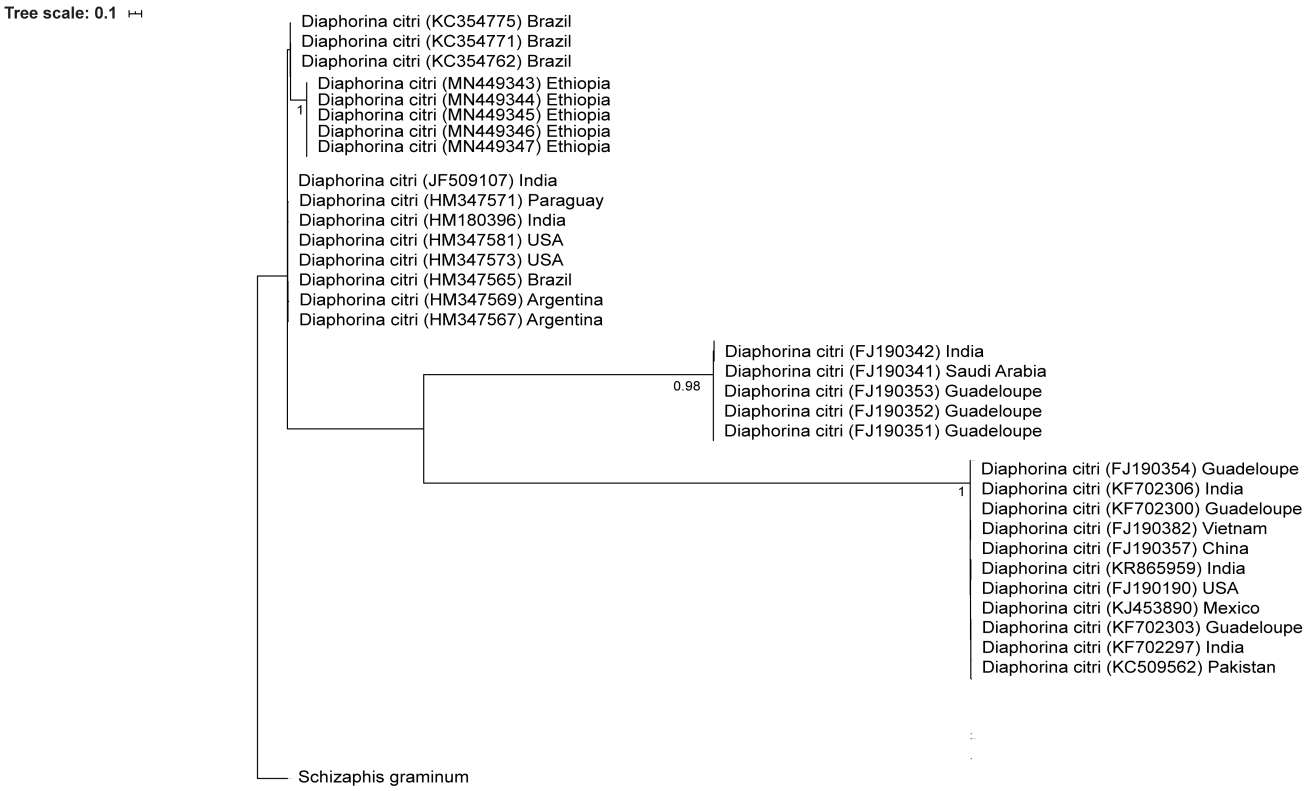

Figure 4.3. Maximum-Likelihood tree based on mitochondrial cytochrome oxidase 1 (COI) genes of *Diaphorina citri* from Ethiopia and representative sequences from global collections with *Schizaphis graminum* as an outgroup. Branch support was based on 1000 bootstrap replicates. Numbers in the brackets represent the GenBank accession numbers

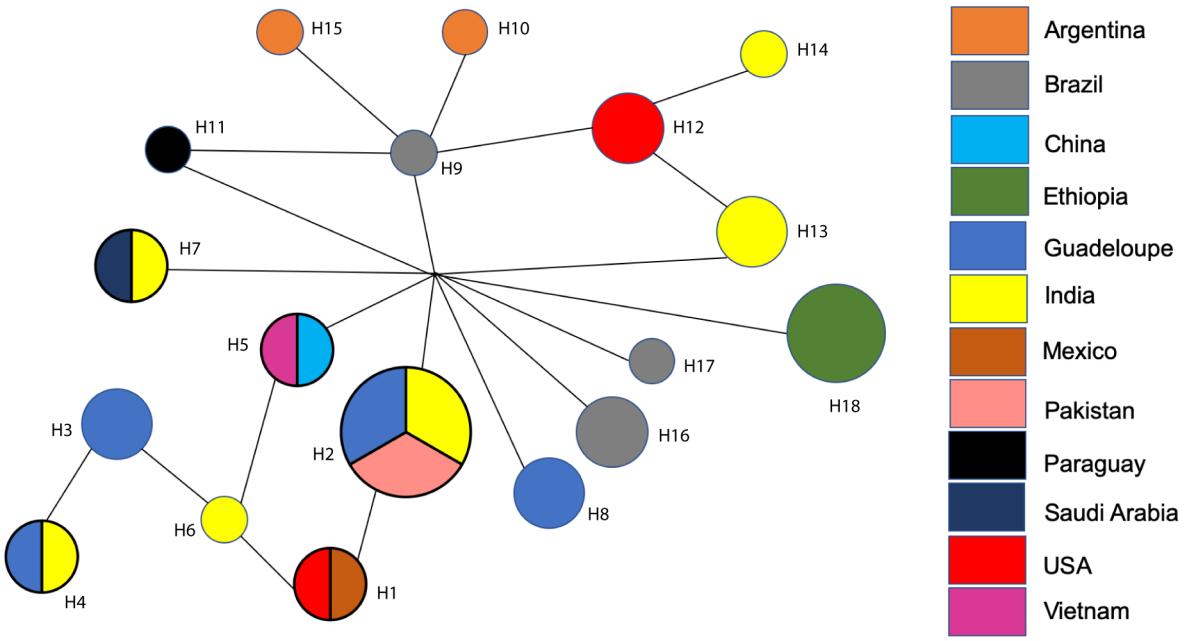

Figure 4.4. Haplotype network of *Diaphorina citri* partial mitochondrial cytochrome oxidase 1 sequences from Ethiopia and representative haplotypes from different countries obtained from GenBank for 17 haplotypes (H_1 to H_17). Node size is proportional to number of samples within each haplotype

Discussion

The first report of ACP on the African continent was in Tanzania (Shimwela et al., 2016). Subsequently, the pest was detected by Rwomushana et al., (2017) in Kenya and other parts of Tanzania. Our study established the presence of ACP in Ethiopia, where CLas associated HLB is also present (Saponari et al., 2010). The identification of the pest using molecular tools confirmed the specimens to be ACP; thus, highlighting the escalated risk of spread of HLB from Ethiopia to other citrus-producing countries. Indeed, this is the first detection of ACP in Ethiopia.

The presence of ACP at altitudes ranging between 1,619 masl and 2,112 masl in Mersa and Abuabu and its absence at altitudes below 1000 masl was in contrast to the native altitudinal range (<800 masl) of this species (Jenkins et al., 2015). Although, the average maximum temperature range of the detection sites of 25°C, was within the ideal temperature range for the population development of ACP (25-28°C) (Liu and Tsai, 2000). The species is heat tolerant (Bové 2014a), and the distribution of ACP has been shown to be affected by climatic conditions in America and Asia (Halbert and Manjunath, 2004; Grafton-Cardwell et al., 2013; Hall et al., 2013).

The ACP detection from our study was clustered around locations from Mersa to Hayk in North Wollo where HLB has been reported (Saponari et al., 2010), while the insect was absent in the regions of Gondar and Gojjam where ACT was predominant (Ajene et al., 2019). This suggests a

movement of the pest and possible spread of HLB within the north-eastern region of the country southwards towards Nura Hera, Awassa and Jimma where citrus production is high. Therefore, preventative measures including surveillance, containment and pest control are required to slow the movement of the pest to the un-infested and HLB-free regions of the country. The adult psyllids have been reported to have a dispersal range of 2 km within 12 days (Lewis-Rosenblum et al., 2015); therefore, the migration of the pest southwards is imminent.

The source of the introduction of ACP into Ethiopia is unknown. Suggestions on the introduction route from Asia into East Africa (Tanzania and Kenya) through the trade of *M. koenigii,* which is a preferred host for ACP have been made (Rwomushana et al., 2017). However, the probability of this route of invasion into Ethiopia is low due to the geographic location of the detection region. Although, wind-assisted dispersal of ACP leading to long range spread (90 -470 km) have been reported (Bové, 2006; Setamou et al., 2008; Kobori et al., 2011). The locations of ACP detection in our study (North Wollo region) suggests short-distance movement within the country. However, the movement of plant materials which may carry the eggs and nymphs of the pest may assist long-distance proliferation of the pest and its establishment in new areas given climatic conditions favourable for the development of the pest. Furthermore, ecological models using bioclimatic data predicted large areas of suitability for ACP in Ethiopia if the pest is introduced (Grafton-Cardwell et al., 2013, Shimwela et al., 2016). Therefore, the potential establishment of the pest in the part of Ethiopia (Nura Hera) where it was not detected in this study is imminent if control strategies are not put in place to prevent long-distance dispersal of the pest.

Phylogenetic relationship among the ACP populations was inferred using the mitochondrial COI gene, which has been used to infer population dynamics of ACP populations (Boykin et al., 2012; Guidolin and Consoli, 2013; Lashkari et al., 2014; De León et al., 2011). The phylogenetic tree showed a monophyletic relationship between the ACP populations. The clustering patterns inferred from the tree suggests a different origin for the ACP in Ethiopia and the ACP in Kenya and Tanzania, as reported by Rwomushana et al., (2017). The phylogeny showed a close genetic relationship between the ACP from Ethiopia and the ACP from Brazil. Therefore, the possible origin of ACP in Ethiopia is South America. The analysis of the COI sequences from Ethiopia revealed a new haplotype of the psyllid present in Ethiopia, which is linked to the haplotype from Brazil. This was observed in the maximum likelihood tree, thus, confirming the phylogenetic analysis.

The vector of CLaf (*T. erytreae*), was observed at high altitude locations. This vector is heat sensitive (da Graça et al., 2015); therefore, its presence in colder highland areas was characteristic. ACT was found on citrus plants and other host plants such as *Casimiroa edulis*

and *Clausena anisata*. The detection of CLas in ACT in the Ethiopian highlands (Ajene et al., 2019) highlights a new dimension to the proliferation of CLas in the absence of its common vector, *D. citri*. Niche overlap was observed between ACP and ACT in our study with the sites of detections ranging between 1619 m.a.s.l to 2112 masl. This phenomenon has been reported at mid altitudes (Shimwela et al., 2016). Rwomushana et al., (2017) highlighted niche overlaps between the two species in Kenya and Tanzania, which extends to higher altitudes than that reported by Shimwela et al., (2016). Furthermore, the two vectors have been shown to occur at similar altitudinal ranges but in different ecologies (Garnier and Bové, 1996; Bové, 2006). The presence of ACP in Ethiopia highlights a significant limitation to the management of HLB in Africa. The movement of ACP, plants, plant parts and the probable transmission of CLas by ACT increases the likelihood of spread of CLas into other countries in the region. Therefore, ecological and human-mediated prospects for the spread of the pathogen in eastern Africa exist, and efforts at managing the spread of the disease need to be implemented urgently.

In conclusion, the presence of ACP in addition to CLas associated HLB in Ethiopia highlights a significant threat to citrus production in Africa. The proliferation of the disease is accelerated by the presence of the vector; therefore, the management of the disease is linked inherently to the control of the vector coupled with the removal of inoculum. Urgent control strategies targeted at the control of the pest to curb its spread to other citrus-growing areas in the low-altitude regions in the country need to be implemented. Increased surveillance in citrus-producing areas where neither the disease nor the vector has been detected needs to be carried out as well as the establishment of insect-free citrus nurseries with HLB-free seedlings. Furthermore, treatment of ACP infested orchards with systemic insecticides such as imidacloprid may be useful in reducing the pest population. Additionally, phytosanitary and quarantine measures need to be enforced strictly to restrict the movement of citrus plants within the region. Further research into the genetic diversity and invasion history of ACP into Africa are needed to elucidate the population structure and invasion history of ACP in Africa in order to develop a sustainable management strategy for HLB within the continent.

First report of field population of *Trioza erytreae* carrying the Huanglongbing associated pathogen, "*Candidatus* Liberibacter asiaticus", in Ethiopia.

***Disease note: Submitted to Plant disease Journal**

African Citrus greening is a destructive disease of citrus that has been reported in South Africa since the 1920s. The disease is associated with "*Candidatus* Liberibacter africanus" (CLaf) and is transmitted by *Trioza erytreae* (McClean, 1974; Cook et al., 2014). The related bacteria *"Candidatus* Liberibacter asiaticus" (CLas), which is associated with the much more severe

Huanglongbing disease and is transmitted by *Diaphorina citri,* was recently reported in Ethiopia (Saponari et al., 2010). Experimentally, *T. erytreae* has been proven to transmit CLas (Massonié et al., 1976), but natural occurrence of CLas in field populations of this psyllid has not been reported. A survey was conducted for the citrus greening vector *T. erytreae* in the Amhara region of Ethiopia in November 2017. *Trioza erytreae* adults were identified as per the descriptions of OEPP/EPPO, (2005). Sampling sites included large and small-scale citrus orchards (in both the highland and lowland areas), and citrus trees grown in backyard gardens. *T. erytreae* were found and collected from sweet orange, lemon and tangerine trees in backyard gardens and a small-scale commercial orchard. Voucher specimens were deposited at the International Centre of Insect Physiology and Ecology repository. Adult *T. erytreae* collected were screened for the presence of various strains of Liberibacter bacteria. The samples were surface-sterilised using 3% sodium hypochlorite and rinsed with distilled water. Genomic DNA was extracted from individual insects using the Isolate II Genomic DNA Kit (Bioline, United Kingdom), following the manufacturer's instructions. Leaf samples from citrus trees on which the psyllids were collected were also tested and plant total DNA was extracted from individual petioles. DNA quality and quantity checks were performed using a Nanodrop 2000/2000c Spectrophotometer (Thermo Fischer Scientific, USA). Conventional PCR assays were done to amplify the 50s ribosomal protein L10 gene region (*rplA-rplJ*) of CLas and CLaf using primers A2 and J5 (Hocquellet et al., 1999), generating the expected 650-bp product from 70 insect samples and the plant samples from each site. Amplicons were purified and bi-directionally sequenced. The *rplA-rplJ* sequences were aligned with reference CLas sequences retrieved from GenBank (www.ncbi.nlm.nih.gov/genbank/) using the MUSCLE tool in MEGA X (Kumar et al., 2018). Sequences from this study (GenBank Accession No. MH809485) had a 100% base-pair match with CLas (GenBank Accession No. MG418842.1). A maximum likelihood phylogenetic tree constructed for the ribosomal protein gene sequences revealed that the Liberibacter obtained from *T. erytreae* clustered with CLas and clustered separately from CLaf and *Candidatus* Liberibacter solanacearum species (Fig 4.4). To the best of our knowledge, this is the first report of field populations of *T. erytreae* carrying CLas in Ethiopia. Furthermore, the detection of CLas (initially reported to be solely transmitted by *D. citri*) in sweet orange, lemon and tangerine trees in an area with the presence of *T. erytreae* highlights the potential of this psyllid to transmit CLas. Therefore, this study provides new insight into a possible alternate route of proliferation of CLas in the absence of *D. citri* and it raises the need to determine the transmission efficiency, vector competency and the vector-pathogen relationships in field populations of the psyllid (*T. erytreae*).

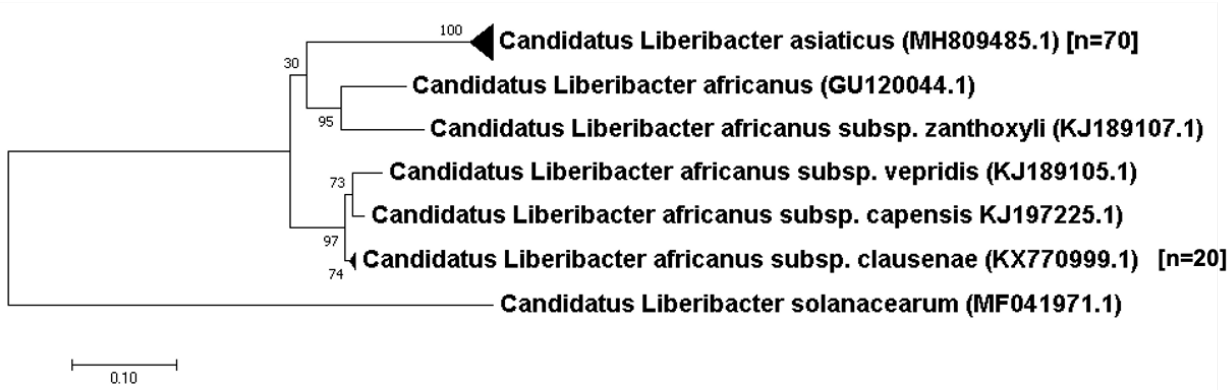

Figure 4.5. Maximum-Likelihood tree based on a 650 bp alignment of 70 sequences of the Liberibacter 50S ribosomal protein L10 (rplA-rplJ) gene from *Trioza erytreae* samples collected from Ethiopia compared to species of the genus Liberibacter. Bootstrap values based on 1000 replicates are indicated at branches, GenBank accession numbers are shown on the tree for sequences included in analyses. The number of sequenced Liberibacter positive samples is indicated in brackets. *Candidatus* Liberibacter solanacearum was used as the outgroup.

Table 4.3. Detection of "*Candidatus* Liberibacter asiaticus" by conventional PCR in specimens of *Trioza erytreae* and citrus plants collected in Ethiopia

Region	**Location**	**Latitude, Longitude**	**Altitude (m.a.s.l)**	**PCR +/Total psyllids tested**	**Plants Tested (PCR)**	**Host plant species**	**Symptoms**	**Citrus system**
Amhara	Dangila	11.26105, 36.84836	2116	12/15	Positive	Sweet orange	Leaf galls	Urban backyard trees
Amhara	Shuwabere	11.35555, 36.95422	1979	10/15	Positive	Lemon	Leaf galls	Urban backyard trees
Amhara	Insude	11.41575, 37.16275	1959	10/15	Positive	Tangerine	Leaf galls, dieback	Rural backyard trees
Amhara	Achabere	11.48809, 37.29512	1983	12/15	Positive	Sweet orange	Leaf galls, dieback	Rural backyard trees
Amhara	Zenzelima	11.598, 37.44383	1868	11/15	Positive	Sweet orange	Leaf galls, yellowing	Small-scale commercial orchard
Amhara	Sasaberete	11.60664, 37.45234	1892	15/15	Positive	Sweet orange	Leaf galls, dieback	Rural backyard trees

Chapter Five: Comparative Analyses of *Diaphorina citri* Mitogenome revealed two different African Populations which are linked to Populations from USA and China

Abstract

The Asian citrus psyllid (*Diaphorina citri* Kuwayama) is a key pest of *Citrus* sp. Worldwide, as the vector for "*Candidatus* Liberibacter asiaticus" (CLas), the bacterial pathogen which causes citrus Huanglongbing (HLB). *D. citri* has been reported in Kenya, Tanzania and more recently in Ethiopia. An assessment of the diversity of *D. citri* in Africa in relation to populations from Asia and America will give an insight into the source of introduction of the psyllid into Africa. In this study, populations of *D. citri* were obtained from China, Ethiopia, Kenya, Tanzania and USA. Next generation sequencing was done on psyllid DNA samples and the mitochondrial genome (mitogenome) sequences from each of the populations were obtained. Each mitogenome contained 13 protein coding genes, two ribosomal RNA and 21 transfer RNA genes. Our analysis identified two groups, with the *D. citri* mitogenome sequences from Kenya, Tanzania and China being identical to the reference mitogenome from China (99.9%) but had a 3% dissimilarity with the sequences from Ethiopia and USA which was identical (99.9%) to the *D. citri* reference mitogenome from USA. Further analyses of the tRNA genes confirmed the variation between the two clusters. We conclude that the *D. citri* populations in Africa have different origins. The Ethiopian *D. citri* population has its origins from USA while the Kenyan and Tanzanian populations have their origins from China.

Introduction

The Asian citrus psyllid, *Diaphorina citri* (Kuwayama) (Hemiptera: Psyllidae), is one of the most destructive pests of citrus worldwide. *Diaphorina citri* causes direct damage to citrus plants through feeding, which results in curling and notching of leaves, and the production of honeydew by the insect on the plant encourages the growth of sooty mold. The most damaging activity of the psyllid is the transmission of the phloem-limited bacterium "*Candidatus* Liberibacter asiaticus" (CLas), the pathogen responsible for Huanglongbing (HLB) (Bové, 2006). CLas is widespread in Asia, North and South America (Grafton-Cardwell, Stelinski, & Stansly, 2013; Halbert & Manjunath, 2004; Hall et al., 2013).

HLB transmitted by *D. citri* is a major phytosanitary concern worldwide and has been responsible for the destruction of several citrus industries in Asia and America (Manjunath et al., 2008). In Africa, CLas was reported for the first time in Ethiopia (Saponari et al., 2010) but *D. citri,* its primary vector, was not detected in the country at that time. CLas was later reported in

Uganda (Kalyebi et al., 2016) but the results represented a misidentification (Roberts et al., 2017). More recently, the pathogen was detected in Kenya (Ajene et al., 2020a).

Diaphorina citri was shown to transmit the HLB pathogen in India, the Philippines (Capoor & Viswanath 1967, Martinez & Wallace 1967), and China (Guangdong Agriculture and Forestry College, 1977). The geographic origin of *D. citri* is likely Southwest Asia (Halbert & Manjunath, 2004, Beattie et al., 2009). The insect has been now reported in 55 countries across Asia, Africa, the Americas and Oceania (EPPO 2020). *Diaphorina citri* was first detected in Florida in 1998, and it was subsequently detected in other parts of the south-eastern USA (French Kahlke & Da Graca 2001, Halbert et al. 2002).

The genetic diversity of *D. citri* populations from different geographical regions has been mostly assessed using mitochondrial cytochrome oxidase 1 (*COI*) sequences (De León et al. 2011, Boykin et al. 2012, Guidolin & Consoli, 2013, Lashkari et al. 2014). This strategy showed that the presence of *D. citri* in the Americas resulted from two separate introductions of (De León et al. 2011). Furthermore, two major mitochondrial groups have been identified between south-western and south-eastern Asia, allowing for the tracing back the *D. citri* invasion of Florida (USA) and Mexico to south-western Asia (Boykin et al. 2012).

In Africa, *D. citri* was first detected in 2016 in Tanzania (Shimwela et al., 2016), and subsequently in Kenya in 2017 (Rwomushana et al., 2017), and Ethiopia in 2019 (Ajene et al., 2020b). Due to the relatively recent dispersal of *D. citri* into Africa, the genetic diversity and phylogeographic structure of the psyllid in the continent are largely unknown.

Currently, there is no cure for HLB, and prevention of further spread of the disease calls for the management of the psyllid vector. Insights into the genetic diversity and phylogeographic of the insect may inform the design of successful control strategies and contribute to elucidate the invasion history of the species. This work focused on the comparison of new and publicly available mitogenomic and *COI* sequence data of *D. citri* collected in Africa with counterparts from China and the USA.

The objective of this study was to assess the diversity and phylogeography of *D. citri* in Africa as the species represents a new introduction to the continent, by exploring variations in the mitochondrial genome of *D. citri* from the three African countries (Ethiopia, Kenya and Tanzania) where it has been detected in comparison to *D. citri* mitogenomes from China and the USA and the phylogeny of the African *D. citri* based on *COI* and *16S rRNA* gene sequences from publicly available global accessions, with the aim of gaining insights into the invasion history of the species.

Methods

Sample collection and DNA extraction.

Field surveys were carried out for *D. citri* in citrus orchards and backyard gardens in, Ethiopia, Kenya and Tanzania from March 2017 to December 2018. Psyllids encountered were aspirated from the trees and stored in vials with 96% ethanol for later DNA extraction. For the USA samples, psyllids were obtained from the Kingsville Citrus Centre, Texas A&M University (received in alcohol preservation). The psyllids from China were obtained from Fuzhou, Fujian Province, China (received in alcohol preservation) (Appendix 13). Geographic positioning coordinates (GPS) of the sampling sites were obtained using a Garmin eTrex20 instrument (GARMIN, USA) and recorded for each site. One adult specimen representative of the species was imaged and deposited in Biosystematics unit at the International Center of Insect Physiology and Ecology Nairobi, Kenya. One adult specimen per country (China, Ethiopia, Kenya, Tanzania and USA) was randomly chosen for next-generation sequencing (NGS). Total DNA was individually extracted from each adult specimen using the Isolate II Genomic DNA Kit (Bioline, London, UK). DNA extracts were stored at -20°C until further analysis.

Mitogenome sequencing, assembling and annotation.

Total DNA from each of the five specimens was sequenced separately by Macrogen Inc Europe (The Netherlands) using Illumina MiSeq (Illumina, San Diego, CA). Mapping and assembly of the *D. citri* mitogenome sequences was performed in Geneious Prime version 2019.0.4. (https://www.geneious.com) (Kearse et al., 2012). The NGS reads for each sample were mapped and assembled using a publicly available mitochondrial genome sequence of *D. citri* as reference (KU647697). The open reading frames of protein-coding genes (PCGs) were identified using Geneious Prime, with the invertebrate mitochondrial genetic code. Transfer RNAs (tRNAs) were predicted with tRNAscan-SE v.1.21 and ARWEN v.1.2 (http://130.235.244.92/ARWEN/) (Lowe and Eddy 1997, Laslett and Canbäck 2008), using the default composite metazoan mitochondrial code. Overlapping regions and intergenic spacers were counted manually. Nucleotide composition, and AT- and GC-skews were calculated using Geneious Prime, as AT-skew = (A-T)/(A+T) and GC-skew = (G-C)/(G+C).

Comparison of mitogenome nucleotide sequences and Phylogenetic Analyses

The five new *D. citri* complete mitogenome sequences were aligned with two publicly available sequences from China (KU647697) and USA (KY426015) using MAFFT (Katoh et al., 2013) for the identification of single nucleotide polymorphisms (SNPs) within the PCGs and the

tRNAs. To assess the genetic divergence of the African *D. citri* mitogenomes, Multiple sequence alignments of the sequences obtained and 31 publicly available mitogenome sequences (Appendix 14) was performed using MAFFT. Mean genetic distances between the sequences was calculated using p-distances in MEGA X. Standard errors were obtained using 1,000 bootstrap replicates. Multidimensional scaling analysis was carried out using the 'cmdscale' function in R software version 3.5.1 (R development core team 2008) on the genetic distance matrix to generate the plot for principal coordinate axis (PCoA). The tRNA genes were predicted by their cloverleaf secondary structure.

Phylogenetic analyses

The phylogeographic structure of *D. citri* was assessed using a compilation of all the *COI* and 16S rRNA sequences publicly available on GenBank as for October 2019 (Appendix 15). Multiple sequence alignments were performed using the MAFFT algorithm available in Geneious Prime. The final sequence alignment was used to construct a median-joining (MJ) network using Network software version 5 (http://www.fluxus-engineering.com/sharenet.htm), under the default settings (Bandelt, Forster and Röhl, 1999). Genetic divergence among the haplogroups displayed in the MJ network were calculated as pairwise distances (p-distances) using MEGA X (Kumar et al., 2018). A Maximum likelihood (ML) tree was also constructed as an alternative display of the relationships among the sequences. The ML tree was constructed using MEGA X based on the Tamura 3-parameter model (T92) (Tamura, 1992), with 1,000 bootstrap replicates.

Results

NGS, mapping and assembly of complete *D. citri* mitogenomes

The Illumina MiSeq run resulted in an average of 17.6 million reads for each sample, with an average read length of 151 bp. Average GC and AT content were 41% and 59%, respectively. Average Q20 (ratio of bases with phred quality score > 20) was 99% and average Q30 (ratio of bases with phred quality score > 30) was 95% (Appendix 16). The number of assembled reads ranged from 183,235 (China), 95,804 (Ethiopia), 164,94 (Kenya), 41,125 (Tanzania) and 115,700 (USA). Sequence average coverage ranged from 414x (Tanzania), 965x (Ethiopia), 1,165x (USA), 1,661x (Kenya) to 1,845x (China) (Fig. 5.1).

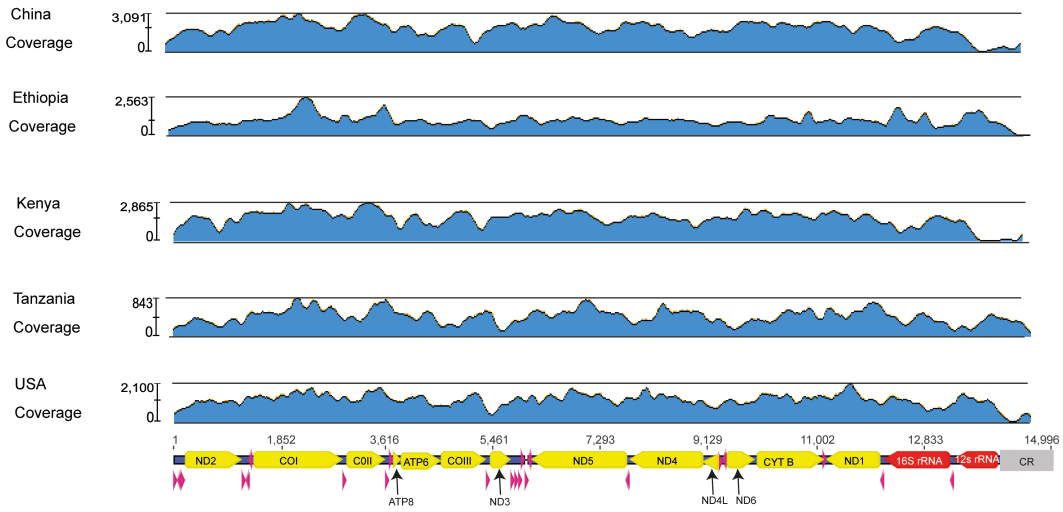

Figure 5.1. Schematic representation of mitogenome sequences coverage of *Diaphorina citri* from China, Ethiopia, Kenya, Tanzania and USA in reference to publicly available *Diaphorina citri* mitogenome sequence (KU647697).

General features of the *D. citri* mitogenomes

As expected, the mitogenomes of *D. citri* were identical in the main features, and had the typical Metazoan complement of 13 (protein-coding genes) PCGs, 22 transfer RNA (tRNA) genes, two ribosomal RNA (rRNA) genes, and an AT-rich non-coding region generally assumed to contain the control for transcription and replication. The complete mitogenome sequences had an average total size of 14,995 bp, similar to the length of the *D. citri* mitogenome (KU647697) used as a reference in the mapping and assembly (14,996 bp). The gene order was identical to the previously reported *D. citri* mitogenomes and the other species in the family Psyllidae, and identical to the hypothetical ancestral mitogenome organisation in insects (Boore, 1999). Twenty-three genes were located on the majority strand (J-strand), and the other 14 genes on the minority strand (N-strand) (Fig. 5.2).

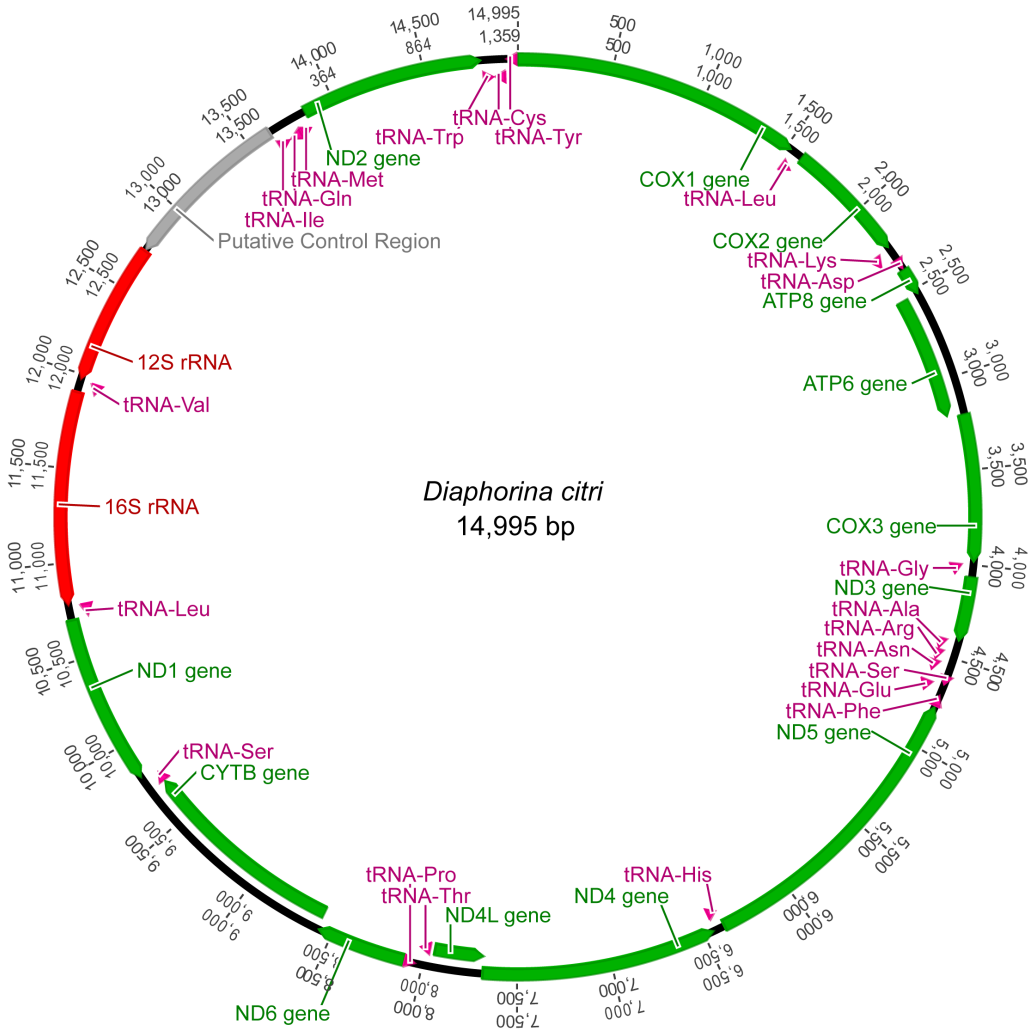

Figure 5.2. General organization of the complete mitochondrial genome of the Asian citrus psyllid *Diaphorina citri* (Hemiptera: Psyllidae). The arrows represent the direction of the genes.

Protein-coding genes, Non-coding AT-rich, intergenic and overlapping regions

The average combined length of the 13 protein coding genes (PCGs) was 10,798 bp, and varied between ND5 (1,618 bp) and ATP8 (153 bp) (Table 1). The size of the PCGs were similar to the other members of the family Psyllidae, which had an average combined PCG length of 10,814 bp. The large rRNA gene (16s rRNA; 1,134 bp) was located between $tRNA^{Leu1}$ and $tRNA^{Val}$, and the rRNA gene (12s rRNA; 758 bp) was located between $tRNA^{Val}$ and the AT-rich region The large rRNA gene (16s rRNA; 1,134 bp) was located between tRNALeu1 and tRNAVal, and the rRNA gene (12s rRNA; 758 bp) was located between tRNAVal and the AT-rich region. The large rRNA gene (16s rRNA; 1,134 bp) was located between $tRNA^{Leu1}$ and $tRNA^{Val}$, and the rRNA gene (12s rRNA; 758 bp) was located between $tRNA^{Val}$ and the AT-rich region (Table 5.1). The complete complement of 22 tRNAs was successfully identified with ARWEN software, and tRNA sizes varied between 56 bp ($tRNA^{Ser1}$) and 70 bp ($tRNA^{Lys}$). The typical clover-leaf structure was predicted for all tRNAs except $tRNA^{Ser1}$, for which the DHU arm was

reduced to a simple loop, as commonly observed in metazoans (Bernt, Braband, Schierwater, & Stadler, 2013) (Fig. 5.3).

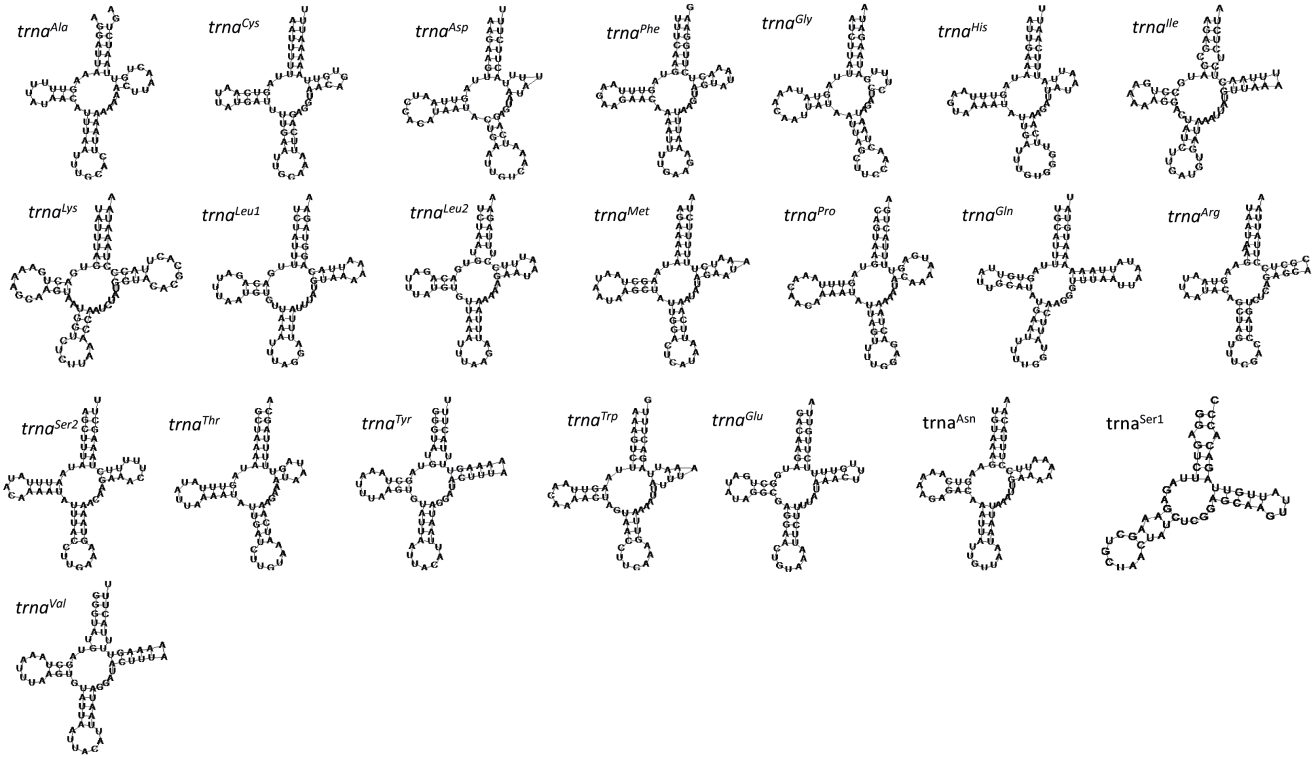

Figure 5.3. Predicted structure of the 22 tRNAs in the complete mitochondrial genome of the Asian citrus psyllid *Diaphorina citri* (Hemiptera: Psyllidae). Inferred canonical Watson-Crick bonds are represented by lines.

The five mitogenomes were equally compact, with 10 short gene overlaps (maximum overlap = 11 bp between $tRNA^{Glu}$ and $tRNA^{Phe}$). Intergenic regions were found at nine locations representing a total average of 69 bp, the longest of which was between $tRNA^{ser}$ and *ND1* (24 bp). The largest non-coding region (902 bp), located between the *12s rRNA* and the $tRNA^{Ile}$-$tRNA^{Gln}$-$tRNA^{Met}$ cluster, was annotated as the AT-rich region (Table 5.1).

Table 5.1. Gene composition and order of the complete mitochondrial genomes of the Asian citrus psyllid *Diaphorina citri* (Hemiptera: Psyllidae) collected in China, Ethiopia, Kenya, Tanzania and the USA. N – majority strand; J – minority strand; IGN – number of intergenic nucleotides (negative values indicate overlapping between genes).

Gene	Code	Start	Stop	Strand	Coordinates	Size bp	IGN
COI		ATG	TAA	J	1-1530	15330	2
$tRNA^{Leu2}$	L2	-	-	J	1534-1594	61	3
COII		ATT	T--	J	1595-2258	664	-
$tRNA^{Lys}$	K	-	-	J	2259-2328	70	-
$tRNA^{Asp}$	D	-	-	J	2327-2387	61	-2
ATP8		ATA	TAA	J	2388-2540	153	-

ATP6		ATG	TAA	J	2534-3208	675	-7
COIII		ATG	TAA	J	3208-3990	783	-1
tRNA^{Gly}	G	-	-	J	4003-4065	63	12
ND3		ATA	T--	J	4064-4414	351	-2
tRNA^{Ala}	A	-	-	J	4413-4472	60	-2
tRNA^{Arg}	R	-	-	J	4473-4533	61	-
tRNA^{Asn}	N	-	-	J	4534-4601	66	-
tRNA^{Ser1}	S1	-	-	J	4601-4656	56	-1
tRNA^{Glu}	E	-	-	J	4657-4717	61	2
tRNA^{Phe}	F	-	-	N	4707-4768	62	-11
ND5		AAC	ACA	N	4769-6386	1618	-
tRNA^{His}	H	-	-	N	6387-6446	60	-
ND4		ACA	TAA	N	6447-7690	1244	-
ND4L		AAT	TAA	N	7685-7959	276	-5
tRNA^{Thr}	T	-	-	J	7973-8036	64	13
tRNA^{Pro}	P	-	-	N	8035-8100	66	2
ND6		ATA	TAA	J	8103-8585	483	2
CYTB		ATA	TAG	J	8579-9721	1141	7
tRNA^{Ser2}	S2	-	-	J	9720-9782	63	-2
ND1		ATA	TAG	N	9807-10714	909	24
tRNA^{Leu1}	L1	-	-	N	10716-10779	64	1
16s rRNA		-	-	N	10780-11913	1136	-
tRNA^{Val}		-	-	N	11914-11977	64	-
12s rRNA		-	-	N	11978-12735	758	-
AT-Rich region		-	-	N	12736-13637	902	-
tRNA^{Ile}	I	-	-	J	13638-13702	65	-
tRNA^{Gln}	Q	-	-	N	13708-13774	67	5
tRNA^{Met}	M	-	-	J	13775-13839	65	-
ND2		ATA	TAA	J	13840-14809	970	-2
tRNA^{Trp}	W	-	-	J	14810-14870	61	-
tRNA^{Cys}	C	-	-	N	14871-14932	62	-
tRNA^{Tyr}	Y	-	-	N	14932-14993	62	-2

Nucleotide composition and strand asymmetry

The complete mitogenomes had the high A+T content typically found of insects, with values higher than 74.3% (complete sequence) in all genes (Appendix 17).The average A+T content of the AT-rich region (85.9%) was higher than the average for the complete sequence (74.4%), the combined tRNAs (75.1%) and the two rRNAs (76.9%). The nucleotide composition of the five mitogenomes showed that all PCGs had negative GC-skews. Four PCGS (*ND5, ND4, ND4L* and *ND1*) had positive AT-skews while nine PCGs (*COII, ATP6, ATP8, COIII, ND3 ND6, CYTB* and *ND2*) had negative AT-skews.

Comparison of *D. citri* mitogenomes from Africa, China and the USA

In the PCGs, the highest number of single nucleotide polymorphisms (SNPs) among the mitogenomes of *D. citri* was observed in *COI*, *ND4* and *ND5*, whereas *ND4L* was completely conserved. In Africa, Kenya and Tanzania had almost identical mitogenomes which diverged from Ethiopia by 40 SNPs (nucleotide pairwise differences = 0.44%). The mitogenomes from the USA (KY426015) and Kenya/Tanzania had an average of 39 SNPs. In contrast, there was only one SNP between USA (KY426015) and Ethiopia. The mitogenome from China (KU647697) was highly similar to Kenya and Tanzania, with an average of only three SNPs. In contrast, China (KU647697) and Ethiopia were separated by 40 SNPs (Fig. 5.4). The sequences from Kenya and Tanzania diverged from the sequence from China by 0.12% and diverged from the sequence from USA by 0.43%. The sequence from Ethiopia diverged from the sequence from China by 0.43% and diverged from the sequence from USA by 0.05% (Table 5.2). The new sequences from China, Kenya and Tanzania (hereon referred to as Group 1) and the new sequences from Ethiopia and USA (hereon referred to as Group 2) were separated by an average of 39 SNPs (0.41% nucleotide pairwise differences) (Fig. 5.5)

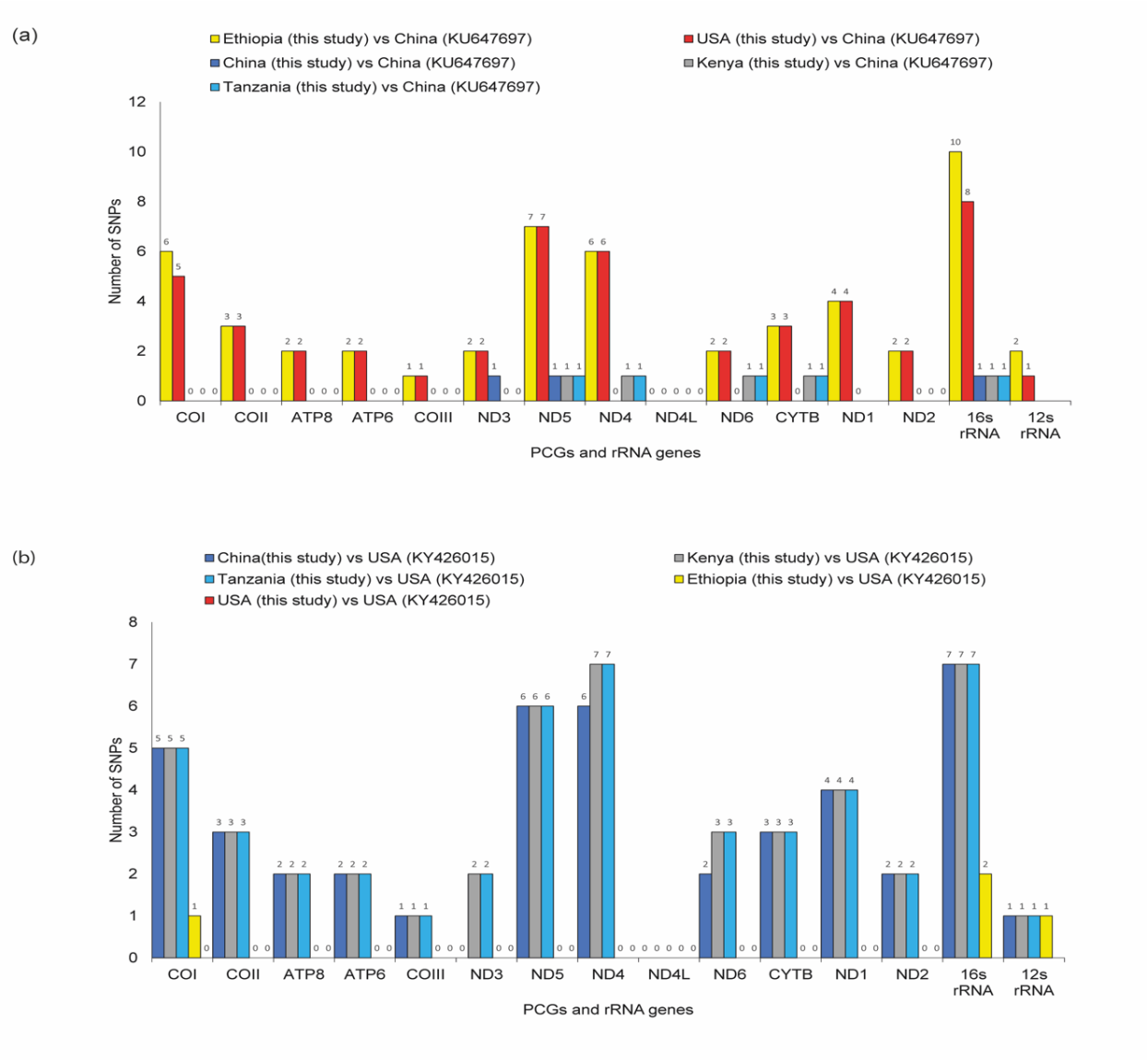

Figure 5.4. Nucleotide pairwise differences in the mitochondrial protein coding genes (PCGs) and ribosomal RNA (rRNA) genes between five *Diaphorina citri* mitogenomes generated in this study and (a) a reference mitogenome from China and (b) a reference mitogenome from USA.

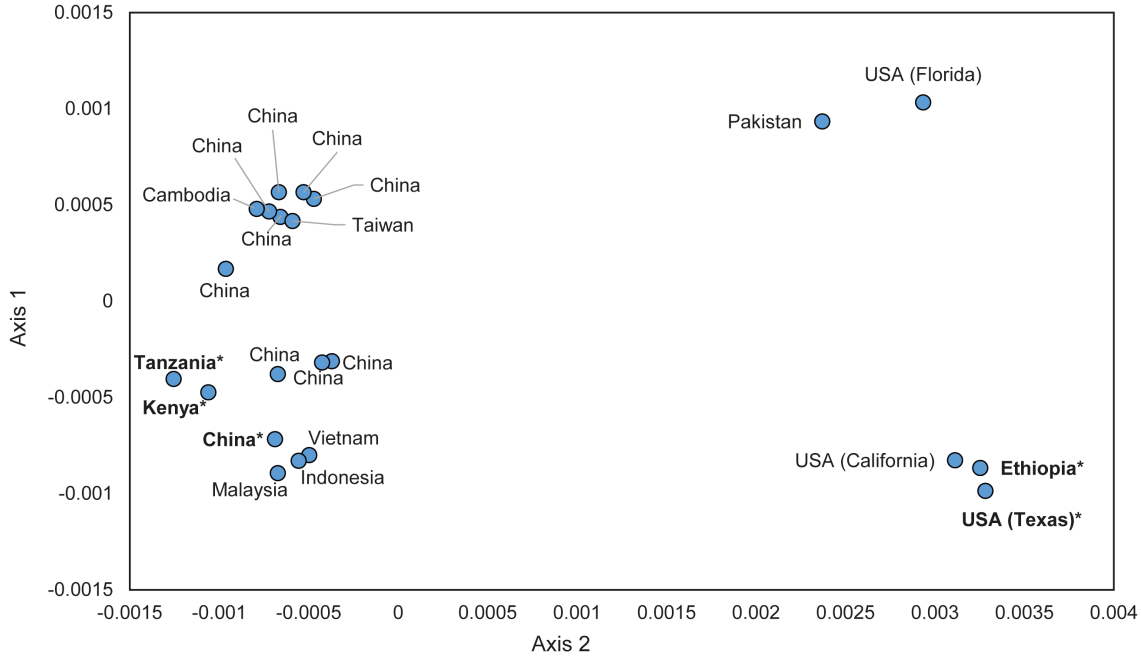

Figure 5.5. Principal Coordinate Analysis (PCoA) plot representing the genetic distances among *Diaphorina citri* mitogenome sequences from China, Ethiopia, Kenya, Uganda, USA and publicly available sequences in GenBank computed using the classic multidimensional scaling function 'cmdscale' in R version 3.5.1.

Table 5.2. Genetic divergence of complete mitochondrial genome among Asian citrus psyllid *Diaphorina citri* (Hemiptera: Psyllidae) from China, Ethiopia, Kenya, Tanzania and USA (in bold) and publicly available *Diaphorina citri* calculated as percentage of pairwise distances (p-distances) under the Tamura 3-parameter model.

		1	2	3	4	5	6	7	8	9	10	11	12	13
1	China	-												
2	Vietnam	0.001	-											
3	Taiwan	0.000	0.001	-										
4	Pakistan	0.003	0.003	0.003	-									
5	Malaysia	0.001	0.000	0.001	0.004	-								
6	Indonesia	0.001	0.000	0.001	0.003	0.000	-							
7	USA	0.004	0.004	0.003	0.001	0.004	0.004	-						
8	Cambodia	0.001	0.001	0.000	0.003	0.001	0.001	0.004	-					
9	**China***	0.001	0.000	0.001	0.004	0.001	0.000	0.004	0.001	-				
10	**Kenya***	0.001	0.001	0.001	0.004	0.001	0.001	0.004	0.001	0.001	-			
11	**USA***	0.004	0.004	0.004	0.001	0.004	0.004	0.001	0.004	0.004	0.004	-		
12	**Ethiopia***	0.004	0.003	0.004	0.001	0.004	0.004	0.001	0.004	0.004	0.004	0.000	-	
13	**Tanzania***	0.001	0.001	0.001	0.004	0.001	0.001	0.004	0.001	0.001	0.000	0.004	0.005	-

The total number of substitutions between the two groups (39) showed 34 transitions and five transversions (Appendix 18). The analyses of the tRNA sequences between Group 1 and Group 2

showed variation in three tRNAs: a U-C change in the TΨC in *tRNA*^{Phe}, an additional A on the TΨC in in *tRNA*^{Asn} (Group 1), and a U-C change in the variable loop of *tRNA*^{Ser1} (Fig. 5.6)

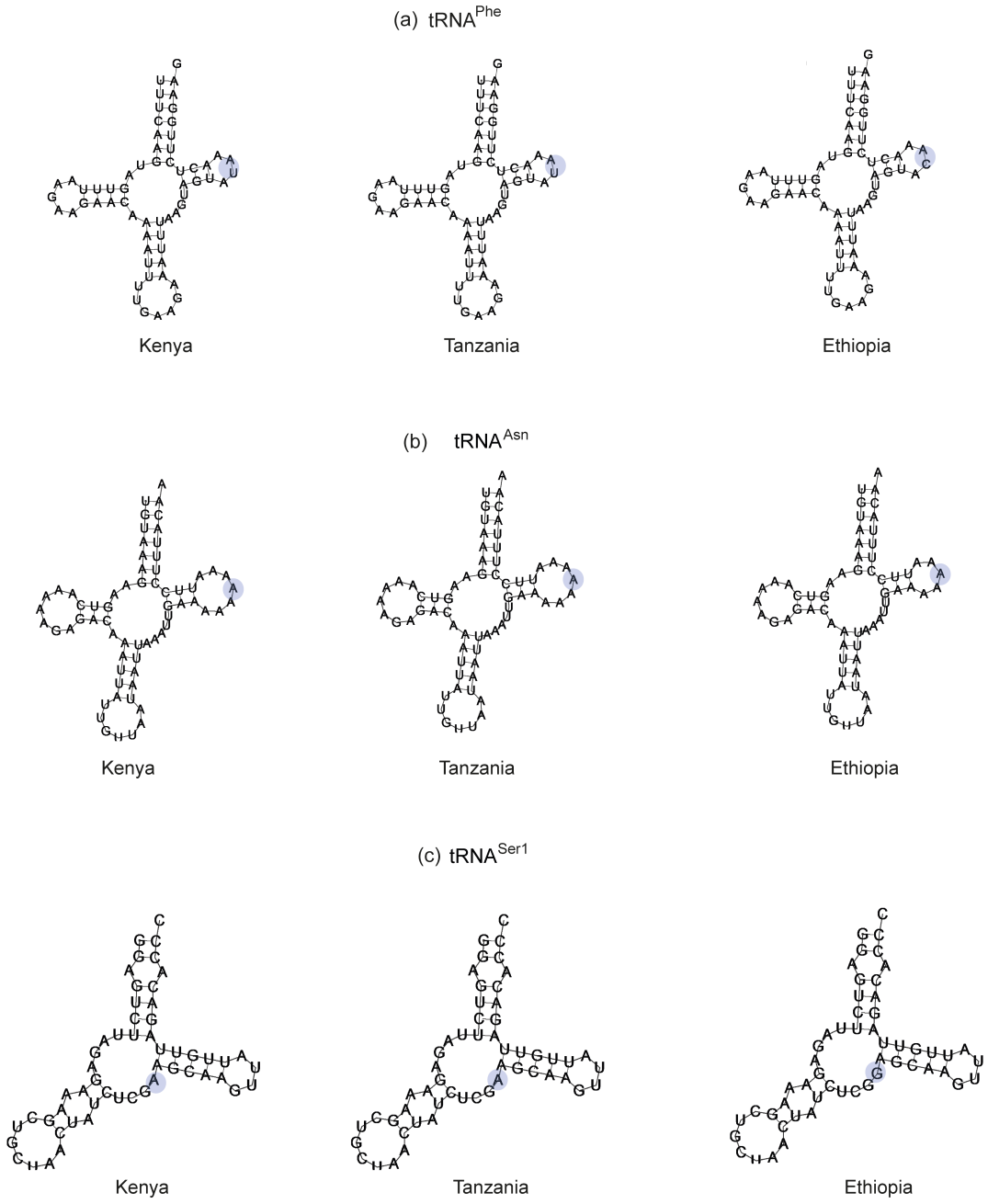

Figure 5.6. Variation in the secondary structures of the tRNA genes (a) *trna*^{Phe} (b) *trna*^{Asn} (c) *trna*^{Ser1}, as predicted in the mitochondrial genome of *Diaphorina citri* from Africa. Bases highlighted in blue indicated the difference in structure among tRNAs from Ethiopia, Kenya and Tanzania.

Phylogeographic structure and genetic diversity of *D. citri*

The phylogeographic structure of *D. citri* in Africa was assessed in the context of *COI* and *16S rRNA* sequences generated in previous studies from specimens collected in Asia and the Americas. using a median-joining (MJ) network, a maximum-likelihood (ML) tree and a principal coordinate analysis (PCoA) plot.

The MJ network showed a total of 21 haplotypes distributed among Africa, Asia and the Americas. Sequences from Asia comprised of 12 haplotypes with five shared haplotypes and seven singletons (China (H5, H7, H10, H11), India (H16), Pakistan (H4), Thailand (H9), sequences from the Americas comprised 13 haplotypes with five shared haplotypes and eight singletons (Argentina (H17), Brazil (H2, H20 and H21), Guadeloupe (H1), Mexico (H8), and USA (H15 and H18) (Fig 5.7).

The largest haplotype (H6) comprised of sequences from all the regions except the middle east sequences (Iran and Saudi Arabia), Guadeloupe, Paraguay and Ethiopia. The Asian sequences that had shared haplotypes (H3, H12, H13 and H19)with the sequences from the Americas were the southwest and middle east Asian sequences (India, Pakistan, Iran and Saudi Arabia). The new sequences from Kenya, Tanzania and China shared the same haplotype (H6) with sequences from China and 12 other countries (Argentina, Brazil, Cambodia, India, Indonesia, Malaysia, Mexico, Pakistan, Thailand, Taiwan, USA and Vietnam. The sequence from Ethiopia represented a singleton (H14), while the new sequence from USA shared the same haplotype with the public sequences from USA, Puerto Rico, Mexico, Guadeloupe, India and Iran (H13) (Fig. 5.8).

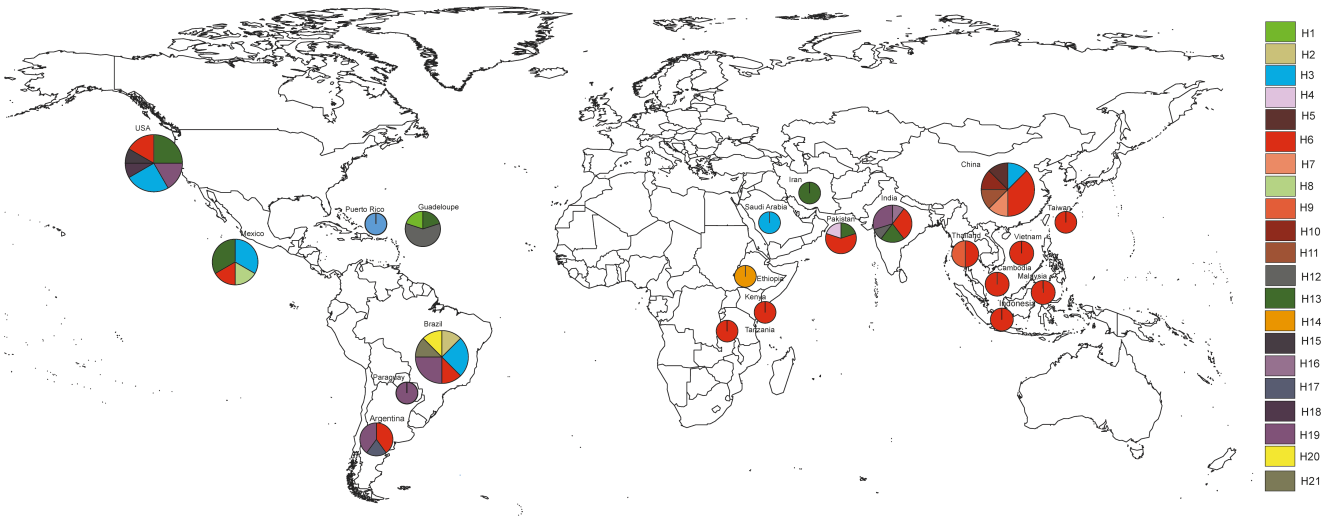

Figure 5.7. Geographic distribution of *Diaphorina citri* cytochrome c oxidase subunit 1 haplotypes of (n = 62), showing the phylogeographic structure

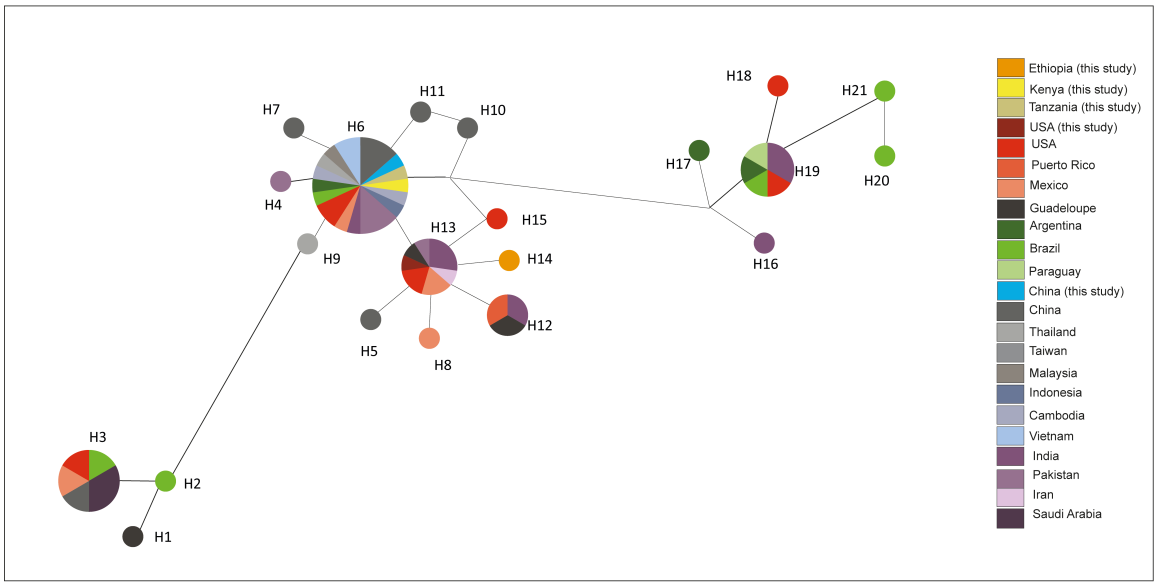

Figure 5.8. Median-joining network of cytochrome c oxidase subunit 1 (*COI*) gene (874 bp) of *Diaphorina citri* (n = 62), showing the relationships between haplotypes according to geographic origin. The size of the circles is proportional to the number of individuals sharing the same haplotype.

The *COI* ML tree recovered three distinct branches (Branch I-III). The new sequences, represented by the 12 closely related haplotypes (H4 – H15) seen in the MJ network, formed Branch I, along with most sequences from Asia, the Americas and the Caribbean. Branch II was also formed by sequences from Asia, the Americas and the Caribbean. Branch III was formed by six haplotypes (H16 – H21) exclusively from Asia and the Americas (Fig 5.9).

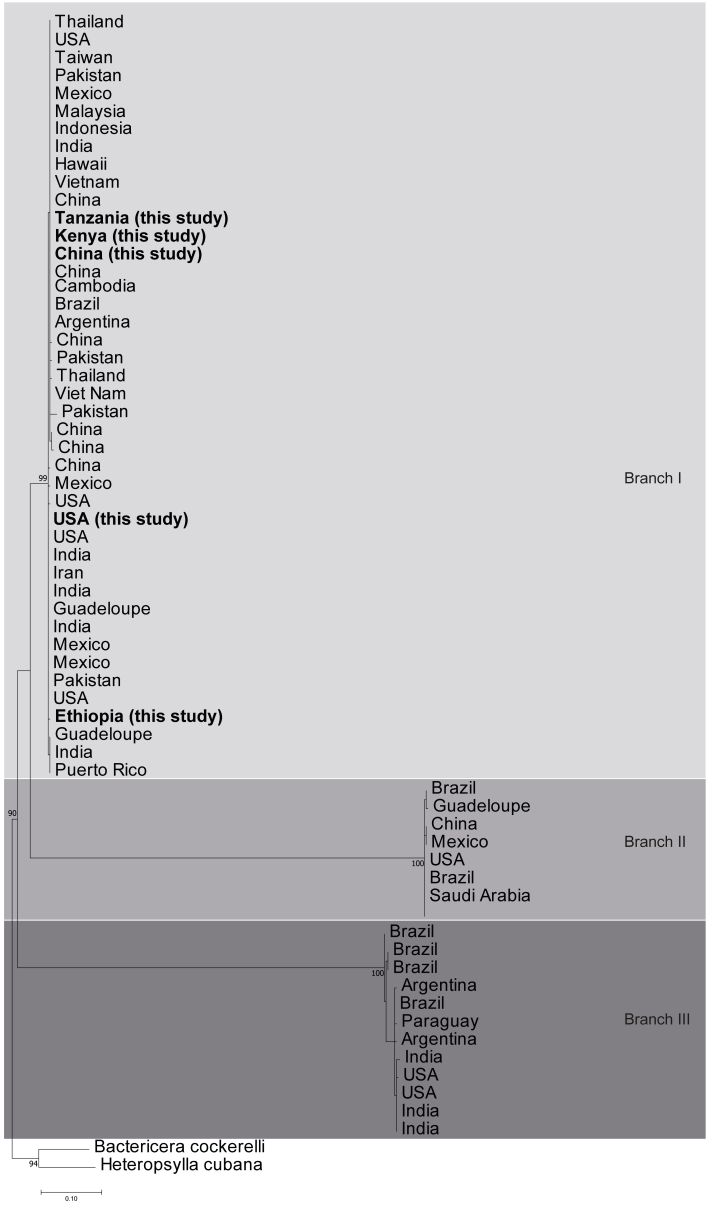

Figure 5.9. Maximum likelihood tree showing the relationships among haplotypes of *Diaphorina citri* from Africa and other world regions. The tree was constructed using an 874-bp alignment of cytochrome oxidase 1 sequences with *Bactericera cockerelli* and *Heteropsylla cubana* as outgroups. Nodal support was calculated using 1,000 bootstrap replicates.

The ML tree based on the *16S rRNA* sequences, recovered two distinct branches. The new sequences from China, Kenya and Tanzania formed one Branch, along with all sequences from Asia while the second branch was formed by the new sequence from Ethiopia and sequences from USA and Pakistan (Fig 5.10).

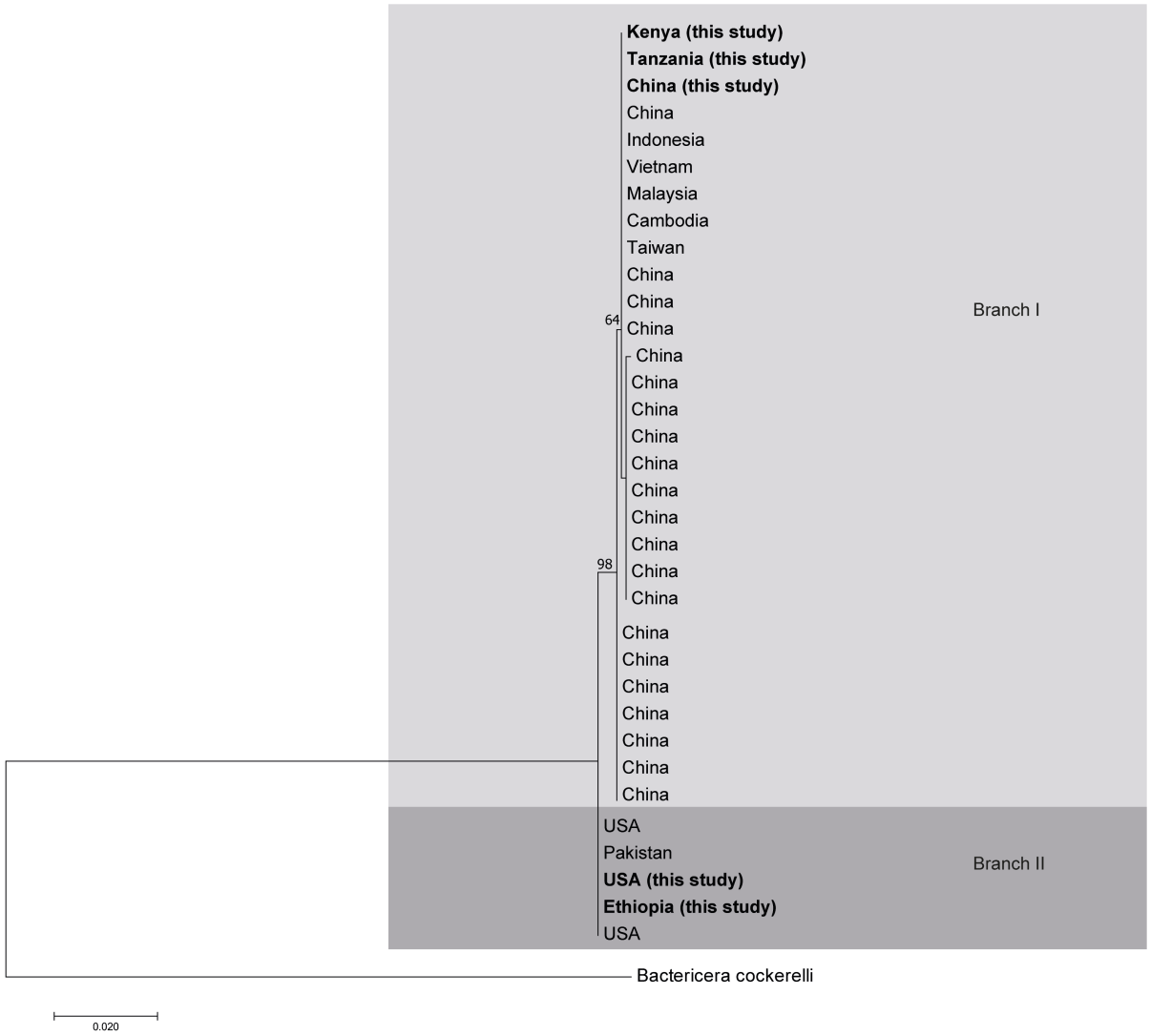

Figure 5.10. Maximum likelihood tree showing the relationships among *Diaphorina citri* from Africa and other world regions. The tree was constructed using a 1,500-bp alignment of 16s ribosomal RNA sequences with *Bactericera cockerelli* an outgroup. Nodal support was calculated using 1,000 bootstrap replicates. The length of the branches is proportional to the number of substitutions per site.

In the pairwise genetic distance analyses of the *COI* sequences, the divergence of the Ethiopian *D. citri* sequence was evident. The singleton *D. citri* sequence from Ethiopia in this study had a lower genetic divergence from the sequence from USA (0.24%) than the Kenyan, Tanzanian and Chinese *D. citri* sequences (0.72%). (Table 5.3).The principal component analysis (PCoA) plot based on genetic distances showed an overlap of the new and publicly available *D. citri* from China, Kenya and Tanzania, and an overlap between the new and publicly available *D. citri* from USA (Fig 5.11). The sequence from Ethiopia was positioned closer to the USA cluster than to the other African sequences.

Table 5.3. Genetic divergence of the Asian citrus psyllid (*Diaphorina citri*) from China, Ethiopia, Kenya, Tanzania and USA from this study (in bold) and global populations available in GenBank (n =18) based on an 874 bp alignment of the *COI* gene. Distances were calculated as percentage of pairwise distances (p-distances) under the Tamura 3-parameter model. Standard error estimates are shown above the diagonal.

	1	2	3	4	5	6	7	8	9	10	11	12	13	14	15	16	17	18	19	20	21	22	23
China	-	0.00	0.01	0.00	0.00	0.00	0.00	0.00	0.00	0.00	0.00	0.00	0.00	0.00	0.00	0.00	0.00	0.08	0.08	0.08	0.08	0.08	0.08
Argentina	0.24	-	0.00	0.00	0.00	0.00	0.00	0.00	0.00	0.00	0.00	0.00	0.00	0.00	0.00	0.00	0.00	0.08	0.08	0.08	0.08	0.08	0.08
Brazil	1.20	0.96	-	0.00	0.00	0.00	0.00	0.01	0.00	0.00	0.00	0.00	0.01	0.00	0.00	0.00	0.00	0.08	0.08	0.08	0.08	0.08	0.08
Iran	0.72	0.48	0.96	-	0.00	0.00	0.00	0.00	0.00	0.00	0.00	0.00	0.00	0.00	0.00	0.00	0.00	0.08	0.08	0.08	0.08	0.08	0.08
Malaysia	0.24	0.00	0.96	0.48	-	0.00	0.00	0.00	0.00	0.00	0.00	0.00	0.00	0.00	0.00	0.00	0.00	0.08	0.08	0.08	0.08	0.08	0.08
Mexico	0.72	0.48	0.96	0.00	0.48	-	0.00	0.00	0.00	0.00	0.00	0.00	0.00	0.00	0.00	0.00	0.00	0.08	0.08	0.08	0.08	0.08	0.08
Pakistan	0.72	0.48	0.96	0.00	0.48	0.00	-	0.00	0.00	0.00	0.00	0.00	0.00	0.00	0.00	0.00	0.00	0.08	0.08	0.08	0.08	0.08	0.08
Puerto Rico	0.48	0.24	1.20	0.24	0.24	0.24	0.24	-	0.00	0.00	0.00	0.00	0.00	0.00	0.00	0.00	0.00	0.08	0.08	0.08	0.08	0.08	0.08
Thailand	0.24	0.00	0.96	0.48	0.00	0.48	0.48	0.24	-	0.00	0.00	0.00	0.00	0.00	0.00	0.00	0.00	0.08	0.08	0.08	0.08	0.08	0.08
USA	0.72	0.48	0.96	0.00	0.48	0.00	0.00	0.24	0.48	-	0.00	0.00	0.00	0.00	0.00	0.00	0.00	0.08	0.08	0.08	0.08	0.08	0.08
Cambodia	0.24	0.00	0.96	0.48	0.00	0.48	0.48	0.24	0.00	0.48	-	0.00	0.00	0.00	0.00	0.00	0.00	0.08	0.08	0.08	0.08	0.08	0.08
China	0.24	0.00	0.96	0.48	0.00	0.48	0.48	0.24	0.00	0.48	0.00	-	0.00	0.00	0.00	0.00	0.00	0.08	0.08	0.08	0.08	0.08	0.08
Ethiopia	0.96	0.72	1.20	0.24	0.72	0.24	0.24	0.48	0.72	0.24	0.72	0.72	-	0.00	0.00	0.00	0.00	0.08	0.08	0.08	0.08	0.08	0.08
Kenya	0.24	0.00	0.96	0.48	0.00	0.48	0.48	0.24	0.00	0.48	0.00	0.00	0.72	-	0.00	0.00	0.00	0.08	0.08	0.08	0.08	0.08	0.08
Tanzania	0.24	0.00	0.96	0.48	0.00	0.48	0.48	0.24	0.00	0.48	0.00	0.00	0.72	0.00	-	0.00	0.00	0.08	0.08	0.08	0.08	0.08	0.08
USA	0.72	0.48	0.96	0.00	0.48	0.00	0.00	0.24	0.48	0.00	0.48	0.48	0.24	0.48	0.48	-	0.00	0.08	0.08	0.08	0.08	0.08	0.08
Taiwan	0.24	0.00	0.96	0.48	0.00	0.48	0.48	0.24	0.00	0.48	0.00	0.00	0.72	0.00	0.00	0.48	-	0.08	0.08	0.08	0.08	0.08	0.08
Saudi Arabia	7.90	7.91	8.08	7.82	7.91	7.82	7.82	7.81	7.91	7.82	7.91	7.91	7.76	7.91	7.91	7.82	7.91	-	0.00	0.00	0.00	0.00	0.00
Guadeloupe	7.77	7.78	7.95	7.69	7.78	7.69	7.69	7.69	7.78	7.69	7.78	7.78	7.64	7.78	7.78	7.69	7.78	0.72	-	0.00	0.00	0.00	0.00
India	7.90	7.91	8.08	7.82	7.91	7.82	7.82	7.81	7.91	7.82	7.91	7.91	7.76	7.91	7.91	7.82	7.91	0.00	0.72	-	0.00	0.00	0.00
Indonesia	7.90	7.91	8.08	7.82	7.91	7.82	7.82	7.81	7.91	7.82	7.91	7.91	7.76	7.91	7.91	7.82	7.91	0.00	0.72	0.00	-	0.00	0.00
Mauritius	7.72	7.73	7.89	7.64	7.73	7.64	7.64	7.64	7.73	7.64	7.73	7.73	7.58	7.73	7.73	7.64	7.73	0.48	0.72	0.48	0.48	-	0.00
Reunion	7.72	7.73	7.89	7.64	7.73	7.64	7.64	7.64	7.73	7.64	7.73	7.73	7.58	7.73	7.73	7.64	7.73	0.48	0.72	0.48	0.48	0.00	-

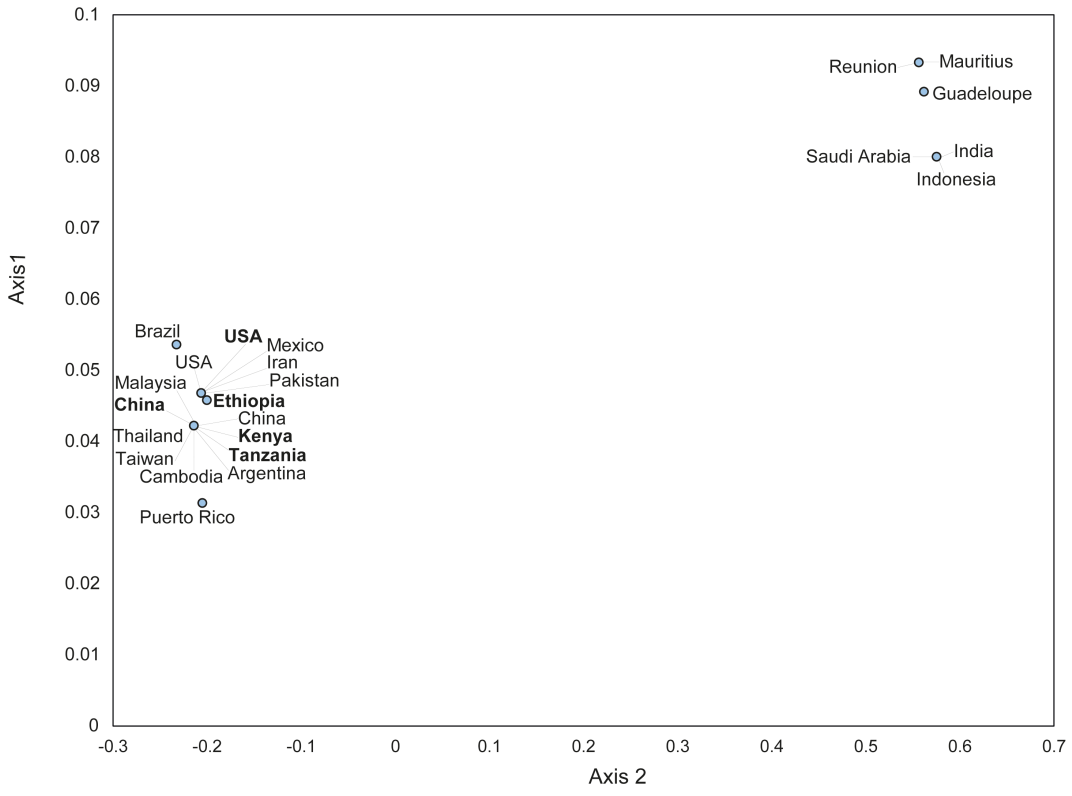

Figure 5.11. Principal Coordinate Analysis (PCoA) plot representing the genetic distances among *Diaphorina citri* Cytochrome oxidase 1 (*COI*) sequences from China, Ethiopia, Kenya, Uganda, USA and publicly available sequences from 18 countries, available in GenBank computed using the classic multidimensional scaling function 'cmdscale' in R version 3.5.1.

Discussion

The recent invasion and rapid spread of the Asian citrus psyllid *D. citri* into Eastern Africa, and the confirmed presence of "*Candidatus* Liberibacter asiaticus" (CLas) in Ethiopia and Kenya, have raised concerns over the threat of HLB to other citrus-producing countries in the continent. A recent study based on complete mitochondrial genomes of *D. citri* concluded that psyllid in California was likely not introduced from China but from somewhere in south-eastern USA (Wu et al., 2017). Based on *COI* sequences, the recently detected *D. citri* in Ethiopia showed a close phylogenetic relationship between *D. citri* from the Americas (Ajene et al., 2020b). In this study, we preliminarily assessed the genetic diversity of *D. citri* in Africa using complete mitochondrial sequences from the three Eastern African countries (Ethiopia, Kenya and Tanzania). We also provide a description of the global phylogeographic structure of the psyllid based on the *COI* and *16S rRNA* sequences.

The comparison of complete *D. citri* mitogenomes from China, Ethiopia, Kenya, Tanzania and the USA revealed two groups. Group 1 was composed by the sequences from China, Kenya and Tanzania, and Group 2 included the sequences from Ethiopia and USA. The African sequences showed no difference between Kenya and Tanzania, which were different from Ethiopia. Albeit at a low level, *D. citri* from Ethiopia was closer to *D. citri* from the USA than to Kenya or Tanzania. All members of Group 1 had the same number of SNPs when compared to the mitogenome sequences from Group 2 and vice versa. This clearly distinguished the two groups in addition to the pairwise comparisons of the p-distances of the complete PCG sequences. Furthermore, the variation of tRNAs between Group 1 and Group 2 showed a similar pattern of variation, with the sequences from Group 1 showing no differences in all tRNAs, while variation was observed in the tRNA sequences of $tRNA^{Phe}$, $tRNA^{Asn}$ and $tRNA^{Ser1}$ between Group 1 and Group 2. Variation in the $tRNA^{Asn}$ was also reported between *D. citri* mitogenomes from USA and China (Wu et al., 2017). Therefore, our results are in agreement with the previous report of two genetic clusters associated with the USA and China identified by analysis of the *D. citri* mitogenome (Wu et al., 2017).

Based on the analyses of the *COI* sequences, the ML tree showed three main branches of *D. citri* all the *D. citri* from this study clustered on Branch I which also included *D. citri* from Asia and America. The phylogeographic structure of *D. citri* from our study showed a bias of the *D. citri* from Ethiopia to *D. citri* from the USA while the *D. citri* from Kenya and Tanzania were closely linked to *D. citri* from China. Furthermore, the NJ network clustered the samples from Kenya and Tanzania in the same haplotype with China and Vietnam while the Ethiopian *D. citri* sequence formed a unique haplotype absent from all other samples. The singleton haplotype seen

in the Ethiopian sequence from this study was also reported by Ajene et al., (2020b) in the detection of *D. citri* from Ethiopia.

Furthermore, the estimates of genetic divergence observed between the *COI* sequences of the African *D. citri* showed no difference between the Kenyan and Tanzanian sequences but revealed diversity (0.72%) with Ethiopia. In comparison to the probable source populations (China and USA), Kenyan and Tanzanian *D. citri* had no variation with the Chinese *D. citri* while the Ethiopian *D. citri* had less variation with the *D. citri* from the USA than the Chinese *D. citri*.

The high substitution rate in *COI* (Mandal et al., 2014) makes it suitable for intraspecific differentiation of insect species but other PCGs such as *ND5* and *CytB* which are highly polymorphic as seen in our study and reported by Wu et al., (2017) can be used as well as the *16S rRNA* gene.

The *16S rRNA* also presents a viable option for differentiation of *D. citri* populations as has been shown in the evaluation of *Bactericera cockerelli* (Swisher & Crosslin 2014). In our study, the *16S rRNA* had the highest number of SNPs across the mitogenome. The phylogenetic analysis of the *16S rRNA* sequences provided better resolution of the phylogeographic differentiation between *D. citri* from Africa, America and Asia. A multi-gene approach to intra-species differentiation will provide a clearer picture of the phylogeographic structure of insect species rather than the use of a single gene. For example, Mitochondrial *COI* gene together with *ND5* has been used for phylogenetic studies of flies (Navajas et al., 1996), *CytB* has been shown to be better than *COI* at recovering population structure in *Athetis lepigone* (Chen et al., 2019) and *COIII* has been used in intraspecific studies of *Ixodes pacificus* (Kain et al., 1999). Previous studies on the phylogeography of *D. citri* populations have relied on analyses of *COI* sequences (De León et al., 2011, Boykin et al., 2012, Guidolin & Consoli, 2013, Lashkari et al., 2014). These studies showed the phylogeographic structure of American and Asian *D. citri* populations, for example, Boykin et al., (2012) identified eight haplotypes of *D. citri* from 16 countries in five regions and concluded that *D. citri* from North America is more closely related to southwestern Asia while *D. citri* from South America is closely related to *D. citri* from south-western and south-eastern Asia. Similarly, our results showed that *D. citri* from the Americas were more closely linked to *D. citri* from south-western and middle east Asia with four out of five shared haplotypes only containing sequences from these two regions. Also, the singleton haplotype from Ethiopia was more closely linked to the American and south-western/middle eastern *D. citri*. Therefore, *D. citri* in Africa seems to have been introduced in separate events. While *D. citri* was likely introduced in Tanzania and Kenya through the shipping routes from China with infested plant material (Rwomushana et al., 2017), the probable route of introduction

of *D. citri* into Ethiopia from the USA is still unknown. Furthermore, the timeline of *D. citri* detections, as well as the locations (coastal and border regions of Kenya and Tanzania) of detections, seem to suggest a scenario of movement of *D. citri* between Tanzania and Kenya, while *D. citri* in Ethiopia was first detected three years later in the north-eastern part of the country (Ajene et al., 2020b).

In the present study, new complete mitogenomes of *D. citri* from China, Kenya, Tanzania and the USA were sequenced and compared. Furthermore, the relationship between the genetic diversity of the psyllid and its geographical origins was assessed based on the *COI* and *16S rRNA* genes. The Kenyan and Tanzanian *D. citri* were found to group with the Chinese *D. citri*, while the Ethiopian *D. citri* was found to group with the USA *D. citri*. These results suggest that *D. citri* in the three African countries was not introduced from the same source. Therefore, the combined evidence from the analyses of the complete mitochondrial genome and specifically the *COI* and *16S rRNA* gene regions in this study reveals a different phylogeographic structure between *D. citri* in Ethiopia and the *D. citri* found in Kenya and Tanzania. In light of this, future research should evaluate the population structure of these two *D. citri* populations (Group 1 and 2) using other techniques which use other genetic methods of differentiation such as nuclear microsatellite loci. The recognition of separate introduction routes of *D. citri* and CLas in Africa could have implications on HLB regulatory strategies in Africa, in particular strategies aimed at preventing the establishment of CLas. This information is of phytosanitary and quarantine regulatory importance for the management of HLB spread in the continent as accurate determination of the origin of the *D. citri* populations in Africa and information on the population genetic structure and diversity of *D. citri* across a wider geographic range will provide greater insight and thereby strengthen the argument for greater quarantine and regulatory policies in these countries.

Chapter Six: Genetic diversity and population structure of the Asian citrus psyllid *Diaphorina citri* in Eastern Africa reveals different invasion histories

Abstract

The Asian citrus psyllid *Diaphorina citri* Kuwayama (Hemiptera: Liviidae) is a damaging pest of citrus which has recently been reported in East Africa. It is the primary vector of the devastating Huanglongbing disease which has been reported in Ethiopia. Despite the economic risk, the population genetics of this invasive pest have remained relatively unexplored in East Africa. This study explores population genetic structure and contemporary gene flow in *D. citri* in the eastern African region and attempts to place observed patterns within the broader geographical context of the species' total range. We assessed the population structure and population differentiation using 10 microsatellite loci on *D. citri* populations from China, Ethiopia, Kenya, Tanzania and USA. The overall genetic structuring in two out of the three African countries was low. The expansion history of this species, including likely human-mediated dispersal, may have played a role in shaping the observed weak structure. We observed two distinct population structures within the African populations, with the populations from Kenya and Tanzania significantly structured from the population from Ethiopia. The study suggested a close relationship between China, Kenya and Tanzania, with evidence for China as the origin of introduction into these countries while a close relationship was seen between Ethiopia and USA, with evidence of USA being the origin of invasion into Ethiopia. The information obtained from this analysis of gene flow and population structure has broad implications for quarantine, trade and management of this pest, especially in Kenya where it is expanding northward. Furthermore, the control of this pest will have a significant impact on the management of Huanglongbing disease in Africa.

Introduction

Diaphorina citri Kuwayama (Hemiptera: Psyllidae) commonly known as the Asian citrus psyllid are pests of citrus. The psyllid causes direct damage on plants through its feeding activities (Grafton-Cardwell et al., 2006). Heavy infestation of flush shoots by psyllids prevents the shoots from normal development and thus making the shoot more likely to break off. *Diaphorina citri* is an efficient vector of "*Candidatus* Liberibacter asiaticus" (CLas) that is associated with Huanglongbing disease and is found in "tropical and subtropical Asia, Afghanistan, Saudi Arabia, Reunion, Mauritius, parts of South and Central America, Mexico, Caribbean, and the

United States", (Grafton-Cardwell et al., 2006) and most recently, it has also been reported in Tanzania (Shimwela et al., 2016), Kenya (Rwomushana et al., 2017) and Ethiopia (Ajene et al., 2019)

The nymphal feeding activities of *D. citri* results in twisting and some curling in new shoots and leaves. Additionally, the production of honeydew by the insect on the plant encourages the growth of sooty mould, which reduces plant productivity. The most significant impact of *D. citri* to citrus plants however is its transmission of the phloem-limited CLas. CLas is closely related to *Candidatus* Liberibacter americanus (CLam) and "*Candidatus* Liberibacter africanus" (CLaf). The latter is transmitted by *Trioza erytreae* and is widespread in East and southern African highlands (Rasowo et al., 2019). CLas has been reported in Asia, North and South America (Grafton-Cardwell et al., 2013; Halbert & Manjunath, 2004; Hall et al., 2013). CLas was reported for the first time in Ethiopia (Saponari et al., 2010) but its primary vector, *D. citri* was not detected until recently (Ajene et al., 2020). *Diaphorina citri* has been shown, albeit experimentally only, to transmit CLaf in laboratorial conditions (Massonie et al., 1976). Given the current context, the invasion of *D. citri*, into Africa is a significant threat to citrus production in Africa.

Genetic diversity studies have potential uses in breeding, evolution, genetic conservation, species classification, taxonomy (Wangari et al., 2013; Wu et al., 1999). Simple sequence repeat (SSR) is an important means for determining genetic variation in living organisms (Sajib, Hossain, & Ali, 2012; Powell et al., 1996; Ma et al., 2011). SSR markers also known as microsatellite markers have some advantages over other genetic marker techniques because, they are easy to use and are highly polymorphic that is they detect both heterozygous and homozygous alleles, and is therefore typically applied in genetic diversity studies, gene mapping (Sajib, et al., 2012; Zhang et al., 2007; Ma et al., 2011) and genetic fingerprinting (Sajib, et al., 2012; Xiao et al., 2006; Ma et al., 2011).

Microsatellite markers are currently being employed in arthropod genetics. One aim of this method in citrus psyllid genetics is to track possible geographical origins of the psyllid introductions (e.g. one or multiple invasions) into Africa. This information will be used in research, targeting the design of appropriate management strategies and monitoring of any expansion of the range of this agricultural pest (Boykin et al., 2007). The potential climate suitability for *D. citri* in citrus growing areas in Africa as reported by Shimwela et al., (2016) poses a potential risk of rapid spread of citrus greening across the African continent (Shimwela et al., 2016).

Studies to investigate the phylogeography of African *D. citri* using the maternally transmitted mitochondrial genome (Ajene et al., Unpublished) revealed two probable parent populations

from China and USA. Therefore, there is a need to establish the population structure and genetic diversity of the African *D. citri* populations using the bi-parentally transmitted microsatellite markers. Furthermore, given the notable rapid spread of *D. citri* in Tanzania and Kenya, the recent detection of *D. citri* in Ethiopia, its economic importance, the risk of this species being introduced, established and invading other regions of eastern and southern Africa is a good reason for the need of greater understanding of population relationships and invasion routes of the insect. Additionally, the incorporation of psyllid populations collected from Asia (China) and the United States provides insight into the origin of the African *D. citri* population. This study provides foundational data for understanding the population dynamics and genetic structure in Eastern Africa.

Methods

Sample collection, DNA extraction, and microsatellite genotyping.

Specimens of *D. citri* (*n*=270) were collected from one site in China, one site in Ethiopia, four sites in Kenya, three sites in Tanzania and one site in USA between 2016 to 2018 (Table 6.1). All Psyllids were stored in 100% ethanol at − 20 °C prior to DNA extraction.

Table 6.1. Collection data of *Diaphorina citri* populations used in this study

Country	Collection Site	Code	Latitude	Longitude	N
China	Fuzhou	CHN	26.07877	119.2969	10
Ethiopia	Goshuha	ETH	11.76407	39.59168	20
Kenya	Awasi	AWA	0.166967	35.0844	30
	Koitamburot	KOT	-0.20731	35.19261	30
	Lungalunga	LUN	-4.56247,	39.1221	30
	Soin	SOI	0.54117	35.18458	30
Tanzania	Mafiga	MAF	-5.22042	37.65931	30
	Mikese	MIK	-4.93511	39.12586	30
	Mlali	MLA	-6.99731	37.57047	30
USA	Texas	USA	30.01501	-96.3425	30

Ten to 30 individuals from each of the 10 locations were genotyped using ten microsatellite markers, namely Dcoi01, Dcoi02, Dcoi03, Dcoi04, Dcoi05, Dcoi07, Dcoi09, Dcoi10, Dcoi11 and Dcoi12 (Boykin et al., 2012). Total DNA was extracted from individual specimens using the Isolate II Genomic DNA kit (Bioline, London, United Kingdom), following the manufacturer's instructions. DNA extracts were checked for quality and concentration using a Nanodrop 2000/2000c Spectrophotometer (Thermo Fischer Scientific, Wilmington, USA). DNA extracts within the $A_{260\ nm}/A_{280nm}$ ratio range of 1.8 to 2.0 were eluted to a final volume of 50 µl, and used for downstream analyses. The forward primers were labeled with one of the three Fluorescent labels (FAM, NED, PET and VIC). PCR reactions were run and fluorescently labeled fragments were detected on an ABI PRISM 3730 DNA analyzer, with Pop-7 as sieving matrix, HiDi

Formamide as single-stranded DNA stabilizer and GeneScan 500 ROX standard as a size marker. ABI PRISM GeneMarker software version 3.0.1 was used to size the alleles.

Marker summary statistics and intra-population genetic diversity.

Data preparation was done using MS Tools (Park 2001) add-in for Microsoft excel. Assessment of population genetic parameters was done in GenAlEx (Peakall and Smouse 2006) add-in for Microsoft excel, standard genetic distance was used to estimate genetic differentiation. Allele Frequencies by Population (AFP), Heterozygosity, F-statistics and Polymorphism by Population (HFP), Allelic Patterns graph (APT), Private Alleles by Population (PAS), Samples with more than one Private Allele (PAL) were performed in GenAlEx.

Population structure analysis

Analysis of molecular Variance (AMOVA) was utilised to test different groupings of the populations to determine whether the meta-population is in panmixia (that is the ability of individuals in the population to mate without restrictions), the component of genetic diversity attributable to variance between and within populations from the different countries was performed in Arlequin (Excoffier and Lischer 2010). Significance for the AMOVA analysis was ascertained using 10,000 permutations. The format conversions for analysing the data in various software programs were achieved using the CONVERT software version 1.31 (Glaubitz, 2004). The exact tests for linkage disequilibrium and deviation from Hardy-Weinberg equilibrium were also conducted using the web version of GENEPOP.

Two methods were used to infer the clustering of the 10 populations: Bayesian clustering and multivariate discriminant analysis of principal components (DAPC). The Bayesian approach was implemented in Structure 2.2 (Pritchard et al., 2000). To determine the most likely number of clusters underlying our samples, K values ranging from 1 to 10 were set. The simulations were run using the admixture model without prior population information (Pritchard et al., 2000). The length of the initial burn-in period was set to 100,000 iterations followed by a run of 1,000,000 Markov chain Monte Carlo (MCMC) repetitions, replicated 10 times to ensure convergence on parameters and likelihood values. To identify the most likely number of sub populations (K) among individuals, we used the Med- and Mean K methods (Puechmaille (2016) which takes into account this sampling bias and corrects for it. Values were computed to select the most likely number of K using the online resource STRUCTURE SELECTOR (Li & Liu, 2018) that explained the structure in data. The multivariate clustering approach was implemented in R version 3.5.1 environment with R-Studio (R Development Core Team, 2008)

GeneClass 2.0 (Piry et al., 2004) was used to assign or exclude reference populations as possible origins of individuals, on the basis of multilocus genotypes. We used the Nei's standard (1972) criterion for assignment of migrant populations. The Monte Carlo resampling method (Paetkau et

al., 2004) is aimed to identify the accurate exclusion / inclusion critical values: our results are based on 10 000 simulated genotypes for each population and on a threshold probability value of 0.05.

Results

Genetic diversity

Our results are based on 10 microsatellite loci detected in 270 psyllids across 10 populations. Over the 10 populations, these loci have different levels of polymorphism, in terms of both number of alleles (from 4 to 16) and allele size range: Dci01: 11 alleles (201 to 221 bp); Dci02: 13 alleles (184 to 204 bp); Dci03: 9 alleles (235 to 250bp); Dci04: 16 alleles (288 to 307 bp); Dci05: 7 alleles (328 to 340 bp); Dci07: 6 alleles (272 to 278 bp); Dci09: 4 alleles (183 to 188 bp); Dci10: 14 alleles (227 to 247 bp); Dci11: 12 alleles (239 to 252 bp) and Dci12: 7 alleles (213 to 220 bp) (Table S1).

The population from Lungalunga, Kenya had the highest number of different alleles (3.30) while the Ethiopian *D. citri* population had the highest number of effective alleles (2.54). All populations had a negative fixation index with the population from Soin, Kenya having the highest fixation index. The population from Mlali, Tanzania had the highest observed heterozygosity, while the population from Mikese, Tanzania had the least. All populations had higher observed heterozygosity than the expected heterozygosity (Table 6.2).

Table 6.2. Genetic variability estimates in samples of *Diaphorina citri* from different 5 countries

Country	Population	N	Na	Ne	I	Ho	He	uHe	F
Kenya	Awasi	2.100	1.700	1.401	0.513	0.500	0.300	0.431	-0.715
China	Fuzhou	1.800	1.400	1.173	0.441	0.475	0.277	0.396	-0.735
Ethiopia	Goshuha	3.900	3.100	2.535	0.870	0.680	0.459	0.551	-0.547
Kenya	Koitamburot	2.000	2.300	1.734	0.627	0.483	0.328	0.448	-0.547
Kenya	Lungalunga	4.400	3.300	2.531	0.910	0.700	0.473	0.565	-0.525
Tanzania	Mafiga	3.000	2.700	2.473	0.794	0.700	0.439	0.584	-0.688
Tanzania	Mikese	4.600	0.800	0.680	0.256	0.300	0.164	0.170	-0.852
Tanzania	Mlali	3.000	2.400	2.230	0.777	0.800	0.470	0.643	-0.753
Kenya	Soin	2.400	2.300	2.000	0.690	0.700	0.410	0.604	-0.787
USA	Texas	5.800	2.300	1.802	0.676	0.583	0.380	0.447	-0.581

Na = No. of Different Alleles, Ne = No. of Effective Alleles = 1 / (Sum pi^2), I = Shannon's Information Index = -1* Sum (pi * Ln (pi)), Ho = Observed Heterozygosity = No. of Hets / N, He = Expected Heterozygosity = 1 - Sum pi^2, uHe = Unbiased Expected Heterozygosity = (2N / (2N-1)) * He,

F = Fixation Index = (He - Ho) / He = 1 - (Ho / He)

Pairwise F_{ST} values were generally low, with F_{ST} ranging from 0.012 to 0.305. No out-of-range high values are observed between any of the African populations and China. Likewise, no out-of-range high values were observed between the African populations and USA. Low values of

differentiation are observed among eastern African populations. There was no significantly different F_{ST} values between the western Kenya populations (Soin, Awasi and Koitamburot) but there was significant divergence between the western Kenya populations and Lungalunga in coastal Kenya. There was also no significantly different F_{ST} value between the populations from Tanzania (Mafiga, Mikese and Mlali) or between the Tanzanian populations and Lungalunga in Kenya.

Table 6.3. Pairwise FST divergence between 10 different geographical populations of *Diaphorina citri*. Fst Values below diagonal. Probability, P (rand >= data) based on 999 permutations is shown above diagonal. ns – not significantly different from zero (P < 0.05)

		1	2	3	4	5	6	7	8	9	10
1	Awasi	-	0.001	0.001	0.017	0.001	0.001	0.001	0.001	0.022	0.001
2	Fuzhou	0.194	-	0.005	0.001	0.005	0.007	0.001	0.001	0.001	0.001
3	Goshuha	0.161	0.059	-	0.001	0.012	0.007	0.001	0.006	0.001	0.001
4	Koitamburot	**0.023** ns	0.138	0.125	-	0.001	0.001	0.001	0.001	0.043	0.001
5	Lungalunga	0.107	0.057	**0.032** ns	0.078	-	0.076	0.002	0.017	0.001	0.001
6	Mafiga	0.113	0.053	0.041	0.080	**0.013** ns	-	0.002	0.010	0.001	0.001
7	Mikese	0.305	0.145	0.100	0.260	0.070	0.082	-	0.004	0.001	0.001
8	Mlali	0.207	0.107	0.056	0.179	**0.038** ns	**0.036** ns	0.051	-	0.001	0.001
9	Soin	**0.022** ns	0.134	0.114	**0.012** ns	0.079	0.086	0.255	0.179	-	0.001
10	Texas	0.280	0.128	0.083	0.248	0.134	0.139	0.189	0.116	0.234	-

Population structure

AMOVA analyses performed across all the groups to test panmixia showed a high variation within the populations (80.5 %) and a low variation among populations (19.5 %) thus showing the populations are in panmixia. (Table 6.4). The analysis performed on groupings as per regions (Africa separated from all other populations) showed, genetic differentiation among groups accounted for 9.8%. All fixation indices, including FCT, FSC, FST, FIS and FIT were highly significant (P < 0.01) (Table 6.4).

Table 6.4. Analysis of molecular variance (AMOVA)

Hypothesis tested	**Source of variation**	**Sum of squares**	**Variance components**	**Percentage variation (%)**	**Fixation Indices**
Panmixia	Among populations	87.505	0.3802	19.50504	F_{ST} = 0.16923
	Within populations	336.439	1.56904	80.49496	
Inter-continent	Among groups	57.123	0.23043	11.55381	F_{CT} = 0.11554 F_{SC} = 0.11050 F_{ST} = 0.21327
	Among populations within groups	30.382	0.19491	9.77288	
	Within groups	336.439	1.56904	78.67331	

Bayesian clustering analysis of microsatellite genotypes implemented in STRUCTURE showed that the maximum value for the estimated likelihood of K was found at K = 2 (Fig. 6.1). The average values of ancestry probabilities (Q) for each population in the two clusters showed that, the psyllids from Texas (USA) had the highest ancestry in one cluster (Q = 0.863), while the psyllids from Mikese (Tanzania) had the highest ancestry in the second cluster (Q = 0.708). from the African populations, the psyllids from Kenya and Tanzania were clustered in one cluster while the psyllids from Ethiopia was in the second cluster (Table 6.5). Visualisation of cluster membership coefficients suggests that psyllids from the sites in China, Ethiopia and USA formed one cluster (red) while the psyllids from Kenya and Tanzania formed another cluster (green) (Fig. 6.2).

Table 6.5 Average coefficient of ancestry obtained from a Structure run with K = 2 for the 270 individuals of *Diaphorina citri* from the 5 countries. Co-ancestry higher than 10% of each population in a cluster is in bold

	Inferred Clusters (K)		
Country	**Population**	**1**	**2**
China	Fuzhou	**0.847**	0.153
Ethiopia	Goshuha	**0.73**	0.27
Kenya	Awasi	0.316	**0.684**
	Koitamburot	0.387	**0.613**
	Lungalunga	0.338	**0.662**
	Soin	0.326	**0.674**
Tanzania	Mafiga	0.416	**0.584**
	Mikese	0.292	**0.708**
	Mlali	0.52	**0.48**
USA	Texas	**0.863**	0.137

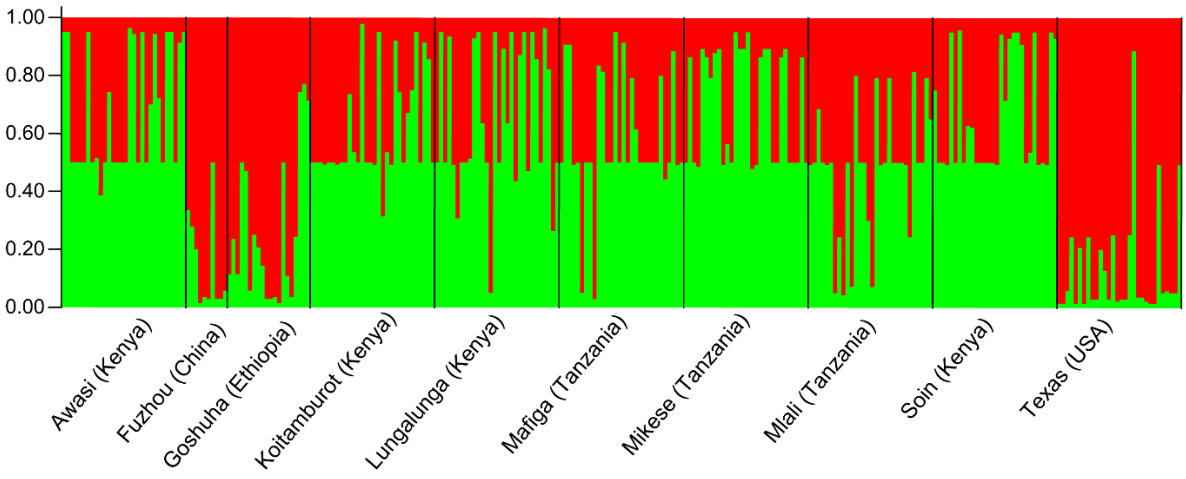

Figure 6.1. Bayesian clustering analysis of *Diaphorina citri* individuals based on 10 microsatellite genotypes using Structure. The two colours (red and green) represent the co-ancestry distribution of the 270 individuals in two hypothetical clusters (K1-K2) respectively.

Bars are partitioned into three shaded segments proportional to the inferred ancestry of each individual to each cluster. Bold vertical lines separate collection sites.

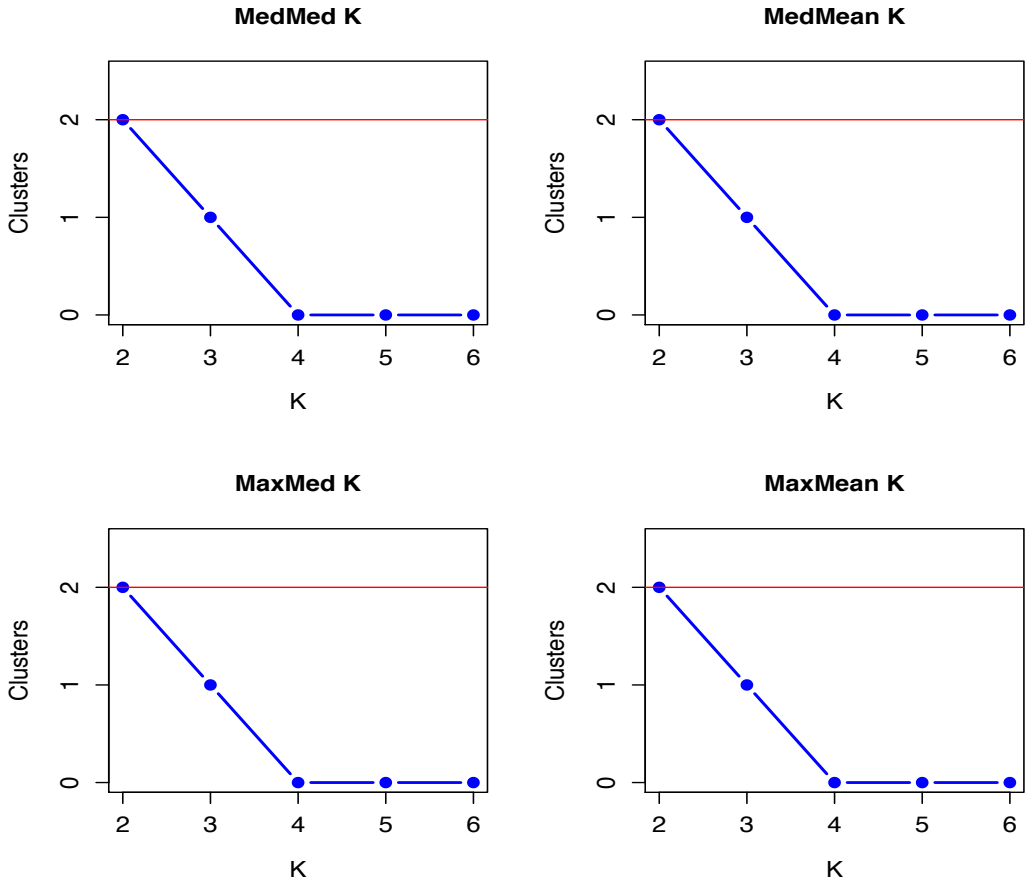

Figure 6.2. Bayesian analysis of 270 *Diaphorina citri* individuals based on 10 microsatellite loci showing optimal number of clusters as inferred by Med- and Mean K values. The optimal K (Y-axis) used to explain predefined 10 populations after removing spurious clusters are indicated by red lines.

The discriminate analysis of principal components also revealed a high clustering pattern between the Kenyan populations and the Tanzanian populations while the population from Ethiopia was clustered with the population from USA. the psyllids from Kenya and Tanzania clustered together while the psyllids from Ethiopia clustered with the psyllids from USA (Fig. 6.3).

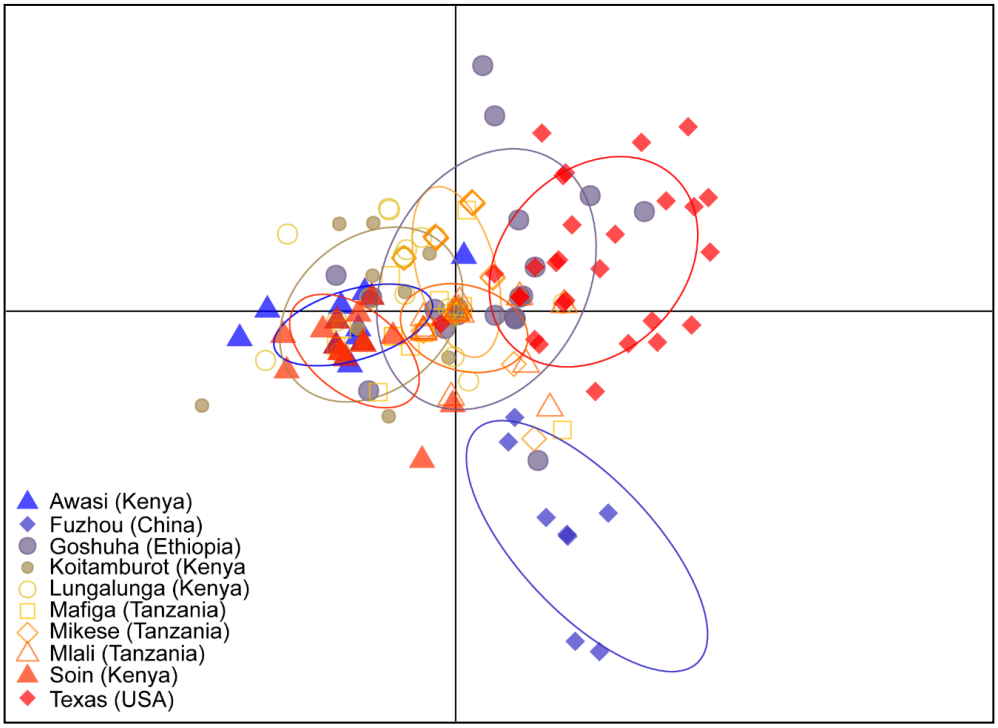

Figure 6.3. Multivariate clustering of 270 *Diaphorina citri* individuals based on 10 microsatellite loci using discriminate analysis of principal components.

Assignment rate

In these analyses, migration rate estimates above 0.500 imply restricted gene flow, whereas moderate to high gene flow is suggested by values greater than 0.500. The migration rates from the Goshuha and Texas populations to other populations were all above 0.500. The migration rate values between the Kenyan populations showed moderate gene flow between Lungalunga and the other Kenyan populations with an average migration rate of 0.997. Interestingly, the average estimated migration rates were high between Lungalunga and the Tanzanian populations (0.210) suggesting high gene flow (Table 6.6).

The migration pattern when visualized by the spanning tree network showed the Lungalunga population was more closely linked to the Tanzanian populations than to the other Kenyan populations (Fig 6.4).

Table 6.6. Mean assignment rate of *Diaphorina citri* individuals into source populations (rows) and aim populations (columns) as calculated using Nei's standard distance in GENECLASS 2.0. Values in bold indicate the distance of individuals assigned to the source population. The distance of individuals assigned to the source populations are underlined.

	Awasi	Fuzhou	Goshuha	Koitamburot	Lungalunga	Mafiga	Mikese	Mlali	Soin	Texas	Assigned migrant
Awasi	0	0.982	0.952	0.632	1.139	1.009	2.695	1.737	0.276	0.937	Soin
Fuzhou	0.982	0	1.032	1.224	0.588	**0.372**	0.69	0.623	1.437	0.992	Mafiga
Goshuha	0.952	1.032	0	1.103	0.584	0.817	0.952	0.613	0.751	0.099	Texas
Koitamburot	0.632	1.224	1.103	0	0.875	0.532	1.767	1.348	0.399	1.711	Soin
Lungalunga	1.139	0.588	0.584	0.875	0	0.297	0.135	0.199	0.917	0.592	Mikese
Mafiga	1.009	0.372	0.817	0.532	0.297	0	0.494	0.227	0.92	0.876	Mlali
Mikese	2.695	0.69	0.952	1.767	0.135	0.494	0	0.187	2.478	0.873	Lungalunga
Mlali	1.737	0.623	0.613	1.348	0.199	0.227	0.187	0	1.712	0.516	Mikese
Soin	0.276	1.437	0.751	0.399	0.917	0.92	2.478	1.712	0	0.942	Awasi
Texas	0.937	0.992	**0.099**	1.711	0.592	0.876	0.873	0.516	0.942	0	Ethiopia

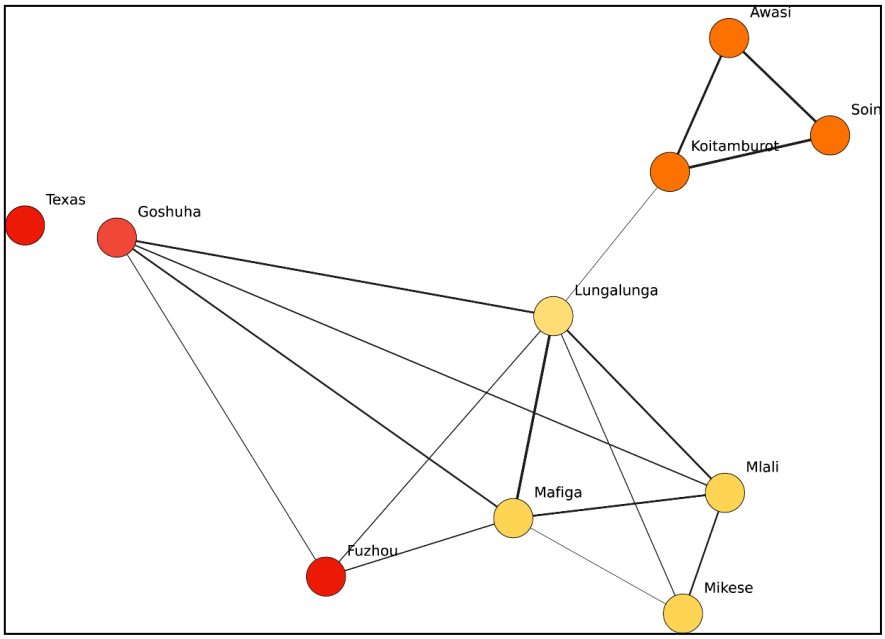

Figure 6.4. Minimum spanning tree network of 270 *Diaphorina citri* individuals from 10 geographic locations based on Fst distance. The lines between circles indicate the similarity between profiles. Nodes are colored based on proportion of shared genotypes.

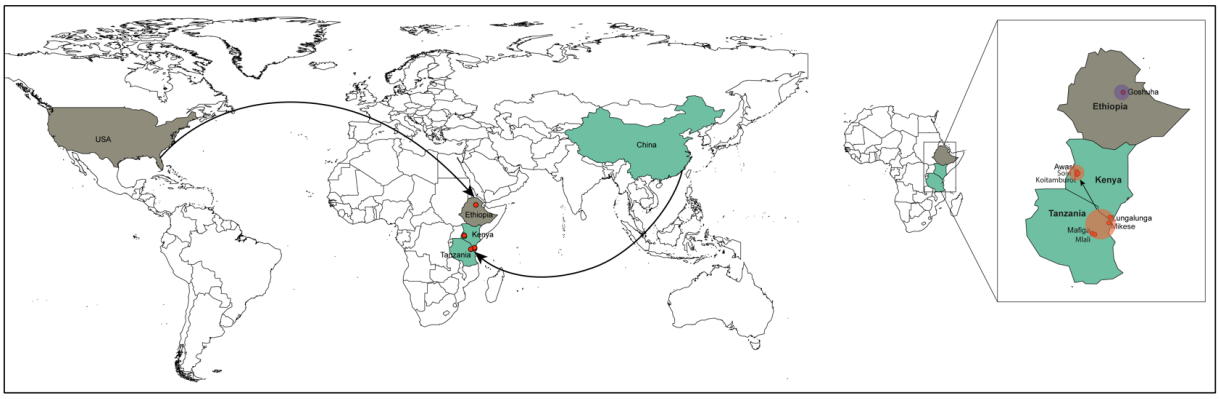

Figure 6.5. Route of introduction of *Diaphorina citri* into Africa and the movement of within eastern Africa based on population structure and genetic diversity. Different populations are separated by color based on population structure.

Discussion

Understanding population structure and gene flow among regions are very important aspects in the management of citrus psyllids. In this study, we obtained data from nuclear DNA markers of an extensive sampling of *D. citri* in countries where the psyllid has been reported in eastern Africa (Ethiopia, Kenya and Tanzania), and collections from China and USA. Our aim was to examine population structure and gene flow within eastern Africa and to place global diversity and structure in a regional context.

The clearest signal of population structure across the sampled locations from Africa, supported the population from Ethiopia, as being significantly structured from all other African populations. This pattern was expressed by low levels of estimated gene flow between this site and all others, and manifests in this site being supported as a separate genetic entity in Bayesian clustering analysis of the microsatellite genotypes. The genotypic assignment of the Ethiopian *D. citri* to the American *D. citri* and its significant separation from the Kenyan and Tanzanian *D. citri* may be representative of a separate origin for the Ethiopian population and strongly supports the suggestion that its origin was from USA. Furthermore, the region in Ethiopia where the *D. citri* populations were found is characterized by steep mountainous topology, potentially disrupting the movement of the insects.

Within the other eastern African populations, the most probable source of introduction of *D. citri* into Tanzania and Kenya is China as the analysis of the minimum spanning tree and the pairwise distances showed low genetic distance between the Chinese *D. citri* and the Tanzanian *D. citri* as well as the *D. citri* from Lungalunga. The low population differentiation patterns seen between the Kenyan and Tanzanian *D. citri* is expected as there are direct trade routes between the sampled locations and no significant geological barriers to prevent the natural movement of the psyllid.

Within the Kenyan populations, a few locations were supported as significantly structured. Awasi, Soin and Koitamburot, situated in the western part of Kenya showed some evidence for genetic differentiation from Lungalunga in the coastal region of Kenya and the Tanzanian populations. This pattern may be associated with the geographic proximity of Lungalunga (which lies at the border with Tanzania) to Mikese, Mlali and Mafiga, as well as the relative distance from the sites in western Kenya which are farther inland. Furthermore, there is a direct trade route between the Tanzanian sites and Lungalunga while there are more geological and physical barriers between Lungalunga and the sites in western Kenya. The *D. citri* populations were seen to be largely panmitic, therefore the genetic differentiation observed between the Kenyan *D. citri* may thus be the result of physical and natural barriers that limited gene flow from Lungalunga inland resulting in the differentiation of the populations in western Kenya. Therefore, the movement of the psyllid inland into Kenya most likely is as a result of a combination of trade practices and geographical barriers to dispersal which may have resulted in the observed differentiation. High gene flow was inferred from the close relationship between Mafiga, Mikese, Mlali and Lungalunga, in contrast to minimal migration inland into Kenya. This pattern has also been seen in *Bactrocera correcta* as well as *Bactrocera dorsalis* in China (Aketarawong et al., 2007; Shi et al., 2012; Qin et al., 2016) and *Bactrocera invadens* in Africa (Khamis et al., 2009).

The use of nuclear microsatellites, which are biparentally inherited makes them more suitable for geneflow analysis. Therefore, we provide evidence based on microsatellite molecular markers that there are two distinct populations of *D. citri* in Africa with different origins and there is a relatively low gene flow among most Kenyan and Tanzanian populations of *D. citri* with the exception of Lungalunga. We also hypothesize the first introduction of the species into East Africa occurring in Tanzania from China, and dispersal inward while the entry into Ethiopia occurring from USA. This confirms the reports of the comparative analyses of the maternally transmitted mitochondrial genome of the African *D. citri* and the phylogeographic analysis using the mt COI coding gene region, which links the *D. citri* from Kenya and Tanzania to China, and the Ethiopian *D. citri* to the Americas (Ajene et al., Unpublished).

These results present a strong case for strict phytosanitary and quarantine measures to be put in place to stem the spread of this invasive species to other African countries thereby reducing the risk of spread of Huanglongbing. Furthermore, we recommend increased surveillance for this pest as well as sustainable management strategies to avoid the invasion into other citrus producing countries.

Chapter Seven: Microbiome analysis of African *Diaphorina citri* from Eastern Africa shows links to China

Abstract

The Asian citrus psyllid (*Diaphorina citri*) is a key pest of *Citrus* sp. worldwide, as it acts as a vector for "*Candidatus* Liberibacter asiaticus" (CLas), the bacterial pathogen associated with the destructive Huanglongbing (HLB) disease. Recent detection of *D. citri* in Africa and reports of CLas-associated HLB in Ethiopia suggest that the citrus industry on the continent is under imminent threat. Endosymbionts and gut bacteria play key roles in the biology of arthropods, especially with regards to vector-pathogen interactions and resistance to antibiotics. Thus, we aim to profile the bacterial genera and to identify antibiotic resistance genes within the microbiome of different populations worldwide of *D. citri*. The metagenome of *D. citri* was sequenced using the Oxford Nanopore full-length 16S metagenomics protocol, and the "What's in my pot" (WIMP) analysis pipeline. Microbial diversity within and between *D. citri* populations was assessed, and antibiotic resistance genes were identified using the WIMP-ARMA workflow. The most abundant genera were key endosymbionts of *D. citri* (*Candidatus* Carsonella, *Candidatus* Profftella, *Wolbachia* and *Halotalea*). The Shannon diversity index showed that *D. citri* from Tanzania had the highest diversity of bacterial genera (1.92), and *D. citri* from China had the lowest (1.34). The Bray-Curtis dissimilarity showed that China and Kenya represented the most diverged populations, while the populations from Kenya and Tanzania were the least diverged. The WIMP-ARMA analyses generated 48 CARD genes from 13 bacterial species in each of the populations. Spectinomycin resistance genes were the most frequently found, with an average of 65.98% in all the populations. These findings add to the knowledge on the diversity of the African *D. citri* populations and the probable introduction source of the psyllid in these African countries.

Introduction

The Asian citrus psyllid, *Diaphorina citri* Kuwayama (Hemiptera: Psyllidae) is a major pest of citrus plants, as it transmits "*Candidatus* Liberibacter asiaticus" (CLas), the pathogen associated with Huanglongbing (HLB) worldwide (Bové 2006). *Diaphorina citri* is native to Asia and widely distributed in southern Asia, but it has also been reported in South America, North America, and more recently, in Africa (Costa Lima, 1942; Catling, 1970; Shimwela et al., 2016; Rwomushana et al., 2016). HLB was responsible for the destruction of several citrus industries in

Asia and America in the past decade (Manjunath et al., 2008). As HLB is currently incurable, prevention of further spread of the disease calls for the management of the psyllid vector. The most commonly employed method for the control of *D. citri* relies on the use of synthetic pesticides such as endosulfan, aldicarb, cypermethrin, abamectin, acetamiprid and clothianidin (Boina and Bloomquist 2015). Unfortunately, insecticides are not species-specific and have negative impact on the environment and continued use can lead to insecticide resistance. Therefore, synthetic chemicals should be complemented or replaced by alternative methods, such as biological control using parasitoids, and the manipulation of endosymbionts.

The presence of endosymbiotic microbes in the insect gut has been shown to benefit the host, and their loss leads to decreased fitness (O'Neill et al., 1992; Kikuchi, 2009). Endosymbionts play a critical role in the reproductive fitness of insects and their ability to transmit pathogens. The presence of the key endosymbionts and their locations within the insect tissue gives insight into their probable effects on the acquisition and transmission of CLas by *D. citri* for example, "*Candidatus* Profftella" and "*Candidatus* Carsonella" which are vertically transferred from mother to offspring, have been shown to be localized in the bacteriome, with "*Candidatus* Carsonella" localizing to the outer layer in the cytoplasm of the bacteriocytes, while "*Candidatus* Profftella" localizes to the inner syncytial cytoplasm while *Wolbachia pipientis* wDi localized the outside layer of the bacteriome (Hosseinzadeh et al., 2019). Furthermore, *Wolbachia pipientis* is present in the Malpighian tubules and within midgut epithelial cells, the outer membrane cells of the scrotal capsule, testes, and accessory glands (Hosseinzadeh et al., 2019). Bacterial symbionts have been considered as a potential tool to manipulate reproduction of *D. citri* or suppress transmission of CLas to citrus plants (Hoffmann et al., 2014). Studies on the endosymbiont densities in different tissues and CLas in healthy and CLas-exposed, male and female *D. citri* individuals showed a variation between the bacterial densities and that CLas has a different effect on the endosymbionts in males and female *D. citri* (Hosseinzadeh et al., 2019). Key endosymbionts of *D. citri* such as *Wolbachia*, *Candidatus* Profftella and *Candidatus* Carsonella have diverse roles within the insect. *Ca.* Carsonella is a putative nutrition provider, while *Ca.* Proftella has been reported as a defensive symbiont (Nakabachi et al., 2013; Dossi et al., 2014). *Wolbachia* is maternally transmitted in the egg cytoplasm and performs reproductive manipulations to increase the fitness of *Wolbachia*-infected matrilines resulting in cytoplasmic incompatibility between uninfected females and infected males (Nakabachi et al., 2013). This activity of *Wolbachia* has been exploited as a potential control measure to decrease insect populations as with *Ceratitis capitata, Aedes aegypti* and *Aedes albopictus* (Zabalou et al., 2004; Xi et al., 2005; Xi et al., 2006; Calvitti et al., 2010).

The study of microbial communities through metagenomics helps to understand their interactions with arthropods, disease transmission, immunity, host resistance and insect host vector competence (Finney et al., 2015; Weiss & Aksoy, 2011). The taxonomic composition of metagenomes can be profiled using short-read high-throughput sequencing followed by mapping the reads to reference genomes, and analysis of k-mer distribution (Brown et al., 2017). However, the taxonomic resolution of the target community to the species level is limited by read length.

Recent reports of the presence of *D. citri* in Tanzania and Kenya (Shimwela et al., 2015; Rwomushana et al., 2016) and CLas in Ethiopia (Saponari et al., 2010; Ajene et al., 2019) highlighted the need to profile the metagenome diversity in the insect vector populations. The identification of key endosymbionts and other bacteria, as well as antibiotic resistance genes in the microbial community within the insect can inform the development of sustainable, integrated pest control strategies. The main objectives of this study were to evaluate microbiome and endosymbiont diversity in *D. citri* populations, and to detect antibiotic resistance genes in the microbiome of the insects.

Methods

Sample collection and DNA extraction

Collection of *D. citri* specimens were carried out in orchards and backyard gardens in Kenya and Tanzania from March 2017 to December 2018. Adult psyllids were aspirated from citrus plants at the collection sites and stored in 96% ethanol. Adult psyllids were also obtained from citrus trees in the Fuzhou, Fujian Province, (China) (Fig 7.1). Five female insect specimens per country collected from sweet orange (*Citrus sinensis*) trees were randomly selected for further analysis. Specimens were surface-sterilised using 3% sodium hypochlorite for three seconds, rinsed thrice with distilled water to remove environmental contaminants, and stored at -80 °C until DNA extraction. Total DNA was extracted from individual specimens using the Isolate II Genomic DNA kit (Bioline, London, United Kingdom), following the manufacturer's instructions. DNA extracts were checked for quality and concentration using a Nanodrop 2000/2000c Spectrophotometer (Thermo Fischer Scientific, Wilmington, USA). DNA extracts within the $A_{260\ nm}/A_{280nm}$ ratio range of 1.8 to 2.0 were eluted to a final volume of 50 µl, and used for downstream analyses.

Figure 7.1. Geographic origin of *Diaphorina citri* populations (China, Kenya and Tanzania) surveyed for assessment of microbiome and endosymbiont diversity, and presence of antibiotic resistance genes.

PCR and Sanger sequencing for identification of endosymbiont

A preliminary screening of the DNA extracts was performed using universal primers for bacterial 16S rRNA (Appendix 19) (Hocquellet et al., 1999). The same gene region was amplified using *Wolbachia*-specific primers (Werren and Windsor, 2000). The sequences generated in this study were deposited in GenBank (accession numbers MN928700 - MN928707). The phylogeny of the key endosymbionts of *D. citri* was assessed using a compilation of selected publicly available 16S sequences on GenBank. Multiple sequence alignments were performed using the MAFFT. The final sequence alignment (n = 1400 bp) was used to construct a Maximum likelihood (ML) tree to display the relationships among the microbial sequences from different regions. The ML tree was constructed using MEGA X based on p-distances under the Tamura-Nei model, with 1,000 bootstrap replicates.

MinION sequencing

The MinION $1D^2$ sequencing chemistry (Oxford Nanopore Technologies, Inc., Oxford, UK) provides high information content in long reads (10,000 -100,000 bp), resulting in longer alignments and, therefore, higher taxonomic resolution and specificity (Brown et al., 2017). For this survey, total DNA from five individuals per country was pooled, and analysed as a single

sample. Sequencing of bacterial 16S rRNA was performed on an Oxford Nanopore Technologies (ONT) MinION device using R9.4 flow cells to obtain the full-length 16S rRNA metagenome (~1,500 bp). Libraries were prepared using the SQK-RAB204 16S Barcoding kit following the ONT "16S Barcoding Kit (SQK-RAB204)" protocol, according to the manufacturer's instructions. The library preparation PCR step was carried out in a total reaction volume of 50 µl containing 5X My Taq reaction buffer (5 mM dNTPs, 15 mM $MgCl_2$, stabilizer and enhancer) (Bioline), 0.5 pmol μl^{-1} of each 16S barcode, 0.0625 U μl^{-1} MyTaq DNA polymerase (Bioline), and 10 ng μl^{-1} of DNA template. Reactions were run in a Mastercycler Nexus gradient thermal cycler (Eppendorf, Germany), under the following conditions: initial denaturation for 2 min at 95°C, followed by 35 cycles of denaturation for 30 s at 95°C, annealing for 40 s at 55°C and extension for 1 min at 72°C, and a final extension step of 10 min at 72°C. Libraries were purified, pooled and diluted to 4 nM prior to MinION sequencer runs, which ranged from 4 to 8 h.

Base calling and read preparation

Live base calling of the MinION reads was performed using the ONT Albacore in the MinKNOW software (v19.05.0). All raw data were deposited in the NCBI database as BioProject: PRJNA598520. Quality assessment of each MinION dataset was performed during the runs via MinKNOW. The raw MinION reads collected during the sequencing runs by MinKNOW were immediately uploaded to the ONT cloud for analyses via EPI2ME (v2.59.1896509), after which base-called data were returned to the host computer, also in the form of FASTQ files. The "What's in my Pot" (WIMP) (Juul et al., 2015) workflow classifies and identifies species in real-time. FASTQ-WIMP (v3.2.1) (Juul et al., 2015) (https://epi2me.nanoporetech.com/) was used to extract and characterize the numbers of reads and assign taxonomy. FASTQ-WIMP, which has been shown to work for long-read data (Irinyi et al., 2019), was used to analyze the datasets and assign taxonomic identification by comparing the reads against a NCBI database for bacteria. WIMP makes use of Centrifuge software (Kim et al., 2016), which is capable of accurately identifying reads when using databases containing multiple highly similar reference genomes, such as different strains of bacterial species. Centrifuge identifies unique segments of those genomes and builds an FM-index that can be used for efficient searches of sequenced reads. The WIMP workflow classifies and identifies species in real time: as soon as a strand of DNA passes through the pore it can be base-called and analysed.

Bacterial diversity statistics

Direct quantitative comparison of abundances was done at the genus level using a stacked bar plot to view the cumulative read counts from the samples for each country. A minimum

abundance cut-off of 0.1% was used to select the most abundant taxa in each sample. Taxa with cumulative read counts below the 0.1% cut-off were collapsed into "Others" category. Viewing composition at higher-levels (e.g. genus) provides a better picture than at lower-levels (e.g. species), when the number of bacterial species in a community is large and diversified. Merging minor taxa helps to better visualize significant taxonomic patterns in the data. Alpha diversity statistics, which included evenness, richness and the Shannon-Wiener index, were used to determine the bacterial diversity in each sample. Beta diversity was computed using the Bray Curtis dissimilarity index (Bray and Curtis, 1957; Beals, 1984) to determine the diversity of bacterial genera among the samples. Inter-population distances were visualized using principal coordinate analyses (PCoA) computed in R software v3.5.3, using the '*vegan'* package (Oksanen et al., 2015).

Antibiotic resistance genes

MinION reads from the WIMP workflow were searched for antibiotic resistance genes (ARGs) using the ARMA workflow in EPI2ME (https://epi2me.nanoporetech.com/). The workflow is integrated with the Comprehensive Antibiotic Resistance Database (CARD) to identify ARGs. The CARD model used in this analysis was the rRNA mutation model. Depth of coverage, alignment details, and resistance profile from the CARD database were generated for specific genes.

Results

Identification of endosymbionts using Sanger sequencing

PCR and Sanger sequencing of individual *D. citri* specimens using universal primers for bacteria (27F/149R) generated sequences (accession nos MN928700 - MN928703) which showed homology with *Wolbachia sp.* (100%)*, Candidatus* Profftella armatura (98%), *Pseudomonas sp.* (97%), *Candidatus* Carsonella ruddii (98%), *Enterobacteriaceae sp.* (96%), and *Syncytium* endosymbiont (96%) respectively (Appendix 20) in all samples. The *Wolbachia*-specific primers (wspecF/wspecR) generated sequences identified as *Wolbachia sp*., based on sequence homology using BLAST. The sequences from this study (accession nos MN928704 - MN928707) had 100% identity with *Wolbachia* endosymbiont of *D. citri* sequences in GenBank. The Maximum-Likelihood tree was built using 16S rRNA sequences obtained from the samples in this study combined with 16S rRNA sequences of the representative sequences available in GenBank to assess the phylogeographic structure of the key endosymbionts of *D. citri*. The tree topology indicated that "*Candidatus* Carsonella ruddii" from this study clustered closely with "*Candidatus* Carsonella ruddii" from China while a wider variation was seen between the sequences from this study and the sequences from Australia and the USA. The "*Candidatus*

Profftella" sequences from this study was closely related to the publicly available sequences obtained from China and Japan. The same trend was observed with the *Wolbachia* sequences obtained from this study (Fig. 7.2).

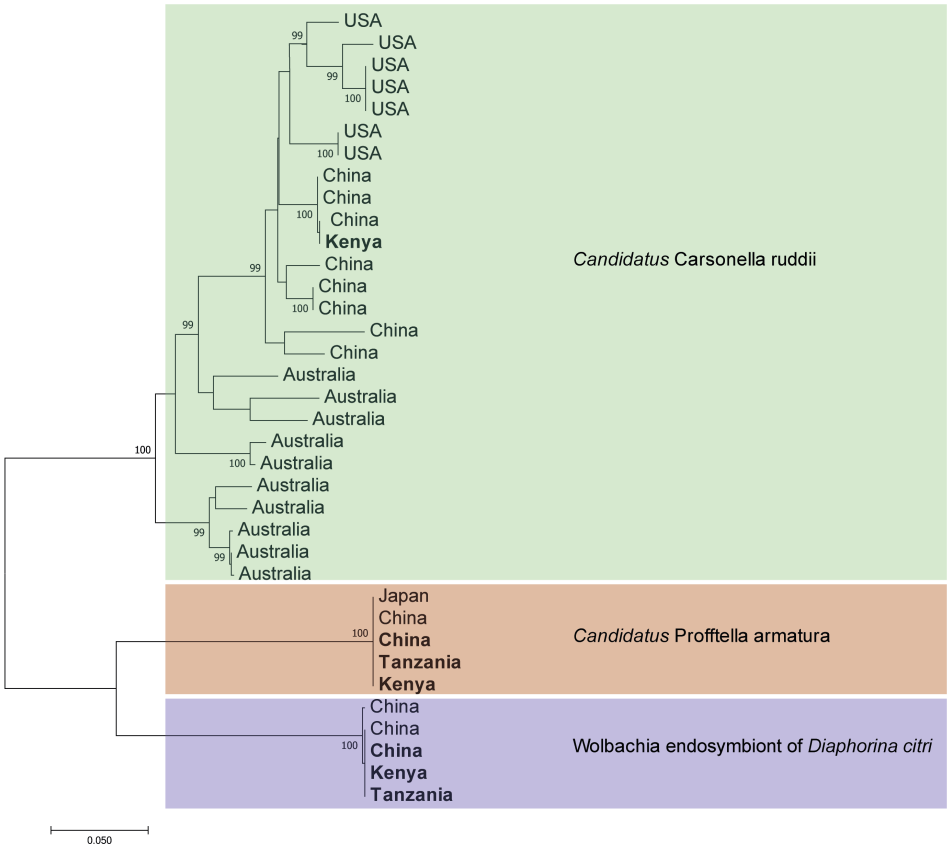

Figure 7.2. Maximum-Likelihood tree based on 16S ribosomal RNA gene sequences of "*Candidatus* Carsonella ruddii", "*Candidatus* Profftella armatura" and *Wolbachia* endosymbiont of *Diaphorina citri* from China, Kenya and Tanzania and representative sequences from publicly available sequences on GenBank. Branch support was based on 1000 bootstrap replicates. Samples from this study are in bold font.

Full length 16S metagenome profiling

Library size and cumulative abundance

Library size was the largest for *D. citri* from Tanzania (812,730 reads), followed by those from China (192,136 reads) and Kenya (80,521 reads) (Fig. 7.3).

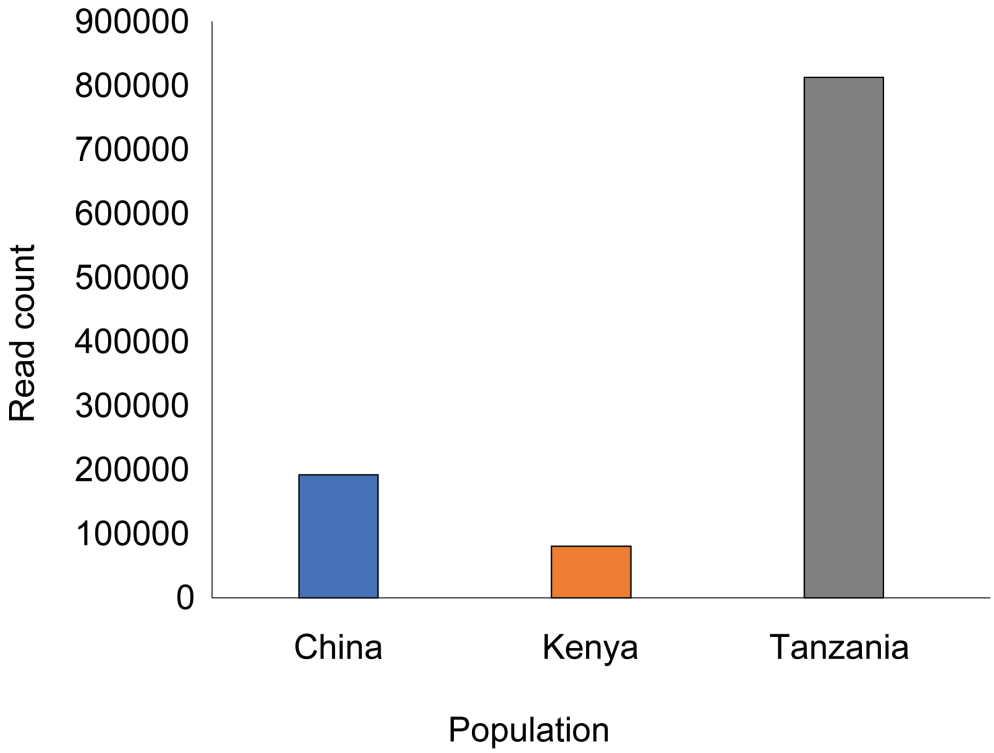

Figure 7.3. Overview of 16S rRNA library size for MinION sequencing of five pooled *Diaphorina citri* individuals collected from each world region (China, Kenya and Tanzania).

The taxonomic composition of the samples and the cumulative abundance of the bacterial genomes present in *D. citri* from the different world regions are presented in figure 7.3 and showed that the most abundant genera in China were *Candidatus* Profftella making up 46.32% of the bacterial population, *Wolbachia* (43.24%) and *Candidatus* Carsonella (1.99%). In Kenya, the most abundant genera were *Candidatus* Carsonella (42.41%), *Candidatus* Profftella (39.94%) and *Wolbachia* (8.33%). In Tanzania, the most abundant genera were *Candidatus* Profftella (43.15%), *Wolbachia* (21.83%) and *Candidatus* Carsonella (15.36%) (Fig. 7.4).

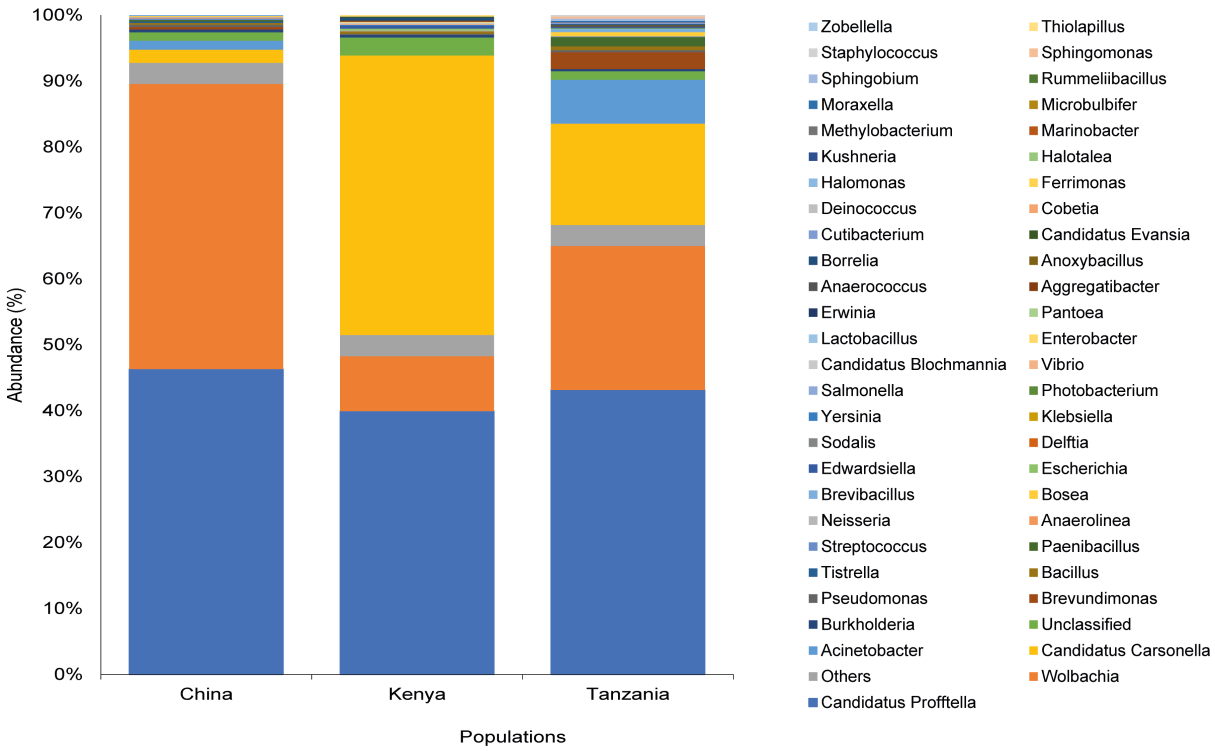

Figure 7.4. Taxonomic composition and percentage of reads of bacteria at the genus level of the bacterial community in *Diaphorina citri* from China, Kenya and Tanzania, using Stacked Bar plot. Taxa with cumulative read counts below the cut-off value of 0.1% were collapsed into 'Others' category.

Bacterial community profiling

Alpha diversity

The analysis showed that *D. citri* from Tanzania had the highest species richness (736), followed by China (477) and Kenya (367) (Appendix 21). The Shannon diversity index showed that *D. citri* from Tanzania had the highest diversity of bacterial genera (1.92), followed by Kenya (1.51) and China (1.34) (Fig. 7.5). The effective diversity (True-Shannon) showed that *D. citri* from Tanzania had the highest effective number of species (6.78), followed by Kenya (4.51), and China (3.81).

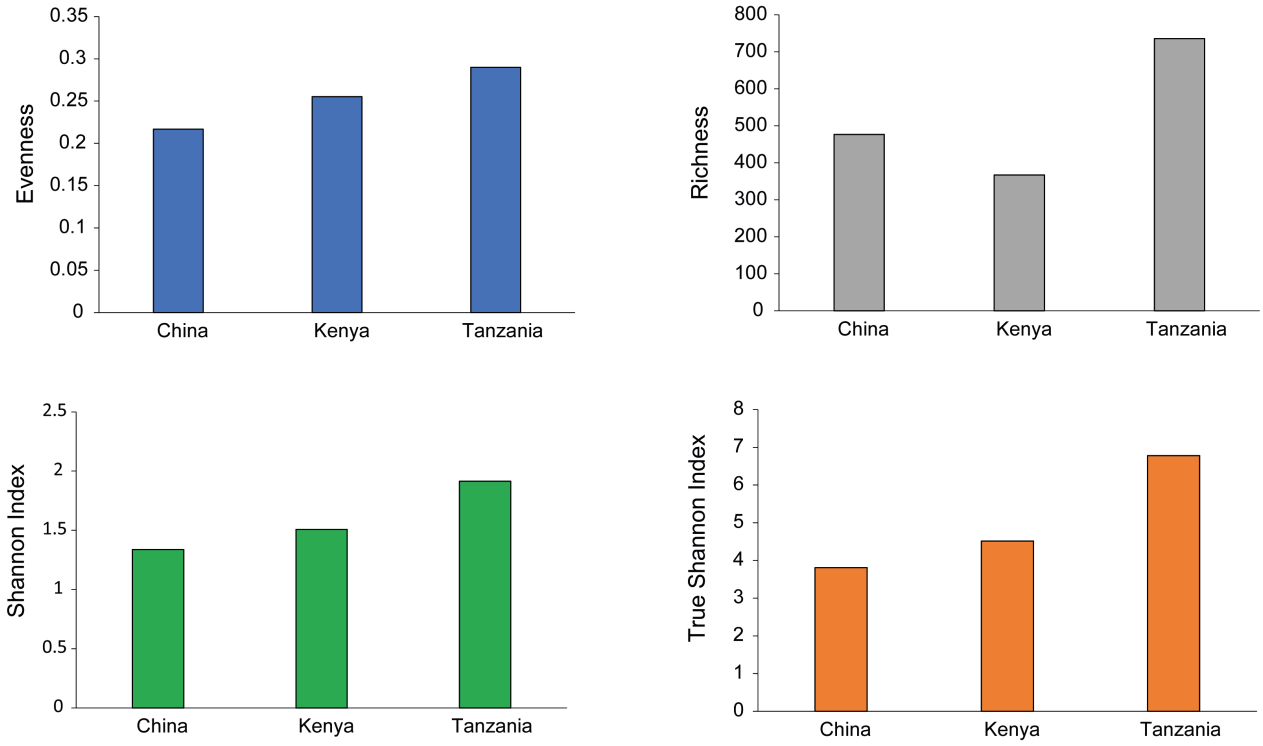

Figure 7.5. Alpha-diversity measures using evenness, Shannon diversity index, and species richness at the genus level across *Diaphorina citri* collected in different word regions (China, Kenya, and Tanzania). The samples were composed by five pooled individual insects, and are represented on the X-axis, and their estimated diversity is represented on the Y-axis.

Beta diversity

The highest value in interpopulation diversity, as estimated with the Bray Curtis dissimilarity index, was obtained between Kenya and China (26.43%) (Table 7.1) while the lowest interpopulation diversity was observed between Kenya and Tanzania (8.72%) (Table 7.1, Fig 7.6).

Table 7.1. Interpopulation beta diversity (%) in the metagenomes of *Diaphorina citri* from different world regions, as estimated using the Bray Curtis dissimilarity index.

	Dissimilarity (%)		
World region	China	Kenya	Tanzania
China	-		
Kenya	26.43	-	
Tanzania	25.61	8.72	-

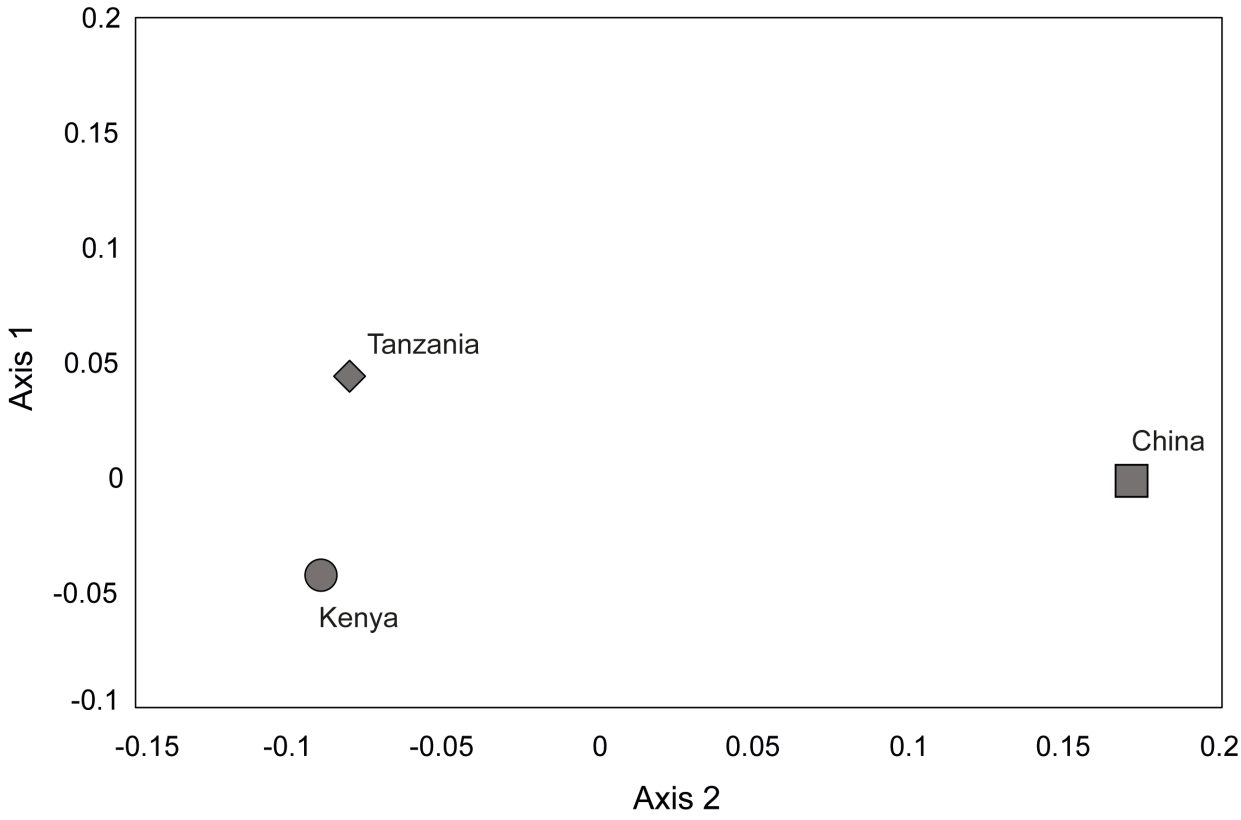

Figure 7.6. Two-dimensional principal coordinate analyses plot of the beta diversity of bacterial genera in *Diaphorina citri* collected from different world regions, estimated using the Bray Curtis dissimilarity index showing.

Abundance of antibiotic resistance genes in *Diaphorina citri*

The number of 16S rRNA reads analysed ranged from 44,455 (Kenya) to 399,992 (Tanzania), with overall average accuracy of the alignments of 75.45% (Appendix 22). The identified ARGs conferred resistance to 16 antibiotic compounds (Table 7.2). Among the detected ARGs in the microbiome of *D. citri*, spectinomycin resistance genes were the most abundant, making up 72.82%, 70.75% and 67.29% of the total ARGs found in Tanzania, China and Kenya. This was followed by tetracycline resistance genes with 17.42%, 10.95% and 7.55% detected in China, Tanzania and Kenya respectively. Streptomycin resistance genes in Kenya (4.43%) and Tanzania (2.71%), and kasugamicin resistance genes were the third most abundant in China (2.74%) (Fig 7.7).

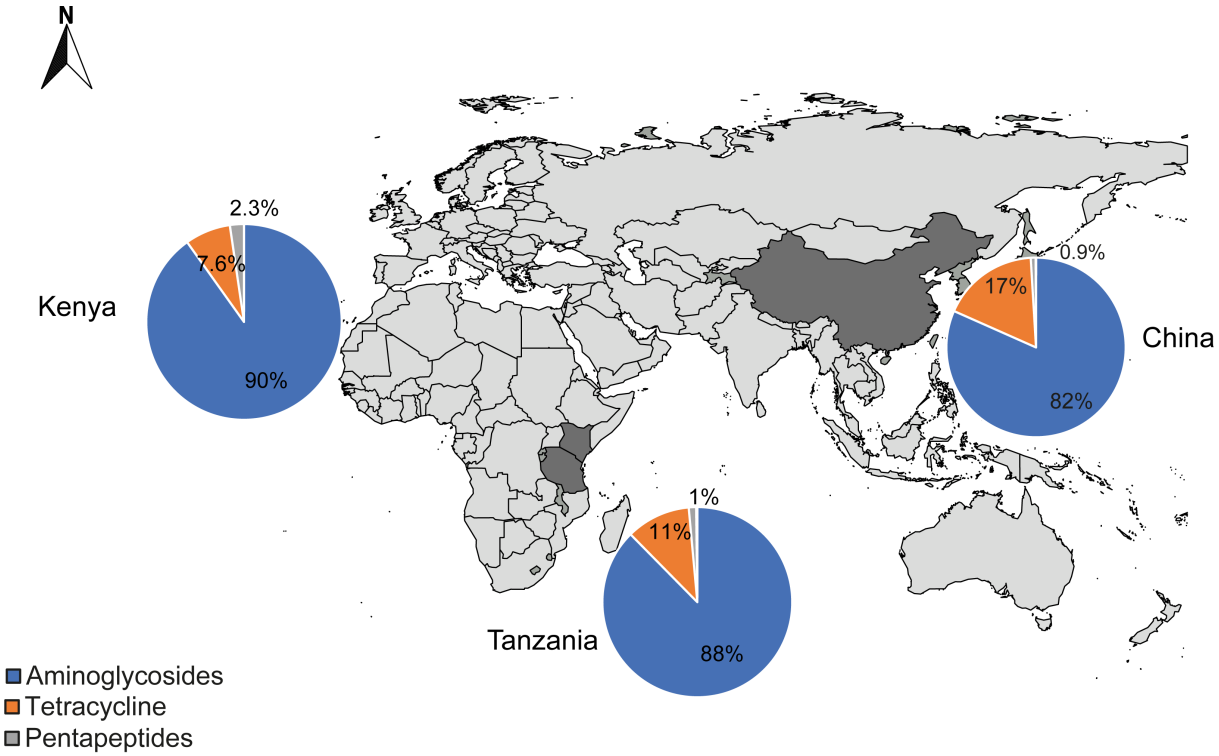

Figure 7.7. Relative abundance of genes for resistance to antibiotics identified in the microbiome of *Diaphorina citri* from China, Kenya and Tanzania.

Table 7.2. Antibiotic resistance genes found in the microbiome of the citrus psyllid *Diaphorina citri,* as obtained from Comprehensive Antibiotic Resistance Database.

Taxon	**Gene**	**Conferred antibiotic resistance**
Borrelia burgdorferi	*Borrelia burgdorferi* 16S rRNA mutation	resistance to gentamicin, kanamycin and spectinomycin
Chlamydia psittaci 6BC	*Chlamydophila psittaci* 16S rRNA mutation	resistance to spectinomycin
Escherichia coli K-12	*Escherichia coli* 16S rRNA mutation	resistance to edeine
	Escherichia coli 16S rRNA mutation in the rrnB gene	resistance to spectinomycin, streptomycin and tetracycline
	Escherichia coli 16S rRNA mutation in the rrsB gene	resistance to G418, gentamicin C, kanamycin A, neomycin, paromomycin, spectinomycin, streptomycin, tetracycline and tobramycin
	Escherichia coli 16S rRNA mutation in the rrsC gene	resistance to kasugamicin
	Escherichia coli 16S rRNA mutation in the rrsH gene	resistance to spectinomycin
Helicobacter pylori 26695	*Helicobacter pylori* 16S rRNA mutation	resistance to tetracycline
Mycobacterium abscessus	*Mycobacterium abscessus* 16S rRNA mutation	resistance to amikacin, gentamicin, kanamycin, neomycin and tobramycin

Mycobacterium	*Mycobacterium chelonae* 16S rRNA mutation	resistance to amikacin, gentamicin C, kanamycin A, neomycin and tobramycin
Mycobacterium smegmatis str. MC2 155	*Mycobacterium smegmatis* 16S rRNA mutation in the rrsA gene	resistance to hygromycin B, kanamycin A, neomycin and viomycin
	Mycobacterium smegmatis 16S rRNA mutation in the rrsB gene	resistance to hygromycin B, kanamycin A, neomycin, streptomycin and viomycin
Mycobacterium tuberculosis H37Rv	*Mycobacterium tuberculosis* 16S rRNA mutation	resistance to amikacin, kanamycin, streptomycin and viomycin
Neisseria gonorrhoeae	*Neisseria gonorrhoeae* 16S rRNA mutation	resistance to spectinomycin
Neisseria meningitidis	*Neisseria meningitidis* 16S rRNA mutation	resistance to spectinomycin
Pasteurella multocida 36950	*Pasteurella multocida* 16S rRNA mutation	resistance to spectinomycin
Propionibacterium acnes	*Propionibacterium acnes* 16S rRNA mutation	resistance to tetracycline
Salmonella enterica subsp. *salamae*	*Salmonella enterica* serovar *Typhimurium* 16S rRNA mutation in the rrsD gene	resistance to spectinomycin

Discussion

The standard methodology in metagenomics involves sequencing and annotation of whole genomes extracted directly from samples to profile the microbial composition (Eisenstein 2012). Efforts to use this technology to study diverse environmental communities have been limited (Edwards et al., 2016), and there has been a limited assessment of the best strategies for data analysis in nanopore-based environmental metagenomics (Brown et al., 2017). In this study, we assessed the microbiome diversity and presence of bacterial antibiotic resistance genes in a pool of five *D. citri* specimens collected from each of four countries (China, Kenya and Tanzania), using ONT long-read sequencing of the full length 16S metagenome. The nanopore sequencing resulted in good read coverage (up to 800,000 reads). The bacterial community profiling in this study relied on the cumulative read count generated from the FASTQ-WIMP and is presented as a percentage of reads of specific bacterial genera amongst reads to all bacterial genera.

The preliminary screening of bacteria in *D. citri* using Sanger sequencing with universal and *Wolbachia*-specific primers revealed the presence of the key endosymbionts *Candidatus* Carsonella, *Candidatus* Profftella and *Wolbachia,* along with other bacterial species. The full-length 16S metagenome analysis correlated with the preliminary screening, showing that the dominant genera in three of the four samples representing each country were similarly comprised of *Candidatus* Proftella, *Candidatus* Carsonella and *Wolbachia*, which are key endosymbionts of *D. citri* (Nakabachi et al., 2006). This agrees with previous studies on the microbiota of *D. citri*

which identified "*Candidatus* Profftella", "*Candidatus* Carsonella" and *Wolbachia* as the endosymbionts with the highest composition (Chu et al., 2016; Wang et al., 2017; Hosseinzadeh et al., 2019; Meng et al., 2019).

Candidatus Proftella had the highest abundance in three of the four populations tested, while *Wolbachia* had the second-highest abundance in Tanzania and third highest abundance in Kenya. Previously, *Candidatus* Profftella was reported to be present in all *D. citri* populations (Nakabachi et al., 2013). The difference in the microbial population composition between the Kenyan and Tanzanian population could be a result of the age of the psyllids as previous reports have shown that gender and age could be factors affecting the densities of endosymbionts between populations (Chu et al., 2016). Our study specifically considered the microbiota composition in females partly because it has been reported that "*Candidatus* Profftella" and "*Candidatus* Carsonella" show an increase in the female ovaries in the presence of CLas and thus a potentially greater effect on the reproductive ability of *D. citri.* Also, higher densities of "*Candidatus* Profftella" and "*Candidatus* Carsonella" in the bacteriome of CLas-infected females as compared to CLas-infected males have been reported (Hosseinzadeh et al., 2019). This could account for the higher density of the two endosymbionts seen in the current study. *Wolbachia* is known to cause cytoplasmic incompatibility between uninfected females and infected males resulting in increased infected lineages in the host population (Nakabachi et al., 2013). The ability of *Wolbachia* to cause incompatibility in insects can be exploited as a potential control measure to control *D. citri* in addition to other control methods, as has been shown in the Mediterranean fruit fly and the olive fruit fly (Zabalou et al., 2009, Apostolaki et al., 2011). Additionally, *Wolbachia* can play a crucial role in the reduction in transmission efficiency of CLas by *D. citri* by causing a reduction in the production of saliva in the psyllid, as the Liberibacter is transmitted through the saliva during feeding. This has been shown to be effective in mosquitoes where *Wolbachia*-infected *Aedes aegypti* produce smaller volumes of saliva (Moreira et al., 2009). Furthermore, as *Wolbachia* has been shown to display an increased density in CLas-exposed males, the possibility of vector manipulation using Wolbachia that may affect the ability of *D. citri* to transmit CLas has been hypothesized (Hosseinzadeh et al., 2019).

Our study showed that *D. citri* from the Tanzania had the highest degree of homogeneity (high evenness index), while the population from China was the most heterogeneous. This suggests that all bacterial species within the *D. citri* from the Tanzania have a higher rate of equal abundance within the microbiome compared to the other populations, as evenness is a measure of the homogeneity in terms of species abundance (MacDonald et al., 2017). Species richness (a measure of the number of species or other taxonomic levels present in a population) showed that the *D. citri* from Tanzania had the most bacterial taxa and is therefore likely to harbour a more

ecologically complex microbiome. Criticisms of the Shannon–Wiener index due to the log-transformation of species proportion values, which weakens the discriminating power of the index (Magurran 2013), informed the use of True-Shannon index (effective number of species) (Jost 2006) to yield an effective number of species in this study. The True-Shannon diversity or the effective number of species, which considers species richness, as well as the dominance of a species, is a more complex measure of how many different types of taxa are present in a population (Jost 2006). The True-Shannon diversity showed that *D. citri* from the Tanzania had the most diverse microbiome, followed by Kenya. *Diaphorina citri* from China, which was richer in bacterial species than *D. citri* from Kenya, had lower diversity. The negative correlation between Shannon diversity and richness observed in this study agrees with the report of the negative correlation between species richness and Shannon-Weiner diversity (MacDonald et al., 2017). The species richness and evenness were positively correlated in this study. Wilsey et al., (2005) also found that species richness and evenness were positively correlated within invertebrate communities.

Interpopulation comparison, as estimated by Bray-Curtis dissimilarity index, showed that *D. citri* microbiomes had the highest diversity between the China and Kenya. Additionally, the diversity between the *D. citri* metagenome from China and Tanzania was similar to the diversity between China and Kenya. Overall, the alpha and beta diversity of the metagenome of *D. citri* support the hypothesis of a close genetic relationship between the African and the Chinese *D. citri*. Furthermore, the phylogeny of the key endosymbionts showed close relationship between the *D. citri* from Kenya/Tanzania and *D. citri* from China in relation to *D. citri* from other regions. Most evident was the clustering of the "*Candidatus* Carsonella rudii" sequences where significant variation was seen between sequences from Australia/USA and the sequences from Kenya and China. Previous studies on the endosymbiont variation in *D. citri* have shown that the distribution of "*Candidatus* Carsonella ruddii" had a strong geographical structure in China (Wang et al., 1999), thereby informing the inference of a possible invasion route of *D. citri* from China into Eastern Africa. This highlights the need for further studies on the resolution of the origins of *D. citri* in Africa by assessing the population structure and genetic diversity using bi-parentally transmitted microsatellite markers.

The WIMP-ARMA workflow generated 48 Comprehensive Antibiotic Resistance Database (CARD) genes from 13 bacterial species in each of the samples. The identified genes for antibiotic resistance conferred resistance to 16 antibiotic compounds belonging to different groups: aminoglycosides (amikacin, gentamicin, gentamicin C, hygromycin B, kanamycin, kanamycin A, kasugamicin, neomycin, paromomycin, spectinomycin, streptomycin and tobramycin), pentapeptides (edeine), tetracycline, and tuberactinomycin (viomycin), in varying

frequency across the four countries. The most abundant type of antibiotic resistance gene was spectinomycin resistance, across all the samples from each country, followed by tetracycline resistance. Antibiotics have been used in several countries in attempts to control HLB (McManus et al., 2002), with positive results of reduced symptoms in the treated trees as evaluated in China, Reunion Island, and the Philippines (Zhao 1981, Aubert & Bové 1981), and also on "*Candidatus* Liberibacter africanus" infected trees in South Africa (Schwarz and Van Vuuren 1971). However, the use of antibiotics may have accelerated the development of resistance genes within the gut microbiome in *D. citri* as a response to selective pressure (Ignasiak and Maxwell 2017). For example, tetracycline resistance genes were present in all samples tested in our study, and tetracycline has been used in direct injection into the trunks of HLB-affected citrus trees in China and India (Zhao 1981, Aubert & Bové 1981). The effect of antibiotics on the microbiome of insects is a cause for concern, since the microbiome may serve as reservoirs for resistance genes that can be transferred to pathogens (Salyers et al., 2004; Marshall et al., 2009; Sommer et al., 2009), as well as to the host plant (Zurek & Ghosh, 2014). Furthermore, the use of antibiotics in controlling infections by pathogens also impacts beneficial bacteria since the selective pressure caused by an antibiotic can cause the buildup of resistance determinants within the microbiome community members (Zurek & Ghosh 2014).

The combination of the variation shown in the phylogenetic reconstruction of the 16S sequences, the microbiome composition and diversity as well as the composition of antimicrobial resistance genes identified in this study presents a case for the probable route of invasion of the *D. citri* into Kenya and Tanzania from China. Although, further research into the genetic diversity of these populations is required to confirm the origins. Furthermore, the elucidation of the endosymbionts, and microbiome community and its antibiotic resistance genes in *D. citri* provide valuable information on potential integrated pest control measures which can be used to curb the spread of the psyllid and its ability to transmit diseases. For example, manipulation of cytoplasmic incompatibility conferred by *Wolbachia* can be used to interrupt the capacity of the insect to transmit diseases (Sinkins, 2004; Kambris et al., 2009; McMeniman et al., 2009; Iturbe-Ormaetxe et al., 2011), in addition to strategies aimed at reducing *Candidatus* proftella within the psyllid in order to enhance predation. The presence of polyketide synthase (PKS) genes in *Candidatus* proftella, which are responsible for the synthesis of diaphorin (a bioactive polyketide), indicates that *Candidatus* Profftella is a defensive symbiont. Diaphorin creates inhibitory effects on predators such as the Asian lady beetle *Harmonia axyridis* (Nakabachi et al., 2013). Therefore, decreased *Candidatus* Proftella within *D. citri* will increase the susceptibility of the insect to predators. Furthermore, the influence of *Wolbachia* on the increased susceptibility of the psyllid to parasitoids (Van Nouhuys et al., 2016) can be exploited.

These factors, combined with knowledge of the possible transfer of ARGs from the psyllid to the plant, can inform integrated pest control strategies. Therefore, a comprehensive assessment of the role of *Candidatus* Proftella and *Wolbachia* in *D. citri* should be evaluated in order to increase the potential of biological control applications using predators and *Wolbachia* induced cytoplasmic incompatibility, whilst encouraging a reduction in the use of antibiotics for the control of HLB. Furthermore, research on the population structure and genetic diversity of the citrus psyllids in Africa needs to be carried out for complementing the knowledge on the microbiome and endosymbiont composition of *D. citri* on the continent. These findings are critical to the implementation of integrated pest management strategies to curb the rapid spread of the pest and the associated pathogen "*Candidatus* Liberibacter asiaticus" to other parts of Africa.

Preceding chapters in this thesis have described the distribution of *Candidatus* Liberibacter species associated with citrus greening disease in three Eastern African countries (Ethiopia, Kenya and Uganda) and determined the potential spread of CLas associated Huanglongbing (HLB)in the region. The population structure of the invasive vector of "*Candidatus* Liberibacter asiaticus" (CLas), *D. citri,* was also unravelled using nuclear microsatellite markers and the complete mitochondrial genome to identify the probable sources of introduction of *D. citri* into the three African countries where it has established. Furthermore, the microbiome of the vector was assessed using Oxford Nanopore Technologies (ONT) long-read sequencing of the full length 16S metagenome to identify key endosymbionts and antibiotic resistant genes; important information which will prove useful in the development of sustainable management strategies utilizing novel approaches aimed at psyllid endosymbiont mitigation to decrease the fitness and vector potential of the insect to control spread of HLB.

The current distribution of the Liberibacter species varied among the three countries, with Ethiopia having a larger distribution of CLas and was identified in Kenya for the first time in the coastal region of the country, while "*Candidatus* Liberibacter africanus subspecies clausenae" (CLafCl) was more widespread in Uganda. CLas in Ethiopia was widespread in the highlands where the symptoms were severe, in contrast to reports that they are less pronounced and disappear above 1,500 m (Aubert 1987). In Uganda, CLafCl infected plants showed severe symptoms similar to the HLB infected plants observed in Ethiopia. In contrast, the citrus plants in the western region of the country, which were infected by "*Candidatus* Liberibacter africanus" (CLaf), had milder symptoms typical of African citrus greening disease (ACGD). The detection of low concentrations of Liberibacter in asymptomatic plants has been problematic even with sensitive diagnostic methods (Manjunath et al., 2008). The bacterial quantities detected in citrus plants from Ethiopia and Uganda were high, suggesting that the establishment of the pathogen in the plant had happened over a long period as suggested by Halbert and Manjunath (2004). Although the bacterial titers of the CLas detected in citrus material was generally low in the Kenyan samples, the Liberibacter was unambiguously identified in plants and vectors highlighting a recent invasion of the pathogen in the country. The phylogenetic analysis of the Liberibacter species from this study unveiled an interesting observation; the interspecies diversity showed low genetic divergence between the "subspecies" of CLaf ("*Candidatus* Liberibacter africanus subspecies clausenae" (CLafCl), "*Candidatus* Liberibacter africanus subspecies

capensis" (CLafC) and "*Candidatus* Liberibacter africanus subspecies vepridis" (CLafV) with an average genetic distance of 3.63%. These Liberibacter are currently classified as subspecies of CLaf and clustered separately from CLaf in the analysis. Furthermore, the genetic divergence between CLaf and the "subspecies" group was similar to the divergence between CLas and the subspecies cluster. On the basis of this, we suggest that the CLafCl/CLafC/CLafV represent a different species complex rather than subspecies of CLaf. Further research involving other informative regions of the *Candidatus* Liberibacter genome such as the 16S and ribonucleotide reductase (RNR)-PCR derived from the five-copy nrdB gene and 4CP-PCR system (Zheng et al., 2016), a four-copy genomic locus in addition to the rplJ region will be necessary to confirm this assertion. The visual expression of the symptoms on the plants was also considered in this study. Although symptomatic expression of the Liberibacters could be a function of the environmental conditions as well as the age of the plant, we observed that plants of similar age carrying different Liberibacter species showed a difference in the severity of the associated disease, with CLas and CLafCl infected trees showing more severe symptoms than CLaf infected trees of the same age. This also suggests that the variation between the three pathogen groups may be linked to the phenotypic expression of the disease symptoms. Overall, our survey clearly confirms that CLas is present in Kenya and that the distribution of CLafCl in Uganda and CLas in Ethiopia is much more widespread than previously described.

We demonstrated the potential of an ensemble approach using bioclimatic variables to model the distribution of plant pathogens and predict future habitat suitability of Liberibacter species. In Eastern Africa, the modelling for the potential distribution of CLas showed large areas of optimum habitat suitability for the pathogen in Ethiopia and marginal suitability for CLas in eastern Uganda, where most commercial citrus is grown. Large areas of Tanzania showed marginal to optimal suitability for the pathogen, and the regions where *D. citri* has been detected (Rwomushana et al., 2017) were highly suitable. The coastal and western regions of Kenya, where citrus production is high, showed optimum suitability**.** The detection of *D. citri* previously in these regions (Rwomushana et al., 2017) and the subsequent detection of CLas in our study shows a heightened risk of proliferation of the disease to the citrus-producing parts of the central region of Kenya. The ensemble approach to plant-pathogen predictive modelling carried out in this study corroborates previous vector-based approaches to HLB prediction. Our results highlight the potential distribution of CLas in Africa and show that large areas of Central Africa, Eastern Africa, Southern Africa, and some parts of Western Africa are highly suitable for HLB establishment. ACG, which has only been reported in Africa thus far was modelled globally and our predictive maps showed large areas of the Americas, Asia and Australia included in the potential distributional range of ACG in the world. In Europe, only the Iberian Peninsula showed

suitability for the disease, although marginal. Thus, the prediction of potential habitat suitability of the bacteria in other areas of the world provides valuable information required for monitoring and implementation of preventive measures. Our projections of the distribution of CLas will inform; closer vector monitoring in citrus-producing areas with high suitability for HLB establishment, as well as periodic testing of asymptomatic citrus plants in these high-risk areas. Our approach presents an early warning system for citrus-producing regions where HLB and ACG are not yet present. Plant protection strategies based on future habitat suitability of plant pathogens would be an important inclusion in the integrated pest management systems for citrus production.

The vectors of HLB and ACG (*D. citri* and *T. erytreae*) were found during the study. *T. erytreae* adults were found on citrus trees in Ethiopia and Uganda, while *D. citri* adults were found in Ethiopia for the first time and in Kenya. In the three countries, both insect species tested positive for generic Liberibacter. CLas was detected for the first time in high concentrations in field populations of *T. erytreae* in the Ethiopian highlands where CLas infected trees were also found. This finding supports the postulation of the probable transmission of CLas by *T. erytreae* (McLean and Oberholzer 1965; Aubert et al., 1988; Da Gracia, 1991) which was shown experimentally previously. *T. erytreae* and *D. citri* could both transmit ACG and HLB (Massonie et al., 1976; Lallemand and Bove, 1986). *Diaphorina citri* which is the efficient vector of CLas is suited to areas with higher temperatures while *T. erytreae* thrives in highland areas where the temperatures are cooler, but niche overlap between these two species has been observed by Rwomushana et al., (2017). Therefore, the detection of CLas in field populations of *T. erytreae* in this study, suggests that this species has the potential for also transmitting HLB, particularly to citrus groves at the mid to higher altitude areas of Eastern Africa. We propose further studies into the transmission efficiency of both vectors in the field and the epidemiology of citrus greening amid both pathogens.

The detection of *D. citri* in Tanzania, Kenya and now Ethiopia prompted the research into the population structure of the vector to identify the probable source of introduction of the vector into the continent as well as its genetic diversity to provide information that will assist in the development of management strategies to curb its spread to other citrus-producing countries in Africa. The genetic diversity of *D. citri* from Kenya, Tanzania and Ethiopia was assessed in relation to *D. citri* from China and the USA. For this, the complete mitochondrial genomes of *D. citri* from these countries were compared, and the simple sequence repeats in the nuclear genome using microsatellite markers were analysed and the potential parent populations were identified. The mitochondrial genome, which is maternally transmitted, assessed all 13 protein-coding genes, as well as the 21 transfer RNA genes, showed that the *D. citri* from Kenya and Tanzania closely

linked to the *D. citri* from China, while the *D. citri* from Ethiopia had homology with the *D. citri* from the USA. Therefore, the probable origin of the Ethiopian *D. citri* is USA while the probable origin of the Kenyan and Tanzanian *D. citri* is China.

This was further confirmed by the use of nuclear microsatellites which are biparentally transmitted, making them more suitable for geneflow analysis. The analysis showed the difference in the population structure of the African *D. citri* populations and identified the source of introduction of *D. citri* into Kenya and Tanzania as China as there was a low genetic distance between the Chinese *D. citri* and the Tanzanian *D. citri.* Low population differentiation patterns were seen between the Kenyan and Tanzanian *D. citri* and this is probably as a result of direct trade routes between the sampled locations with no significant geological barriers to prevent the natural movement of the psyllid.

Within the Kenyan populations, the population from the western region of the country were significantly structured and showed some evidence for genetic differentiation from the population from the coastal part which shares a similar population structure to the Tanzanian populations. The *D. citri* populations were seen to be largely panmictic, therefore this pattern may be associated with the geographic proximity of the coastal population (which lies at the border with Tanzania) to the Tanzanian population. Also, the relative distance from the sites in western Kenya which are farther inland is a factor. Furthermore, there are more geological and physical barriers between the coastal population and the sites in western Kenya. The movement of the psyllid inland into Kenya most likely is as a result of a combination of trade practices and geographical barriers to dispersal which may have resulted in the observed differentiation. High gene flow was inferred from the close relationship between Mafiga, Mikese, Mlali and Lungalunga, in contrast to minimal migration inland into Kenya. Therefore, the evidence based on microsatellite molecular markers also showed that there are two distinct populations of *D. citri* in Africa with different origins. We also conclude that the first introduction of the species into East Africa occurring in Tanzania from China, and dispersal inward while the entry into Ethiopia occurring from the USA.

The assessment of the microbiome of *D. citri* from Kenya and Tanzania in relation to *D. citri* from China further revealed the link between the Kenyan and Tanzanian *D. citri* to the Chinese *D. citri* as the three most abundant bacterial species present in the microbiome of *D. citri* from Kenya, Tanzania and China were the same (*Candidatus* Profftella, *Candidatus* Carsonella and Wolbachia). Due to practical limitations in the novelty of the minion sequencing procedures (DNA isolation, library preparation, sequencing runs and bioinformatics) the sample size was limited (five individual samples each from four countries). Nonetheless, the data generated were

significant and provide critical insight into the microbiome of adult female *D. citri*. The diversity statistics showed that the probable parent population China had the highest degree of heterogeneity. The identification of high abundance of the primary endosymbionts of *D. citri* (*Candidatus* Proftella, *Candidatus* Carsonella and *Wolbachia*) in the Kenyan and Tanzanian populations is significant in the development of management strategies to reduce the *D. citri* populations as "*Candidatus* proftella" is a known defensive symbiont. The polyketide synthase (PKS) genes in "*Candidatus* proftella", is responsible for the synthesis of diaphorin (a bioactive polyketide), which creates inhibitory effects on predators such as the Asian lady beetle *Harmonia axyridis* (Nakabachi et al., 2013). Therefore, strategies aimed at decreasing "*Candidatus* Proftella" within *D. citri* will increase the susceptibility of the insect to predators. Furthermore, we recommend the exploitation of cytoplasmic incompatibility between uninfected females and infected males as well as the reduction in transmission efficiency of CLas by *D. citri* caused by *Wolbachia* as a potential control measure in addition to other control methods.

The identification of antibiotic resistance genes in *D. citri* adds to the information necessary in the development of key management strategies. As seen from our study, the most abundant type of antibiotic resistance gene was spectinomycin resistance genes, across all the samples from each country, followed by tetracycline resistance genes. The application of antibiotics in attempts to control HLB with the positive effects of reduced symptoms has been shown in China, Reunion Island, and the Philippines (Zhao 1981, Aubert & Bové 1981), and also on CLaf infected trees in South Africa (Schwarz and Van Vuuren 1971). The downside to this is the accelerated development of resistance genes within the gut microbiome in *D. citri* as a response to selective pressure (Ignasiak and Maxwell 2017). The effect of antibiotics on the microbiome of insects is a cause for concern, since the microbiome may serve as reservoirs for resistance genes that can be transferred to pathogens (Salyers et al., 2004, Marshall et al., 2009, Sommer et al., 2009), as well as to the host plant (Zurek & Ghosh, 2014). Furthermore, the use of antibiotics in controlling infections by pathogens also impacts beneficial bacteria since the selective pressure caused by an antibiotic can cause the build-up of resistance determinants within the microbiome community members (Zurek & Ghosh, 2014). The identification of the endosymbionts and the antibiotic resistant genes in *D. citri* presents a viable strategy on the potential integrated pest control measures which can be used to slow the spread of the psyllid and its ability to transmit diseases. Therefore, a comprehensive assessment of the role of "*Candidatus* Proftella" and *Wolbachia* in *D. citri* should be evaluated in order to increase the potential of biological control applications using predators and *Wolbachia* induced cytoplasmic incompatibility, whilst encouraging a reduction in the use of antibiotics for the control of HLB.

In conclusion, this thesis brings valuable contributions to the understanding of the distribution of *Candidatus* Liberibacter species associated with citrus greening disease in Eastern Africa and *D. citri* population diversity and has implications on HLB regulatory practices. The results present a strong case for strict phytosanitary and quarantine measures to be put in place to halt the spread of the disease as well as the vector to other African. Furthermore, we recommend increased surveillance for this pest as well as sustainable management strategies to avoid the invasion into other citrus-producing countries.

References

Aidoo, O. F., Tanga, C. M., Khamis, F. M., Rasowo, B. A., Mohamed, S. A., Badii, B. K., Salifu, D., Sétamou, M., Ekesi, S., & Borgemeister, C. (2018). Host suitability and feeding preference of the African citrus triozid Trioza erytreae Del Guercio (Hemiptera: Triozidae), natural vector of "*Candidatus* Liberibacter africanus." Journal of Applied Entomology 143(3), 262–270.

Ajene, I. J., Khamis, F., Adediji, A. O., Atiri, G., Kazeem, S., Mohammed, S., and S. Ekesi. 2019a. First report of '*Candidatus* Liberibacter africanus'' associated with citrus greening disease in Nigeria.' Plant Disease. https://doi.org/10.1094/PDIS-11-19-2380-PDN

Ajene, I. J., Khamis, F., Mohammed, S., Rasowo, B., Ombura, F. L., Pietersen, G., B. van Asch, and S. Ekesi. 2019b. First Report of Field Population of *Trioza erytreae* Carrying the Huanglongbing-Associated Pathogen, ' *Candidatus* Liberibacter asiaticus ', in Ethiopia . *Plant Disease*, *103*(7), 1766–1766. https://doi.org/10.1094/pdis-01-19-0238-pdn

Ajene I. J, Khamis F, Ballo S, Pietersen G, van Asch B, Seid N, Azerefegne F, Ekesi S, & Mohamed S (2020). Detection of *Diaphorina citri* in Ethiopia A new haplotype and its implication to the proliferation of Huanglongbing. *Journal of Economic Entomology*.

Aketarawong N, Bonizzoni M, Thanaphum S, Gomulski, L M Gasperi, G Malacrida, A R Guglieminoet C R (2007). Inferences on the population structure and colonization process of the invasive oriental fruit fly, Bactrocera dorsalis (Hendel). Mol Ecol. 2007;16(17):3522-3532. doi:10.1111/j.1365-294X.2007.03409.x

Akhtar, M. A., & Ahmad, I. (1999) Incidence of citrus greening in Pakistan. Pakistan Journal of Phytopathology 11, 1–5.

ANR, (2010). Citrus bacterial canker disease and Huanglongbing (citrus greening). Publication 8218. California, USA: University of California, Agriculture and Nature Resources. http://anrcatalog.ucdavis.edu

Apostolaki, A., Livadaras, I., Saridaki, A., Chrysargyris, A., Savakis, C., Bourtzis, K. 2011. Transinfection of the olive fruit fly Bactrocera oleae with Wolbachia: Towards a symbiont-based population control strategy. *J. Appl. Entomol*. 135, 546–553.

Araujo, M. B, Cabeza, M., Thuiller, W., Hannah, L., & Williams, P. H. (2004). Would climate change drive species out of reserves? An assessment of existing reserve-selection methods. Global Change Biology 10: 1618–1626.

Araujo, M. B. & New, M. (2007) Ensemble forecasting of species distributions. Trends in Ecology & Evolution 22, 42–47.

Araujo, M. B., & Peterson, A. T. (2012) Uses and misuses of bioclimatic envelope modeling. Ecology 93(7): 1527-1539.

Aubert, B. & Bové, J. 1980. Effect of penicillin or tetracycline injections of citrus trees affected by greening disease under field conditions in Reunion Island. Proc Intern Org Citrus Virology.

Aubert, B. (1987). *Trioza erytreae* del Guercio and *Diaphorina citri* Kuwayama (Homoptera: Psylloidea), the two vectors of citrus greening disease: Biological aspects and possible control strategies. *Fruits.* 42, 149-162

Aubert, B., Garnier, M., Cassin, J. C. and Bertin, Y. (1988). Citrus greening disease survey in eastern and western African countries south of Sahara. In *Proceedings of the 10th Conference of the International Organization of Citrus Virologists*. pp. 231-237. Edited by L. W. Timmer, S. M. Garnsey and L. Navarro. Riverside, CA: University of California

Aurambout, J. P., Finlay, K. J., Luck, J., & Beattie, G. A. C. (2009). A concept model to estimate the potential distribution of the Asiatic citrus psyllid Diaphorina citri Kuwayama in Australia under climate change—A means for assessing biosecurity risk. Ecological Modelling, 220(19), 2512–2524.

Bandelt, H. J., Forster, P., & Rohl, A. (1999). Median-joining networks for inferring intraspecific phylogenies. *Molecular Biology and Evolution.* 16(1), 37–48.

Bao, M., Zheng, Z., Sun, X., Chen, J., & Deng, X. (2019). Enhancing PCR capacity to detect '*Candidatus* Liberibacter asiaticus' utilizing whole genome sequence information. *Plant Disease*, PDIS-05-19-0931-RE. https://doi.org/10.1094/PDIS-05-19-0931-RE

Barbet-Massin, M., Jiguet, F., Albert, C. H., & Thuiller, W. (2012). Selecting pseudo-absences for species distribution models: How, where and how many? Methods in Ecology and Evolution, 3(2), 327–338. https://doi.org/10.1111/j.2041-210X.2011.00172.x

Barrows, C. W, Rotenberry, J. T, & Allen, M. F. (2010). Assessing sensitivity to climate change and drought variability of a sand dune endemic lizard. Biological Conservation 143: 731–736.

Bassanezi, R. B., & Gottwald, T. R. (2009) Epidemiology of HLB and potential pathways for introduction. Taller internacional de plagas cuarentenarias de los citricos. Villahermosa, Tabasco, México 27-31.

Batool, A., Iftikhar, Y., Mughal S. M., Khan, M. M., Jaskani, M. J., Abbas, M., & Khan, A. (2007) Citrus Greening Disease–A major cause of citrus decline in the world–A Review. *Hort. Sci.(Prague) 34*(4): 159-166

Beals, E. 1984. Bray-Curtis ordination: an effective strategy for analysis of multivariate ecological data. Adv. Ecol. Res. 14, 1–55.

Bernt, M., Braband, A., Schierwater, B., & Stadler, P. F. (2013). Genetic aspects of mitochondrial genome evolution. Molecular Phylogenetics and Evolution, 69(2), 328–338. https://doi.org/10.1016/j.ympev.2012.10.020

Boina, D. R. & Bloomquist, J. R. (2015). Chemical control of the Asian citrus psyllid and of huanglongbing disease in citrus *Pest Manag Sci* (2015) DOI 10.1002/ps.3957

Boore, J. L. (1999). Animal mitochondrial genomes. Nucleic Acids Research, 27(8), 1767–1780. https://doi.org/10.1093/nar/27.8.1767

Booth, T. H., Nix, H. A., Busby, J. R., & Hutchinson, M. F. (2014) BIOCLIM: the first species distribution modelling package, its early applications and relevance to most current MAXENT studies. Diversity and Distributions, 20(1): 1-9.

Bové, J. M. (2006). Huanglongbing: a destructive, newly-emerging, century old disease of citrus. *Journal of Plant Pathology*, *88*(1), 7–37.

Bove, J. M. (2014). Heat-tolerant Asian HLB meets heat-sensitive African HLB in the Arabian Peninsula! Why? Journal of Citrus Pathology, 1(1)

Bové, J. M. (2014b). Huanglongbing or yellow shoot, a disease of Gondwanan origin: Will it destroy citrus worldwide? *Phytoparasitica*, *42*(5), 579–583. https://doi.org/10.1007/s12600-014-0415-4

Boykin, L. M., Shatters, R. G. J., Rosell, R. C., McKenzie, C. L., Bagnall, R. A., De Barro, P., & Frohlich, D. R. (2007). Global relationships of Bemisia tabaci (Hemiptera: Aleyrodidae) revealed using Bayesian analysis of mitochondrial COI DNA sequences. Molecular Phylogenetics and Evolution, 44(3), 1306–1319. https://doi.org/10.1016/j.ympev.2007.04.020

Boykin, L.M., De Barro, P., Hall, D.G., Hunter, W.B., McKenzie, C.L., Powell, C.A. & Shatters, R.G. (2012). Overview of worldwide diversity of Diaphorina citri Kuwayama mitochondrial cytochrome oxidase 1 haplotypes:two old world lineages and a new world invasion. B. Entomol. Res. 102, 573–582.

Bray, J. R., & Curtis, J. T. (1957). An ordination of upland forest communities of southern Wisconsin. Ecol. Monogr. 27, 325–349.

Brown, B. L., Watson, M., Minot, S. S., Rivera, M. C., & Franklin, R. B. (2017). nanopore sequencing of environmental metagenomes: a synthethic approach Gigascience. 1;6(3):1-10. doi: 10.1093/gigascience/gix007.

Bruce, D.S., Duan, Y.P, Halbert, S, Sun, Schubert, X.A, T. & W. Dixon (2005). Detection and identification of citrus Huanglongbing (greening) in Florida, Proceedings of the Second International Citrus Canker and Huanglongbing Research Workshop. Orlando, Fl.

Buitendag, C. H. & von Broembsen, L. A. (1993). Living with citrus greening in South Africa. In: Moreno P, da Grata JV, Timmer LW, eds. Proceedings of the 12th Conference of the International Organization of Citrus Virologists. University of California, Riverside, USA: IOCV, 269-273

CABI, (2018). "Candidatus Liberibacter asiaticus". In: Invasive Species Compendium. Wallingford, UK: CAB International. Retrieved 7/1/2018 from https://www.cabi.org/isc/datasheet/16565

CABI/EPPO, (1998). Liberobacter africanum. [Distribution map]. Distribution Maps of Plant Diseases, October (Edition 1). Wallingford, UK: CAB International, Map 765

CABI/EPPO, (2017). *Candidatus* Liberibacter asiaticus. [Distribution map]. In: Distribution Maps of Plant Diseases , (No.April) Wallingford, UK: CABI.Map 766 (Edition 4).

Calvitti, M., Moretti, R., Lampazzi, E., Bellini, R., & Dobson, S. L. (2010) Characterization of a new Aedes albopictus (Diptera: Culicidae)-Wolbachia pipientis (Rickettsiales: Rickettsiaceae) symbiotic association generated by artificial transfer of the wPip strain from Culex pipiens (Diptera: Culicidae). J Med Entomol 47: 179–187

Capener, A. L. (1970). Southern African Psyllidae (Homoptera): Some new species of Diaphorina Löw. J. Entomol. Soc. Southern Africa 33: 201-226.

Capoor, S. P., Rao, D. G., & Viswanath, S. M. (1974) Greening disease of citrus in the Deccan Trap Country and its relationship with the vector, Diaphorina citri Kuwayama. In *International Organization of Citrus Virologists Conference Proceedings (1957-2010)* (Vol. 6, No. 6)

Capener, A. L. (1970). Southern African Psyllidae (Homoptera): Some new species of Diaphorina Löw. J. Entomol.

Castresana, J. (2000) Selection of conserved blocks from multiple alignments for their use in phylogenetic analysis. *Molecular Biology and Evolution*, 17 (4), 540-52.

Catling, H. D. (1970). The bionomics of the South African citrus psylla Trioza erytreae (Del Guercio) 4. The influence of predators. Journal of the Entomological Society of Southern Africa 32: 273–290.

Catling, H. D., & Atkinson, P. R. (1974). Spread of greening by Trioza erytreae (Del Guercio) in Swaziland, pp. 33-39 In L. G. Weathers and M. Cohen [eds.], Proc. 6th Conference of the International Organization of Citrus Virologists. University of California, Richmond.

Chen, L., Huang, J.-R., Dai, J., Guo, Y.-F., Sun, J.-T., & Hong, X.-Y. (2019). Intraspecific mitochondrial genome comparison identified CYTB as a high-resolution population marker in a new pest Athetis lepigone. Genomics, 111(4), 744–752. https://doi.org/10.1016/J.YGENO.2018.04.013

Chhetri, B., Badola, H. K., & Barat, S. (2018). Predicting Climate-Driven Habitat Shifting of the near Threatened Satyr Tragopan (Tragopan Satyra; Galliformes) in the Himalayas. Avian Biology Research, 11(4), 221–230.

Chu, C., Gill, T. A., Hoffmann, M., Kirsten, S. & Pelz-Stelinski, K. S. (2016). Inter-population variability of endosymbiont densities in the asian citrus psyllid (*Diaphorina citri* Kuwayama). Microb Ecol. 2016; 71:999–1007 DOI 10.1007/s00248-016-0733-9

Clarke, L. E., Edmonds, J. A., Jacoby, H. D., Pitcher, H., Reilly, J. M., & Richels, R. (2007) Scenarios of greenhouse gas emissions and atmospheric concentrations. Sub-report 2.1a of Synthesis and Assessment Product 2.1. Climate Change Science Program and the Subcommittee on Global Change Research, Washington DC

Cocuzza, G. E. M., Alberto, U., Hernández-Suárez, E. Siverio, F., Di Silvestro, S., Tena, A. & Rapisarda, C. (2017). A review on Trioza erytreae (African citrus psyllid), now in mainland Europe, and its potential risk as vector of huanglongbing (HLB) in citrus. J Pest Sci (2017) 90: 1. https://doi.org/10.1007/s10340-016-0804-1

Cook, G., Maqutu, V., & Van Vuuren, S. (2014) Population dynamics and seasonal fluctuation in the percentage infection of Trioza erytreae with '*Candidatus*' Liberibacter africanus, the African citrus greening pathogen, in an orchard severely infected with African greening and transmission by field-collected Trioza erytreae. Afr Entomol 22:127–135Costa Lima, A. M. DA. 1942. Homópteros. Insetos do Brazil illus. Esc. Na. Agron. Min. Agr. 3: 1-327, 267

Cuscó, A., Catozzi, C., Viñes, J., Sanchez, A., & Francino, O. (2018). Microbiota profiling with long amplicons using Nanopore sequencing: full-length 16S rRNA gene and whole rrn operon. F1000Res. 6;7:1755.

Da Graça, J. V. (1991). Citrus greening disease. *Annu Rev Phytopathol.* 29, 109-136

da Graça, J. V. & Korsten, L. (2004). Citrus huanglongbing: Review, present status and future strategies. In Diseases of fruits and vegetables volume I (pp. 229–245). Springer.

Damsteegt, V.D., E.N. Postnikova, A.L. Stone, M. Kuhlmann, C. Wilson, A. Sechler, N.W., Schaad, Brlansky, R.H. & Schneider, W.L. (2010). Murraya paniculata and related species as potential hosts and inoculum reservoirs of '*CandidatusLiberibacterasiaticus*', causal agent of Huanglongbing. Plant Disease 94: 528-533.

Darriba, D., Taboada, G. L., Doallo, R., & Posada, D. (2015). jModelTest 2: more models, new heuristics and high-performance computing Europe PMC Funders Group. Nature Methods, 9(8), 772. https://doi.org/10.1038/nmeth.2109.jModelTest

De León, J. H., Sétamou, M., Gastaminza, G. A., Buenahora, J., Cáceres, S., Yamamoto, P. T., Bouvet, J. P. & Logarzo, G. A. (2011). Two separate introductions of Asian citrus psyllid populations found in the American continents. Ann. Entomol. Soc. Am. 104, 1392–1398

Dereeper, A., Guignon, V., Blanc, G., Audic, S., Buffet, S., Chevenet, F., Dufayard, J. F., Guindon, S., Lefort, V., Lescot, M., Claverie, J. M., & Gascuel, O. (2008). Phylogeny.fr: robust phylogenetic analysis for the non-specialist. Nucleic acids research, 36(Web Server issue), W465–W469. https://doi.org/10.1093/nar/gkn180

Dormann, C.F., Elith, J., Bacher, S., Buchmann, C., Carl, G., Carré, G., Marquéz, J.R.G., Gruber, B., Lafourcade, B., Leitão, P.J., Münkemüller, T., McClean, C., Osborne, P.E., Reineking, B., Schröder, B., Skidmore, A.K., Zurell, D. and Lautenbach, S. (2012), Collinearity: a review of methods to deal with it

and a simulation study evaluating their performance. Ecography, 36: 27-46. doi:10.1111/j.1600-0587.2012.07348.x

Dossi, F. C., da Silva, E. P., & Consoli, F. L. (2014). Population dynamics and growth rates of endosymbionts during Diaphorina citri (Hemiptera, Liviidae) ontogeny. Microb Ecol 68(4):881–889.

Edwards, A., Debbonaire A. R., Nicholls S. M., Rassner S.M.E., Sattler B., Cook J. M., Davy T., Soares A., Mur L.A.J., & Hodson A.J. (2019). In-field metagenome and 16S rRNA gene amplicon nanopore sequencing robustly characterize glacier microbiota. bioRxiv doi: https://doi.org/10.1101/073965

Eisenstein, M. (2012). Oxford Nanopore announcement sets sequencing sector abuzz. *Nat Biotechnol.* 2012;30:295–6.

Ekesi, S. (2012). Arthropod pest composition and farmers perceptions of pest and disease problems on citrus in Kenya. Book of Abstract, pp. 283. *XII International Citrus Congress,* Valencia, Spain.

EPPO global database. (2018). Data Sheet on Liberibacter asiaticus. Retrieved 7/1/2018 from https://gd.eppo.int/taxon/LIBEAS

EPPO, (2014). PM 7/121 (1) '*Candidatus* Liberibacter africanus', '*Candidatus* Liberibacter americanus' and '*Candidatus* Liberibacter asiaticus'. Bulletin OEPP/EPPO Bulletin, 44(3):376-389. http://onlinelibrary.wiley.com/journal/10.1111/(ISSN)1365-2338

EPPO, (2014). PM 7/121 (1) '*Candidatus* Liberibacter africanus', '*Candidatus* Liberibacter americanus' and '*Candidatus* Liberibacter asiaticus'. Bulletin OEPP/EPPO Bulletin, 44(3):376-389. http://onlinelibrary.wiley.com/journal/10.1111/(ISSN)1365-2338

EPPO, (2018). PM 7/121 (1) '*Candidatus* Liberibacter africanus', '*Candidatus* Liberibacter americanus' and '*Candidatus* Liberibacter asiaticus'. Bulletin OEPP/EPPO Bulletin, 44(3):376-389. http://onlinelibrary.wiley.com/journal/10.1111/(ISSN)1365-2338

EPPO, 2020. EPPO Global database. In: EPPO Global database, Paris, France: EPPO. https://www.cabi.org/isc/search/index?q=do:%22EPPO%20Global%20database%22. [accessed 1 May 2020].

FAOSTAT (2018). Food and agriculture data. http://faostat.fao.org.

Fernandes, A., & Franquinho Aguiar, A. (2001). Evoluçao das pragas de quarenta Toxoptera citrida (KIRKALDY) *Trioza erytreae* (DEL GUERCIO) no Archipiélago da Madeira. *Boletín de Sanidad Vegetal. Plagas*, *27*(1), 51–58.

Fick, S. E. & Hijmans, R. J. (2017). Worldclim 2: New 1-km spatial resolution climate surfaces for global land areas. International Journal of Climatology. 37: 4302-4315. doi:10.1002/joc.5086

Fielding, A. H., & Bell, J. F. (1997). A review of methods for the assessment of prediction errors in conservation presence/absence models. Environ. Conserv. 24, 38–49.

Finney, C. A. M., Kamhawi, S., & Wasmuth, J. D. (2015). Does the Arthropod Microbiota Impact the Establishment of Vector-Borne Diseases in Mammalian Hosts? PLoS Pathogens, 11(4), 1–8. https://doi.org/10.1371/journal.ppat.1004646

Forester, B. R., Dechaine, E. G., & Bunn, A. G. (2013). Integrating ensemble species distribution modelling and statistical phylogeography to inform projections of climate change impacts on species distributions. Diversity and Distributions, 19(12), 1480–1495. https://doi.org/10.1111/ddi.12098

Friedman, J.H. (2001). Greedy function approximation: a gradient boosting machine. The Annals of Statistics 29: 1189-1232

Garnier, M. & J. M. Bové. (1993). Citrus greening disease, pp. 212-219 *In* P. Moreno, J. V. da Graça, and L. W. Timmer [eds.], Proc. 12th Conference of the International Organization of Citrus Virologists (IOCV). University of California, Riverside

Garnier, M., & Bové, J. M. (1983). Tranmission of the organism associated with citrus greening disease from sweet orange to periwinkle by dodder. *Phytopathology.* 73(10):1358-1363

Garnier, M., & Bové, J. M. (1996) Distribution of the huanglongbing (greening) Liberobacter species in fifteen African and Asian countries. In *International Organization of Citrus Virologists Conference Proceedings (1957-2010)* (Vol. 13, No. 13)

Garnier, M., Jagoueix-eveillard, S., Cronje, P. R., Le Roux, H. F. & Bove, J. M. (2000). Genomic characterization of a liberibacter present in an ornamental rutaceous tree, Calodendrum capense, in the Western Cape province of South Africa. Proposal of '*Candidatus* Liberibacter africanus subsp. capensis'. *Int J Syst Evol Microbiol*. 6(6), 2119–2125

Garnier, M., Jagoueix, S., Toorawa, P., et al (1996) Both huanglongbing (greening) liberobacter species are present in Mauritius and Reunion. In *International Organization of Citrus Virologists Conference Proceedings (1957-2010)* (Vol. 13, No. 13)

Gottwald, T. R. (2010). Current epidemiological understanding of citrus huanglongbing. Annual Review of Phytopathology, 48, 119–139.

Grafton-Cardwell, E. E., J. G. Morse, N. V. O'Connell, P. A. Phillips, Kallsen, C. E. & Haviland, D. R. (2006). UC IPM pest management guidelines: citrus insects, mites and snails. University of California Agriculture and Natural Resources Publication 3441.

Grafton-Cardwell, E. E., L. L. Stelinski, & P. A. Stansly. (2013). Biology and Management of Asian Citrus Psyllid, Vector of the Huanglongbing Pathogens. *Annual Review of Entomology*, *58*(1), 413–432. https://doi.org/10.1146/annurev-ento-120811-153542

Grenouillet, G., Buisson, L., Casajus, N., & Lek, S. (2011) Ensemble modelling of species distribution: the effects of geographical and environmental ranges. Ecography, 34, 9–17.

Gritti, E. S., Smith, B., & Sykes, M. T. (2006). Vulnerability of Mediterranean Basin ecosystems to climate change and invasion by exotic plant species. Journal of Biogeography 33: 145–157.

Guidolin, A. S. & Consoli, F. L. (2013). Molecular characterization of Wolbachia strains associated with the invasive Asian citrus psyllid Diaphorina citri in Brazil. Microbial Ecol. 65, 475–486

Gutierrez, A. P., & Ponti, L. (2013). Prospective analysis of the geographic distribution and relative abundance of Asian citrus psyllid (Hemiptera:Liviidae) and citrus greening disease in North America and the Mediterranean Basin. Florida Entomologist, 96(4), 1375–1391.

Hailu, T., & Wakgari, M. (2019). Distribution and Damage of African Citrus Psyllids (*Trioza erytreae*) in Casimiroa edulis Producing Areas of the Eastern Zone of Ethiopia. *International Journal of Environment, Agriculture and Biotechnology*, *4*(3), 741–750. https://doi.org/10.22161/ijeab/4.3.22

Halbert, S. E., Niblett, C. L., Manjunath, K. L., Lee, R. F. & Brown, L. G. (2002). Establishment of two new vectors of citrus pathogens in Florida. Proc. Intl. Soc. E. Citricult. IX Congr. 1016–1017 (2002).

Halbert, S. E., & Manjunath, K. L. (2004). Asian citrus psyllids (Sternorrhyncha: Psyllidae) and greening disease in citrus: a literature review and assessment of risk in Florida. Florida Entomologist, 87,(3), 330-354 –353. https://doi.org/10.1653/0015-4040(2004)087[0330:acpspa]2.0.co;2

Halbert, S. E., Manjunath, K. L. Ramadugu, C., Brodie, M. E., Webb, S. E., & Lee, R. E. (2010). Trailers transporting oranges to processing plants move Asian citrus psyllids. Florida Entomol. 93:33-38.

Halbert, S. E., Manjunath, K., Ramadugu, C., & Lee, R. F. (2012). Incidence of huanglongbing-associated "Candidatus Liberibacter asiaticus" in Diaphorina citri (Hemiptera: Psyllidae) collected from plants for sale in Florida. Florida Entomologist, 95(3), 617–624.

Hall, D. G., & M. G. Hentz. 2010. Sticky trap and stem-tap sampling protocols for the Asian citrus psyllid (Hemiptera: Psylli-dae). J Econ Entomol 103:541–549. doi:10.1603/EC09360

Hall, D. G., Richardson, M. L., Ammar, E. D. & Halbert, S. E. (2013). Asian citrus psyllid, *Diaphorina citri*, vector of citrus huanglongbing disease. Entomol Exp Appl. **146,** 207-223

Hall, T. A. (1999). BioEdit: a user-friendly biological sequence alignment editor and analysis program for Windows 95/98/NT. *Nucl. Acids. Symp*. Ser. **41,** 95-98

Hebert P. D. N., Stoeckle M. Y., Zemlak, T. S. & Francis, C. M. (2004). Identification of birds through DNA barcodes. PLoS Biol 2(10):e312

Hebert, P. D., Cywinska, A., Ball, S. L. & deWaard, J. R. (2003). Biological identifications through DNA barcodes. *Proc. R. Soc. B Biol. Sci.* **270,** 313-321

Heikkinen, R. K., Marmion, M., & Luoto, M. (2012) Does the interpolation accuracy of species distribution models come at the expense of transferability? Ecography, 35, 276–288.

Hijmans, R. J., Cameron, S. E., Parra, J. L., Jones, P. G., & Jarvis, A. (2005). Very high resolution interpolated climate surfaces for global land areas. International Journal of Climatology, 25(15), 1965–1978.

Hijmans, R. J., Phillips, S., Leathwick, J., and Elith, J. (2017). Package 'dismo'. Available online at: http://cran.r-project.org/web/packages/dismo/index.html.

Hocquellet, A., Toorawa, P., Bove, J. M. & Garnier, M. (1999). Detection and identification of the two *Candidatus* Liberobacter species associated with citrus huanglongbing by PCR amplification of ribosomal protein genes of the beta-operon. *Mol. Cell. Probes* **13,** 373-379

Hollis, D. (1987). A new citrus-feeding psyllid from the Comoro Islands, with a review of the Diaphorina amoena species group (Homoptera). Systematic Entomol.12: 47-61.

Hoffmann, M., Coy, M. R., Gibbard, H. N. K., & Pelz-Stelinski, K. S. (2014).Wolbachia infection density in populations of the Asian citrus psyllid (Hemiptera: Liviidae). Environ Entomol. 2014; 43(5):1215–1222

Horino, O., Mew, T. W., & Yamada, T. (1982). The effect of temperature on the development of bacterial leaf blight on rice. Ann Phytopath Soc Japan 48:72–75.

Hosseinzadeh S, Shams-Bakhsh M, Mann M, Fattah-Hosseini S, Bagheri A, Mehrabadi M, & Heck M. (2019). Distribution and variation of bacterial endosymbiont and *Candidatus* Liberibacter asiaticus titer in the Huanglongbing insect vector, *Diaphorina citri* Kuwayama. Microbial Ecology. 2019;78(1):206-222. https://doi.org/10.1007/s00248-018-1290-1

Ignasiak, K., & Maxwell, A. (2017). Antibiotic-resistant bacteria in the guts of insects feeding on plants: prospects for discovering plant-derived antibiotics. BMC Microbiology.; 17:223 doi10.1186/s12866-017-1133-0

Irinyi, L., Hu, Y., Hoang, M., Pasic, L., Halliday, C., Jayawardena, M., Basu, I., McKinney, W., Morris, A. J., Rathjen, J., Stone, E., Chen, S., Sorrell, T. C., Schwessinger, B., & Meyer, W. (2019). Long-read sequencing based clinical metagenomics for the detection and confirmation of Pneumocystis jirovecii directly from clinical specimens: A paradigm shift in mycological diagnostics. Medical mycology, myz109. Advance online publication. https://doi.org/10.1093/mmy/myz109

Islam, M. S., Glynn, J. M., Bai, Y., Duan, Y-P., Coletta-Filho, H. D., Kuruba, G., Civerolo E. L. & Lin, H. (2012). Multilocus microsatellite analysis of "Candidatus Liberibacter asiaticus" associated with citrus Huanglongbing worldwide. *BMC Microbiology.* **12(1),** 39

Iturbe-Ormaetxe, I., Walker, T., & O'Neill, S.L. 2011. Wolbachia and the biological control of mosquito-borne disease. EMBO Rep., 12, 508–518.

Jagoueix, S., Bove, J. M. & Garnier, M. (1996). PCR detection of the two '*Candidatus* liberibacter' species associated with greening disease of citrus. *Molecular and Cellular Probes.* 10, 43-50

Jagoueix, S., Bove, J. M. & Garnier, M. (1994).The phloem-limited bacterium of greening disease of citrus is a member of the α subdivision of the proteobacteria. *International Journal of Systematic Bacteriology*. **44,** 379-386

Jenkins, D. A., Hall, D. G. & Goenaga, R. (2015). *Diaphorina citri* (Hemiptera: Liviidae) abundance in puerto rico declines with elevation. *Journal of Economic Entomology*, *108*(1), 252–258. https://doi.org/10.1093/jee/tou050

Jepson, S. B., (2009). Citrus greening disease (Huanglongbing). OSU Plant Clinic. Corvallis, Oregon, USA: Oregon State University

Jost, L. (2006). Entropy and diversity. Oikos 113(2):363–375. doi:10.1111/j.2006.0030-1299.14714.x

Juul, S., Izquierdo, F., Hurst, A., Dai, X., Wright, A., Kulesha, E., Pettett, R., & Turner, D.J. (2015). What's in my pot? Real-time species identification on the MinION. bioRxiv. 2015:030742. doi: 10.1101/030742.

Kain, D. E., Sperling, F. H., Daly, H.V., & Lane R.S., (1999). Mitochondrial DNA in Ixodespacificus (Acari: Ixodidae), Heredity, 1999, 83, 378-386

Kalyebi, A., Aisu, G., Ramathani, I., Ogwang, J., McOwen, N., & Russell, P. (2016). Detection and identification of etiological agents (Liberibacter spp.) associated with citrus greening disease in Uganda. Uganda J Agric Sci, 16(1), 43. https://doi.org/10.4314/ujas.v16i1.4

Kambris, Z., Cook, P.E., Phuc, H.K., & Sinkins, S.P. Immune activation by life-shortening Wolbachia and reduced filarial competence in mosquitoes. Science 2009, 326, 134–136.

Kandasamy, C. (1986). Taxonomy of South Indian psyllids. Records of the Zoological Survey of India. Miscellaneous Publication Occasional Paper No. 84. iv + 111 pp.

Katoh, K. & Standley, D. M. (2013). MAFFT multiple sequence alignment software version 7: improvements in performance and usability. *Mol Biol Evol*. **30(4),** 772-80

Kerr, J.T. (2001). Butterfly Species Richness Patterns in Canada: Energy, Heterogeneity, and the Potential Consequences of Climate Change. Conservation Ecology 5(1):10

Khamis, F. M., Karam, N., Ekesi, S., De meyer, M., Bonomi, A., Gomulski, M., Scolari, F., Gabrieli, P., Siciliano, P., Masiga, D., Kenya, E. U., Gasperi, G., Malacrida A. R. and Guglielmino C. R. (2009). Uncovering the tracks of a recent and rapid invasion: the case of the fruit fly pest Bactrocera invadens (Diptera: Tephritidae) in Africa. Molecular Ecology (2009) doi: 10.1111/j.1365-294X.2009.04391.x

Kikuchi, Y. (2009). Endosymbiotic bacteria in insects: their diversity and culturability. 351 Microbes and Environments, 24:195–204.

Kilalo, D., Olubayo, F., Obukosia, S. & Shibairo, S. I. (2009). Farmer management practices of citrus insect pests in Kenya. *Afr. J. Hortic*. Sci. **2,** 168-176.

Kim, D., Song, L., Breitwieser, F. P., & Salzberg, S. L. (2016). Centrifuge: rapid and sensitive CLassification of metagenomic sequences. Genome Research, 26(12), 1721–1729. https://doi.org/10.1101/gr.210641.116

Kobayashi, T., Ishiguro, K., Nakajima, T., Kim, H. Y., Okada, M., & Kobayashi, K. (2006). Effects of elevated atmospheric CO2 concentration on the infection of rice blast and sheath blight. Phytopathology 96:425–431.

Kobori, Y., Nakata, Ohto, T. Y., & Takasu, F. (2011). Dispersal of adult Asian citrus psyllid, *Diaphorina citri* Kuwayama (Homoptera: Psyllidae), the vector of citrus greening disease, in artificial release experiments. *Applied Entomology and Zoology*, *46*, 27–30. https://doi.org/10.1007/s13355-010-0004-z

Kobori, Y., Takasu, F., & Ohto, Y. (2012). Development of an individual-based simulation model for the spread of citrus greening disease by the vector insect Diaphorina citri. INTECH Open Access Publisher. http://cdn.intechopen. com/pdfs/32853.pdf

Korsten L, Jagoueix S, Bové JM et al. (1996). Huanglongbing (greening) detection in South Africa. In *International Organization of Citrus Virologists Conference Proceedings (1957-2010)* (Vol. 13, No. 13)

Krishna, P. P. (2015). Technological Advances in Huanglongbing (HLB) or Citrus Greening Disease Management. Journal of Nepal Agricultural Research Council Vol 1:41-50, August 2015

Kuhn, M., Wing, J., Weston S., Williams, A., Keefer, C., Engelhardt, A., … Candan, C. (2016). caret: CLassification and Regression Training. R package version 6.0-71. https://CRAN.R-project.org/package=caret

Kumar, S., Stecher, G., Li M., Knyaz C., & Tamura K. (2018). MEGA X: Molecular Evolutionary Genetics Analysis across computing platforms. *Molecular Biology and Evolution* 35:1547-1549.

Kuwayama, S. (1908). Die psylliden Japans. Transactions of the Sopporo Natural History Society 2 (parts I and II): 149-189. (*D. citri*: p. 160-161, Plate III, Fig. 16).

Lallemand, J., Fos, A. & Bove, J. M. (1986). Transmission de la bacterie associee al a forme africaine de la maladie du "greening" par le psylla asiatique *Diaphorina citri* Kuwayama. *Fruits.* 41, 341-343

Lashkari, M., Manzari, S., Sahragard, A., Malagnini, V., Boykin, L. M. & Hosseini R. (2014). Global genetic variation in the Asian citrus psyllid, Diaphorina citri (Hemiptera: Liviidae) and the endosymbiont Wolbachia: links between Iran and the USA detected. Pest Manag. Sci. 70, 1033–1040

Laslett, D., & Canbäck, B. (2008). ARWEN: A program to detect tRNA genes in metazoan mitochondrial nucleotide sequences. Bioinformatics, 24(2), 172–175. https://doi.org/10.1093/bioinformatics/btm573

Lee, J. A., Halbert, S. E., Dawson, W. O., Robertson, C. J., Keesling, J. E., & Singer, B. H. (2015). Asymptomatic spread of huanglongbing and implications for disease control. Proceedings of the National Academy of Sciences. doi:10. 1073/pnas.1508253112.

Lewis-Rosenblum, H., Martini, X., Tiwari, S. & Stelinski L. L. (2015). Seasonal Movement Patterns and Long-Range Dispersal of Asian Citrus Psyllid in Florida Citrus. *Journal of Economic Entomology*, *108*(1), 3–10. https://doi.org/10.1093/jee/tou008

Li Y-L & Liu J-X. (2018). STRUCTURESELECTOR: A web-based software to select and visualize the optimal number of clusters using multiple methods. Mol Ecol Resour. 2018;18:176–177. https://doi.org/10.1111/1755- 0998.12719

Li, J., Li, L., Pang, Z., Kolbasov, V. G., Ehsani, R., Carter, E. W., & Wang, N. (2019). Developing Citrus Huanglongbing (HLB) Management Strategies Based on the Severity of Symptoms in HLB-Endemic Citrus-Producing Regions. Phytopathology, 109(4), 582–592.

Li, W., Hartung, J. S. & Levy, L. (2006). Quantitative real-time PCR for detection and identification of *Candidatus* Liberibacter species associated with citrus Huanglongbing. *J. Microbiol. Methods.* **66,** 104-115.

Liu, Y. H, & Tsai, J. H. (2000). Effects of temperature and life table parameters of the Asian citrus psyllid, Diaphorina citri Kuwayama (Homoptera: Psyllidae). Ann. Appl. Biol. 137:201–6

Lopes, S. A., & Frare, G. F. (2007). Graft transmission and cultivar reaction of citrus to *Candidatus* Liberibacter americanus. Plant Disease, 92(1), 21–24.

Ma, H., Yin, Y., Guo, Z. F., Cheng, L. J., Zhang, L., Zhong, M., Shao, G.J. (2011). Establishment of DNA fingerprinting of Liaojing series of japonica rice. Middle-East Journal of Scientific research, 8(2): 384-392.

MacDonald, Z. G., Nielsen, S. E. & Acorn J. H. (2017). Negative relationships between species richness and evenness render common diversity indices inadequate for assessing long-term trends in butterfly diversity. Biodivers.Conserv 26:617–629 DOI 10.1007/s10531-016-1261-0

Magarey, R. D., Sutton, T. B., & Thayer, C. L. (2005). A simple generic infection model for foliar fungal plant pathogens. Phytopathology 95:92–100.

Magomere, T. Obukosia, S. D., Mutitu, E., Ngichabe, C., Olubayo, F. & Shibairo S. (2009).PCR detection and distribution of Huanglongbing disease and psyllid vectors on citrus varieties with changes in elevation in Kenya. *J Biol Sci.* **9,** 697- 709

Magurran AE., 2013. Measuring biological diversity. Wiley, New Jersey

Mandal De, Chhakchhuak, Gurusubramanian, G., & Kumar, S. (2014). Mitochondrial markers for identification and phylogenetic studies in insects – A Review. Barcodes, (1), 1–. https://doi.org/10.2478/dna-2014-0001

Mangrauthia, S. K., Singh Shakya, V. P., Jain, R. K., & Praveen, S. (2009). Ambient temperature perception in papaya for papaya ringspot virus interaction. Virus Genes. 38:429–434.

Manjunath, K. L., Halbert, S. E., Ramadugu, C., Webb, S. & Lee, R. F. (2008). Detection of '*Candidatus* Liberibacter asiaticus' in *Diaphorina citri* and its importance in the management of citrus Huanglongbing in Florida. *Phytopathology.* 98, 387-396

Marmion, M., Parviainen, M., Luoto, M., Heikkinen, R. K. & Thuiller, W. (2009) Evaluation of consensus methods in predictive species distribution modelling. Diversity and Distributions 15, 59–69.

Marshall, B. M., Ochieng, D. J., & Levy, S. B. (2009). Commensals: underappreciated reservoirs of resistance. Microbe. 4:231–238.

Massonie, G., Garnier, M. & Bove, J. M. (1976). Transmission of Indian citrus decline by Trioza erytreae (Del Guercio), the vector of South Africa greening, p. 18-20. *In Proc. 8th Conf. IOCV. IOCV, Riverside*.

Mather, R. N. (1975). Psyllidae of the Indian Subcontinent. Indian Council of Agricultural Research, New Delhi. 429 pp.

McLean, A. P. D. & Oberholzer, P. C. J. (1965). Citrus psylla, a vector of the greening disease of sweet orange. *S Afr J Agric Sci.* 8, 297-298

McClean, R. E., (1970). Greening or blotchy-mottle disease of citrus. *Phytophylactica 2*(3): 177-194.

McManus, P. S., Stockwell, V. O., Sundin, G. W. & Jones, A. L. 2002. Antibiotic use in plant agriculture. Ann Rev Phytopatho 40: 443-465.

McMeniman, C. J., Roxanna, L.V., Bodil, C.N., Amy, F. W. C., Manpreet, S., Wang, Y. F., & O'Neill, S. L. 2009. Stable introduction of a life-shortening Wolbachia infection into the mosquito Aedes aegypti. Science, 323, 141–145.

Mendonça, L. B. P., Zambolim, L., & Badel, J. L. (2017). Bacterial Citrus Diseases: Major Threats and Recent Progress. Journal of Bacteriology & Mycology: Open Access 5:4 – 2017.

Mendoza, M. L. Z., Sicheritz-Ponten T., & Gilbert, M. T. P. (2015). Environmental genes and genomes: understanding the differences and challenges in the approaches and software for their analyses. Briefings in Bioinformatics;1–14. doi: 10.1093/bib/bbv001.

Meng, L., Li, X., Cheng, X., & Zhang H. (2019). 16S rRNA Gene Sequencing Reveals a Shift in the Microbiota of Diaphorina citri During the Psyllid Life Cycle. Front Microbiol. 2019; 10: 1948. doi: 10.3389/fmicb.2019.01948

Ministry of Agriculture (1982). Citrus Greening Disease in Kenya and Recommendations for Its Control. A Report to the Director of Agriculture by the Committee on Greening Disease in Citrus and Fruit Nursery Management : 80pp

Moll, J. N., Van Vuuren, S.P., & Milne, D.L. (1980) Greening disease, the South African situation. In *Proc. 8th Conf. Int. Org. Citrus Virol., Univ. Calif* (pp. 109-117)

Moreira LA, Saig E, Turley AP, Ribeiro JM, O'Neill SL, McGraw EA (2009b) Human probing behavior of Aedes aegypti when infected with a life-shortening strain of Wolbachia. PLoS Negl Trop Dis 3: e568.

Nakabachi, A., Ueoka, R., Oshima, K., Teta, R., Mangoni, A., Gurgui, M., Oldham, N. J., van Echten-Deckert, G., Okamura, K., Yamamoto, K., Inoue, H., Ohkuma, M., Hongoh, Y., Miyagishima, S. Y., Hattori M., Piel, J. & Fukatsu, T. (2013). Defensive bacteriome symbiont with a drastically reduced genome. Curr Biol. 2013 Aug 5;23(15):1478-84. doi: 10.1016/j.cub.2013.06.027. Epub 2013 Jul 11.

Narouei-Khandan, H. A., Halbert, S. E., Worner, S. P. & VanBruggen, A. H. C. (2016). Global climate suitability of citrus huanglongbing and its vector, the Asian citrus psyllid, using two correlative species distribution modelling approaches, with emphasis on the USA. *Eur J Plant Pathol* DOI 10.1007/s10658-015-0804-7

Navajas, M., Gutierrez, J., Lagnel, J., & Boursot, P. (1996). Mitochondrial cytochrome oxidase I in tetranychid mites: A comparison between molecular phylogeny and changes of morphological and life history traits. Bulletin of Entomological Research, 86(4), 407-417. doi:10.1017/S0007485300034994

Nei M. (1972). Genetic distance between populations. AmericanNaturalist106:283–292.

Nyambo, B. (2009). Integrated pest management plan (IPMP): the Agricultural Sector Development Program - Republic of Tanzania.

O'Neill, S. L., Giordano, R., Colbert, A. M., Karr, T. L., & Robertson, H. M. (1992). 16s rRNA phylogenetic analysis of the bacterial endosymbionts associated with cytoplasmic incompatibility in insects. Proceedings of the National Academy of Sciences of the United States of America, 89:2699-2702.

Oberholzer, P. C. J., Von Standen, D. F. A. & Basson, W. J. (1965). Greening disease of sweet orange in South Africa. In Proc. 3rd Conf. Conference of the International Organization of Citrus Virologists (IOCV), p. 213-219. Gainesville, Univ. Fla. Press.

Obukosia, S. & Waithaka, K. (2000). Nucellar culture of Citrus sinensis L. and Citrus limon L. *African Crop Science Journal.* 8(2) 1-8

OEPP/EPPO (2005a). EPPO Standards PM 7/52(1). Diagnostic protocol for Diaphorina citri. Bulletin OEPP/EPPO Bulletin 35:331–333. doi:10.1111/j.1365-2338.2005.00839.x

OEPP/EPPO (2005b). EPPO Standards PM 7/57(1). Diagnostic protocol for Trioza erytreae. Bull OEPP/EPPO Bull 35:357–360. doi:10.1111/j.1365-2338.2005.00832.x

Oksanen, J., Blanchet, F., Kindt, R., Legendre, Minchin, P., Hara, P.O. R., Simpson, G. L., Solymos, P., Stevens, M. H. H. & Wagner, H. (2015). Vegan Community Ecology Package. R package version 2.2-1. Available online at: https://cran.r-project.org/web/packages/vegan/index.html

Paetkau, D., Slade, R., Burden, M. & Estoup, A. (2004). Genetic assignment for the direct, real-time estimation of migration rate: a simulation-based exploration of accuracy and power. Mol. Ecol. 13, 55–65

Pérez-Rodríguez, J., Krüger, K., Pérez-Hedo, M., Ruíz-Rivero, O., Urbaneja, A. & Tena, A. (2019). *Ca. L. asiaticus* sical biological control of the African citrus psyllid *Trioza erytreae*, a major threat to the European citrus industry. *Scientific Reports*, *9*(1), 9440. https://doi.org/10.1038/s41598-019-45294-w

Pettey, F. W. (1924). South African psyllids. Entomology Memoirs of the Department of Agriculture of the Union of South Africa 2: 21-30.

Phahladira, M. N., Viljoen, R., & Pietersen, G. (2012). Widespread occurrence of "*Candidatus* Liberibacter africanus subspecies capensis" in Calodendrum capense in South Africa. *Eur J Plant Pathol.* **134,** 39–47

Phillips, S. J., Anderson, R. P., & Schapire, R. E. (2006). Maximum entropy modelling of species geographic distributions. Ecological Modelling, 190(3), 231–259.

Piry, S., Alapetite, A., Cornuet, J.-M., Paetkau, D., Baudouin, L. & Estoup, A. (2004). GENECLASS2: A Software for Genetic Assignment and First-Generation Migrant Detection, Journal of Heredity, Volume 95, Issue 6, November/December 2004, Pages 536–539, https://doi.org/10.1093/jhered/esh074

Pole, F. N., Ndung'u, J. M., Kimani, J. M., & Kagunu, E. (2010). Citrus farming in Kwale district: a case study of Lukore location, pp. 629–635. In Proceedings of the 12th KARI Biennial conference: Transforming Agriculture for improved livelihoods through agricultural product value chains, November 8–12, 2010. KARI Headquarters, Nairobi, Kenya.

Porfirio, L. L., Harris, R. M. B., Lefroy, E. C., Hugh, S., Gould, S. F., Lee, G., Bindoff, N. L. & Mackey B. (2014). Improving the Use of Species Distribution Models in Conservation Planning and Management under Climate Change. PLoS ONE 9(11): e113749. doi:10.1371/journal.pone.0113749

Powell W., Machray G. C., & Provan J. (1996). Polymorphism revealed by simple sequence repeats.*Trends Plant Sci.* 1 215–222. 10.1016/S1360-1385(96)86898-0

Powell, C., Cleca, V., Sinno, M., van Staden, M., van Noort, S., Rhode, C., Allsopp, E. & van Asch B. (2018). Barcoding of parasitoid wasps (Braconidae and Chalcidoidea) associated with wild and cultivated olives in the Western Cape of South Africa. *Genome*. **62(3),** 183–199

Pritchard, J. K, Stephens, M., & Donnelly, P. (2000) Inference of population structure using multilocus genotypic data. Genetics, 155, 945–959.

Puechmaille, S. J (2016) The program structure does not reliably recover the correct population structure when sampling is uneven: subsampling and new estimators alleviate the problem. *Molecular Ecology Resources*, 16:608–627.

Pyke, C. R., & Fischer, D. T. (2005). Selection of bioclimatically representative biological reserve systems under climate change. Biological Conservation 121: 429–441.

Pyke, C. R., Andelman, S. J., & Midgley, G. (2005). Identifying priority areas for bioclimatic representation under climate change: a case study for Proteaceae in the Cape Floristic Region, South Africa. Biological Conservation 125: 1–9.

QGIS Development Team (2016). QGIS Geographic Information System. Open Source GeospatialFoundation Project. http://qgis.osgeo.org".

QGIS Development Team QGIS Geographic Information System. Open Source Geospatial Foundation Project. http://qgis.osgeo.org" (2016).

Qin, Y.-J., Buahom, N., Krosch, M. N., Du, Y., Wu, Y., Malacrida, A. R., Deng, Y.-L., Liu, J.-Q., Jiang, X.-L. & Li, Z.-H. (2016). Genetic diversity and population structure in Bactrocera correcta (Diptera: Tephritidae) inferred from mtDNA cox1 and microsatellite markers. Sci. Rep. 6, 38476; doi: 10.1038/ srep38476

R Development Core Team (2008). R: A language and environment for statistical computing. R Foundation for Statistical Computing, Vienna, Austria. ISBN 3-900051-07-0, URL http://www.R-project.org.

Rasowo, B. A., Khamis, F. M., Mohamed, S. A., Ajene, I. J., Aidoo, O. F., Ombura, F.L., Sétamou, M., Ekesi, S. & Borgemeister, C. (2019). African Citrus Greening Disease in East Africa: Incidence, Severity and Distribution Patterns. Journal of Economic Entomology, toz167, https://doi.org/10.1093/jee/toz167

Riahi, K., Grübler, A., & Nakicenovic, N. (2007). Scenarios of long-term socio-economic and environmental development under climate stabilization. Technol Forecast Soc Chang 74:887–935

Roberts, R. & Pietersen, G. (2017). A novel subspecies of '*Candidatus* Liberibacter africanus' found on native Teclea gerrardii (Family: Rutaceae) from South Africa. *Antonie van Leeuwenhoek*. 110(3), 437-444

Roberts, R., Cook, G., Grout, T. G., Khamis, F., Rwomushana, I., Nderitu, P. W., Seguni, Z., Materu, C. L., Steyn, C., Pietersen, G., Ekesi, S. & le Roux, H. F. (2017). Resolution of the identity of ' *Candidatus* Liberibacter' species from Huanglongbing-affected citrus in East Africa. Plant Disease, (August), PDIS-11-16-1655-RE. https://doi.org/10.1094/PDIS-11-16-1655-RE

Roberts, R., Steenkamp, E. T., & Pietersen, G. (2015). Three novel lineages of "*Candidatus* Liberibacter africanus" associated with native rutaceous hosts of Trioza erytreae in South Africa. Int J Syst Evol Microbiol. 65 (2):723-31. doi: 10.1099/ijs.0.069864-0. Epub 2014 Nov 13.

Robson, J. D., Wright, M. G., & Almeida, R. P. P., (2007). Biology of Pentalonia nigronervosa (Hemiptera, Aphididae) on banana using different rearing methods. Environ Entomol 36:46–52.

Roistacher, C. N. (1996). The economics of living with citrus diseases: huanglongbing (greening) in Thailand. In *International Organization of Citrus Virologists Conference Proceedings (1957-2010)* (Vol. 13, No. 13)

Rosentrater, L. D. (2010). Representing and using scenarios for responding to climate change. Wiley Interdisciplinary Reviews-Climate Change 1: 253–259.

Ross, H. A., Murugan, S. & Li, W. L. S. (2008). Testing the reliability of genetic methods of species identification via simulation. *Syst. Biol.* **57(2),** 216-230

Rwomushana, I., Khamis, F. M., Grout, T. G., Mohamed, S. A., Sétamou, M., Borgemeister, C., Heya, H. M., Tanga, C. M. Nderitu, P. W., Seguni, Z. S., Materu, C. L. & Ekesi, S. (2017). Detection of *Diaphorina citri* Kuwayama (Hemiptera: Liviidae) in Kenya and potential implication for the spread of Huanglongbing disease in East Africa. *Biological Invasions*, 1–11. https://doi.org/10.1007/s10530-017-1502-5

Sajib, A. M., Hossain, M., & Ali, S. (2012). SSR marker-based molecular characterization and genetic diversity analysis of aromatic landreces of rice (Oryza sativa L .). J. BioSci. Biotech. 2012, 1(2): 107-116, 1(2), 107–116.

Salibe, A. A., & Cortez, R. E. (1966). Studies on the Leaf Mottling Disease of Citrus in the Philippines. *FAO Plant Prot. Bull* 14: 141–44

Salyers, A. A., Gupta, A., & Wang, Y. (2004). Human intestinal bacteria as reservoirs for antibiotic resistance genes. Trends Microbiol. 12:412–416.

Saponari, M., De Bac, G., Breithaupt, J., Loconsole, G., Yokomi, R. K., & Catalano, L. (2010). First report of '*Candidatus* Liberibacter asiaticus' associated with huanglongbing in sweet Orange in Ethiopia. Plant Disease, 94,482.

Schapire, R.E. (2003) The Boosting Approach to Machine Learning: An Overview. In: Denison D.D., Hansen M.H., Holmes C.C., Mallick B., Yu B. (eds) Nonlinear Estimation and CLassification. Lecture Notes in Statistics, vol 171. Springer, New York, NY

Schwarz, R., & Van Vuuren, S. (1971). Decrease in fruit greening of sweet orange by trunk injection of tetracycline's. Plant Dis Reptr.55:747-50

Sengoba, T., Hakiza, J. J., Kalunda, P., Ameo, M. & Ogwang, Y. (2002). Introduction and evaluation of improved Citrus and Mangoes through Farmers Field Schools. Project Supported by NARO/DFID COARD Project.

Setamou, M., Flores, D., French, J. & Hall D. (2008). Dispersion Patterns and Sampling Plans for *Diaphorina citri* (Hemiptera: Psyllidae) in Citrus. *Journal of Economic Entomology*, *101*, 1478–1487. https://doi.org/10.1603/0022-0493(2008)101[1478:DPASPF]2.0.CO;2

Shen, W., Halbert, S. E., Dickstein, E., Manjunath, K. L., Shimwela, M. M., & van Bruggen, A. H. C. (2013). Occurrence and in-grove distribution of citrus Huanglongbing in north Central Florida. Journal of Plant Pathology, 95, 361–371.

Shi, W., Kerdelhue, C. & Ye, H. (2012). Genetic structure and inferences of potential source areas for Bactrocera dorsalis (Hendel) based on mitochondrial and microsatellite markers. Plos One 7, e37083

Shimwela, M. M., Narouei-Khandan, H. A., Halbert, S. E., Keremane, M. L., Minsavage, G. V., Timilsina, S., Massawe D. P., Jones J. B., Ariena, H. C. & van Bruggen A. H. C. (2016). First occurrence of *Diaphorina citri* in East Africa, characterization of the Ca. Liberibacter species causing huanglongbing (HLB) in Tanzania, and potential further spread of *D. citri* and HLB in Africa and Europe. *European Journal of Plant Pathology*, *146*(2), 349–368. https://doi.org/10.1007/s10658-016-0921-y

Sinkins, S.P. (2004). Wolbachia and cytoplasmic incompatibility in mosquitoes. Insect Biochem. Mol. Biol., 34, 723–729.

Siverio, F., Marco-Noales E., Bertolini, E., Teresani, G. R., Penalver, J., Mansilla P., … Lopez, M. M. (2019). Survey of huanglongbing associated with '*Candidatus* Liberibacter' species in Spain: analyses of citrus plants and Trioza erytreae. Phytopathologia Mediterranea, [S.l.], v. 56, n. 1, p. 98-110, may. 2017. ISSN 1593-2095. Available at: <http://www.fupress.net/index.php/pm/article/view/18679>. Date accessed: 07 May. 2019. doi:10.14601/Phytopathol_Mediterr-18679.

Sommer, M. O., Dantas, G., & Church, G. M. (2009). Functional characterization of the antibiotic resistance reservoir in the human microflora. Science. 325:1128–1131.

Swai, I. S., Evers, G., Gumpf, D.J. & Lana, A. F. (1992). Occurrence of citrus greening disease in Tanzania. *Plant disease 76*(11)

Swets, K.A. (1988). Measuring the accuracy of diagnostic systems. Science 240: 1285-1293.

Swisher, K. D. & Crosslin, J. M. Restriction digestion method for haplotyping the potato psyllid, Bactericera cockerelli. Southwest Entomol. 39, 49–56 (2014).

Tabachnick W. J. (2015) Diaphorina citri (Hemiptera: Liviidae) vector competence for the citrus greening pathogen '*Candidatus* Liberibacter asiaticus'. *Journal of economic entomology 108*(3): 839-848

Tamura, K. & Nei, M. (1993). Estimation of the number of nucleotide substitutions in the control region of mitochondrial DNA in humans and chimpanzees. *Molecular Biology and Evolution.* **10,** 512-526

Tang J., Toe L., Back C., & Unnasch T.R. (1995). Mitochondrial alleles of Simulium damnosum sensu lato infected with Onchocerca volvulus, Int. J. Parasitol., 1995, 25, 1251-1254

Taylor, K. E., Stouffer, R. J. & Meeh, G.A. (20l2). An Overview of CMIP5 and the experiment design." Bull. Amer. Meteor. Soc., 93, 485-498, doi:10.1175/BAMS-D-11-00094.1, 2012

Teixeira, D. C. (2005). First report of a Huanglongbing-like disease of citrus in São Paulo, Brazil, and association of a new *Liberibacter* species, "*Candidatus* Liberibacter americanus" with the disease. *Plant Dis.* 89, 107.

Tellez-Valdes, O., & Davila-Aranda, P. (2003). Protected areas and climate change: A case study of the cacti in the Tehuacan-Cuicatlan biosphere reserve, Mexico. Conservation Biology 17: 846–853.

Thomas, C. D., Cameron, A., Green, R. E., Bakkenes, M., Beaumont, L. J., Collingham, Y. C., Erasmus, B. F., De Siqueira, M. F., Grainger, A., Hannah, L., Hughes, L., Huntley, B., Van Jaarsveld, A. S., Midgley, G. F., Miles, L., Ortega-Huerta, M. A., Peterson, A. T., Phillips, O. L., & Williams, S. E. (2004). Extinction risk from climate change. Nature, 427(6970), 145–148. https://doi.org/10.1038/nature02121

Thuiller, W., Arau´jo, M. B., & Lavorel, S. (2003). Generalised models versus CLassification tree analysis: a comparative study for predicting spatial distributions of plant species at different scales. Journal of Vegetation Science, 14(5):669-681.

Thuiller, W., Lafourcade, B., Engler, R. & Araujo, M.B. (2009) BIOMOD – a platform for ensemble forecasting of species distributions. Ecography 32, 369–373.

Torres-Pacheco, I., López-Arroyo, J., Aguirre-Gómez, J., Guevara-González, R., Yänez-López, R., Hernández-Zul, M., & Quijano-Carranza, J. (2013). Potential distribution in Mexico of Diaphorina citri (Hemiptera: Psyllidae) vector of Huanglongbing pathogen. Florida Entomologist, 96(1), 36– 47.

Tschirley, D. L., Muendo, K. M., & Weber, M. T. (2004) Improving Kenya's domestic horticultural production and marketing system: current competitiveness, forces of change, and challenges for the future (volume II: horticultural marketing) (No. 55156). Michigan State University, Department of Agricultural, Food, and Resource Economics

Van de Merwe, A. J. & Andersen, F. G. (1937). Chromium and manganese toxicity. Is it important in Transvaal citrus greening? *Farming S Afr.* **12,** 439-440

Van den Berg, M. A., Van Vuuren, S. P., & Deacon, V. E. (1992). Studies on greening disease transmission by the citrus psylla, Trioza erytreae (Hemiptera: Triozidae). *Israel Journal of Entomology 25*:51-56

Van Nouhuys, S., Kohonen, M. & Duplouy, A. (2016). Wolbachia increases the susceptibility of a parasitoid wasp to hyperparasitism. J. Exp. Biol., 219, 2984–2990.

Van Vuuren, S. P. and da Graca, J. V. (1978). Effects of exposure time and monocrotophos on citrus greening transmission by psylla (Trioza erytreae Del G.). *Citrus and sub-tropical fruit journal*. 536: 13–14

Váry, Z., Mullins, E., McElwain, J. C., & Doohan, F. M. (2015). The severity of wheat diseases increases when plants and pathogens are acclimatized to elevated carbon dioxide. Glob Chang Biol 21:2661–2669.

Velásquez, A. C., Castroverde, C. D. M., & He, S. Y. (2018). Plant-Pathogen Warfare under Changing Climate Conditions. Current Biology : 28(10), R619–R634. https://doi.org/10.1016/j.cub.2018.03.054

Wangari, N. P., Gacheri, K. M., Theophilus, M. M., & Box, P. O. (2013). Use of SSR markers for genetic diversity studies in mulberry accessions grown in Kenya. 4(June), 38–44. https://doi.org/10.5897/IJBMBR11.057

Weaver, C. P., Lempert, R. J., Brown, C., Hall, J. A., Revell, D & Sarewitz, D. (2013). Improving the contribution of climate model information to decision making: the value and demands of robust decision frameworks. Wiley Interdisciplinary Reviews: Climate Change 4: 39–60.

Weinert, M. P., Jacobson, S. C., Grimshaw, J. F., Bellis, G. A., Stephens, P. M., Gunua, T. G., Kame, M. F. & Davis, R. I. (2004). Detection of huanglongbing (citrus greening disease) in Timor-Leste (East Timor) and in Papua New Guinea. *Australasian Plant Pathology 33*(1): 135-136

Weiss, B., & Aksoy, S. (2011). Microbiome influences on insect host vector competence. Trends in Parasitology, 27(11), 514–522. https://doi.org/10.1016/j.pt.2011.05.001

Werren, J. H., & Windsor, D. M. (2000). Wolbachia infection frequencies in insects: evidence of a global equilibrium? Proc. Biol. Sci. 267:1277-1285.

Wiens, J. A., Stralberg, D., Jongsomjit, D., Howell, C. A., & Snyder, M. A. (2009). Niches, models, and climate change: Assessing the assumptions and uncertainties. Proceedings of the National Academy of Sciences of the United States of America 106: 19729–19736.

Williams, S. E., Bolitho, E. E., & Fox, S. (2003). Climate Change in Australian Tropical Rainforests: An Impending Environmental Catastrophe. Proceedings: Biological Sciences 270: 1887–1892

Wilsey, B. J., Chalcraft, D. R., Bowles, C. M. & Willig, M. R. (2005) Relationships among indices suggest that richness is an incomplete surrogate for grassland biodiversity. Ecology 86(5):1178–1184. doi:10.1890/04-0394

Wise, M., Calvin, K., Thomson, A., Clarke, L., Bond-Lamberty, B., Sands, R., Smith, S. J., Janetos, A., & Edmonds, J. (2009). Implications of limiting CO2 concentrations for land use and energy. Science (New York, N.Y.), 324(5931), 1183–1186. https://doi.org/10.1126/science.1168475

Wang Y, Xu C, Tian M, Deng X, Cen Y, & He Y. (2017). Genetic diversity of Diaphorina citri and its endosymbionts across East and Southeast Asia. Pest Manag Sci. 2017;73(10):2090-2099. doi: 10.1002/ps.4582

Wu, J., Krutovskii, K. V., & Strauss, S. H. (1999). Nuclear DNA diversity, population differentiation, and phylogenetic relationships in the Califonia closed-clone pines based on RAPD and allozyme markers, Genome 42:893-908.

Xi, Z., Khoo, C. C., & Dobson, S. L. (2005) Wolbachia establishment and invasion in an Aedes aegypti laboratory population. Science 14: 326–328

Xi, Z. Y., Khoo, C. C. H., & Dobson, S. L. (2006) Interspecific transfer of Wolbachia into the mosquito disease vector Aedes albopictus. Proc Royal Soc Lond B Biol Sci 273: 1317–1322

Xiao, X. Y., Wang, Y. P., Zhang, J. Y., Li, S. G., & Rong, T. Z. (2006). SSR marker-based genetic diversity fingerprinting of hybrid rice in Sichuan, China. Chin. J. Rice. Sci., 20(1): 1-7.

Zabalou, S., Apostolaki, A., Livadaras, I., Franz, G., Robinson, A.S., Savakis, C. & Bourtzis, K. (2009). Incompatible insect technique: Incompatible males from a Ceratitis capitata genetic sexing strain. Entomol. Exp. Appl., 132, 232–240.

Zabalou, S., Riegler, M., Theodorakopoulou, M., Stau_er, C., Savakis, C. & Bourtzis, K. (2004). Wolbachia-induced cytoplasmic incompatibility as a means for insect pest population control. Proc. Natl. Acad. Sci. USA, 101, 15042–15045.

Zardoya R. & Meyer A. (1996). Phylogenetic Performance of Mitochondrial Protein-Coding Genes in Resolving Relationships Among Vertebrates, Mol. Biol. Evol., 1996, 13, 933-942

Zhang, S. B., Zhu, Z., Zhao, L., Zhang, Y. D., Chen, T., Lin, J., & Wang, C. L. (2007). Identification of SSR markers closely linked to eui gene in rice. Yi Chuan (Hereditas-Beijing), 29(3): 365-370.

Zhao, X. Y. (1981). Citrus yellow shoot disease (huanglongbing) in China – a review. In: Matsumoto K (ed.), Proc 4th Intern Soc Citric Cong. Tokyo, Japan, 9-12 November 1981.

Zheng Z, Xu M, Bao M, Wu F, Chen J, & Deng X. (2016). Unusual Five Copies and Dual Forms of nrdB in '*Candidatus* Liberibacter asiaticus': Biological Implications and PCR Detection Application. Scientific Reports. 2016; 6:39020.

Zurek, L., & Ghosh, A. (2014). Insects represent a link between food animal farms and the urban environment for antibiotic resistance traits. Appl Environ Microbiol. 80:3562–3567.

Appendix 1. Symptoms typical of Huanglongbing disease found in citrus plants in Ethiopia. a) Severe yellowing of leaves, b) Lopsided fruit and yellowing of leaves, c) Leaf galls caused by *T*rioza *erytreae* nymph feeding, and d) Defoliation, yellowing and dieback on an orange tree.

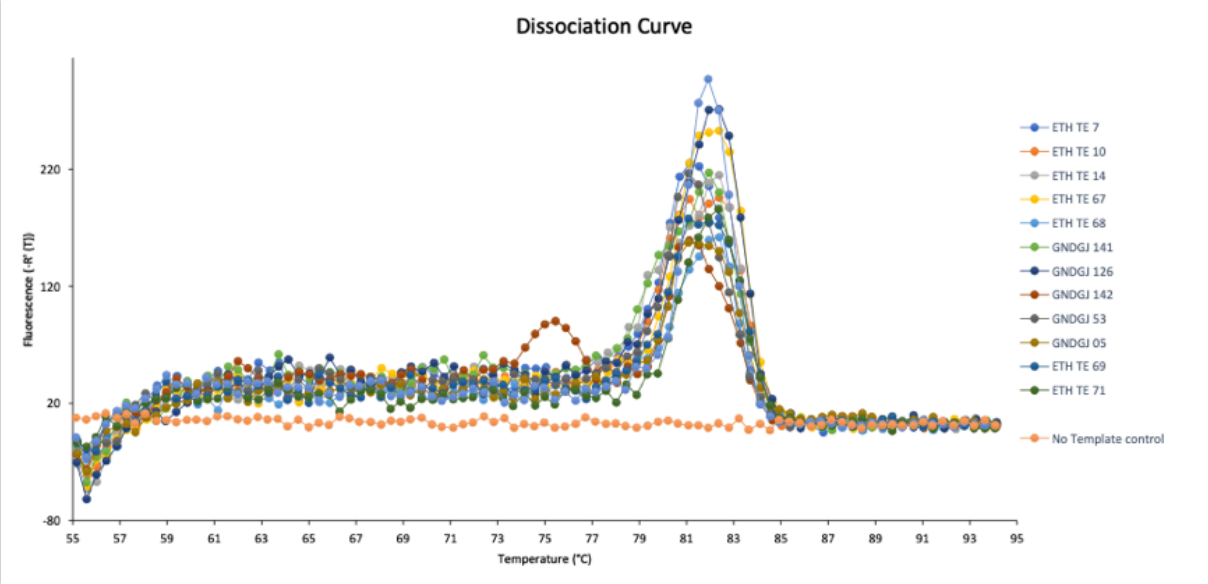

Appendix 2. Melting curve for Liberibacter 16S ribosomal DNA gene in representative plant and insect vector samples. ETH TE - Liberibacter samples from *Trioza erytreae* vector, GNDGJ. Liberibacter samples from citrus plants.

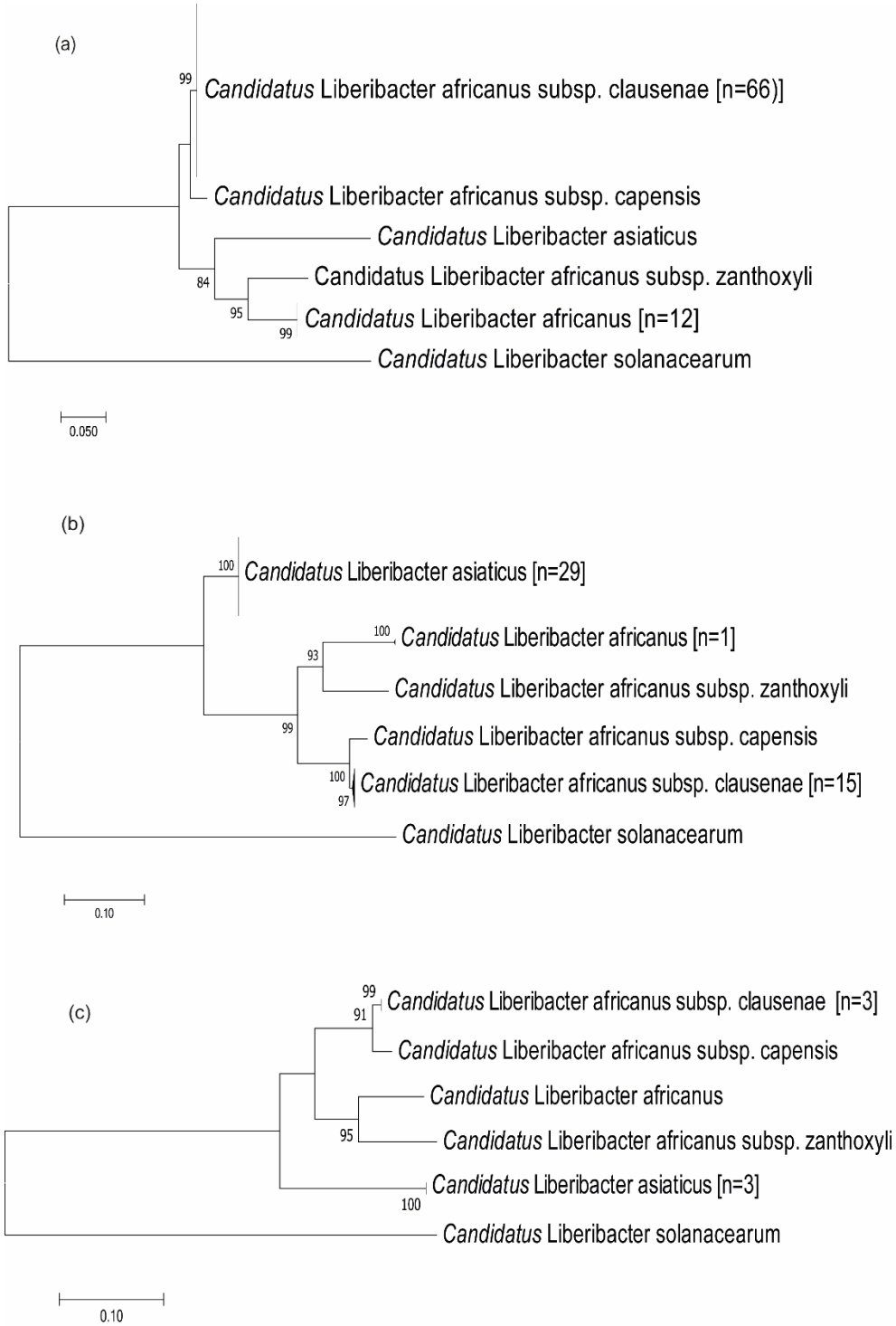

Appendix 3.Maximum-likelihood trees based on a 650 bp alignment of 129 sequences of the 50S ribosomal protein L10 (*rplJ)* gene of Liberibacters found on symptomatic citrus samples collected from (a) Ethiopia (n = 45), (b) Kenya (n = 6), and (c) Uganda (n = 78), and publicly available representative Liberibacter sequences with *Candidatus* Liberibacter solanacearum as an outgroup. The number of Liberibacter sequences obtained in this study is indicated in square brackets. Bootstrap values were based on 1,000 replicates.

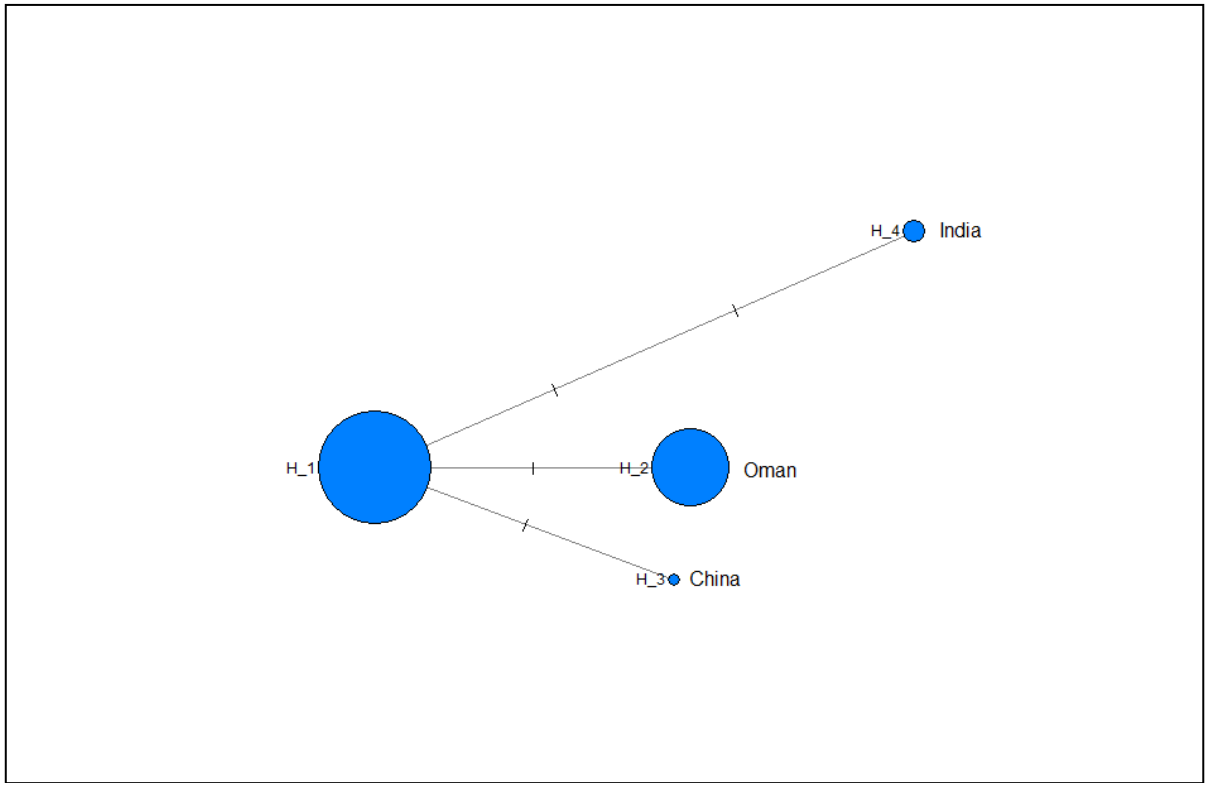

Appendix 4. Haplotype network representing the relationships among the new and publicly available *Candidatus* Liberibacter asiaticus sequences used in this study. The size of the circles is proportional to the number of sequences in each haplotype.

Appendix 5. Sampling locations where *Candidatus* Liberibacter species were identified from citrus plants by *rplJ* gene in Uganda, Ethiopia and Kenya. Las: "*Candidatus* Liberibacter asiaticus", CLaf: "*Candidatus* Liberibacter africanus", CLafCl: "*Candidatus* Liberibacter subspecies Clausenae".

Country	**Region**	**Location**	**Altitude (m.a.s.l)**	**Citrus system**	**Liberibacter Identity (*rplJ*)**	**Vector Found**
Uganda	Western	Naro Zardi	1457	Research Orchard	LafCl	*T. erytreae*
		Katojo	1439	Backyard garden	LafCl	*T. erytreae*
		Kyarwabugunda	1419	Backyard garden	LafCl	*T. erytreae*
		Ruharo	1415	Small scale rural farm	Laf	*T. erytreae*
	Central	Kyabigondo	1259	Backyard garden	LafCl	*T. erytreae*
		Lyatonde3	1332	Backyard garden	LafCl	*T. erytreae*
		Kyanasanjya	1228	Backyard garden	LafCl	*T. erytreae*
		Kijjasi	1258	Backyard garden	LafCl	*T. erytreae*

		Mukusamvu	1175	Backyard garden	LafCl	*T. erytreae*
		Lukoma	1189	Backyard garden	LafCl	*T. erytreae*
		Kawuto	1164	Small scale rural farm	LafCl	*T. erytreae*
		Namabare	1262	Small scale rural farm	LafCl	*T. erytreae*
		Makondo	1279	Backyard garden	LafCl	*T. erytreae*
		Kiswera	1262	Backyard garden	LafCl	*T. erytreae*
		Kaswa	1292	Backyard garden	LafCl	*T. erytreae*
		Bajja3	1180	Backyard garden	LafCl	*T. erytreae*
		Buganga	1168	Backyard garden	LafCl	*T. erytreae*
		Buganga2	1143	Small scale rural farm	LafCl	*T. erytreae*
		Bubule3	1167	Backyard garden	LafCl	*T. erytreae*
		Kyengeza	1278	Backyard garden	Laf	*T. erytreae*
		Kaswa	1260	Backyard garden	Laf	*T. erytreae*
		Kyamenyamingo	1288	Backyard garden	Laf	*T. erytreae*
		Kasana	1279	Backyard garden	Laf	*T. erytreae*
		Bajja	1180	Backyard garden	Laf	*T. erytreae*
		Bubule	1167	Backyard garden	Laf	*T. erytreae*
		Bugonzi	1216	Backyard garden	Laf	*T. erytreae*
	Eastern	Teibu	1056	Small scale rural farm	LafCl	*T. erytreae*
		Akere	1058	Small scale rural farm	LafCl	*T. erytreae*
		Akere 2	1056	Backyard garden	LafCl	*T. erytreae*
		Hospital Atik	1051	Small scale rural farm	LafCl	*T. erytreae*
		Atik	1040	Backyard garden	LafCl	*T. erytreae*
		Agulo	1038	Commercial	LafCl	*T.*

				orchard		*erytreae*
		Aboko	1037	Commercial orchard	LafCl	*T. erytreae*
		Aduku	1048	Commercial orchard	LafCl	*T. erytreae*
		Akoremo	1059	Commercial orchard	LafCl	*T. erytreae*
		Abedi-woro	1092	Commercial orchard	LafCl	*T. erytreae*
		Ngetta	1076	Commercial orchard	LafCl	*T. erytreae*
		Telela	1102	Commercial orchard	LafCl	*T. erytreae*
		Telela2	109	Commercial orchard	LafCl	*T. erytreae*
		Aminyango	108	Commercial orchard	LafCl	*T. erytreae*
		Gweng Abara	1121	Commercial orchard	LafCl	*T. erytreae*
		Ocokcan	1099	Commercial orchard	LafCl	*T. erytreae*
		Adidun	1045	Commercial orchard	LafCl	*T. erytreae*
		Akani	1077	Commercial orchard	LafCl	*T. erytreae*
		Awase	1067	Commercial orchard	LafCl	*T. erytreae*
		Serere TC	1130	Research orchard	LafCl	*T. erytreae*
		Oburen	1108	Small scale rural farm	LafCl	*T. erytreae*
		Sapir	1118	Small scale rural farm	LafCl	*T. erytreae*
		Omukunyo	1094	Small scale rural farm	LafCl	*T. erytreae*
		Otaba	1101	Small scale rural farm	LafCl	*T. erytreae*
		Otete	1098	Commercial orchard	LafCl	*T. erytreae*
		Arabaka	1092	Commercial orchard	LafCl	*T. erytreae*
		Busitema Uni	1122	Research orchard	LafCl	*T. erytreae*
		Arapai Uni	1102	Research orchard	LafCl	*T. erytreae*
		Opero	1103	Commercial orchard	LafCl	*T. erytreae*

		Alake	1087	Commercial orchard	LafCl	*T. erytreae*
		Awoja	1049	Commercial orchard	LafCl	*T. erytreae*
		Kapir	1061	Commercial orchard	LafCl	*T. erytreae*
		Olupe	1106	Commercial orchard	LafCl	*T. erytreae*
		Okutai	1081	Commercial orchard	LafCl	*T. erytreae*
		Obokora	1103	Commercial orchard	LafCl	*T. erytreae*
		Aoloko	1132	Commercial orchard	LafCl	*T. erytreae*
		Kapokina	1113	Commercial orchard	LafCl	*T. erytreae*
		Bukedea	1133	Commercial orchard	LafCl	*T. erytreae*
		Kachumbala	1142	Commercial orchard	LafCl	*T. erytreae*
		Butuwongore	1082	Commercial orchard	LafCl	*T. erytreae*
		Namalemba	1103	Commercial orchard	LafCl	*T. erytreae*
		Nakawunje	1115	Commercial orchard	LafCl	*T. erytreae*
		Namutumba	1119	Commercial orchard	LafCl	*T. erytreae*
		Buyange	1085	Commercial orchard	LafCl	*T. erytreae*
		Butamba	1075	Commercial orchard	LafCl	*T. erytreae*
		Mazuba	1067	Commercial orchard	LafCl	*T. erytreae*
		Kibuku	1081	Commercial orchard	LafCl	*T. erytreae*
		Nakatende	1107	Commercial orchard	LafCl	*T. erytreae*
		Lambo	1159	Commercial orchard	LafCl	*T. erytreae*
		Molo1	1193	Commercial orchard	LafCl	*T. erytreae*
Ethiopia	Amhara	Dangila	2122	Small scale rural farm	Laf	*T. erytreae*
		Dangila2	2123	Small scale rural farm	LafCl	*T. erytreae*
		Dangila3	2116	Backyard garden	Las	*T.*

						erytreae
		Shuwabere	1978	Small scale rural farm	Las	*T. erytreae*
		Abchbele-mariam	1970	Small scale rural farm	Las	*T. erytreae*
		Insude	1959	Small scale rural farm	Las	*T. erytreae*
		Insude2	1964	Small scale rural farm	Las	*T. erytreae*
		Insude3	1992	Small scale rural farm	Las	*T. erytreae*
		Insude4	2005	Small scale rural farm	Las	*T. erytreae*
		Achabere	1982	Backyard garden	LafCl	*T. erytreae*
		Achabere2	1958	Backyard garden	LafCl	*T. erytreae*
		Matafa duda	1936	Backyard garden	LafCl	*T. erytreae*
		Addis Zemen	1920	Backyard garden	LafCl	*T. erytreae*
		Addis Zemen2	1923	Backyard garden	LafCl	*T. erytreae*
		Bohona	1922	Backyard garden	LafCl	*T. erytreae*
		Zenzelima	1867	Backyard garden	Las	*T. erytreae*
		Zenzelima2	1876	Backyard garden	LafCl	*T. erytreae*
		Sasaberete	1891	Backyard garden	Las	*T. erytreae*
		Bure	2460	Small scale rural farm	LafCl	*T. erytreae*
		Bureau of Agric	2021	Commercial orchard	LafCl	*T. erytreae*
	Wollo	Mola gerado	1953	Small scale rural farm	Las	-
		Goshuha	1880	Backyard garden	Las	-
		Gola	1935	Backyard garden	Las	-
		Weira Amba	1891	Commercial orchard	Las	-
		Mersa	161	Backyard garden	Las	-
		Mersa2	1679	Backyard garden	Las	-
		Mersa3	1592	Backyard garden	Las	-
		Ambasel	1725	Backyard garden	Las	-
		Jare	1685	Backyard garden	Las	-

		Pasomile	1805	Backyard garden	Las	-
		Hayk	2002	Backyard garden	Las	-
		Hayk2	2029	Backyard garden	Las	-
		Abuabu	2113	Backyard garden	Las	-
		Milamile	1436	Small scale rural farm	Las	-
	Tigray	Adishewi	1657	Backyard garden	Las	-
Kenya	Coast	Lunga-Lunga	50	Backyard garden	Las	*D. citri*
		Matuga	55	Research orchard/ Nursery	Las	*D. citri*
		Muhaka	55	Research orchard	Las	*D. citri*
	Western	Awasi	1344	Backyard garden	LafCl	*D. citri*
		Soin	1543	Backyard garden	LafCl	*D. citri*
		Koitamburot	1409	Backyard garden	LafCl	*D. citri*

*For GPS coordinates refer to Appendix 11

Appendix 6. Intraspecific mean uncorrected p-distances (%) for citrus greening associated *Candidatus* Liberibacter species: based on a 649 bp alignment of 273 new and publicly available 50S ribosomal protein L10 gene region sequences. Standard error estimates (SE) are shown in the last column. CLas – "*Candidatus* Liberibacter asiaticus, CLaf – "*Candidatus* Liberibacter africanus", CLafCl – "*Candidatus* Liberibacter africanus subsp. clausenae", CLafC – "*Candidatus* Liberibacter africanus subsp. capensis" and CLafV – "*Candidatus* Liberibacter africanus subsp. vepridis".

	Number of sequences	Number of haplotypes	Intraspecific p-distance (mean, %)	SE
LafCl (this study)	84	1	0.00	0.000
LafCl (GenBank)	3	1	0.00	0.000
LafC (GenBank)	4	1	0.00	0.000
Laf (GenBank)	14	1	0.00	0.000
Laf (this study)	13	1	0.00	0.000
Las (GenBank)	123	4	0.10	0.001
Las (this study)	32	1	0.00	0.000

Appendix 7. Primers used in the qPCR assay for the detection of generic Liberibacter, and PCR amplification and bidirectional sequencing of the 50S ribosomal protein L10 region in *Candidatus* Liberibacter species (in bold) for species and sub-species identification. Liberibacter DNA was obtained from citrus plants, and the insect vectors *Trioza erytreae* and *Diaphorina citri* in Uganda, Ethiopia and Kenya.

Primer	Assay	Primer sequence (5'-3')	PCR product (bp)
LibUF	qPCR	GGCAGGCCTAACACATGC	˜1160
HLBr		5'-GCGTTATCCCGTAGAAAAAGGTAG	˜1160
A2	**PCR**	**TATAAAGGTTGACCTTTCGAGTTT**	**˜650**

J5		**ACAAAAGCAGAAATAGCACGAACAA**	**˜650**

Appendix 8. List of publicly available and new ribosomal protein L10 (rplJ) sequences (excluding sequences: shorter than 650 bp and containing nucleotide ambiguities) used in the phylogenetic analyses of *Candidatus* Liberibacter species recovered from citrus plants in Uganda, Ethiopia and Kenya, with GenBank accession numbers. Sequences generated in this study are shown in bold.

Organism	**Accession**	**Country (region)**
***Candidatus* Liberibacter africanus**	**MK542518.1**	**Uganda**
Candidatus Liberibacter africanus	GU120033.1	
Candidatus Liberibacter africanus	GU120041.1	
Candidatus Liberibacter africanus	GU120034.1	
Candidatus Liberibacter africanus	GU120037.1	
Candidatus Liberibacter africanus	GU120038.1	
Candidatus Liberibacter africanus	GU120043.1	
Candidatus Liberibacter africanus	GU120032.1	
Candidatus Liberibacter africanus	GU120042.1	
Candidatus Liberibacter africanus	GU120040.1	
Candidatus Liberibacter africanus	GU120036.1	
Candidatus Liberibacter africanus	GU120044.1	
Candidatus Liberibacter africanus	GU120039.1	
Candidatus Liberibacter africanus	GU120035.1	South Africa
Candidatus Liberibacter africanus subsp. capensis	JF419553.1	
Candidatus Liberibacter africanus subsp. capensis	JF419554.1	
Candidatus Liberibacter africanus subsp. capensis	JF419555.1	South Africa
Candidatus Liberibacter africanus subsp. capensis	KJ197225.1	
Candidatus Liberibacter africanus subsp. clausenae	KX770999.1	Tanzania
Candidatus Liberibacter africanus subsp. clausenae	KX770998.1	
***Candidatus* Liberibacter africanus subsp. clausenae**	**MK542519.1**	**Uganda**
Candidatus Liberibacter africanus subsp. clausenae	KJ189106.1	South Africa
Candidatus Liberibacter africanus subsp. vepridis	KJ189105.1	South Africa
Candidatus Liberibacter asiaticus	JX430435.1	
Candidatus Liberibacter asiaticus	KR919749.1	
Candidatus Liberibacter asiaticus	JX455746.1	USA
Candidatus Liberibacter asiaticus	MF041971.1	
Candidatus Liberibacter asiaticus	JF346109.1	Bhutan
Candidatus Liberibacter asiaticus	FJ394022.1	Cuba
Candidatus Liberibacter asiaticus	GQ890155.1	
Candidatus Liberibacter asiaticus	GQ890156.1	
Candidatus Liberibacter asiaticus	**MK542517.1**	**Ethiopia**

Candidatus Liberibacter asiaticus	MK542517.1	
Candidatus Liberibacter asiaticus	KC133067.1	China
Candidatus Liberibacter asiaticus	KC133068.1	
Candidatus Liberibacter asiaticus	KC133065.1	
Candidatus Liberibacter asiaticus	JN211021.1	
Candidatus Liberibacter asiaticus	JN211020.1	
***Candidatus* Liberibacter asiaticus**	JN211014.1	
Candidatus Liberibacter asiaticus	JN211015.1	
Candidatus Liberibacter asiaticus	JN211016.1	
Candidatus Liberibacter asiaticus	JN211017.1	
Candidatus Liberibacter asiaticus	DQ303211.1	
Candidatus Liberibacter asiaticus	JN211018.1	
Candidatus Liberibacter asiaticus	JN211019.1	
Candidatus Liberibacter asiaticus	KF699074.1	French West Indies
Candidatus Liberibacter asiaticus	KF699075.1	
Candidatus Liberibacter asiaticus	KF699076.1	
Candidatus Liberibacter asiaticus	KF699081.1	
Candidatus Liberibacter asiaticus	KF699077.1	
Candidatus Liberibacter asiaticus	KF699088.1	
Candidatus Liberibacter asiaticus	KF699078.1	
Candidatus Liberibacter asiaticus	KF699080.1	
Candidatus Liberibacter asiaticus	KF699082.1	
Candidatus Liberibacter asiaticus	KF699089.1	
Candidatus Liberibacter asiaticus	KF699090.1	
Candidatus Liberibacter asiaticus	KF699083.1	
Candidatus Liberibacter asiaticus	KF699091.1	
Candidatus Liberibacter asiaticus	KF699084.1	
Candidatus Liberibacter asiaticus	KF699085.1	
Candidatus Liberibacter asiaticus	KF699092.1	
Candidatus Liberibacter asiaticus	KF699086.1	
Candidatus Liberibacter asiaticus	KF699079.1	
Candidatus Liberibacter asiaticus	KF699087.1	
Candidatus Liberibacter asiaticus	MG418842.1	Venezuela
Candidatus Liberibacter asiaticus	MG418841.1	
Candidatus Liberibacter asiaticus	LC090236.1	Indonesia
Candidatus Liberibacter asiaticus	AB859772.1	Mexico
Candidatus Liberibacter asiaticus	AB859773.1	
Candidatus Liberibacter asiaticus	AB859774.1	
Candidatus Liberibacter asiaticus	HQ335314.1	Iran
Candidatus Liberibacter asiaticus	KY990824.1	
Candidatus Liberibacter asiaticus	JF261098.1	
Candidatus Liberibacter asiaticus	KY990823.1	
Candidatus Liberibacter asiaticus	KC596024.1	
Candidatus Liberibacter asiaticus	KC477386.1	India

Candidatus Liberibacter asiaticus	KC477383.1	
Candidatus Liberibacter asiaticus	KC477380.1	
Candidatus Liberibacter asiaticus	KC477381.1	
Candidatus Liberibacter asiaticus	KC477384.1	
Candidatus Liberibacter asiaticus	Q973894.1	
Candidatus Liberibacter asiaticus	JQ973895.1	
Candidatus Liberibacter asiaticus	KC816565.1	
Candidatus Liberibacter asiaticus	KC477375.1	
Candidatus Liberibacter asiaticus	GU074017.1	
Candidatus Liberibacter asiaticus	KC477376.1	
Candidatus Liberibacter asiaticus	MF767288.1	
Candidatus Liberibacter asiaticus	MF694639.1	
Candidatus Liberibacter asiaticus	JQ973890.1	
Candidatus Liberibacter asiaticus	JQ973891.1	
Candidatus Liberibacter asiaticus	KM889670.1	
Candidatus Liberibacter asiaticus	KM889671.1	
Candidatus Liberibacter asiaticus	KT164846.1	
Candidatus Liberibacter asiaticus	JX284242.1	
Candidatus Liberibacter asiaticus	JX284243.1	
Candidatus Liberibacter asiaticus	KC137980.1	
Candidatus Liberibacter asiaticus	MF767289.1	
Candidatus Liberibacter asiaticus	JX284244.1	
Candidatus Liberibacter asiaticus	MF769715.1	
Candidatus Liberibacter asiaticus	MF769714.1	
Candidatus Liberibacter asiaticus	MF769717.1	
Candidatus Liberibacter asiaticus	KT164840.1	
Candidatus Liberibacter asiaticus	KT164841.1	
Candidatus Liberibacter asiaticus	KT164842.1	
Candidatus Liberibacter asiaticus	KT164843.1	
Candidatus Liberibacter asiaticus	KT164844.1	
Candidatus Liberibacter asiaticus	KT164845.1	
Candidatus Liberibacter asiaticus	KC137978.1	
Candidatus Liberibacter asiaticus	JQ973892.1	
Candidatus Liberibacter asiaticus	KY550692.1J	
Candidatus Liberibacter asiaticus	KY550693.1	
Candidatus Liberibacter asiaticus	KY550694.1	
Candidatus Liberibacter asiaticus	KY550690.1	
Candidatus Liberibacter asiaticus	KY550695.1	
Candidatus Liberibacter asiaticus	KY550696.1	
Candidatus Liberibacter asiaticus	KY550697.1	
Candidatus Liberibacter asiaticus	KY550698.1	
Candidatus Liberibacter asiaticus	KY550704.1	
Candidatus Liberibacter asiaticus	KY550705.1	
Candidatus Liberibacter asiaticus	KY550706.1	Oman

Candidatus Liberibacter asiaticus	KY550707.1	
Candidatus Liberibacter asiaticus	KY550699.1	
Candidatus Liberibacter asiaticus	KY550700.1	
Candidatus Liberibacter asiaticus	KY550701.1	
Candidatus Liberibacter asiaticus	KY550702.1	
Candidatus Liberibacter asiaticus	KY550708.1	
Candidatus Liberibacter asiaticus	KY550709.1	
Candidatus Liberibacter asiaticus	KY550685.1	
Candidatus Liberibacter asiaticus	KY550678.1	
Candidatus Liberibacter asiaticus	KY550679.1	
Candidatus Liberibacter asiaticus	KY550680.1	
Candidatus Liberibacter asiaticus	KY550681.1	
Candidatus Liberibacter asiaticus	KY550682.1	
Candidatus Liberibacter asiaticus	KY550683.1	
Candidatus Liberibacter asiaticus	KY550686.1	
Candidatus Liberibacter asiaticus	KY550688.1	
Candidatus Liberibacter asiaticus	KY550703.1	
Candidatus Liberibacter asiaticus	KY550684.1	
Candidatus Liberibacter asiaticus	KY550691.1	
Candidatus Liberibacter asiaticus	KY550687.1	
Candidatus Liberibacter asiaticus	KY550689.1	
Candidatus Liberibacter asiaticus	KY550672.1	
Candidatus Liberibacter asiaticus	KY550673.1	
Candidatus Liberibacter asiaticus	KY550674.1	
Candidatus Liberibacter asiaticus	KY550676.1	
Candidatus Liberibacter asiaticus	KY550675.1	
Candidatus Liberibacter asiaticus	KY550677.1	

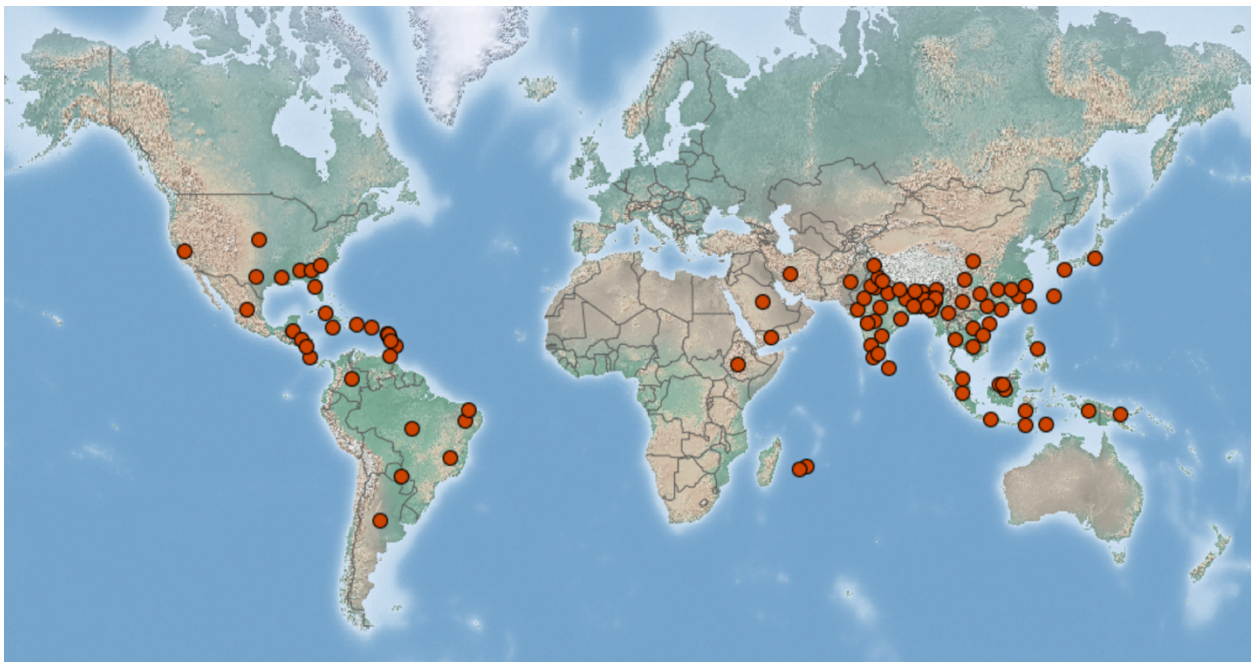

Appendix 9 Global occurrence of citrus Huanglongbing disease (HLB) caused by the bacterial pathogen *Candidatus* Liberibacter asiaticus (Las), as reported in previous studies. Source: Centre for Agriculture and Bioscience International CABI/EPPO, 2017. *Candidatus* Liberibacter asiaticus. [Distribution map]. In: Distribution Maps of Plant Diseases, (No.April) Wallingford, UK: CABI.Map 766 (Edition 4).

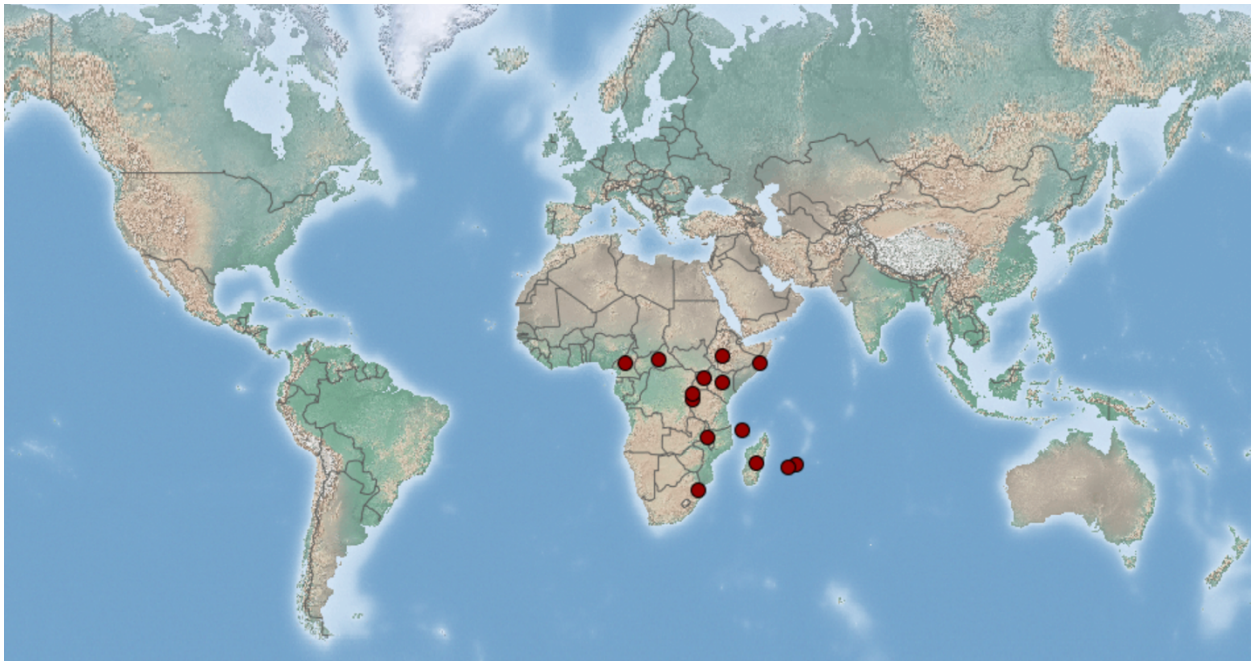

Appendix 10. Occurrence of African citrus greening disease caused by the bacterial pathogen "*Candidatus* Liberibacter africanus" (CLaf), as reported in previous studies. Source: Centre for Agriculture and Bioscience International CABI/EPPO, 1998. Liberibacter africanum. [Distribution map]. Distribution Maps of Plant Diseases, October (Edition 1). Wallingford, UK: CAB International, Map 765

Appendix 11. Presence points for "*Candidatus* Liberibacter asiaticus" (CLas) and "*Candidatus* Liberibacter africanus" (CLaf) in Ethiopia, Kenya, Uganda and Tanzania obtained during this survey on the incidence of HLB and African citrus greening. * Identity of Liberibacter species as determined by PCR testing of symptomatic plants.

Country	Region	District	Location	Latitude	Longitude	Altitude	Identity*
Ethiopia	Amhara	Agew Awi	Dangila	11.255714	36.848322	2122.52	Laf
			Dangila3	11.261051	36.848362	2116.26	Las
		West Gojjam	Shuwabere	11.355548	36.954216	1978.46	Las
			Abchibele Mariam	11.360449	36.961524	1970.74	Las
			Insude	11.399672	37.096003	1959.42	Las
			Acha bere	11.48809	37.295119	1982.59	Laf
			Matafa duda	11.531406	37.311268	1936.47	Laf
			Zenzelima	11.598003	37.443825	1867.91	Las
			Zenzelima	11.602138	37.447285	1877.05	Laf
			Sasaberete	11.606641	37.452338	1891.66	Laf
			Bure	10.716565	37.066553	2460.56	Laf
		North Gondar	Bohona	12.533765	37.164483	1915.09	Laf
		South Gondar	Addis Zemen	12.117811	37.77603	1920.51	Laf
		North Wollo	Mola gerado	11.782162	39.584961	1953.19	Las
			Goshuha	11.761833	39.595538	1861.48	Las
			Gola	11.740891	39.608093	1935.65	Las
			Weira Amba	11.743527	39.628531	1899.71	Las
			Mersa	11.673971	39.656038	1619.47	Las
			Ambasel	11.390236	39.634393	1724.56	Las
			Jare	11.374817	39.649231	1684.67	Las
			Pasomile	11.355098	39.662071	1804.60	Las
			Hayk	11.285255	39.682494	2028.54	Las
			Abuabu	11.26593	39.681838	2112.56	Las
	Tigray	Eastern	Adishewi	12.684336	39.645854	1657.05	Las
	Oromia	Oromia	Milamile	10.766333	39.832743	1435.62	Las
Kenya	Central	Machakos	Kathiani	-0.5378333	37.3066111	1815.00	Laf
		Meru	Tigania East	0.1251	37.1655667	1298.00	Laf
			Tigania West	0.04713333	37.15375	1381.00	Laf
		Embu	Mbeere North	0.54663889	37.5857222	1223.00	Laf

		Kirinyaga	Mwea East	0.55963889	37.3879722	1340.00	Laf
		Nyeri	Karatina	0.46272222	37.0909167	1778.00	Laf
		Murang'a	Sabasaba	0.87994444	37.15375	1385.00	Laf
			Kigumo	0.85347222	37.1252222	1434.00	Laf
			Kigumo	0.84463889	37.1028889	1495.00	Laf
	Western	Kisumu	Awasi	0.00828333	35.08785	1271.00	Laf
			Ahero	0.18378333	34.0794	1153.00	Laf
		Kericho	Soin	0.09243333	35.1469333	1483.00	Laf
			Soin	0.23453333	35.1407833	1403.00	Laf
			Soin	0.05411667	35.1845833	1398.00	Laf
Uganda	Western	Mbarara	Naro Zardi	-0.6027222	30.61075	1457.00	Laf
			Katojo	-0.5699167	30.5485	1439.00	Laf
			Kyarwabugunda	-0.5483333	30.6171389	1419.00	Laf
	Central	Lyatonde	Kyabigondo	-0.4891944	31.22175	1259.00	Laf
		Lyatonde	Lyatonde3	-0.5143611	31.2383611	1332.00	Laf
		Rakai	Kyanasanjya	-0.4964444	31.5547778	1228.00	Laf
			Kijjasi	-0.5053889	31.4594167	1258.00	Laf
			Mukusamvu	-0.9813333	31.4188889	1175.00	Laf
			Lukoma	-0.9231667	31.4292222	1189.00	Laf
			Kawuto	-0.8459444	31.4838056	1164.00	Laf
		Luwengo	Namabare	-0.5346389	31.38225	1262.00	Laf
			Makondo	-0.5098611	31.4854722	1279.00	Laf
		Masaka	Kiswera	-0.4174444	31.5504444	1262.00	Laf
			Kaswa	-0.3682778	31.6619722	1292.00	Laf
		Kalungu	Bajja	-0.1582222	31.8675278	1180.00	Laf
		Mpigi	Buganga	-0.0388333	32.101	1143.00	Laf
			Bubule	0.17611111	32.2764444	1167.00	Laf
	Eastern	Akere	Akere	1.958776	32.532672	1058.31	Laf
		Lira	Telela	2.317064	32.909521	1102.82	Laf
		Serere	Serere	1.518456	33.468837	1096.52	Laf
		Bukedea	Bukedea	1.284829	34.080013	1133.58	Laf
		Kalangala	Buyange	0.879634	33.719727	1082.17	Laf
Tanzania	Morogoro	Morogoro	Musumbe	-5.0871389	37.57175	552.00	Laf
			Misegese	-5.003	37.5721111	785.00	Laf

			Langali	-6.9406111	37.5833333	1229.00	Laf
			Langali	-6.9561944	37.57125	1018.00	Laf
			Mlali	-6.9973056	37.5704722	812.00	Laf
			Mlari	-5.0138333	37.5610833	651.00	Laf
			Kisiwani	-4.8989444	38.6493889	486.00	Laf
	Tanga	Tanga	Amani	-4.8990833	38.6337222	898.00	Laf

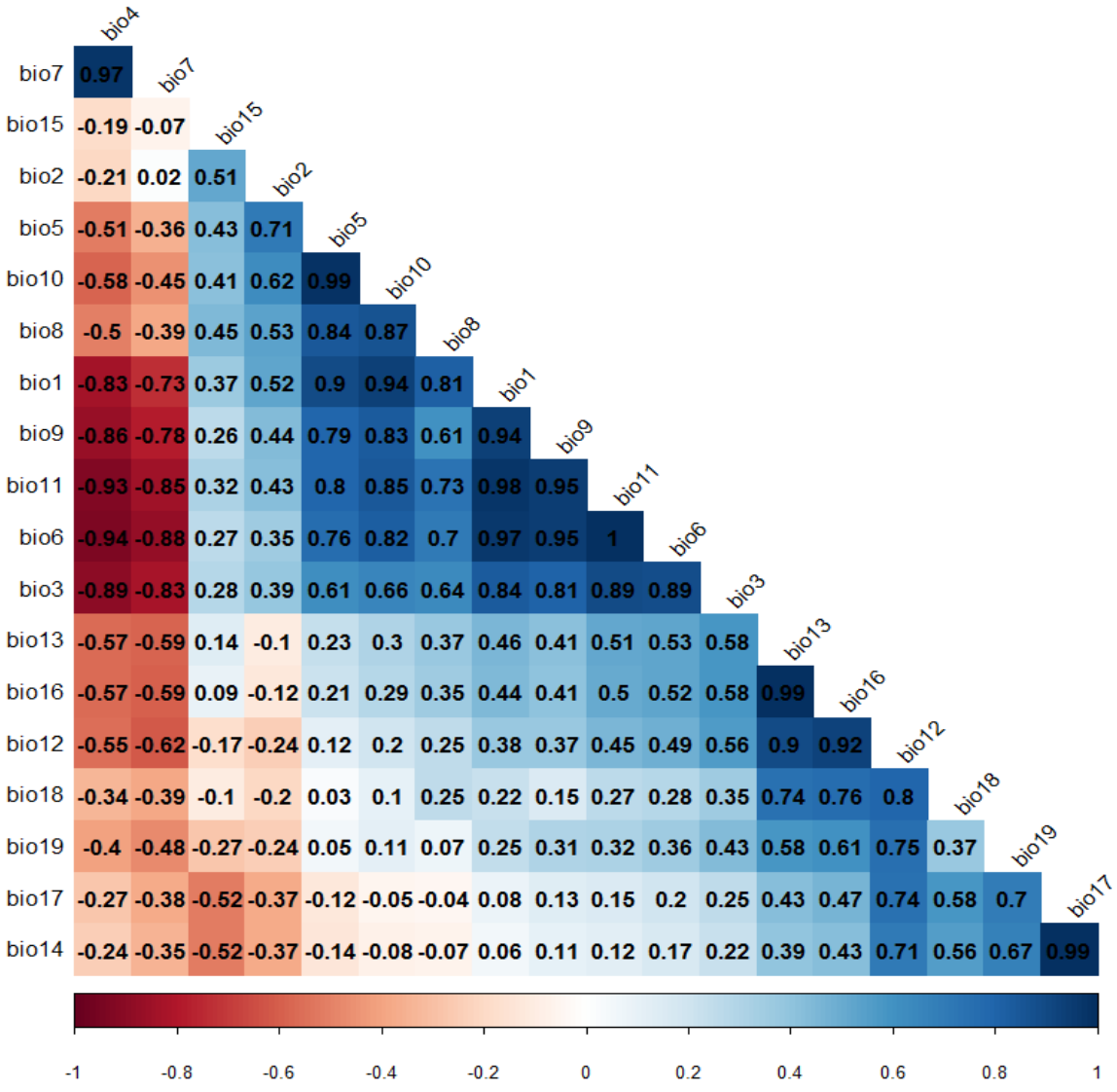

Appendix 12. Collinearity matrix for predictor bioclimatic variables used for modelling the ecological niche for "*Candidatus* Liberibacter asiaticus" and "*Candidatus* Liberibacter africanus", the pathogenic agents associated with Huanglongbing and African citrus greening diseases. Darker shades of blue and red colours indicate high collinearity between variables, while light shades indicate low collinearity between variables.

Appendix 13. Sample data of the adult specimens of the Asian citrus psyllid *Diaphorina citri* (Hemiptera: Psyllidae) collected in China (DC-CHN), Ethiopia (DC-ETH), Kenya (DC-KEN) Tanzania (DC-TZN) and USA (DC-USA) on *Citrus sinensis* (L.) Osbek and used for next-generation sequencing of the complete mitochondrial genomes.

Sample code	**Species**	**Country**	**Region**	**GPS**	**Host**	**Use**
DC-CHN	*Diaphorina citri*	China	Fuzhou	26.07877, 119.2969	Citrus sinensis	Complete mitogenome
DC-ETH	*Diaphorina citri*	Ethiopia	Goshuha	11.76407, 39.59168	Citrus sinensis	Complete mitogenome
DC-KEN	*Diaphorina citri*	Kenya	Lungalunga	-4.56247, 39.1221	Citrus sinensis	Complete mitogenome
DC-TZN	*Diaphorina citri*	Tanzania	Mikese	-4.93511, 39.12586	Citrus sinensis	Complete mitogenome
DC-USA	*Diaphorina citri*	USA	Texas	30.01501, -96.3425	Citrus sinensis	Complete mitogenome

Appendix 14. List of publicly available *Diaphorina citri* (Hemiptera: Psyllidae) mitogenomes used for the analysis of genetic divergence between samples from different world regions.

Country	GenBank Accession
Cambodia	MF614824
China	NC_030214
	MG489916
	MF614803 -MF614822
	MF426268
	KX073968
	KU647697
Indonesia	MF614827
Malaysia	MF614825
Pakistan	MF614828
Taiwan	MF614823
USA	KY426015
	KY426014
Vietnam	MF614826

Appendix 15. List of publicly available and new cytochrome oxidase 1 sequences (n = 573) identified as *Diaphorina citri* (Hemiptera: Psyllidae) used for the construction of a median-joining network, and a maximum likelihood tree.

Country	**GenBank accession**	**Reference**
Argentina	KY001577	Chu et al. 2019
Brazil	KC011223 - KC011243	Guidolin & Consoli 2013
	KC354739 - KC354785	Guidolin & Consoli 2013
	FJ190228 - FJ190333	Boykin et al. 2012
Cambodia	KU941172 - KU941176	Wang et al. 2018

China	MH970587- MH970829	Zhang & Xia 2018
	MF140371 - MF140373	Qasim et al.2019
	KU940421 - KU941158	Wang et al. 2018
	MH001384	Fuentes et al 2018
	FJ190357 - FJ190368	Boykin et al. 2012
	MK804829 - MK804888	Luo & Fu, 2019
	FJ190297 -FJ190299	Boykin et al. 2012
Guadeloupe	FJ190346 - FJ190356	Boykin et al. 2012
India	FJ190342 - FJ190345	Boykin et al. 2012
	KU050675	Das, 2009
	KR865959 - KR865960	Das, 2009
Indonesia	KU941145 - KU941149	Wang et al. 2018
	FJ190264 - FJ190336	Boykin et al. 2012
Iran	KC509563 - KC509572	Lashkari et al. 2013
Malaysia	KU941150 - KU941154	Wang et al. 2018
Mauritius	FJ190312 - FJ190316	Boykin et al. 2012
Mexico	MH001383	Fuentes et al 2018
	FJ190300 - FJ190305	Boykin et al. 2012
	KJ453889 - KJ453897	Sanchez, 2014
	FJ190306 - FJ190309	Boykin et al. 2012
Pakistan	FJ190288 - FJ190292	Boykin et al. 2012
	MH001373 - MH001379	Fuentes et al 2018
	KY001579	Chu et al. 2019
	KC509561 - KC509562	Lashkari et al. 2013
	MF140365 - MF140370	Qasim et al.2019
	KU941179 - KU941184	Wang et al. 2018
Puerto Rico	FJ190260 - FJ190262	Boykin et al. 2012
Reunion	FJ190317 - FJ190319	Boykin et al. 2012
Saudi Arabia	FJ190337 - FJ190341	Boykin et al. 2012
Taiwan	FJ190283 - FJ190287	Boykin et al. 2012
Thailand	MH001380	Fuentes et al 2018
	KY001580	Chu et al. 2019
	KU941177 - KU941178	Fuentes et al 2018
	FJ190293 - FJ190296	Boykin et al. 2012
USA	MH001381 - MH001382	Fuentes et al 2018
	KY001578	Chu et al. 2019
	KU941185 - KU941204	Wang et al. 2018
	FJ190187-FJ190241	Boykin et al. 2012
Vietnam	FJ190273 - FJ190378	Boykin et al. 2012
	KU941155 - KU941162	Chu et al. 2019

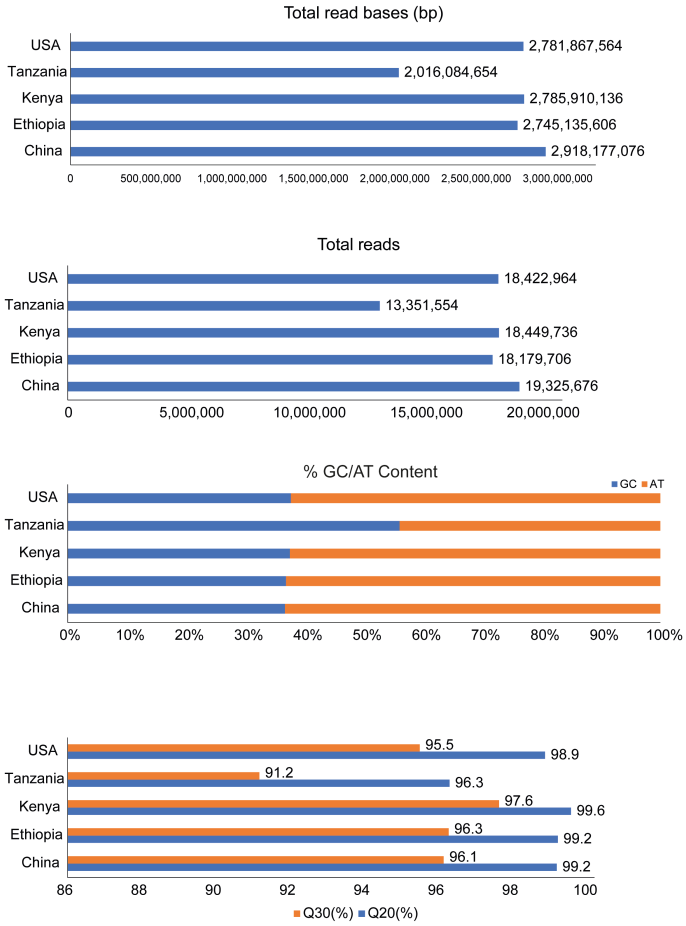

Appendix 16. Illumina MiSeq sequencing summary statistics for *Diaphorina citri* (Hemiptera: Psyllidae) from China, Ethiopia, Kenya, Tanzania and USA.

Appendix 17 Nucleotide composition of the complete mitochondrial sequence of Five African citrus triozids *Diaphorina citri* (Hemiptera: Psyllidae) collected in (a) China, (b) Ethiopia, (c) Kenya, (d) Tanzania and (e) USA. AT-skew = (A - T)/(A + T); CG-skew = (G - C)/(G + C).

(a) DC-CHN										
Region	**A%**	**C%**	**G%**	**T%**	**A+T%**	**G+C%**	**AT-skew**	**GC-skew**	**bp**	**% (size)**
COI	32.4	17.7	13.2	36.7	69.1	30.9	-0.06	-0.15	1,530	10.21
COII	34.8	17.6	10.4	37.2	72.0	28.0	-0.03	-0.26	664	4.43
ATP8	35.9	20.9	4.6	38.6	74.5	25.5	-0.04	-0.64	153	1.02
ATP6	36.6	17.0	8.7	37.6	74.2	25.7	-0.01	-0.32	675	4.51
COIII	36.5	15.7	10.7	37.0	73.5	26.4	-0.01	-0.19	783	5.23
ND3	37.8	13.5	8.3	40.4	78.2	21.8	-0.03	-0.24	349	2.33
ND5	43.9	17.0	10.2	28.9	72.8	27.2	0.21	-0.25	1,618	10.80
ND4	46.3	18.0	8.6	27.1	73.4	26.6	0.26	-0.35	1,244	8.31
ND4L	50.4	14.9	5.4	29.3	79.7	20.3	0.26	-0.47	276	1.84
ND6	33.3	16.6	6.0	44.1	77.4	22.6	-0.14	-0.47	483	3.22
CYTB	31.9	18.2	11.0	38.8	70.7	29.2	-0.10	-0.25	1,141	7.62
ND1	46.4	16.8	11.1	25.8	72.2	27.9	0.29	-0.20	912	6.09

16s rRNA	41.5	16.0	6.6	35.9	77.4	22.6	0.07	-0.42	1,134	7.57
12s rRNA	40.1	16.1	8.0	35.8	75.9	24.1	0.06	-0.34	758	5.06
ND2	36.0	16.3	8.0	39.7	75.7	24.3	-0.05	-0.34	970	6.48
PCGs	**38.6**	**17.1**	**9.9**	**34.4**	**73.0**	**27.0**	**0.06**	**-0.27**	**10,798**	**72.09**
tRNAs	39.8	14.8	10.2	35.3	75.1	25.0	0.06	-0.18	1386	9.25
rRNAs	41.0	16.0	7.2	35.8	76.8	23.2	0.07	-0.38	1892	12.63
AT-rich region	38.9	9.0	5.0	47.1	86.0	14.0	-0.10	-0.29	902	6.02
Complete mtDNA	**39.0**	**16.3**	**9.3**	**35.4**	**74.4**	**25.6**	**0.05**	**-0.27**	**14978**	**100.00**

(b) DC-ETH

Region	**A%**	**C%**	**G%**	**T%**	**A+T%**	**G+C%**	**AT-skew**	**GC-skew**	**bp**	**% (size)**
COI	32.6	17.6	13.1	36.7	69.3	30.7	-0.06	-0.15	1,530	10.21
COII	34.6	17.3	10.4	37.7	72.3	27.7	-0.04	-0.25	664	4.43
ATP8	35.9	20.3	5.2	38.6	74.5	25.5	-0.04	-0.59	153	1.02
ATP6	36.9	17.0	8.4	37.6	74.5	25.4	-0.01	-0.34	675	4.51
COIII	36.4	15.7	10.9	37.0	73.4	26.6	-0.01	-0.18	783	5.23
ND3	38.1	13.5	8.0	40.4	78.5	21.5	-0.03	-0.26	349	2.33
ND5	44.0	16.9	10.1	28.9	72.9	27.1	0.21	-0.25	1,618	10.80
ND4	46.1	18.1	8.8	27.0	73.1	26.9	0.26	-0.35	1,244	8.31
ND4L	50.4	14.9	5.4	29.3	79.7	20.3	0.26	-0.47	276	1.84
ND6	33.3	16.6	6.0	44.1	77.4	22.6	-0.14	-0.47	483	3.22
CYTB	31.8	18.3	11.0	38.8	70.6	29.4	-0.10	-0.25	1,141	7.62
ND1	46.4	16.7	11.2	25.8	72.2	27.9	0.29	-0.20	912	6.09
16s rRNA	41.8	15.8	6.4	36.0	77.8	22.3	0.07	-0.42	1,134	7.57
12s rRNA	40.1	16.1	8.0	35.8	75.9	24.1	0.06	-0.34	758	5.06
ND2	35.9	16.2	8.1	39.8	75.7	24.3	-0.05	-0.33	970	6.48
PCGs	**38.6**	**17.0**	**9.9**	**34.4**	**73.0**	**26.9**	**0.06**	**-0.26**	**10,798**	**72.09**
tRNAs	39.8	14.5	10.1	35.6	75.4	24.6	0.06	-0.18	1386	9.25
rRNAs	41.1	15.9	7.1	35.9	77.0	23.0	0.07	-0.38	1892	12.63
AT-rich region	39.4	9.1	4.8	46.8	86.2	23.0	-0.09	-0.31	902	6.02
Complete mtDNA	**39.0**	**16.3**	**9.3**	**35.3**	**74.3**	**25.6**	**0.05**	**-0.27**	**14978**	**100.00**

(c) DC-KEN

Region	**A%**	**C%**	**G%**	**T%**	**A+T%**	**G+C %**	**AT-skew**	**GC-skew**	**bp**	**% (size)**
COI	32.4	17.7	13.2	36.7	69.1	30.9	-0.06	-0.15	1,530	10.21
COII	34.8	17.6	10.4	37.2	72.0	28.0	-0.03	-0.26	664	4.43
ATP8	35.9	20.9	4.6	38.6	74.5	25.5	-0.04	-0.64	153	1.02
ATP6	36.6	17.0	8.7	37.6	74.2	25.8	-0.01	-0.32	675	4.51
COIII	36.5	15.7	10.7	37	73.5	26.4	-0.01	-0.19	783	5.23

ND3	38.1	13.5	8.0	40.4	78.5	21.5	-0.03	-0.26	349	2.33
ND5	43.9	17.0	10.2	28.9	72.8	27.2	0.21	-0.25	1,618	10.80
ND4	46.2	18.0	8.7	27.1	73.3	26.7	0.26	-0.35	1,244	8.31
ND4L	50.4	14.9	5.4	29.3	79.7	20.3	0.26	-0.47	276	1.84
ND6	33.3	16.8	6.0	43.9	77.2	22.8	-0.14	-0.47	483	3.22
CYTB	32.0	18.2	11.0	38.8	70.8	29.2	-0.10	-0.25	1,141	7.62
ND1	46.4	16.8	11.1	25.8	72.2	27.9	0.29	-0.20	912	6.09
16s rRNA	41.5	16.0	6.6	35.9	77.4	22.6	0.07	-0.42	1,134	7.57
12s rRNA	40.1	16.1	8.0	35.8	75.9	24.1	0.06	-0.34	758	5.06
ND2	36.0	16.3	8.0	39.7	75.7	24.3	-0.05	-0.34	970	6.48
PCGs	**38.6**	**17.1**	**9.9**	**34.4**	**73.0**	**27.0**	**0.06**	**-0.27**	**10,798**	**72.09**
tRNAs	39.6	14.9	10.3	35.3	74.9	25.1	0.06	-0.18	1386	9.25
rRNAs	41.0	16.0	7.2	35.8	76.8	23.2	0.07	-0.38	1892	12.63
AT-rich region	39.0	9.0	4.9	47.1	86.1	13.9	-0.09	-0.29	902	6.02
Complete mtDNA	**39.0**	**16.3**	**9.3**	**35.4**	**74.4**	**25.6**	**0.05**	**-0.27**	**14978**	**100.00**

(d) DC-TZN										
Region	**A%**	**C%**	**G%**	**T%**	**A+T%**	**G+C%**	**AT-skew**	**GC-skew**	**bp**	**% (size)**
COI	32.4	17.7	13.2	36.7	69.1	30.9	-0.06	-0.15	1,530	10.21
COII	34.8	17.6	10.4	37.2	72.0	28.0	-0.03	-0.26	664	4.43
ATP8	35.9	20.9	5.2	38.6	74.5	26.1	-0.04	-0.60	153	1.02
ATP6	36.6	17.0	8.7	37.6	74.2	25.8	-0.01	-0.32	675	4.51
COIII	36.5	15.7	10.7	37	73.5	26.4	-0.01	-0.19	783	5.23
ND3	38.1	13.5	8.0	40.4	78.5	21.5	-0.03	-0.26	349	2.33
ND5	43.9	17.0	10.2	28.9	72.8	27.2	0.21	-0.25	1,618	10.80
ND4	46.2	18.0	8.7	27.1	73.3	26.7	0.26	-0.35	1,244	8.31
ND4L	50.4	14.9	5.4	29.3	79.7	20.3	0.26	-0.47	276	1.84
ND6	33.3	16.8	6.0	43.9	77.2	22.8	-0.14	-0.47	483	3.22
CYTB	32.0	18.2	11.0	38.8	70.8	29.2	-0.10	-0.25	1,141	7.62
ND1	46.4	16.8	11.1	25.8	72.2	27.9	0.29	-0.20	912	6.09
16s rRNA	41.5	16.0	6.6	35.9	77.4	22.6	0.07	-0.42	1,134	7.57
12s rRNA	40.1	16.1	8.0	35.8	75.9	24.1	0.06	-0.34	758	5.06
ND2	36.0	16.3	8.0	39.7	75.7	24.3	-0.05	-0.34	970	6.48
PCGs	**38.6**	**17.1**	**9.9**	**34.4**	**73.0**	**27.0**	**0.06**	**-0.27**	**10,798**	**72.09**
tRNAs	39.7	14.9	10.2	35.3	75.0	25.1	0.06	-0.19	1482	9.89
rRNAs	41.0	16.0	7.2	35.8	76.8	23.2	0.07	-0.38	1892	12.63
AT-rich region	39.1	9.3	4.8	46.8	85.9	14.1	-0.09	-0.32	902	6.02
Complete mtDNA	**39.0**	**16.3**	**9.3**	**35.4**	**74.4**	**25.6**	**0.05**	**-0.27**	**14978**	**100.00**

(e) DC-USA										
Region	**A%**	**C%**	**G%**	**T%**	**A+T%**	**G+C%**	**AT-**	**GC-**	**bp**	**%**

							skew	skew		(size)
COI	32.5	17.6	13.1	36.7	69.2	30.7	-0.06	-0.15	1,530	10.21
COII	34.6	17.3	10.4	37.7	72.3	27.7	-0.04	-0.25	664	4.43
ATP8	35.9	20.3	5.2	38.6	74.5	25.5	-0.04	-0.59	153	1.02
ATP6	36.9	17.0	8.4	37.6	74.5	25.5	-0.01	-0.34	675	4.51
COIII	36.4	15.7	10.9	37.0	73.4	26.6	-0.01	-0.18	783	5.23
ND3	38.1	13.5	8.0	40.4	78.5	21.5	-0.03	-0.26	349	2.33
ND5	44.0	16.9	10.1	28.9	72.9	27.1	0.21	-0.25	1,618	10.80
ND4	46.1	18.1	8.8	27.0	73.1	26.9	0.26	-0.35	1,244	8.31
ND4L	50.4	14.9	5.4	29.3	79.7	20.3	0.26	-0.47	276	1.84
ND6	33.3	16.6	6.0	44.1	77.4	22.6	-0.14	-0.47	483	3.22
CYTB	31.8	18.3	11.0	38.8	70.6	29.4	-0.10	-0.25	1,141	7.62
ND1	46.4	16.7	11.2	25.8	72.2	27.9	0.29	-0.20	912	6.09
16s rRNA	41.7	15.8	6.4	36.0	77.7	22.3	0.07	-0.42	1,134	7.57
12s rRNA	40.1	16.0	8.0	35.9	76.0	24.0	0.06	-0.33	758	5.06
ND2	35.9	16.2	8.1	39.8	75.7	24.3	-0.05	-0.33	970	6.48
PCGs	**38.3**	**17.0**	**10.1**	**34.6**	**72.9**	**27.1**	**0.05**	**-0.25**	**10,798**	**72.09**
tRNAs	39.6	14.8	10.3	35.3	74.9	25.1	0.06	-0.18	1386	9.25
rRNAs	41.1	15.9	7.1	36.0	77.1	23.0	0.07	-0.38	1892	12.63
AT-rich region	39.1	9.0	5.0	46.1	85.2	14.0	-0.08	-0.29	902	6.02
Complete mtDNA	**39.0**	**16.3**	**9.3**	**35.4**	**74.4**	**25.6**	**0.05**	**-0.27**	**14978**	**100.00**

Appendix 18. Pairwise comparison of two groups of *Diaphorina citri* specimens collected in China/Kenya/Tanzania (group 1) and Ethiopia/USA (group 2) given as the number of single nucleotide polymorphisms (SNPs) and non-synonymous amino acid substitutions (NS) in the complete complement of 13 mitochondrial protein coding genes.

Gene	Amino Acid Change	Change	Codon Change	Polymorphism Type	Protein Effect
COI		G -> A	CCG -> CCA	SNP (transition)	None
		G -> A	TGG -> TGA	SNP (transition)	None
		C -> T	CTA -> TTA	SNP (transition)	None
	T -> A	A -> G	ACT -> GCT	SNP (transition)	Substitution
	H -> Q	C -> A	CAC -> CAA	SNP (transversion)	Substitution
		G -> A	TGG -> TGA	SNP (transition)	None
COII	M -> L	A -> T	ATA -> TTA	SNP (transversion)	Substitution
		C -> T	ACC -> ACT	SNP (transition)	None
		C -> T	TAC -> TAT	SNP (transition)	None
ATP8		C -> T	ATC -> ATT	SNP (transition)	None
	Y -> D	T -> G	TAT -> GAT	SNP (transversion)	Substitution
ATP6		G -> A	TGG -> TGA	SNP (transition)	None
		G -> A	TCG -> TCA	SNP (transition)	None
COXIII		A -> G	TCA -> TCG	SNP (transition)	None
ND3		C -> T	CTA -> TTA	SNP (transition)	None

		T -> C	AAT -> AAC	SNP (transition)	None
ND5		T -> C	AAA -> AAG	SNP (transition)	None
		C -> T	ATG -> ATA	SNP (transition)	None
		C -> T	GTG -> GTA	SNP (transition)	None
		T -> C	GGA -> GGG	SNP (transition)	None
	L -> F	G -> A	CTT -> TTT	SNP (transition)	Substitution
	V -> M	C -> T	GTA -> ATA	SNP (transition)	Substitution
ND4		A -> G	CCT -> CCC	SNP (transition)	None
		G -> A	CTA -> TTA	SNP (transition)	None
		T -> C	ATA -> ATG	SNP (transition)	None
		A -> G	TTT -> TTC	SNP (transition)	None
		A -> G	ATT -> ATC	SNP (transition)	None
		G -> A	CAC -> CAT	SNP (transition)	None
		A -> G	GGT -> GGC	SNP (transition)	None
ND6		T -> C	GTT -> GTC	SNP (transition)	None
	L -> F	CTC -> TTT	CTC -> TTT	Substitution	Substitution
CYTB		A -> G	GGA -> GGG	SNP (transition)	None
		A -> T	GGA -> GGT	SNP (transversion)	None
		T -> C	CCT -> CCC	SNP (transition)	None
ND1	G -> S	C -> T	GGA -> AGA	SNP (transition)	Substitution
		T -> C	GAA -> GAG	SNP (transition)	None
		A -> G	ATT -> ATC	SNP (transition)	None
	A -> S	C -> A	GCT -> TCT	SNP (transversion)	Substitution
ND2	I -> V	A -> G	ATT -> GTT	SNP (transition)	Substitution
	S -> F	C -> T	TCC -> TTC	SNP (transition)	Substitution

Appendix 19. Universal 16S primers and *Wolbachia*-specific (in bold) primers used in the PCR amplification and bidirectional sequencing of endosymbionts of the citrus psyllid *Diaphorina citri.*

Primer	Primer sequence (5'-3')	Reference
27F	AGAGTTTGATCCTGGCTCAG	Hocquellet et al. 1999
148R	TACGGTACCTTGTTACGACTT	Hocquellet et al. 1999
wspecF	**CATACCTATTCGAAGGGATAG**	Werren and Windsor, 2000
wspecR	**AGCTTCGAGTGAAACCAATTC**	Werren and Windsor, 2000

Appendix 20. List of publicly available sequences with homology to the 16S sequences of *Diaphorina citri* from this study using 27F/148R primers

Population	Taxon	GenBank accession	Percentage identity

China	*Pseudomonas sp.*	KM253123	100%
	Candidatus Profftella armatura	CP012591	100%
	Wolbachia sp.	MK277439.1	100%
Kenya	*Enterobacteriaceae sp*	EF088376	97%
	Candidatus Carsonella ruddii	AF211136.1	96%
	Wolbachia sp	MK277439.1	100%
Tanzania	*Syncytium sp*	EF433792	100%
	Wolbachia sp	MK277439.1	100%

Appendix 21. Alpha diversity statistics for the bacterial metagenomes of the citrus psyllid *Diaphorina citri* collected in four countries (Kenya, Tanzania and China).

	EVENNESS	RICHNESS	SHANNON	TRUE_SHANNON
China	0.21	477	1.34	3.81
Kenya	0.26	367	1.51	4.51
Tanzania	0.29	736	1.91	6.78

Appendix 22. Summary statistics for the analyses of the presence of genes for antibiotic resistance in the microbiome of the citrus psyllid *Diaphorina citri* in three countries, obtained from the ARMA workflow in EPI2ME.

	China	Kenya	Tanzania
Reads analysed	119,988	44,455	399,992
Alignments	112,462	41,227	379,386
Average accuracy (%)	74.40	74.20	75.40
CARD genes	48	48	48

PUBLICATIONS IN DISSERTATIONS AND AUTHOR DECLARATION

DECLARATION BY THE CANDIDATE

With regard to **Chapters 2 to 7 (pages 8 -108)** the nature and scope of my contribution were as follows:

Nature of contribution	Extent of contribution (%)
Conceptualization	20
Data Curation	35
Formal Analysis	80
Investigation	100
Writing – Original Draft Preparation	100
Writing	30

The following co-authors have contributed to chapter 2 to 7 (pages 8 -100):

Name	Email address	Nature of contribution	Extent of contribution (%)
Pietersen Gerhard	gpietersen@sun.ac.za	Supervision Resources Writing	25 10 25
Van Asch Barbara	bva@sun.ac.za	Supervision Formal analysis Resources Writing	25 20 10 25
Ekesi Sunday	sekesi@icipe.org	Supervision Conceptualization Funding Acquisition Resources	25 30 40 40
Khamis Fathiya	fkhamis@icipe.org	Supervision Conceptualization Funding Acquisition Resources Writing	25 30 25 20 20
Mohammed Samira	sfaris@icipe.org	Conceptualization Funding Acquisition Resources	20 25 10
Rwomushana Ivan	rwomivan@gmail.com	Funding Acquisition	10
Subramanian Sevgan	ssubramania@icipe.org	Resources	10
Ombura Fidelis Levi	lombura@icipe.org	Data Curation	10
Seid Nurhussen	nurhusseinsy@yahoo.com	Data Curation	10
Rasowo Brenda A.	bre.rasowo@gmail.com	Data Curation	5

Tanga Chrysantus	ctanga@icipe.org	Data Curation	5
Sétamou Mamoudou	Mamoudou.Setamou@tamuk.edu	Data Curation	5
Komivi Akutse	kakutse@icipe.org	Data Curation	5
Wairimu Anne	Annewambui814@yahoo.com	Data Curation	5
Momanyi George	gmomanyi@kephis.org	Data Curation	5
Finyange Pole	finyange@gmail.com	Data Curation	5
Ballo Shifa	sballo@icipe.org	Data Curation	5
Azerefegne Ferdu	azeref@gmail.com	Data Curation	5

Declaration with signature in possession of candidate and supervisor.